# Mechanisms of evasion of the African Trypanosome: *Trypanosoma brucei* from the host innate and adaptive immune system

BY

**CHEUNG Jackie Lok-Yee**

BSc. Imperial College London; MRes. Imperial College London

Joint Degree of Doctor of Philosophy at The University of Hong Kong and

Imperial College London

September 2017

Abstract of the thesis entitled

**Mechanisms of evasion of the African Trypanosome: *Trypanosoma brucei* from the host innate and adaptive immune system**

Submitted by

**CHEUNG Jackie Lok-Yee**

For the degree of Doctor of Philosophy at The University of Hong Kong in September 2017

The extracellular bloodstream form *Trypanosoma brucei* is the causative agent of Human African Trypanosomiasis (HAT). It is highly adapted to escape both the innate and adaptive immune systems of the mammalian host, which is mediated through a dense Variant Surface Glycoprotein (VSG) coat. Two main mechanisms of evasion are known to provide protection for the parasite in the bloodstream: antigenic variation and high rates of host opsonin removal. VSG is essential for trypanosome survival and blocking its synthesis triggers growth inhibition and a precytokinesis cell cycle arrest *in vitro*, but are rapidly cleared in mice.

In this study, I showed that blocking the synthesis of VSG resulted in an increase in trypanosome phagocytosis by mouse macrophages but only if the parasite had been opsonised with anti-VSG antibodies. Further analysis revealed that the induction of *VSG* RNAi caused a change in swimming behaviour, as stalled cells swam with increased velocity and directionality. Blocking VSG synthesis also resulted in a significant reduction of anti-VSG antibody removal from the parasite surface. However, this was not due to defects in endocytosis as the rates of internalisation of bulk surface VSG, or endocytic markers like tomato lectin, transferrin or dextran were not significantly affected by the VSG synthesis block. Antibody-VSG complexes could enter the trypanosome and reach the lysosome but the kinetics at which antibodies were internalised was reduced, which indicates that selective perturbation of anti-VSG antibody complexes may be operating at the flagellar pocket. These results highlight the importance of efficient elimination of anti-VSG-antibody complexes from the trypanosome cell surface for trypanosome evasion of macrophages.

Trypanosome evasion from the host adaptive immune system is known to mainly involve dampening the pro-inflammatory response elicited in the early phases of infection. Here, I demonstrated that *in vitro*, *T. brucei* hinders the process of maturation and antigen uptake in dendritic cells (DC). As a consequence, led to in a shift in cytokine production to a type II profile, accompanied by an unusual surge in IL-8, a neutrophil recruiting cytokine. The capacity at which *T. brucei* stimulated DCs could activate naïve T-cells also decreased over time. While naïve T-cells were able to proliferate in response, there were significant changes in the cytokine profiles. The Th1 cytokine IFN-γ was upregulated while expression of the Th2 cytokine IL-4 was suppressed, indicating a general pro-inflammatory response was induced by *T. brucei*. Interestingly, I showed for the first time, that Th17 cells may be involved in infection control as Th17-associated cytokines were universally upregulated.

Finally, a preliminary drug study in this thesis, showed the potential of the pegylated human recombinant arginase, BCT-100 as an alternative HAT treatment. Depletion of arginine using BCT-100 resulted in growth inhibition and a cell cycle arrest. This study highlights several key aspects regarding evasion from host immunity by bloodstream form *T. brucei*. Further investigation will allow us to gain insight into the mechanisms involved in mounting an effective response against *T. brucei* infections and develop novel therapies for the treatment of Human African Trypanosomiasis.

---

**An abstract of exactly 497 words**

## Statement of Originality

I declare that this thesis represents my own work, except where due acknowledgement is made, and that it has not been previously included in a thesis, dissertation or reported submitted to this University or to any other institution for a degree, diploma or other qualifications.

Signed …….....

CHEUNG Jackie Lok-Yee

## Copyright Declaration

The copyright of this thesis rests with the author and is made available under a Creative Commons Attribution Non-Commercial No Derivatives licence. Researchers are free to copy, distribute or transmit the thesis on the condition that they attribute it, that they do not use it for commercial purposes and that they do not alter, transform or build upon it. For any reuse or redistribution, researchers must make clear to others the licence terms of this work

Signed …….....

CHEUNG Jackie Lok-Yee

## Acknowledgements

First and foremost, I would like to thank my parents for their unconditional love and support throughout the years and for teaching me to work hard and have fun while doing it. To my brother Jonny, thank you for taking care of me and sharing some of my greatest memories of my time in London. I would like to thank Bom, who has shared countless ups and downs with me throughout this PhD and has always been my biggest cheerleader.

To my ICL supervisor Gloria, thank you for giving me the opportunity to embark on one of the most challenging yet rewarding experiences of my life. I have learned so much from you both inside and outside the lab. To my HKU supervisor, Professor Chan, thank you for being my mentor and for your constant encouragement and advice throughout various challenges in the past 7 years.

I would also like to thank my wonderful lab mates in ICL, Louise, CP and Sophie, who have always been there for me even from 6000 miles away. Some of my fondest memories of the UK were shared with you and I will treasure them forever.

To my lab family in HKU, Carmen, Aikha, Anita, Lin, Ho and Victoria, thank you for making my transition back to Hong Kong so much easier. Thank you all for the countless number of times you have helped me, given me advice, made me exercise, listened to my rants and made me feel loved. I would also like to show my appreciation to all other members of the CFC group and staff of the Department of Paediatrics and Adolescent Medicine, for your help and advice.

To my oldest friends, Sonja, Faye, Becca, Wendy, Nicky, Karl and Ronald: Thank you for always giving me your support and love even though we are all working in different countries and in different fields. I love you all.

# Table of Contents


**Chapter 1** ..... 1

**Introduction** ..... 1

1.1 Epidemiology of Human African Trypanosomiasis ..... 1

1.2 Disease progression ..... 3

1.3 *T. brucei* life cycle ..... 4

1.4 Cell cycle progression of bloodstream form *T. brucei* ..... 5

1.5 Variant Surface Glycoprotein ..... 7

1.6 Antigenic variation ..... 9

1.7 Endocytosis and vesicular transport ..... 11

1.8 Movement of VSG on the trypanosome cell surface ..... 13

1.9 Trypanosome motility ..... 14

1.10 Strategies of innate immune evasion ..... 16

1.11 Immunomodulation of antigen presenting cells ..... 19

1.12 T-cell defects induced by *T. brucei* infection ..... 20

1.13 Current Human African Trypanosomiasis treatments ..... 22

1.14 Objectives ..... 25

**Chapter 2** ..... 26

**Materials and Methods** ..... 26

2.1 Trypanosoma brucei strains ..... 26

2.2 Media and buffers ..... 30

2.3 Primary and secondary antibodies ..... 31

2.4 Trypanosome growth and DNA characterisation ..... 33

2.5 Macrophage culture ..... 33

2.6 Trypanosome phagocytosis assay ..... 33

2.7 Immunofluorescence microscopy ..... 34

2.8 Surface VSG-antibody clearance and uptake ..... 34

2.9 Biotinylated VSG uptake assay ..... 35

2.10 Western blotting and LiCor Imaging ..... 36

2.11 Endocytosis assays ..... 37

2.12 Time-lapse live cell video microscopy ..... 38

2.13 Isolation of peripheral blood mononuclear cells from human peripheral blood ..... 39

2.14 Differentiation of PBMCs into monocyte-derived dendritic cells ..... 39

2.15 Human dendritic cell and *T. brucei* co-culture ..... 40

**2.16 Surface markers staining** ..... 40
**2.17 Dendritic cells phagocytosis assay** ..... 40
**2.18 Purification of VSG** ..... 40
**2.19 Isolation of CD3 positive T-cells from PBMCs** ..... 41
**2.20 T-cell proliferation assay** ..... 41
**2.21 Multiplex Bead Based Immunoassays** ..... 42
**2.22 BCT-100 treatment of *T. brucei*** ..... 43

**Chapter 3** ..... 44

**The role of VSG in the immune evasion from macrophages** ..... 44
**3.1 Introduction** ..... 44
**3.2 Experimental outline** ..... 46
**3.3 Validation of the functionality of the RNAi machinery in the *T. brucei* 221VG1.1 cell line** ..... 47
**3.4 Quantification of phagocytosis using the endogenous eGFP signal from *T. brucei* 221VG1.1 after the induction of *VSG221* RNAi** ..... 49
**3.5 Inhibition of VSG synthesis in *T. brucei* led to an increase in phagocytosis by** ..... 55
**3.6 Blocking VSG synthesis in the presence of anti-VSG221 antibodies resulted in an increase in adherence and phagocytosis of trypanosomes by macrophages.** ..... 58
**3.7 Discussion** ..... 60

**Chapter 4** ..... 63

**Mechanistic effects of a VSG synthesis block on *Trypanosoma brucei* immune evasion** 63
**4.1 Introduction** ..... 63
**4.2 Experimental outline** ..... 64
**4.3 Blocking VSG synthesis results in reduced clearance of surface-bound anti-VSG221 antibodies** ..... 65
**4.4 Decrease in surface VSG corresponded to an increase in anti-VSG antibody binding to the trypanosome surface** ..... 72
**4.5 Blocking VSG synthesis results in impairment of internalisation but not the degradation of anti-VSG antibodies** ..... 78
**4.6 The early endocytic pathway was not significantly affected by the VSG synthesis block** . 80
**4.7 Blocking VSG synthesis increased trypanosome swim velocity** ..... 82
**4.8 *VSG221* RNAi induction resulted in reduced tumbling and increased directional swimming** ..... 84
**4.9 Discussion** ..... 90

**Chapter 5** ..... 96

**Immunomodulation of human dendritic cells by *T. brucei in vitro*** ..... 96

**5.1 Introduction** ..... 96

**5.2 Experimental outline** ..... 97

**5.3 *T. brucei* downregulates human dendritic cell maturation markers** ..... 98

**5.4 *T. brucei* reduces the capacity of antigen uptake by moDCs** ..... 101

**5.5 Soluble VSG suppresses maturation of moDCs** ..... 104

**5.6 Inflammatory cytokine regulation** ..... 110

**5.7 Discussion** ..... 115

**Chapter 6** ..... 120

**Immunomodulation of human T-cells by *T. brucei in vitro*** ..... 120

**6.1 Introduction** ..... 120

**6.2 Experimental outline** ..... 122

**6.3 Naïve CD3 positive T-cells were activated by *T. brucei* exposure** ..... 123

**6.4 T-cells were activated but activation markers were downregulated upon prolonged co-culture with *T. brucei* stimulated moDCs** ..... 127

**6.5 *T. brucei* stimulated moDCs triggered CD3+ T-cell proliferation** ..... 128

**6.6 Th17 cells were involved in generating a pro-inflammatory microenvironment** ..... 133

**6.7 Th2 cytokines were simultaneously upregulated** ..... 136

**6.8 Discussion** ..... 140

**Chapter 7** ..... 144

**Potential therapeutic use of pegylated-arginase (BCT-100) in the treatment of Human African Trypanosomiasis** ..... 144

**7.1 Introduction** ..... 144

**7.2 Experimental outline** ..... 147

**7.3 BCT-100 inhibited *T. brucei* growth and caused parasite lysis *in vitro*** ..... 148

**7.4 Number of abnormal parasites in the G2/M cell cycle stage increased after BCT-100 treatment** ..... 151

**7.5 *T. brucei* cell cycle arrest was coupled with DNA arrangement abnormalities** ..... 153

**7.6 Discussion** ..... 156

**The data presented in this chapter are only the initial steps to explore the potential use of BCT-100 as a therapeutic treatment for HAT. Although preliminary data showed promise in trypanosome killing, more detail analysis regarding cellular toxicity must be performed** ..... 159

**Chapter 8** ..... 160

**Final conclusions and future perspectives** ..... 160

**8.1 High rate of host antibody clearance is key to macrophage evasion ..... 160**

**8.2 *T. brucei* dampens dendritic cell response to avoid activating T-cells ..... 162**

**8.3 Th17 cells are involved in to the perpetuation of the pro-inflammatory response against *T. brucei* infection ..... 164**

**8.4 BCT-100 as a potential drug treatment for Human African Trypanosomiasis ..... 165**

**References ..... 168**

**Publication ..... 190**

**Award ..... 190**

**Conference Presentations ..... 190**

## List of Figures


| | | Page number |
|---|---|---|
| **Chapter 1** | | |
| **Figure 1.1** | Global distribution of Human African Trypanosomiasis | 2 |
| **Figure 1.2** | The life cycle of *Trypanosoma brucei* | 5 |
| **Figure 1.3** | Cell cycle progression in bloodstream form *T. brucei* | 6 |
| **Figure 1.4** | Antigenic variation during a *T. brucei* infection | 10 |
| **Figure 1.5** | Mechanisms of VSG switching | 11 |
| **Figure 1.6** | Hydrodynamic drag forces generated by forward swimming preferentially sort antibody-VSG complexes into the flagellar pocket | 14 |
| **Figure 1.7** | Different subsets of CD4+ T helper cells | 21 |
| **Chapter 2** | | |
| **Figure 2.1** | Schematic illustrations of the bloodstream form *T. brucei* cell lines used in this study | 28 |
| **Chapter 3** | | |
| **Figure 3.1** | Phenotypes of bloodstream form *T. brucei* after blocking VSG221 synthesis | 48-49 |
| **Figure 3.2** | The effect of opsonisation on the viability of *T. brucei* after the induction of *VSG* RNAi | 51 |
| **Figure 3.3** | Anti-VSG221 antibody was not in saturation | 52 |
| **Figure 3.4** | Immunofluorescence microscopy analysis of the phagocytosis of *T. brucei* 221VG1.1 cells | 53 |
| **Figure 3.5** | Microscopic categorisation of *T. brucei* phagocytosis | 55 |
| **Figure 3.6** | Phagocytosis of *T. brucei* by macrophages increased significantly in the presence of anti-VSG221 antibodies | 58 |
| **Figure 3.7** | Analysis of *T. brucei* attachment and internalisation by RAW264.7 macrophages | 60 |
| **Chapter 4** | | |

**Figure 4.1** Immunofluorescence microscopy analysis of surface anti-VSG221 antibody clearance by *T. brucei* 67
**Figure 4.2** Flow cytometry analysis of the surface clearance of anti-VSG221 antibodies after blocking VSG synthesis 69-70
**Figure 4.3** Quantitation of the reduced clearance of anti-VSG221 antibody after blocking VSG221 or TDP1 synthesis 72
**Figure 4.4** Total amount of VSG221 protein decreased after 8h of *VSG221* RNAi induction 74
**Figure 4.5** Biotinylation of surface VSG decreased while anti-VSG221 antibody binding increased following the induction of *VSG221* RNAi 77
**Figure 4.6** Rate of biotinylated VSG internalisation was unchanged after blocking VSG synthesis 78
**Figure 4.7** Blocking VSG synthesis impaired the internalisation of VSG221 antibodies 80
**Figure 4.8** The rate of transferrin, tomato-lectin and dextran internalisation was unaffected by *VSG221* RNAi induction 82
**Figure 4.9** *T. brucei* swim speed was not affected by the VSG synthesis block 84
**Figure 4.10** *T. brucei* swim velocity increased after 8h of VSG synthesis block 86
**Figure 4.11** *T. brucei* swam more directionally after the induction of *VSG221* RNAi 88
**Figure 4.12** Heterogeneity of angular persistence increased presumably as individual cells were affected differently by *VSG* RNAi 90

**Chapter 5**

**Figure 5.1** Downregulation of dendritic cell maturation markers by *T. brucei* in a time-dependent manner 101
**Figure 5.2** Antigen uptake by dendritic cells decreased over time after co-culture with *T. brucei* 104
**Figure 5.3** Purification of VSG protein 107
**Figure 5.4** Soluble VSG is insufficient to activate human moDCs 110

**Figure 5.5** Downregulation of inflammatory cytokines MCP-1, TNF-α and IL-6 by moDCs after stimulation by *T. brucei* 113
**Figure 5.6** Upregulation of the inflammatory cytokines IL-8 and IL-10 by moDCs after stimulation by *T. brucei* 114

**Chapter 6**
**Figure 6.1** Flow cytometry gating of CD3+ cells after selection 124
**Figure 6.2** Size of CD3+ T-cells increased after co-culture with moDCs presenting *T. brucei* antigens 126-127
**Figure 6.3** CD3+ T-cells were activated by moDCs presenting *T. brucei* antigens 129
**Figure 6.4** Flow cytometry gating of CFSE-stained CD3+ T-cells 130
**Figure 6.5** moDCs treated by *T. brucei* for 72h promoted CD3+ T-cell proliferation 132-133
**Figure 6.6** Increase of Th17 cytokine release by CD3+ T-cells after co-culture with *T. brucei* 136-137
**Figure 6.7** IFN-γ expression increased while IL-4 was downregulated 138
**Figure 6.8** Expression of Th2 cytokines were simultaneously upregulated 140

**Chapter 7**
**Figure 7.1** Schematic illustration of the first steps of trypanosome polyamine synthesis 148
**Figure 7.2** Growth of bloodstream form 221VG1.1 *T. brucei* after BCT-100 treatment 150
**Figure 7.3** *T. brucei* were lysed by BCT-100 after 24 hours of treatment 151
**Figure 7.4** Proportion of *T. brucei* in the G2/M cell cycle stage increased after BCT-100 treatment 153
**Figure 7.5** Changes in DNA arrangement in 2N2K cells after BCT-100 treatment 155
**Figure 7.6** Characterisation of DNA content arrangement in BF 221VG1.1 after BCT-100 treatment 156-157

## List of Tables

**Chapter 2**


| | | |
|---|---|---|
| **Table 2.1** | Frequently used transgenic bloodstream form *T. brucei* | 29 |
| **Table 2.2** | Concentrations of drugs used in the maintenance of bloodstream form *T. brucei* | 29 |
| **Table 2.3** | Composition of frequently used media and buffers | 30 |
| **Table 2.4** | Frequently used primary and secondary antibodies | 31 |
| **Table 2.5** | Antibodies used for flow cytometry analysis of human immune cells | 32 |


**Chapter 4**


| | | |
|---|---|---|
| **Table 4.1** | Changes in the amount of surface VSG versus the amount of anti-VSG221 antibody binding after the induction of *VSG221* RNAi for 8h | 76 |


**Chapter 5**


| | | |
|---|---|---|
| **Table 5.1** | Summary of the panel of cytokines screened after moDCs were co-cultured with *T. brucei*. | 115-116 |

## List of Abbreviations

| | |
|---|---|
| AC | Adenylate cyclase |
| APC | Antigen presenting cell |
| BBB | Blood brain barrier |
| BF | Bloodstream form |
| BSA | Bovine serum albumin |
| CATT | Card Agglutination Trypanosomiasis Test |
| CFSE | Carboxyfluorescein succinimidyl ester |
| CNS | Central nervous system |
| CSF | Cerebrospinal fluid |
| DAPI | 4',6-diamidino-2-phenylindole |
| DC | Dendritic cell |
| DFMO | Alpha-Difluoromethylornithine |
| DIC | Differential interference contrast |
| DMEM | Dulbecco's Modified Eagle's Medium |
| DMG | Dimyristoylglycerol |
| DNA | Deoxyribonucleic acid |
| eGFP | Enhanced green fluorescent protein |
| EGTA | Ethylene glycol-bis(β-aminoethyl ether)-N,N,N',N'-tetraacetic acid |
| ES | Expression site |
| FCS | Foetal calf serum |
| FITC | Fluorescein isothiocyanate |
| FMK-024 | morpholinourea-phenylalanine-homophenylalanine-fluoromethylketone |
| FP | Flagellar pocket |
| GIP | Glycosylphosphatidyinositol phosphate |
| HAT | Human African Trypanosomiasis |
| HEPES | 4-(2-hydroxyethyl)-1-piperazineethanesulfonic acid |
| IFN-γ | Interferon gamma |
| ISG | Invariant Surface Glycoproteins |
| ISG | Invariant Surface Glycoprotein |
| kbp | Kilo basepair |

| | |
|---|---|
| KCL | Potassium chloride |
| $KH_2PO_4$ | Potassium dihydrogen phosphate |
| LPS | Lipopolysaccharides |
| MCP-1 | Monocyte chemoattractant protein 1 |
| MFI | Mean fluorescence intensity |
| $MgSO_4$ | Magnesium sulphate |
| MHCII | Major histocompatibility class II |
| moDC | Monocyte-derived dendritic cells |
| MyD88 | Myeloid differentiation primary-response protein 88 |
| $Na_2HPO_4$ | Sodium hydrogen phosphate |
| NaCl | Sodium chloride |
| $NaH_2PO_4$ | Sodium dihydrogen phosphate |
| NMS | Normal mouse serum |
| ODC | Ornithine decarboxylase |
| P/S | Penicillin-streptomycin |
| PAMP | Pathogen associated molecular pattern |
| PBMC | Peripheral blood mononuclear cell |
| PF | Procyclic form |
| PFA | Paraformaldehyde |
| PFR2 | Paraflagellar rod protein 2 |
| PLC | Phospholipase C |
| PRR | Pattern recognition receptors |
| PSG | Phosphate saline glucose |
| RNAi | RNA interference |
| RPMI | Roswell Park Memorial Institute medium |
| SDS | *Sodium dodecyl sulphate* |
| SRA | Serum resistance-associated protein |
| sVSG | Soluble variant surface glycoprotein |
| TDB | Trypanosome dilution buffer |
| TLR | Toll-like receptor |
| TNF-α | Tumour necrosis factor |
| VSG | Variant Surface Glycoprotein |
| WBC | White blood cell |

# Chapter 1

# Introduction

## 1.1 Epidemiology of Human African Trypanosomiasis

Human African Trypanosomiasis (HAT), also known as African sleeping sickness is a vector-borne parasitic disease that is prevalent in 36 Sub-Saharan African countries, threatening over 60 million lives in the region (Brun *et al*. 2010; WHO 2017). The causative agent of HAT, and the animal form of the disease Nagana, is a unicellular eukaryotic parasite of the *Trypanosoma brucei* sub species. HAT is transmitted by the Tsetse flies. These are only found in the sub-Saharan region of Africa, and only Tsetse flies of the *Glossina* genus are vectors of *T. brucei*.

Two subspecies of *Trypanosoma brucei* are responsible for the human infectious form of HAT: *T. b. rhodesiense* and *T. b. gambiense*. These two subspecies have distinct epidemiology and disease progression in the host. *T. b. rhodesiense* causes the acute form of HAT and is common in 13 countries in the eastern and southern parts of Africa, and makes up approximately 3% of the reported cases. *T. b. gambiense* is found in 24 countries in west and central Africa, and accounts for 97% of the cases (Figure 1.1). *T. b. gambiense* causes a chronic HAT infection with minimal symptoms for months and even years (Simarro *et al*. 2012). Often by the time symptoms show, the patient is at an advanced stage of HAT where the parasite has invaded the central nervous system (CNS) (Franco *et al*. 2014; WHO 2017). Other *Trypanosoma* species are pathogenic to animals, *T. brucei brucei* infects domestic animals such as cattle, and causes the disease Nagana, causing extensive economic burden (WHO 2017).

There has been a significant drop in the number of cases in the last 10 years through the efforts of HAT surveillance programmes and increased vector and animal reservoir control.

Nevertheless, difficulty in reaching remote rural areas, social and political unrest and complexity of drug administration still poses challenges to eliminate HAT.

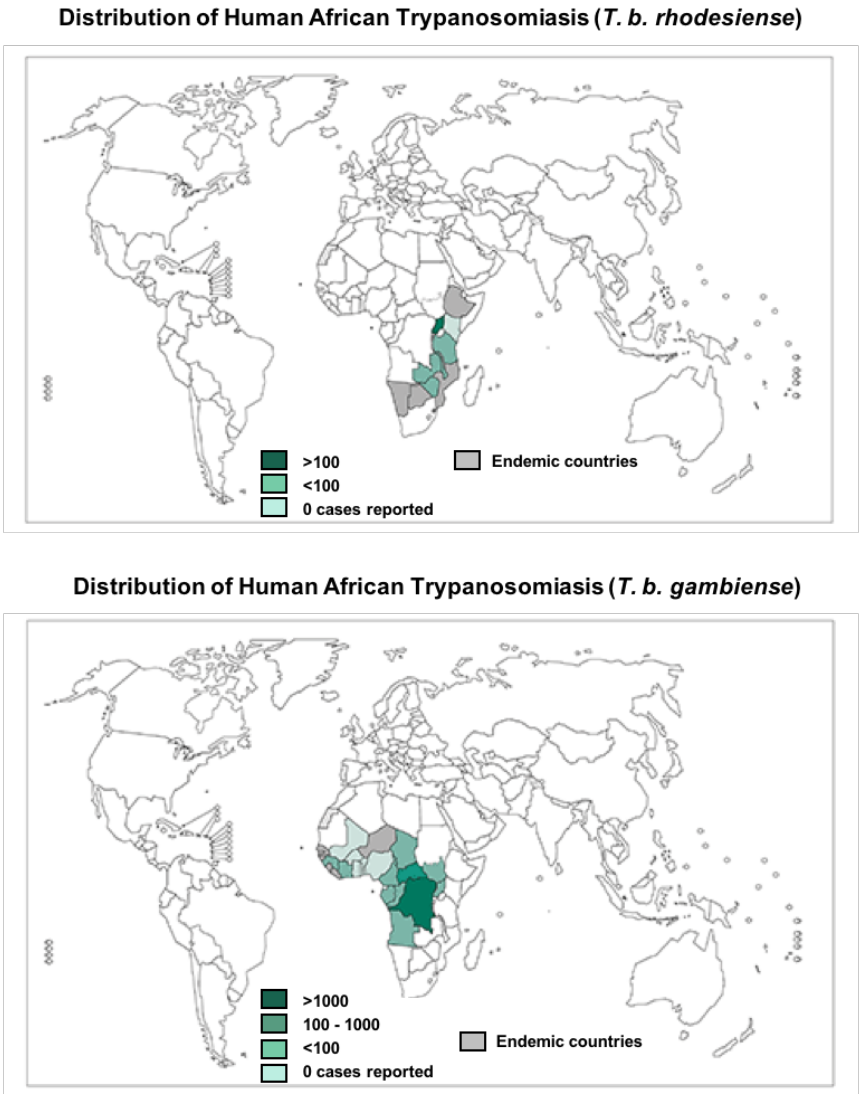



**Figure 1.1 Global distribution of Human African Trypanosomiasis.** The distribution pattern of HAT caused by either *T. b. rhodesiense* (upper panel) or *T. b. gambiense* (lower panel) in 2014 is represented by the green shaded areas on the map. The number of reported cases is proportional to the shade of green on the map. Areas shaded in grey indicate endemic countries that have not reported any cases in 2014. Data and graphs are obtained and modified from the World Health Organisation (WHO 2017).

### 1.2 Disease progression

There are two clinical stages of HAT infection, the early haemolymphatic stage followed by the meningoencephalitic stage (Kennedy 2013; WHO 2017). After the bite of a Tsetse fly, *T. brucei* is transferred into the bloodstream of the mammalian host. The haemolymphatic phase occurs one to three weeks after infection, as the parasite proliferates in the blood and lymphatic system. Patients at this stage of infection are often presented with symptoms such as fever, fatigue and anaemia. An inflammatory response is mounted by the host which leads to enlargement of the spleen and liver. Later in the infection, the parasite migrates across the blood brain barrier (BBB) into the CNS and causes a range of psychological disorders including disruptions in the sleep cycle, loss of sensory and motor skills and seizures (MacLean *et al*. 2012; Sternberg 2004). If untreated and the patient is allowed to progress to an advanced stage, death is the inevitable result. Both *T. b. rhodesiense* and *T. b. gambiense* share the same sequence of disease progression but at different rates. *T. b. rhodesiense* triggers an acute infection and progression to late stage often takes between weeks to months. *T. b. gambiense* on the other hand, causes a chronic infection that takes months or years to develop (Checchi *et al*. 2008; WHO 2017).

Since the clinical manifestations of HAT are not specific enough for diagnosis, current methods to diagnose HAT require finding parasites microscopically in body fluid, primarily in the blood and lymph (Mitashi *et al*. 2012). The most common serological test is the Card Agglutination Trypanosomiasis Test (CATT), which was developed in the 1970s to screen for *T. b. gambiense* specific antibodies (Magnus *et al*. 1978). *T. b. rhodesiense* progresses much quicker than *T. b. gambiense*, and is therefore easier to detect microscopically in the blood. Staging of the disease is then performed by the examination of the cerebrospinal fluid (CSF) for the presence of trypanosomes and white blood cells (WBC) (Kennedy 2013). However, in

the case of *T. b. gambiense* infections, parasite numbers in the early stages can be below the detection limit, which would require multiple serological tests to confirm the infection. Therefore, the development of new tests that are both sensitive and easy to use in the field are still required with urgency.

## 1.3 *T. brucei* life cycle

To complete its life cycle, *T. brucei* must cycle between the procyclic form (PF) in the Tsetse fly vector and the bloodstream form (BF) in the mammalian host (Figure 1.2) (Barrett *et al*. 2003). This requires the parasite to be highly adaptive to the internal environments of both host and vector species. When the Tsetse fly vector ingests a blood meal from an infected mammalian host, the bloodstream form *T. brucei* travels from the mammalian bloodstream to the midgut of the fly. This rapid change in environment induces bloodstream form *T. brucei* to differentiate into the procyclic form. During this transition, the parasite sheds its dense, protective variant surface glycoprotein (VSG) coat and acquires a new coat of proteins called procyclin that are unique to the procyclic form (Acosta-Serrano *et al*. 2001). The parasite then migrates from the midgut of the fly to the salivary glands, while undergoing differentiation into epimastigotes. The VSG coat is regained in the non-proliferative metacyclic stage to prepare the parasite for invasion of the mammalian host (Matthews 2005).

*T. brucei* undergoes numerous morphological changes throughout its life cycle, and one of the most important is the changing of the surface coats between the procyclic and bloodstream forms. Although the role of procyclin remains elusive, the VSG coat of bloodstream form *T. brucei* has been the subject of intense interest due to its role in immune evasion. The role of VSG will be discussed in detail in the following sections.

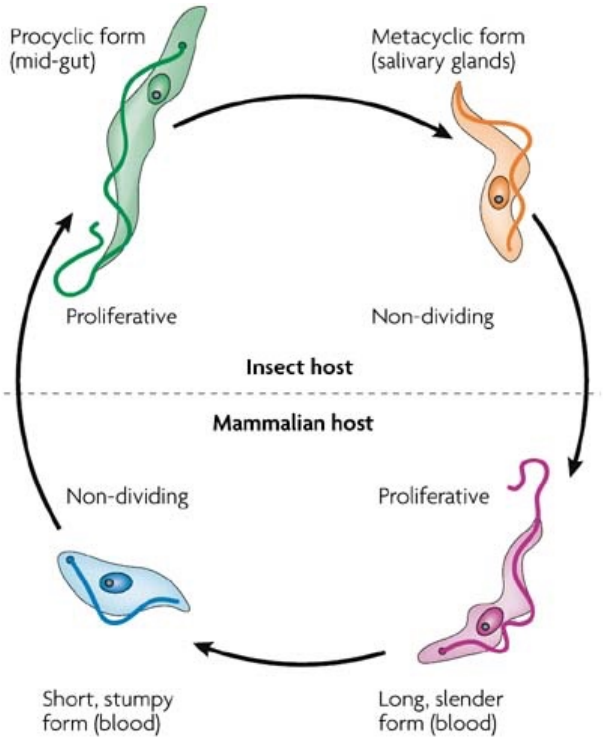



**Figure 1.2 The life cycle of *Trypanosoma brucei*.** The parasite cycles between the mammalian host and the insect vector, the Tsetse fly, throughout its life cycle. In the mammalian bloodstream, the parasite assumes a slender morphology and is covered in a dense coat of Variant Surface Glycoprotein (VSG) molecules. When a certain parasite density is reached, the bloodstream form *T. brucei* differentiates into the non-proliferative stumpy form in preparation for the uptake by the Tsetse fly. Once inside the insect vector, *T. brucei* exchanges its VSG coat for procyclin, the surface coat of the insect (procyclic) form of the parasite. The parasite then eventually migrates to the salivary glands of the fly and differentiates into the metacyclic form, which will re-enter the mammalian host via a Tsetse fly bite. Image is adapted from (Lee *et al*. 2007).

### 1.4 Cell cycle progression of bloodstream form *T. brucei*

*T. brucei* divides by binary fission in the bloodstream, and must carefully coordinate events during the cell cycle to ensure faithful replication and segregation of all cellular components. BF *T. brucei* follows the typical eukaryotic cell cycle, where cells undergo DNA replication in the S-phase and mitosis in the M-phase. These two stages are spaced in between by the G1 and G2 gap phases (Li 2012; Hammarton 2007). In addition to the nucleus,

trypanosomes must also replicate the mitochondrial DNA, which is organised into a disc-like structure called the kinetoplast, which has a distinct DNA synthesis cycle compared to the nuclear DNA. One cell cycle takes approximately 8.5 hours to complete (McKean 2003). Mitochondrial replication precedes that of nuclear replication, resulting in a cell with one nucleus and two kinetoplasts (1N2K) (Figure 1.3). Following S phase, the kinetoplasts and the Golgi begin to segregate. In trypanosomes, mitosis is a closed process, during which the nuclear envelope is not disrupted and the cell is now defined by two nuclei and two kinetoplasts (2N2K). Finally, the cell completes cytokinesis, where a cleavage furrow forms along the longitudinal axis of the cell from the anterior end, passing through the segregated kinetoplasts and nuclei towards the posterior end, producing two daughter cells with 1N1K.

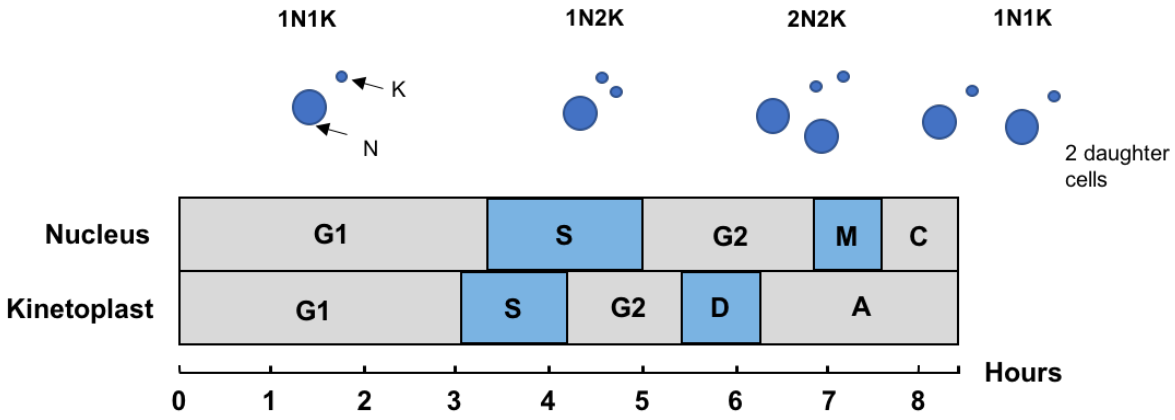



**Figure 1.3 Cell cycle progression in bloodstream form *T. brucei*.** Each cell cycle lasts approximately 8.5 hours. Each BF *T. brucei* cell contains one nucleus (N) and one kinetoplast (K), which contains mitochondrial DNA. Kinetoplast replication takes place before the synthesis of nuclear DNA (S), resulting in a 1N2K cell. Therefore, the segregation of the kinetoplasts (D) occurs before the onset of mitosis (M) of the nuclear DNA. After the kinetoplasts have separated, they continue to move apart (A) while the nuclear DNA completes mitosis, which results in 2N2K cells. Finally, cell division (C), occurs and give rise to two 1N1K daughter cells. Image is adapted from (McKean 2003).

### 1.5 Variant Surface Glycoprotein

Unlike most parasites, *T. brucei* proliferates extracellularly in the bloodstream of the mammalian host, which means the parasite is exposed to the constant attack of the host immune cells. As a result, BF *T. brucei* has evolved a dense surface coat known as the Variant Surface Glycoprotein (VSG) that envelops the entire trypanosome, protecting the parasite from complement or antibody-mediated lysis by shielding invariant components on the cell membrane. The surface coat is made up of approximately $10^7$ glycoprotein molecules, densely arranged in homodimers. Each VSG monomer is approximate 45-60 kDa, depending on the VSG variant and is attached to the membrane via a GPI-anchor at the C-terminus (Cross 1975; Ferguson 1999). The N-terminus of the VSG is on the external face of the membrane and contains 350–400 residues. These residues are arranged in a 10 nm coiled coil structure that is oriented perpendicular to the plane of the cell membrane. The conserved C-terminus of VSG molecules has been shown to be inaccessible to anti-VSG antibodies. This suggests that the dense packing of VSGs can effectively shield conserved moieties from host immune attacks (Schwede *et al*. 2011). Although the sequences between different VSG variants can vary, the overall structure of the VSG monomers remain conserved to ensure tight packing of the homodimers and dense coverage of the cell (Jones *et al*. 2008).

Although the trypanosome surface is dominated by VSG molecules, they are by no means the only cell surface molecules in bloodstream form *T. brucei*. The VSG coat is interspersed with a number of other transmembrane proteins. An estimation of around 2500 copies of transferrin receptors have been detected on the cell surface of the flagellar pocket, and are essential for the uptake of host transferrin, the source of iron for parasite growth (Steverding 2000; Field & Carrington 2009). Adenylate cyclases were also shown to be expressed on the *T. brucei* surface and contribute to innate immune evasion (Salmon *et al*.

2012). Amongst the dense coat of VSG molecules, there are also Invariant Surface Glycoproteins (ISG). ISGs have similar structures and transmembrane domains as VSGs, but exist at much lower copy numbers, around 0.5% of the total number of VSG molecules. Two ISGs with molecular weights of 65 and 75 kDa are similar in structure to VSGs, containing transmembrane domains and small intracellular domains (Chung *et al*. 2004; Ziegelbauer & Overath 1993; Lila Koumandou *et al*. 2013). Although the ligands and functions of ISGs have not been identified, there is evidence that they may be involved in drug interactions and immune evasion (Alsford *et al*. 2012).

The VSG coat is essential to the survival of bloodstream form *T. brucei*, as blocking the synthesis of VSG results in a rapid growth inhibition and a precise cell cycle arrest (Sheader *et al*. 2005). These cells are stalled after the completion of mitosis, but before the onset of cytokinesis. Interestingly, the phenotype of the stalled cells show a striking contrast to other types of cell cycle arrest. The arrested cells show a 4N DNA content; with two kinetoplasts (K; mitochondrial DNA) and two nuclei (N), which differ from the naturally occurring 2N2K population. The cells have a rounder shape, with parallel arrangement of the kinetoplasts, nuclei and flagella. This particular precytokinesis arrest shows a 2N2K phenotype with no re-initiation of S phase. In other studies, knockdowns of cytokinesis components typically lead to the generation of multinucleated cells due to repeated rounds of re-initiation of S phase and mitosis. Concurrently, a global translation arrest is triggered in these arrested cells, presumably as a protective mechanism to prevent dilution of the protective VSG surface coat (Terry K Smith *et al*. 2009). *In vivo*, the ablation of VSG transcript leads to a rapid clearance of the parasite within 12 hours (Sheader *et al*. 2005).

### 1.6 Antigenic variation

The VSG coat protects the trypanosome from the host immune system via several mechanisms. Antigenic variation in BF *T. brucei* involves switching the existing VSG coat to a different variant with different amino acid sequences, while retaining a conserved VSG structure. The sequencing of the *T. brucei* genome revealed that each trypanosome has a repertoire of up to 2000 VSG genes and pseudogenes (Berriman *et al*. 2005). Most of these VSG genes are located in arrays at the subtelomeres of chromosomes. However, VSG genes are also located at the telomeres of the approximately 100 *T. brucei* minichromosomes (50-100 kb) (Williams *et al*. 1982; Alsford *et al*. 2001). Only one VSG is expressed at a time from one of about 15 telomeric VSG expression sites (Taylor & Rudenko 2006).

As a population of trypanosomes multiplies in the bloodstream, the host eventually mounts an antibody response against the actively expressed VSG variant (Magez *et al*. 2008). In order to prevent eradication of the total population, a *T. brucei* can switch to another VSG variant via mechanisms such as gene rearrangement or activation of silent VSG expression sites (Figure 1.4) (Taylor & Rudenko 2006). This new VSG variant is not recognised by host anti-VSG antibodies and can escape lysis by the immune system. This results in characteristic waves of parasitaemia which coincide with episodes of fever in the infected host. VSG switching therefore ensures–continuous evasion from the host immune system and helps maintain a chronic infection (Donelson *et al*. 1998).

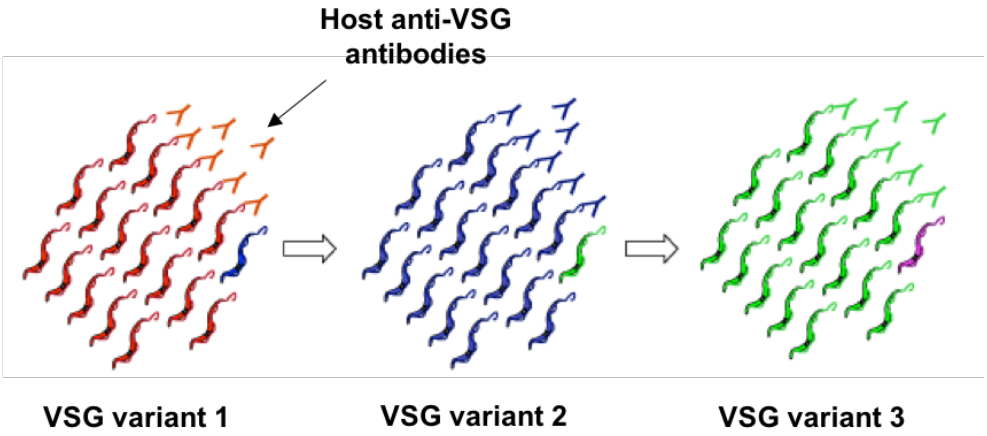



**Figure 1.4 Antigenic variation during a *T. brucei* infection.** A population expressing VSG variant 1 multiplies in the host bloodstream until the host mounts an antibody mediated response to clear the pathogen. A *T. brucei* can switch to express a different VSG variant (VSG variant 2 and 3) these can form a new wave of infection and escape eradication by the host. Continuous VSG switching ensures the survival of the parasite population and helps maintain a chronic infection.

VSG switching can occur predominantly via three different mechanisms: *in situ* (transcriptional) switch, telomere exchange and gene conversion (Taylor & Rudenko 2006; Horn & McCulloch 2010) (Figure 1.5). After an *in situ* switch, a different VSG variant is expressed simply through activation of another VSG expression site. Alternatively, genes encoding other VSG variants can be transferred into the active expression site via gene recombination. As there are simple sequence repeats upstream of each VSG , called 70 bp-repeats, DNA cross-over events can occur here, resulting in a silent VSG gene inserted into the active VSG expression site through telomere exchange (Marcello & Barry 2007; Pays *et al*. 1985). Finally, gene conversion can result in the duplication of a silent VSG gene directly into the active expression site. In more complex gene conversions, chimeric VSGs can be generated by combining different segments of VSG pseudogenes, and therefore infinitely increasing the possibility of VSG variation (Robinson *et al*. 1999). This sophisticated mechanism of antigenic

variation allows *T. brucei* to evade the antibody-mediated host response effectively throughout the course of infection and makes the development of vaccines impossible.

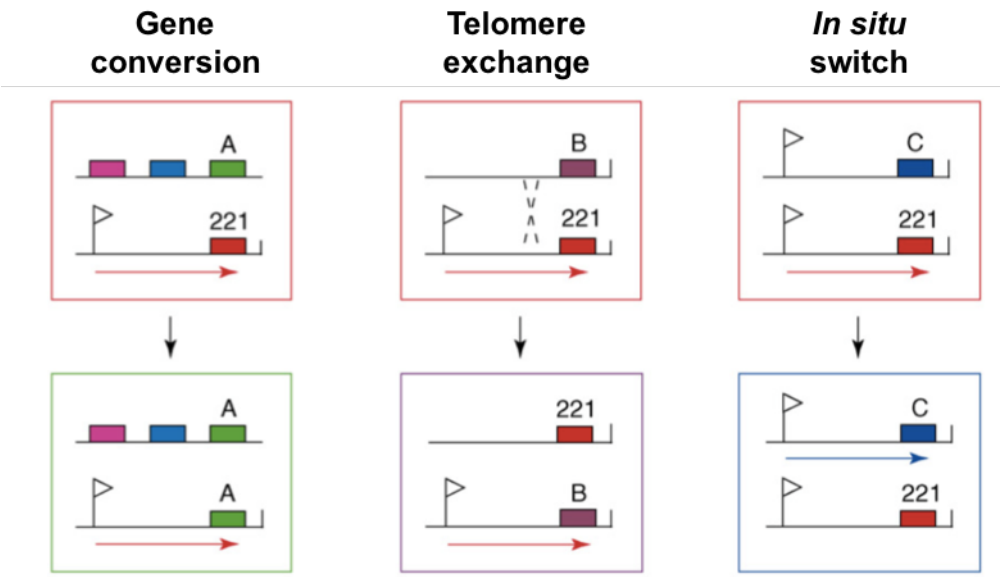



**Figure 1.5 Mechanisms of VSG switching.** VSG switching occurs predominantly via three different mechanisms. Switching via gene conversion involves the duplication of a silent VSG gene (A) into an active VSG expression site. During a telomer exchange, homologous recombination switches a telomeric VSG (B) into the active VSG expression site. Lastly, a silent expression site (C) can be activated spontaneously via an *in situ* switch.
The large boxes indicate trypanosomes, with the colour indicating the VSG that is expressed. Small colour-filled boxes represent the different VSG genes, which are invariably at telomeres or subtelomeres. Each VSG expression site has a promoter (white flag) and transcription of the active expression site is indicated with a red arrow.

### 1.7 Endocytosis and vesicular transport

As the VSG is attached to the trypanosome surface via a GPI-anchor, VSG molecules can move freely over the trypanosome cell surface (Ferguson *et al*. 1988; Jones *et al*. 2008). The highly fluid nature of the VSG coat also supports a unique feature of bloodstream form, and that is the extremely high rates of VSG recycling. Endocytosis in bloodstream form *T. brucei* plays a role in a wide range of cellular activities, such as nutrient uptake, maintenance

of cell surface homeostasis and most importantly, the removal of host opsonins (Allen *et al*. 2003; Grünfelder *et al*. 2003).

All vesicular trafficking in bloodstream form *T. brucei* is restricted to the flagellar pocket (FP), a specialised invagination at the base of the flagellum at the posterior end of the cell body. Remarkably, the FP only makes up 1% of the total trypanosome surface area, but must accommodate the extremely high volume of traffic that passes through continuously (Field & Carrington 2009). In fact, BF *T. brucei* has one of the highest rates of endocytosis amongst eukaryotes, where the entire surface of the cell, including the entire VSG pool is estimated to be endocytosed every 12 minutes (Engstler *et al*. 2004). To achieve this rate of endo- and exocytosis, the entire endosomal structure is organised in a highly polarised manner in *T. brucei*. With the exception of the endoplasmic reticulum, all endocytic and secretory organelles are arranged at the posterior of the cell. This creates a compact system, which facilitates the speed at which endo- and exocytosis occurs (Field & Carrington 2009).

Endocytosis in BF *T. brucei* is strictly clathrin-mediated, as RNAi-mediated knockdown of the heavy chain of clathrin results in a block in endocytosis and the enlargement of the flagellar pocket due to continuous exocytosis (Allen *et al*. 2003). The trypanosome vesicular transport system is defined by the localisation of a family of Rab-GTPases (Pal *et al*. 2002). Molecules enter the trypanosome in clathrin-coated pits that bud off from the cellular membrane forming early endosomes. In bloodstream form *T. brucei* there appears to be further differentiation of the early endosomes into populations of vesicles that co-localise with either Rab5A or Rab5B small GTPases. Compartments marked by Rab5A were shown to co-localise with VSG, VSG-antibody complexes and transferrin, whereas Rab5B positive endosomes are responsible for more general endocytosis and the processing of poly-*N*-acetyllactosamine-containing glycoproteins (Pal *et al*. 2002; Pal *et al*. 2003; Grünfelder *et al*. 2003). Cargo in the

early endosomes can next be delivered to the recycling endosomes marked by Rab11 or the Rab7 positive late endosomes. From the recycling endosomes, VSG and transferrin receptors can be recycled back onto the cell surface. Cargo destined for degradation, such as host antibodies and complement proteins, are transported to the late endosomes, which are located in close proximity to the lysosome and mediate the delivery of cargo to the lysosome (Engstler *et al*. 2004; Silverman *et al*. 2011).

High rates of endocytosis are therefore an additional immune evasion mechanism that protects *T. brucei* from antibody mediated lysis. This mechanism is only effective when the anti-VSG antibody titres rise above a certain threshold which results in the trypanosome being overwhelmed and eliminated from the population.

### 1.8 Movement of VSG on the trypanosome cell surface

The parasite surface is densely packed with $10^7$ VSG molecules, but individual homodimers can freely diffuse within the plane of the plasma membrane by random Brownian motion, which occurs naturally at a diffusion coefficient of $1 \times 10^{-10}$ $cm^2/s$ (Bülow *et al*. 1988). However, this diffusion rate is too low to explain the rapid removal of antibody complexes from the cell surface, which were shown by Engstler *et al* to be internalised within 45 seconds (Engstler *et al*. 2007). This implies that an external force must be operating on the cell surface to actively "sweep" antibody complexes into the posterior flagellar pocket.

It was hypothesised that this external force is provided by the directional swimming of the parasite, which generates a hydrodynamic drag force that pushes antibody-VSG complexes into the flagellar pocket (Figure 1.6). Furthermore, the size of the antibody determines the rate at which it is sorted to the flagellar pocket, as the antibody effectively acts as a "molecular sail" in the face of these hydrodynamic forces. Interestingly, this sorting mechanism appears to be

independent of endocytosis since the RNAi-mediated knockdown of clathrin did not affect cell surface sorting (Engstler *et al*. 2007). Instead, this process was shown to be dependent on cellular motility.

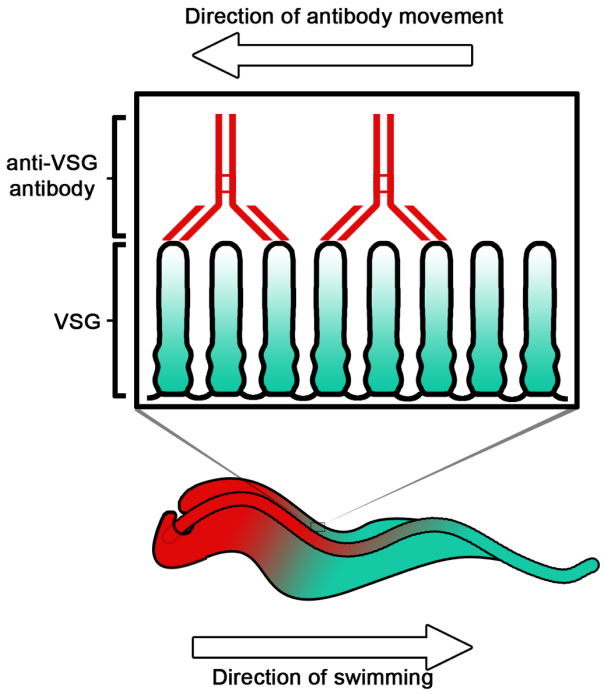



**Figure 1.6 Hydrodynamic drag forces generated by forward swimming preferentially sort antibody-VSG complexes into the flagellar pocket.** Anti-VSG antibodies (red) attached to VSG molecules (green) are sorted on the cell surface towards the posterior flagellar pocket with a rate dependent on their size. Larger, multivalent antibodies are sorted at a higher rate compared with monovalent antibodies. Sorting appears to be dependent on parasite motility rather than endocytosis.

### 1.9 Trypanosome motility

Motility is essential in bloodstream form *T. brucei* and facilitates multiple aspects of the parasite life cycle including morphogenesis, transmission from vector to host, migration and cytokinesis (Ralston *et al*. 2006; Kisalu *et al*. 2014). RNAi-mediated knockdown of

flagellar proteins is lethal, as cytokinesis cannot proceed, producing abnormal parasites which have undergone multiple rounds of replication but are unable to divide (Ralston *et al*. 2006; Broadhead *et al*. 2006).

*T. brucei* has a single external flagellum which extends from the flagellar pocket at the posterior end of the cell, along the cell body towards the anterior end. The trypanosome flagellum is made up of an axoneme, which contains 9 doublet microtubules arranged around a single pair of microtubules (Ralston *et al*. 2009). This structure is anchored at the base of the flagellar pocket via a barrel-like structure called the basal body. The flagellum exits the flagellar pocket at the flagellar pocket collar and is surrounded by its own membrane. Unlike many other flagellated eukaryotes, the trypanosome flagellum is attached to the cell body along the anterior- posterior axis and is only free of the cell body at the distal tip (Rotureau *et al*. 2014).

Until recently, the classical view of trypanosome movement was based on the observation that the flagellum beat is initiated at the tip and moves towards the base of the flagellum. This propels the cell in the opposite direction to the flagellar beat propagation. As a result, the anterior end of trypanosome leads. When the beat propagation reverses, as it does occasionally, the direction of swimming changes, resulting in a tumbling movement. Using high-speed video microscopy, two models have been put forward to investigate trypanosome motility. The “plane rotational” model proposes that the helical movements of trypanosomes are brought about due to the constraints that are imposed by an attached flagellum, and that the flagellum beat is planar (Uppaluri *et al*. 2011; Heddergott *et al*. 2012). In the “bihelical” model, rotational force is generated by alternating beating patterns, a mode of motility that has also been observed in *Plasmodium berghei* (Wilson *et al*. 2013; Rodríguez *et al*. 2009). Neither

model has been proven to be the true mode of trypanosome motility and other modes of flagellum wave propagation could also exist.

It is important to note that the modes of trypanosome swimming change depending on the environment. In culture medium, trypanosomes preferentially tumble, interspersed with periods of forward swimming. In blood, the viscosity is much higher, and trypanosomes swim more directionally (Heddergott *et al*. 2012). Parasite motility in the mammalian host plays an important role in infectivity and is closely associated with disease progression. Migration of the trypanosome, facilitated by motility across the blood brain barrier occurs during the transition of the acute phase of trypanosomiasis into the late meningoencephalitic stage. In the bloodstream, motility was proposed by the Engstler group to facilitate the removal of host opsonins (Engstler *et al*. 2007). Since trypanosomes swim more directionally in the bloodstream, host antibodies and complement proteins would be preferentially pushed by the hydrodynamic forces towards the flagellar pocket for internalisation resulting in their removal. This process would be particularly effective in the early stages of infection when titres of host opsonins are low, allowing the parasite to multiply unrestricted in the mammalian bloodstream.

### 1.10 Strategies of innate immune evasion

Being an extracellular parasite means that *T. brucei* must actively evade detection by host immune cells, particularly macrophages, which form the first line of host defence before activation of the adaptive immune system. Macrophages express a variety of pathogen recognition receptors (PRR) on their cell surface, which allow them to recognise specific pathogen-associated molecular patterns (PAMP) presented by the foreign pathogen. Amongst the different types of PRRs, Toll-like receptors (TLRs) have been the most extensively studied. TLRs a large family of pathogens sensors, some are expressed on the cell surface and some are

located intracellularly (Akira & Takeda 2004). Upon TLR activation, a series of intracellular signalling cascades are initiated, and depending on the TLR activated, different effector functions will be elicited. With the exception of TLR-3, all other TLRs activate the transcription factor NFκB via the adaptor protein, MyD88 (myeloid differentiation primary-response protein 88) for the production of inflammatory cytokines. Drennan *et al* showed in a MyD88 knockout mouse model, that the type I proinflammatory response is MyD88-dependent. In addition, mouse macrophages were activated in a TLR-9 dependent manner (Drennan *et al*. 2005; Drennan *et al*. 2012). However, there is currently limited information on the other types of TLRs that may be involved in a trypanosome infection.

Apart from TLRs, macrophages can bind pathogens through opsonic receptors. These include different types of Fc receptors that bind the Fc regions of antibodies coating the invading pathogen (Plüddemann *et al*. 2011; Nimmerjahn & Ravetch 2006). Alternatively, macrophages can bind pathogens through complement proteins deposited on the pathogen surface. In the absence of an antibody response, which usually takes approximately one week to develop, complement proteins are crucial for opsonising the parasite to facilitate uptake by macrophages. Complement proteins are a family of plasma proteins that are important for pathogen opsonisation and lysis. Three complement pathways can be activated. The lectin pathway is activated by soluble carbohydrate binding proteins called lectins, which bind to carbohydrate moieties on the pathogen surface. In the classical pathway, complement protein C1q binds the Fc region of antibodies coating microorganisms, which can then be recognised by macrophage receptors such as CR1. Finally, the alternative complement pathway is initiated by the spontaneous activation and hydrolysis of the complement C3. All three pathways converge at the point of C3 convertase, an enzyme which cleaves C3. The products of C3 cleavage leaves its product C3b and its degradation products deposited directly on the surface

of the pathogen (Dunkelberger & Song 2010). Macrophage receptors including CR1, CR3 and CR4 can then bind the opsonised pathogen and facilitates recognition and phagocytosis (Bohlson *et al*. 2014). However, there is evidence that *T. brucei* and *T. congolense* are able to inhibit this pathway, as the VSG coat protects the parasite from complement mediated lysis (Ferrante & Allison 1983). Although both C3b and Factor B were detected on the trypanosome surface, activation did not proceed beyond the point of C3 convertase for unknown reasons (Devine *et al*. 1986). This suggests that complement proteins alone are not effective against *T. brucei*.

Upon infection of *T. brucei*, the host is known to mount an early type I proinflammatory response to control parasitaemia. Several parasite derived molecules, such as VSG, and the GPI-anchor moiety of the VSG have been shown to be immunogenic. Host macrophages have been shown to become classically activated, producing pro-inflammatory cytokines such as IL-1, IL-6, IFN- γ, TNF-α and nitric oxide (NO) that are important for parasitaemia control (Baetselier *et al*. 2001; MacLean *et al*. 2001). Although a strong type I response is beneficial to the host, excessive inflammation is associated with pathology, including anaemia and liver damage (Stijlemans *et al*. 2010; Shi *et al*. 2003). Therefore, a successful trypanosome infection requires the parasite to reduce inflammation and create a trypanosome-tolerant environment. In trypanotolerant animals, the switch from a M1 to a M2 phenotype coincides with an increase in IL-10 production. The induction of alternatively activated macrophages is marked by the release of type II cytokines such as L-4, IL-10, IL-13, TGF-ß (Guilliams *et al*. 2009; Namangala *et al*. 2001). This anti-inflammatory state is then sustained by additional mechanisms, which will be discussed further in the upcoming chapters.

Although the trypanosome surface is packed in a dense layer of VSG, other surface receptors and a small proportion of invariant surface glycoproteins (ISG) are found embedded

within the plasma membrane (Ziegelbauer & Overath 1993). Unlike the VSG associated parasite products, which are highly immunogenic, these receptors are able to dampen the inflammatory response. Interestingly, bloodstream form *T. brucei* was found to express over 80 transmembrane receptor-like adenylate cyclases (AC) on its surface. Although no particular functions were found to be associated with these receptors, they were shown to be activated upon cellular stress (Rolin *et al*. 1996). Downregulation of their expression also led to significant inhibition of TNF-α synthesis, suggesting that ACs have role in immunomodulation (Salmon *et al*. 2012; Stijlemans *et al*. 2016).

### 1.11 Immunomodulation of antigen presenting cells

Aside from their primary task as phagocytes, macrophages also function as antigen presentation cells (APCs). Together with the professional antigen presentation cells, dendritic cells (DCs), they serve as a vital link between the innate and adaptive immune systems. When an immature DC encounters a pathogen, it recognises the pathogen associated molecular patterns (PAMPs) through pattern recognition receptors (PRR) expressed on the cell surface. Uptake of the pathogen via phagocytosis and processing of the antigen results in the maturation of the cell. Processed antigens are then presented on the APC surface by major histocompatibility complex molecules (MHC). Concurrently, several cell surface receptors such as CD80, CD86 and CD40 that act as co-receptors for T-cell activation are upregulated.

Like many parasites, *T. brucei* also targets antigen presenting cells to reduce anti-trypanosomal response from the adaptive immune system and contribute to global immunosuppression. There is evidence that trypanosome infections result in the direct depletion of splenic DCs in mice (Taylor R Dagenais *et al*. 2009). Namangala *et al* showed a significant reduction in MHCII expression in mouse macrophages when infected by *T. brucei*,

which resulted in impaired antigen presentation and contributed to T-cell hyporesponsiveness (B. Namangala *et al*. 2000). Several studies have also reported alteration of the DC membrane, interfering with their antigen presentation ability. Without effective antigen presentation, T-cell responses are impaired and downstream effector functions can become severely impacted.

### 1.12 T-cell defects induced by *T. brucei* infection

T-cells are another immune cell population that are targeted by trypanosomes as they are key to activating the rest of the adaptive immune system. When a naïve CD4+ or CD8+ T-cell encounters an APC, its T-cell receptor and the CD4 or CD8 co-receptor interacts with the processed antigen in complex with a MHC molecule on the APC. The co-stimulatory molecule, CD28 expressed on the surface of the T-cell would also interact with the B7 molecule on the APC to deliver a second signal for T-cell activation. In the case of CD4 helper T-cells, cytokines produced by the APC and in the microenvironment will also influence the differentiation of T-cells into different effector T-cells with various functions (Figure 1.7) (Smith-Garvin & Koretzky 2009; Guermonprez *et al*. 2002; Hugues 2010).

A large number of studies have shown a predominant type 1 T helper (Th1) response which shifts to a Th2 response during later stages of infection, correlating with the onset of the chronic stage. Host resistance is correlated with an early polarised Th1 response as the production of IFN-γ by Th1 cells and M1 macrophages is the key to parasite control.

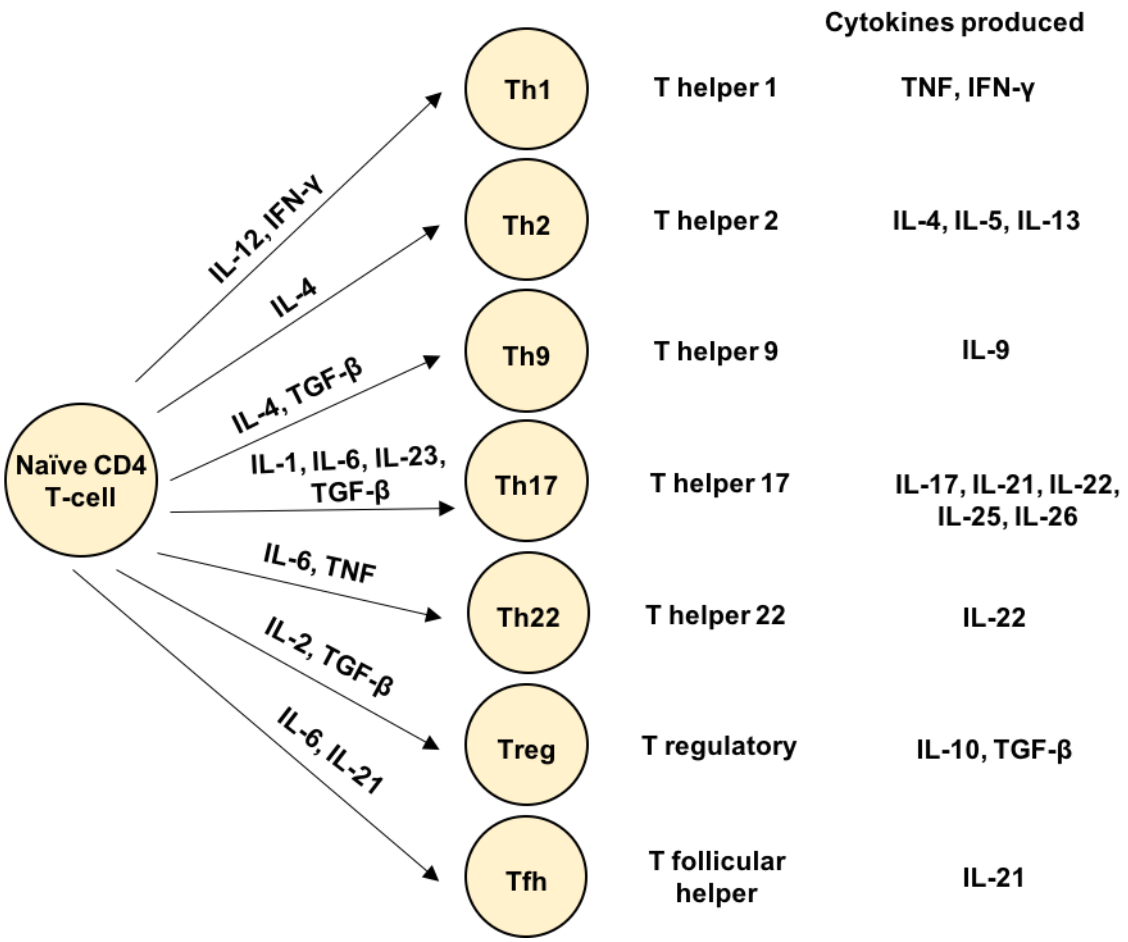



**Figure 1.7 Different subsets of CD4+ T helper cells.** Cytokines secreted by the antigen presenting cell (APC) and in the microenvironment produced by other immune cells can generate different T helper cell subtypes. Schematic illustrations show the different cytokines involved in generating each subset and the cytokines produced by these T helper cell subsets.

However, antigenic variation allows *T. brucei* to escape B-cell and T-cell responses. Alignment of the different VSG sequences revealed a huge diversity between the primary amino acid sequences at the external N-termini (Reinitz *et al*. 1992; Carrington *et al*. 1991). VSG secondary and tertiary structures on the other hand, are conserved, which give VSG molecules the distinct structure that permits dense packing throughout the parasite surface. T-cell responses against *T. brucei* were first characterised using *T. b. rhodesiense* infected mice (Schleifer *et al*. 1993). This study revealed that VSG-specific responses are mediated by CD4+ T helper cells, which are restricted by MHCII. *T. brucei* alone did not appear to be able to

stimulate a direct T helper cell response and processing of VSGs must occur by antigen presenting cells to activate T-cells (Taylor R Dagenais *et al*. 2009). This selectivity of T-cell activation suggests that APCs may be responsible for selection against certain regions of the VSG molecules for presentation to T-cells. As certain VSG epitopes are preferentially presented, one might predict a level of cross-reactivity across different VSG variants but surprisingly, there was not the case. There appears to be another layer of natural selection where antigenically diverse sequences are preferentially presented to T-cells (Taylor R. Dagenais *et al*. 2009; Schopf *et al*. 1998). This possibly explains the biological significance of mosaic gene conversion of VSG genes during VSG switching, which may contribute to T-cell evasion during an infection.

In addition to direct interactions, T helper cells respond to *T. brucei* by secreting a range of cytokines and chemokines which change throughout the infection. Secretion of IFN-γ and TNF-α elicits a polarised Th1 response that is vital for the control of the first wave of parasitaemia, which is often the most aggressive. To limit the tissue damage caused by excessive activation of inflammation, regulatory cytokines are upregulated in late stage trypanosomiasis. IL-10 and IL-6 have both been detected in the cerebrospinal fluid (CSF) in late stage *T. b. rhodesiense* infections (Kato *et al*. 2015). This allows trypanosomes to manipulate host responses and establish a chronic state of infection, effectively avoiding clearance by the host.

### 1.13 Current Human African Trypanosomiasis treatments

Currently only four drugs are registered for the treatment of HAT: melarsoprol, pentamidine, suramin and eflornithine. A fifth drug, nifurtimox is used in combination with eflornithine under authorisation (WHO 2017; Babokhov *et al*. 2013). With the exception of

eflornithine, all were chemotherapy drugs that were discovered in the late 19th and early 20th century.

Suramin and pentamidine were the first two drugs to be discovered after the first large scale epidemic in the 20th century. Suramin is effective against early *T. b. rhodesiense* infections, whereas pentamidine targets early stage *T. b. gambiense* infections. This was followed by the manufacture of the arsenical compound, melarsoprol in the 1940s for the treatment of late stage infections and remains the only treatment for late stage *T. b. rhodesiense* infections (Steverding 2010a; Kennedy 2013). Unfortunately, all four drugs contain a level of toxicity with undesirable side-effects, including seizures, vomiting, paralysis and in some extreme cases, death.

Drug discovery for the treatment of HAT began to slow down in the 1970s as funding and support declined, which led to a resurgence in the number of reported HAT cases (WHO 2017). No treatment alternatives were available until the late 1980s, when eflornithine (alpha-Difluoromethylornithine; DFMO) was discovered. DFMO is an irreversible suicide inhibitor of ornithine decarboxylase (ODC), the first enzyme involved in polyamine biosynthesis, an essential process for cell proliferation and cytokinesis (Van Bogaert & Haemers 1989). DFMO was originally manufactured as an anti-cancer drug in the 70s but was shown to be effective against both early and late stage *T. b. gambiense* infections. However, owing to the short half-life of eflornithine, which lasts only 2-4 hours in adults, treatment with DFMO requires constant dosing (Babokhov *et al*. 2013). This adds to the complication of drug administration, especially in developing countries and areas of remote access. To this day, DFMO remains the only option for late stage *T. b. gambiense* infections.

Although proven to be a safer option compared to melarsoprol, DFMO is not without adverse side-effects, which include fever, hypertension, and gastrointestinal problems (Priotto

*et al*. 2008; Chappuis *et al*. 2005). As a result, nifurtimox, a registered drug for Chagas disease that has shown limited effectiveness against late stage HAT has been used in combination with DFMO. This combination therapy was revealed to improve both the efficacy and safety of DFMO in late stage *T. b. gambiense* treatment (Priotto *et al*. 2007; Checchi *et al*. 2007). Nevertheless, the eflornithine-nifurtimox combination theory must be administered by a skilled professional, which restricts its use in regions with limited medical resources.

In recent years, cases of drug resistance against DFMO have emerged, with *T. brucei* selectively losing the transporter responsible for drug uptake (Delespaux & de Koning 2007; Baker *et al*. 2013). *In vitro* studies have revealed the relative ease with which *T. brucei* develops resistance towards DFMO (Vincent *et al*. 2010). To combat this problem, research efforts have focused on finding alternative treatments in recent years. It is imperative to find treatments that can target both subspecies of trypanosome and ideally are effective against both early and late stages of the disease. To effectively treat late stage infections, the drug must be able to cross the blood brain barrier with minimal side-effects. A focus on developing new treatments possibilities might hopefully allow us to eradicate this neglected tropical disease.

### 1.14 Objectives

My objective of this study is to identify the possible immune evasion mechanisms of African trypanosome, *Trypanosoma brucei* and hopefully discover new therapeutic approaches to eradicate this parasite. My approaches can be summarised into the following steps:

1. Investigate the role of the Variant Surface Glycoprotein in trypanosome evasion from host macrophages

2. Dissect the molecular mechanisms of innate immune evasion using RNAi-mediated knockdown of VSG.

3. Study the interaction between *T. brucei* and human dendritic cells and investigate the immunomodulatory mechanisms utilised by the parasite both to avoid detection and to minimise the host adaptive immune response.

4. Investigate the downstream effects within host adaptive immunity during presentation of *T. brucei* antigens to T-cells.

5. Investigate the potential therapeutic use of a novel anti-cancer drug, BCT-100 in treating Human African Trypanosomiasis as an alternative treatment to current therapeutic options.

# Chapter 2

# Materials and Methods

## Materials

### 2.1 Trypanosoma brucei strains

The bloodstream form (BF) *T. brucei* strains used in this study are outlined in Table 2.1. Bloodstream form *Trypanosoma brucei brucei* 427 was cultured in HMI-9 medium supplemented with 15% heat-inactivated foetal calf serum (FCS) (Hirumi & Hirumi 1989). The schematic illustrations of each cell line are shown in Figure 2.1.

The BF *T. brucei* 221VG1.1 cell line used in the phagocytosis assays is described in (Sheader *et al*. 2005). This cell line is a derivative of *T. brucei* 90-13 (Wirtz *et al*. 1999) and expresses VSG221. A 221GP1 construct containing eGFP and puromycin resistance genes were inserted behind the promoter of the active *VSG221* expression site (Sheader *et al*. 2004). The maintenance of a homogenous cell population that expresses VSG221 is by the selection on puromycin resistance. A construct allowing tetracycline inducible expression of *VSG221* RNAi from two opposing T7 promoters is inserted in a mini-chromosome (Wickstead *et al*. 2002).

The similar BF *T. brucei* 221VB1.2 cell line is also described in (Sheader *et al*. 2005), has a construct containing a blasticidin resistance gene, which was inserted immediately behind the active *VSG221* expression site promoter, and homogeneous expression for VSG221 was ensured by blasticidin resistance. The *T. brucei* 221VB1.2 cell line was used for the surface VSG-antibody clearance assays, endocytosis assays and motility measurements. *VSG221* RNAi was induced in both cell lines for 8 hours using 1 µg/ ml tetracycline. Control experiments were performed with the VSG221 expressing BF *T. brucei* 90-13TDPC1 cell line.

This cell line is derived from BF *T. brucei* 90-13 (Wirtz *et al*. 1999), which also expresses VSG221 but has a fragment from the essential *TDP1* gene inserted between two opposing T7 promoters, allowing the tetracycline inducible expression of *TDP1* RNAi (Narayanan & Rudenko 2013).

Two BF *T. brucei* cell lines were used in the purification of soluble VSG (sVSG) experiments: HNI221+ and HNIVO2+. Expression of VSG221 in the HNI221+ cell line is selected by hygromycin resistance, whereas the expression for VSGVO2 in HNIVO2+ is via neomycin (G418) resistance.

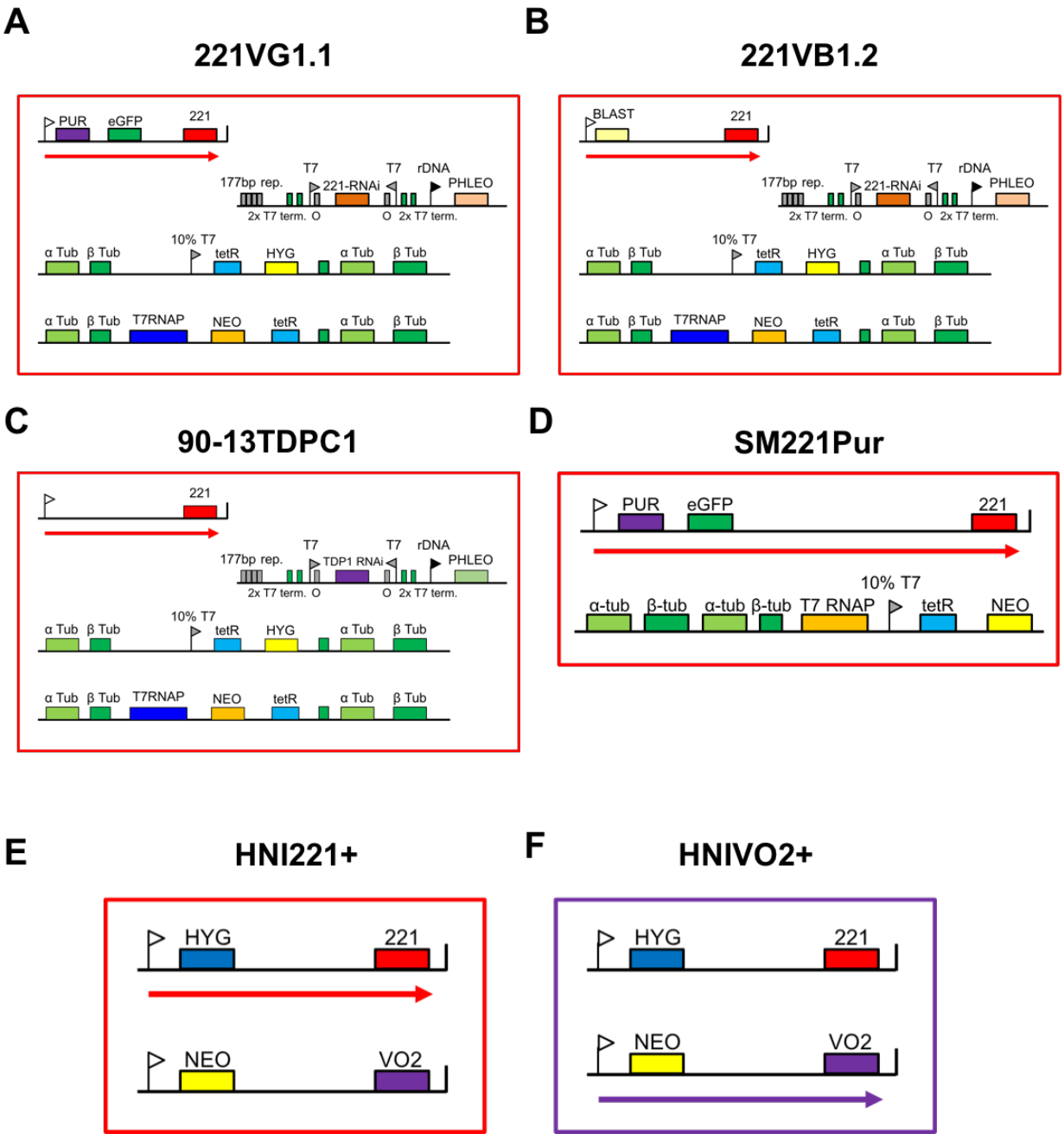



**Figure 2.1 Schematic illustrations of the bloodstream form *T. brucei* cell lines used in this study.** The boxes represent the trypanosome cell membrane and the colour of the boxes corresponds to the VSG variant expressed by each cell line. Cell lines which are capable of tetracycline induced RNAi **(A-C)**, contain an RNAi construct inserted between two opposing T7 promoters to drive the production of double stranded RNA. The expression of the tetracycline repressor (tetR) and T7 RNA polymerase (T7RNAP) are controlled by the hygromycin (HYG) and neomycin (NEO) resistance genes expression. The coloured arrow indicates the active VSG expression site.

| Strain | Active VSG expressed | Drug resistance marker | Selection marker in active ES | References |
|---|---|---|---|---|
| 221VG1.1 | VSG221 | G418<br>Hygromycin<br>Phleomycin<br>Puromycin | Puromycin | (Sheader *et al*. 2004) |
| 221VB1.2 | VSG221 | G418<br>Hygromycin<br>Phleomycin<br>Blasticidin | Blasticidin | (Sheader *et al*. 2005) |
| 90-13TDP1C1 | VSG221 | G418<br>Hygromycin<br>Phleomycin | None | (Narayanan & Rudenko 2013) |
| HNI221+ | VSG221 | G418<br>Hygromycin | Hygromycin | (Rudenko *et al*. 1998a) |
| HNIVO2+ | VSGVO2 | G418<br>Hygromycin | G418 | (Rudenko *et al*. 1998b) |

**Table 2.1**. **Frequently used transgenic bloodstream form *T. brucei*.** Drug resistance markers were used to maintain active VSG expression sites and the tetracycline-inducible RNAi machinery.

| Drug | Source | Concentration used in BF *T. brucei* (µg/ml) |
|---|---|---|
| Neomycin (G418) | Invitrogen, UK | 2 |
| Hygromycin | Roche, UK | 5 |
| Blasticidin | Invitrogen, UK | 5 |
| Puromycin | Sigma, UK | 0.5 |
| Phleomycin | Sigma, UK | 2.5 |

**Table 2.2. Concentrations of drugs used in the maintenance of bloodstream form *T. brucei*.**

## 2.2 Media and buffers

| Medium or buffer | Components |
|---|---|
| HMI-9 medium | HMI-9 was complemented with 15% (v/v) heat-inactivated foetal calf serum (FCS) (Gibco). Appropriate drugs were added to maintain selection on the relevant constructs. |
| 1 x Trypanosome dilution buffer (TDB) | 5 mM KCl; 80 mM NaCl; 1 mM $MgSO_4$; 20 mM $Na_2HPO_4$; 2 mM $NaH_2PO_4$, 20 mM glucose. pH 7.4, filter-sterilised. |
| Stripping buffer | 60% HMI-9 medium; 10% heat-inactivated FCS; 50 mM glutathione. pH 9.0, filter-sterilised. |
| 1 x PSG | 60 mM $Na_2HPO_4$; 3 mM $NaH_2PO_4$; 4.4 mM NaCl; 56 mM glucose. Filtered-sterilised after the addition of glucose. |
| 1X PBS | 1 mM $KH_2PO$; 10 mM $Na_2HPO_4$; 137 mM NaCl; 2.7 mM KCl; pH 7.4; Sterilised by autoclaving. |
| 2% bovine serum albumin (BSA)/ PBS | 2% BSA powder dissolved in autoclaved PBS. Filtered using 0.22 µm filter. |

**Table 2.3**. **Composition of frequently used media and buffers.**

### 2.3 Primary and secondary antibodies

| Primary antibodies | Organism | Source | Dilution for microscopy | Dilution for flow cytometry | Dilution for Western blotting |
|---|---|---|---|---|---|
| Anti-VSG221 | rabbit | A gift from Jay Bangs | 1:1000 | 1:5000 | NA |
| Anti-PFR2 (L8C4) | mouse | A gift from Keith Gull | 1:50 | NA | NA |
| Anti-p67 | mouse | A gift from Jay Bangs | 1:500 | NA | NA |
| Anti-VSG221 | rabbit | Eurogentec | NA | NA | 1:10 000 |
| Anti-VSGVO2 | rabbit | Eurogentec | NA | NA | 1:5000 |
| Anti- HSP70 | rabbit | A gift from Jay Bangs | NA | NA | 1:8000 |
| **Secondary antibodies** | **Organism** | **Source** | **Dilution for microscopy** | **Dilution for flow cytometry** | **Dilution for Western blotting** |
| Anti-rabbit Alexa Fluor 488 | goat | Thermo Fisher Scientific | 1:500 | 1:2000 | NA |
| Anti-mouse Alexa Fluor 594 | goat | Thermo Fisher Scientific | 1:500 | NA | NA |
| Anti-rabbit Alexa Fluor 594 | goat | Thermo Fisher Scientific | 1:500 | NA | NA |
| Streptavidin Alexa Fluor 488 | NA | Thermo Fisher Scientific | 10 µg/ml | 10 µg/ml | NA |
| IRDye 680RD anti-rabbit IgG | donkey | Li-Cor | NA | NA | 1:10 000 |

**Table 2.4 Frequently used primary and secondary antibodies.** Antibody source and dilutions used for each assay are listed. NA indicates the antibody was not used in the assay.

| Antibodies | Source | Conjugation | Host |
|---|---|---|---|
| Anti-HLADR | Biolegend | FITC | Mouse |
| Anti-CD80 | Biolegend | FITC | Mouse |
| Anti-CD86 | Biolegend | PE | Mouse |
| Anti-CD40 | Biolegend | PE | Mouse |
| Anti-CD3 | Biolegend | APC-Cy7<br>Pacific blue | Mouse |
| Anti-CD25 | Biolegend | PE<br>APC | Mouse |
| Anti-CD69 | Biolegend | PerCP-Cy5 | Mouse |

**2.5 Antibodies used for flow cytometry analysis of human immune cells.** The source and fluorescence conjugation are indicated for each antibody. All antibodies were used at a 1:50 dilution.

## Methods

### 2.4 Trypanosome growth and DNA characterisation

Trypanosomes were diluted to a starting density of 1 x $10^5$ cells/ml in 24-well plates. Treatment was added at 0 hours and the number of viable trypanosomes were counted twice daily using a haemocytometer. DNA content of *T. brucei* was stained using Vectashield® mounting medium containing DAPI (1.5 μg/ml) (Vector Laboratories) and visualised by fluorescence microscopy. Cell cycle staging of *T. brucei* was categorised according to the number of the nucleus (N) and kinetoplast (K) in each cell into: 1N1K, 1N2K, 2N2K and others.

### 2.5 Macrophage culture

Murine macrophage cell line RAW264.7 (ATCC® TIB-71™), a kind gift of Prof. Murray Selkirk, Imperial College London (Raschke *et al*. 1978) was cultured in Dulbecco's Modified Eagle's Medium (DMEM) supplemented with 10% FCS, 1% glutamine and 10,000 U/ml penicillin-streptomycin (P/S). Macrophages were plated onto 22 x 22 mm glass coverslips in 6-well plates to adhere for 2 hours at 37ºC. To trigger classical activation, macrophages were primed with 100 ng/ml Lipopolysaccharides *E. coli* (LPS) and 20 ng/ml recombinant mouse interferon gamma (IFN-γ) 24 hours prior to co-culture with trypanosomes (Noda & Amano 1997; Taylor *et al*. 2005).

### 2.6 Trypanosome phagocytosis assay

3 x $10^6$ *T. brucei* 221VG1.1 were opsonised with 10% normal mouse serum (NMS), polyclonal rabbit anti-VSG221 antibodies (gift of Jay Bangs, SUNY Buffalo) or the combination of both NMS and antibodies for 30 minutes at 37ºC. Complement-active NMS

was obtained from CD-1 mice which are wild type for complement C5 (Ooi & Colten 1979)(kind gift of Prof. Paul Morgan, University of Cardiff).

Trypanosomes were then co-cultured with RAW264.7 mouse macrophages for one hour at 37ºC. After one hour, culture medium was removed from each well, and the cells were fixed with 2% paraformaldehyde (PFA) for 20 minutes at room temperature. Cells were subsequently washed with PBS buffer, and permeabilised with methanol at -20ºC for 30 seconds. This was followed by the staining of *T. brucei* flagella with a mouse monoclonal anti-PFR2 antibody (L8C4) (gift of Prof. Keith Gull, University of Oxford) (Kohl *et al*. 1999), and an anti-mouse Alexa Fluor 594 antibody (Molecular Probes, Life Technologies). The coverslips were then removed, mounted onto glass slides and analysed by immunofluorescence microscopy.

**2.7 Immunofluorescence microscopy**

Fixed cells were mounted in Vectashield® mounting medium containing DAPI (1.5 µg/ml) (Vector Laboratories). Microscopic analysis was performed using a Zeiss Imager.M1 microscope and obtained using a Zeiss AxioCam Mrm camera. Subsequent image analysis was performed using the Zeiss AxioVision4.8 software. The ImageJ software was then used to analyse and compile the images.

**2.8 Surface VSG-antibody clearance and uptake**

*T. brucei* 221VB1.2 was first cooled to 4ºC to block endocytosis, then incubated with rabbit polyclonal anti-VSG221 antibody for one hour to coat the cell surface. Cells were subsequently transferred to 37ºC to reactivate endocytosis for 0, 0.5, 1, 2, 4, 8 or 16 minutes and then diluted in trypanosome dilution buffer (TDB). This was followed by cell fixation in

2% PFA for 20 minutes at room temperature and the staining with a secondary antibody (Table 2.5). Fixed cells were permeabilised with 0.1% Triton X-100 for 5 minutes at room temperature and washed in PBS buffer. Cells were next incubated with RNAse A (1 μg/ ml) and propidium iodide (10 μg/ ml) to stain for DNA, before resuspension in PBS buffer for flow cytometry analysis (BD LSRFortessa$^{TM}$ cell analyser) or immunofluorescence microscopy. Quantitation of surface VSG-antibody clearance was calculated from flow cytometry data using FlowJo software as described in (Engstler *et al*. 2007).

The protocol used to visualise internalisation of anti-VSG221 antibodies using immunofluorescence microscopy is described in (Triggs & Bangs 2003). To prevent degradation of anti-VSG221 antibodies in the lysosome, *T. brucei* 221VB1.2 cells were incubated with FMK-024, an inhibitor of cathepsin B and L (morpholinourea-phenylalanine-homophenylalanine-fluoromethylketone) (MP Biochemicals) at a concentration of 20 μM for 1 hour at 37ºC. Cells were then placed at 4ºC in 1% BSA/ TDB and coated with rabbit polyclonal anti-VSG221 antibody for 1 hour. Cells were transferred to 37ºC for 0, 8, 16 and 32 minutes. This was followed by a wash in TDB, fixation in 2% PFA and permeabilised using 0.1% Triton X-100 at room temperature. Cells were then allowed to settle for 1 hour on microscopy slides and blocked with 2% BSA in PBS. To visualise the lysosome, cells were stained with mouse anti-p67 antibody (kind gift of Prof. Jay Bangs). The antibodies were detected using goat anti-rabbit Alexa Fluor 488 or goat anti-mouse Alexa Fluor 594 antibodies, before analysis by immunofluorescence microscopy.

**2.9 Biotinylated VSG uptake assay**

The uptake of surface VSG biotinylation and the subsequent VSG endocytosis, was measured as described in Engstler *et al* (Engstler *et al*. 2004). 1 x $10^7$ cells were collected and

cooled to 4ºC to stop endocytosis. They were then washed in TDB and resuspended at a density of 1 x$10^8$ cells/ ml, followed by a 10 minute incubation with 1 mM EZ-Link$^{TM}$ sulfo-NHS-SS-Biotin (Life Technologies) at 4ºC. 10 mM Tris buffer (pH 7.5) was then added, and cells were transferred to pre-warmed HMI-9 medium with 10% FCS. To reinitiate endocytosis, cells were incubated at 37ºC for 0, 0.5, 1, 1.5, 3, 6 or 12 minutes. Excess ice-cold stripping buffer (60% HMI-9, 10% FCS, 50 mM glutathione pH 9.0) was added to stop endocytosis. Cells were washed in PBS/ 2% bovine serum albumin (BSA), fixed in 2% PFA and resuspended in 100 mM $Na_2HPO_4$/ 100 mM glycine pH 7.2 for 15 minutes. Permeabilisation of the cells were performed using 0.1% Triton X-100 and resuspended in 10 µg/ ml Streptavidin-Alexa Fluor 488 (Molecular Probes, Life Technologies) for one hour in the dark at room temperature. Cells were subsequently analysed by immunofluorescence microscopy or flow cytometry.

**2.10 Western blotting and LiCor Imaging**

For surface VSG quantification experiments, HNIVO2+ and a VSG221 single-expresser cell line with the expression site marked with a puromycin resistance gene (SM221Pur) were used as controls. Cell lysate of the 221VG1.1 cell line was collected at 0h and 8h after *VSG* RNAi induction. Cells were lysed in 50 mM HEPES (pH 7.5); 1 mM EGTA; 1.5 mM $MgCl_2$; 10% (v/v) glycerol, 1% (v/v) Triton X-100 with a cocktail of protease inhibitors (2 µg/ml of leupeptin, chymostatin, pepstatin, and antipain). Protein lysate was then resuspended in loading buffer (62 mM Tris-HCl pH 6.8; 2 % (w/v) SDS; 10 % (v/v) Glycerol; 0.0025 % (w/v) Bromophenol Blue, 12.5 mM DTT) and boiled at 100$^{o}$C for 10 minutes. The equivalent of 2 x $10^4$ cells were loaded per well on 10 % SDS polyacrylamide gels and blotted onto a Hybond-P membrane (GE Healthcare) using wet electrophoresis transfer with protein transfer buffer (20% ethanol; 47.9 mM Tris; 38.6 mM glycine; 1.28 mM SDS). Blots were then

blocked and probed in PBS-Odyssey Blocking buffer (Li-Cor) and washed with 0.1 % PBS-Tween. Proteins were probed with the following rabbit primary antibodies: anti-VSG221 and anti-cytosolic HSP70, followed by IRDye 680RD donkey anti-rabbit IgG (H+L) secondary antibody (Li-Cor). Proteins were visualised and quantified using the Odyssey® Infrared Imaging System. The IRDye signal (for both VSG221 and HSP70) from probed protein was first normalised to that of SM221Pur before normalisation for loading by dividing the VSG221 signal with that of the HSP70 signal for the same sample.

For the VSG purification experiments, the total amount of protein from HNI221+ and HNIVO2+ cell lines were processed in the same manner as above. Protein lysate equivalent to 5 x $10^5$ cells were loaded into each well of the SDS gel and transferred onto a Hybond-P membrane. Proteins were then probed with a rabbit anti-VSG221 antibody or a rabbit anti-VO2 primary antibody. After which, a one-hour incubation with a conjugated secondary antibody: a monoclonal mouse horseradish peroxidase (HRP, 1:1000 dilution) followed. Imaging of the proteins of interest was achieved using Western lightning ECL (PerkinElmer, USA). Chemiluminescence was detected using the BIO-RAD Gel-Doc and Imagelab.

**2.11 Endocytosis assays**

*T. brucei* 221VB1.2 cells (5 x $10^6$) were harvested per condition and cooled to 4ºC to stop endocytosis. Cells were washed and resuspended in TDB with the addition of either Dylight 488 labelled tomato lectin at 5 µg/ml (Vector Labs), Alexa Fluor 488 conjugated human transferrin at 50 µg/ml (Life Technologies) or 10,000 MW Alexa Fluor conjugated dextran at 5 mg/ml (Life Technologies). Cells were subsequently transferred to 37ºC to re-activate endocytosis for 0, 0.5, 1, 2, 4, 8 or 16 minutes (in experiments following uptake of tomato lectin or transferrin) or 0, 1, 2, 4, 8, 16 or 32 minutes (in experiments following uptake

of dextran). Cells were then washed in TDB, fixed in 2% PFA for 20 minutes and analysed by flow cytometry. Statistical analyses of VSG221 antibody clearance or uptake of the various endocytosis markers was performed by first fitting each data set to the non-linear regression model using the GraphPad Prism software. The half-time of uptake was then calculated for each data set and analysed using the Student's t-test.

**2.12 Time-lapse live cell video microscopy**

VSG synthesis was blocked in *T. brucei* 221VB1.2 cells by the induction of *VSG221* RNAi with tetracycline (1 μg/ml) for 8 hours prior to image capture. Cells (10 μl) in HMI-9 medium with the addition of 15% FCS were transferred into a 0.1 mm deep chamber (BIOPTECHS FCS2 & FCS3 closed chamber system), sealed with a coverslip, and allowed to equilibrate at 37ºC for 10 minutes. Cells were observed by bright-field light videomicroscopy using a Leica DM5500B microscope with a 10X NA 0.40 objective lens on a focal point midway through the sample depth. Each image was captured every 200 milliseconds (5 Hz) for 1.7 minutes (512 frames) with an exposure time of 1 millisecond. Analysis of the videomicrographs was performed using custom designed macros on ImageJ (unpublished script written by Dr. R. Wheeler, Oxford). Particles were identified using an intensity maxima algorithm. Tracks were then constructed for each cell by finding the nearest particle to the expected cell location based on its motion in the previous two frames. Tracks were terminated if no particle was found within ten pixels (6.44 μm). Cell mean swimming speed, velocity and directional persistence were calculated from cell tracks as previously described (Zaburdaev *et al*. 2011). Statistical analyses on the mean swimming speed, velocity and directional persistence were performed using the Student's t-test (n=2500).

### 2.13 Isolation of peripheral blood mononuclear cells from human peripheral blood

Buffy coats from health donors were sourced from The Hong Kong Red Cross and processed on the day of collection. Buffy coats were diluted at a 1:1 ratio using PBS and layered over 15ml of Ficoll-Paque. Cells were then centrifuged at 2300 rpm at room temperature for 20 minutes at a low brake setting. The peripheral blood mononuclear cell (PBMC) layer was collected and washed in PBS. Viable PBMCs were then identified by staining with the viability dye, trypan blue and counted using a haemocytometer. This is followed either by further isolation of other mononuclear cell subtypes (Chapters 2.14 and 2.19) or by freezing down into cell stabilates for storage in liquid nitrogen.

### 2.14 Differentiation of PBMCs into monocyte-derived dendritic cells

CD14 positive cells were selected using the MACS® Separation System (MACS Miltenyi Biotec), per the manufacturer's instructions. In brief, PBMCs were magnetically labelled with microbeads conjugated to monoclonal anti-human CD14 antibodies at 4°C for 15 minutes. Stained cells were then washed in PBS and loaded onto a MACS® Column, which was placed in the magnetic field of the MACS Separator. CD14+ cells attached to the microbeads were retained within the column and eluted using PBS. Viable CD14+ cells were counted using a haemocytometer and plated at $1x10^6$ cells/ml in RPMI complemented with 10% FCS and 1% P/S. To differentiate CD14+ monocytes into dendritic cells (DC), 40 ng/ml of human interleukin-4 (IL-4) and human granulocyte-macrophage colony-stimulating factor (GM-CSF) were added. Culture medium and cytokines were replaced every 2 days for 6 days to allow complete DC differentiation.

### 2.15 Human dendritic cell and *T. brucei* co-culture

Half of the medium (RPMI + 10% FCS + 1% P/S) was removed from each well from the DC culture plate on day 6 of differentiation and replaced with equal volumes of trypanosome culture medium (HMI-9 + 15% FCS) containing $1x10^6$ trypanosomes.

### 2.16 Surface markers staining

Cells (DCs or T-cells) were collected and washed in PBS. DCs were stained with human anti-HLADR, anti-CD80, anti-CD86 and anti-CD40 antibodies. T-cells were incubated with human anti-CD3, anti-CD25 and anti-CD69 antibodies. Cells were incubated with antibodies at room temperature for 20 minutes before fixation in 2% PFA and resuspended in PBS. Surface marker expression was analysed using flow cytometry and the fluorescence intensity quantified using the FlowJo software.

### 2.17 Dendritic cells phagocytosis assay

DCs were co-cultured with *T. brucei* for 0, 16, 24, 48 and 72 hours before collected and washed with PBS. $5 \times 10^5$ cells per condition were then resuspended at in fresh RPMI medium. FITC conjugated dextran was used as an endocytosis marker and was added to the cells at a final concentration of 1 mg/ml. Equal volumes of PBS was added to the negative controls for each condition. Cells were then incubated at 37°C for one hour before washing in PBS. Dextran uptake was quantified by the fluorescence intensity of FITC using flow cytometry.

### 2.18 Purification of VSG

$5 \times 10^7$ trypanosomes per condition were collected and washed in PSG (Table 2.3) solution before resuspended in ice-cold sterile milli-Q water containing a cocktail of EDTA-

free protease inhibitors on ice for 5 minutes. Cells were then centrifuged and the supernatant which contained cytoplasmic contents (S1) was collected. The rest of the cells was resuspended in 10 mM sodium phosphate buffer (pH 8.0) with protease inhibitors and incubated at 37°C for 5 minutes. This activated the endogenous *T. brucei* phospholipase-C to cleave the VSG molecules at the GPI-anchor (Wang *et al*. 2003). Cell contents were then centrifuged at 16 000 g for 15 minutes to isolate soluble VSG (sVSG) in the supernatant fraction (S2). Finally, the pellet containing the rest of the cell membrane was collected and resuspended in sodium phosphate buffer (P3).

**2.19 Isolation of CD3 positive T-cells from PBMCs**

Similar to the isolation of CD14+ cell selection, the magnetic MACS® Separation System was used to isolate the CD3+ cell population from PBMCs. CD3+ cells were stained with a human anti-CD3 antibody to ensure the eluted cells meet the 95% purity threshold. Cells were subsequently cultured in RPMI complemented with 10% FCS and 1% P/S.

**2.20 T-cell proliferation assay**

DCs that have been co-cultured with *T. brucei* for 0, 16, 24, 48 and 72 hours were collected. To stop further proliferation of both DCs and *T. brucei*, they were irradiated at 30 gray (Gy). DCs were subsequently spun down and resuspended at 6 x $10^5$ cells/ml in fresh RPMI complemented with 10% FCS and 1% P/S. CD3+ positive T-cells were resuspended at 3 x $10^6$ cells/ml in PBS. This was followed by staining in the dark with 0.05 mM carboxyfluorescein succinimidyl ester (CFSE) at 37°C for 20 minutes. After staining, cells were washed twice with PBS and added to DCs at a density of 3 x $10^6$ cells/ml in RPMI

complemented with 10% FCS and 1% P/S. Cells were then collected 0, 1, 2, 3, 5 and 7 days after co-culturing with DCs. CFSE staining was assessed and quantified by flow cytometry.

### 2.21 Multiplex Bead Based Immunoassays

The LEGENDplex™ Human Inflammation Panel kit was used to screen for 13 human inflammatory cytokines and chemokines: IL-1β, IFN-α, IFN-γ, TNF-α, MCP-1 (CCL2), IL-6, IL-8 (CXCL8), IL-10, IL-12p70, IL-17A, IL-18, IL-23, and IL-33. The LEGENDplex™ Human Th Cytokine Panel kit as used to screen for 13 human T helper cytokines and chemokines: IL-2, IL-4, IL-5, IL-6, IL-9, IL-10, IL-13, IL-17A, IL-17F, IL-21, IL-22, IFN-γ and TNF-α. Screening was performed as per the manufacturer's instructions, using the same principle as traditional sandwich immunoassays. In brief, all 13 antibodies using in the panel are conjugated to fluorescent beads of different sizes and internal fluorescence intensities. These beads were then mixed with supernatant from the co-culture and incubated with a cocktail detection antibodies specific to the antibodies. Streptavidin-phycoerythrin (SA-PE) was subsequently added, which would bind to the biotinylated detection antibodies. The fluorescent signal intensities are in proportion to the amount of bound cytokines. Since the beads are differentiated by size and internal fluorescence intensities, each cytokine population could be separated by these two parameters on a flow cytometer. The concentration of each cytokine was determined using a standard curve generated in the same assay.

### 2.22 BCT-100 treatment of *T. brucei*

The BF 221VG1.1 *T. brucei* cell line was used in all BCT-100 experiments. BCT-100 is a pegylated recombinant human arginase 1 of 329 amino acid residues and is a kind gift from Dr Paul Cheng, The Hong Kong Polytechnic University. The specific enzyme activity of BCT-100 is approximately 400 U/mg. 1 x $10^6$ (per condition) *T. brucei* were treated with 0.1, 1 and 10 U/ml for 0, 24 and 48 hours. One unit of BCT-100 is defined as the amount of enzyme that produces 1 μmol of urea per minute at 30°C, at pH 8.5. *T. brucei* were then processed for either fluorescence microscopy according to the protocol in 2.7. For flow cytometry analysis, *T. brucei* were fixed in 2% PFA and permeablised using 0.1% Triton X-100 before stained with 10 μg/ ml propidium iodide (PI) and 1 μg/ ml RNAse A. 200 μM DFMO (alpha-Difluoromethylornithine) was used as a positive trypanostatic control throughout the experiments.

# Chapter 3

# The role of VSG in the immune evasion from macrophages

## 3.1 Introduction

Being an extracellular parasite, the bloodstream form *Trypanosoma brucei* is under constant attack by the host innate and adaptive immune systems. These include the complement system, antibodies and phagocytic cells such as macrophages. In order to withstand these attacks to survive and proliferate in the bloodstream, *T. brucei* has developed a dense surface coat comprised of over $10^7$ Variant Surface Glycoprotein (VSG) molecules (Cross 1975; Schwede & Carrington 2010). VSG is the most abundant protein in bloodstream form *T. brucei* and the trypanosome surface is dominated by an extremely dense arrangement of VSG homodimers, which form a protective barrier against the host environment (Schwede *et al*. 2011; Barry 1979).

VSG is key to immune evasion from the adaptive immune system through the sophisticated mechanism of antigenic variation. This allows the trypanosome to switch stochastically between different variants of VSG during infection. Each trypanosome expresses a single VSG variant at any given time from one of 15 telomeric expression site (ES) transcription units within its genome (Marcello & Barry 2007; Hertz-Fowler *et al*. 2008). Switching the active *VSG* can be achieved through the activation of another telomeric expression site via an *in situ* switch. Alternatively, the *T. brucei* genome contains a vast repertoire of over 2000 *VSG* pseudogenes that are available for switching into the active expression site via DNA rearrangements, infinitely increasing the possibility of VSG variation (Glover *et al*. 2013; Horn & McCulloch 2010). As a result, antibody production lags behind the rate of VSG switching, allowing the trypanosome to escape antibody-mediated elimination.

Although densely packed with VSG molecules, the VSG surface coat of the trypanosome is surprisingly fluid. In addition, there is an extremely high rate of endocytosis (Engstler *et al*. 2004). In fact, bloodstream form *T. brucei* is known to have one of the highest rates of endocytosis amongst eukaryotes, where the entire surface complement is endocytosed every 12 minutes (Engstler *et al*. 2004). Both endocytosis and exocytosis are limited to a specialised invagination at the base of the flagellum known as the flagellar pocket (Field & Carrington 2009). Any host immune components that are attached to the trypanosome surface are quickly endocytosed, targeted for degradation in the lysosome and prevented from returning to the surface (Overath & Engstler 2004; Engstler *et al*. 2004). VSG is key for maximum virulence of the parasite within its host.

VSG is essential *in vitro* and its synthesis can be blocked using a tetracycline-inducible RNAi system (Sheader *et al*. 2005). The induction of *VSG* RNAi leads to rapid growth inhibition coupled with a precise precytokinesis cell cycle arrest. This is presumably a protective mechanism to reduce the dilution of the VSG coat when new VSG molecules are no longer synthesised (Terry K Smith *et al*. 2009). Since VSG forms the only protective barrier against the host immune system, inhibiting its synthesis would impact on the evasion of trypanosomes from the host immunosurveillance. In addition to evading complement and antibodies, bloodstream form *T. brucei* must also evade phagocytes including macrophages. Although some aspects surrounding the immunology of macrophage activation during a *T. brucei* infection have been investigated (Salmon *et al*. 2012; Stijlemans *et al*. 2010; Beschin *et al*. 2014), little is known about how phagocytosis of trypanosomes by macrophages occurs mechanistically. It has been shown earlier that blocking VSG synthesis *in vitro* leads to stalled trypanosomes which persist for days. However, if *VSG* RNAi is induced *in vivo* in infected mice, trypanosomes were cleared rapidly within hours (Sheader *et al*. 2005). Here, I

investigated to the effect of blocking VSG synthesis on trypanosome phagocytosis by macrophages.

### 3.2 Experimental outline

VSG synthesis was blocked *in vitro* using an inducible RNAi system in the bloodstream form *T. brucei* cell lines 221VG1.1 and 221VB1.2 cell lines for 8 hours. Trypanosomes were then opsonised with various opsonins; complement proteins and anti-VSG antibodies. Using an *in vitro* co-culture system, the opsonised bloodstream form *T. brucei* were co-cultured with RAW264.7 mouse macrophages. Through immunofluorescence microscopy analysis, phagocytosis of the parasites was quantified and categorised to delineate the effect of *VSG* RNAi on the evasion of *T. brucei* from the innate arm of immunity.

### 3.3 Validation of the functionality of the RNAi machinery in the *T. brucei* 221VG1.1 cell line

The *T. brucei* 221VG1.1 cell line used in the phagocytosis assay is capable of tetracycline inducible RNAi against the *VSG221* variant. Induction of *VSG221* RNAi *in vitro* resulted in rapid growth arrest within 8 hours, which was equivalent to the length of one cell cycle (Figure 3.1A). Despite the onset of the growth arrest, these trypanosomes persisted in culture for several days until a small population of cells which had broken free of tetracycline induced *VSG221* RNAi expanded after 60 hours. Cell cycle analysis using immunofluorescence microscopy revealed that the majority of *VSG221* RNAi induced cells (≥ 60%) stalled specifically at the 2N2K cell cycle stage before cytokinesis, characterised by the doubled nuclei and kinetoplast DNA content. There was also an increase in the number of cells with abnormal DNA content i.e. multi-nucleated cells or cells without a nucleus (zoids) (Figure 3.1B). In addition, the arrangement of the nuclei (N) and kinetoplasts (K) in induced cells differed drastically to that in an uninduced cell (Figure 3.1C). Both nuclei and kinetoplasts were positioned much closer to each other in a parallel arrangement. Cell morphology of induced cells appeared rounder and flatter with two external flagella. All of the above phenotypes displayed by the 221VG1.1 cell line matched those described in Sheader *et al* (Sheader *et al*. 2005). Therefore, I could verify that the *VSG221* RNAi machinery is intact and functional in the 221VG1.1 cell line.

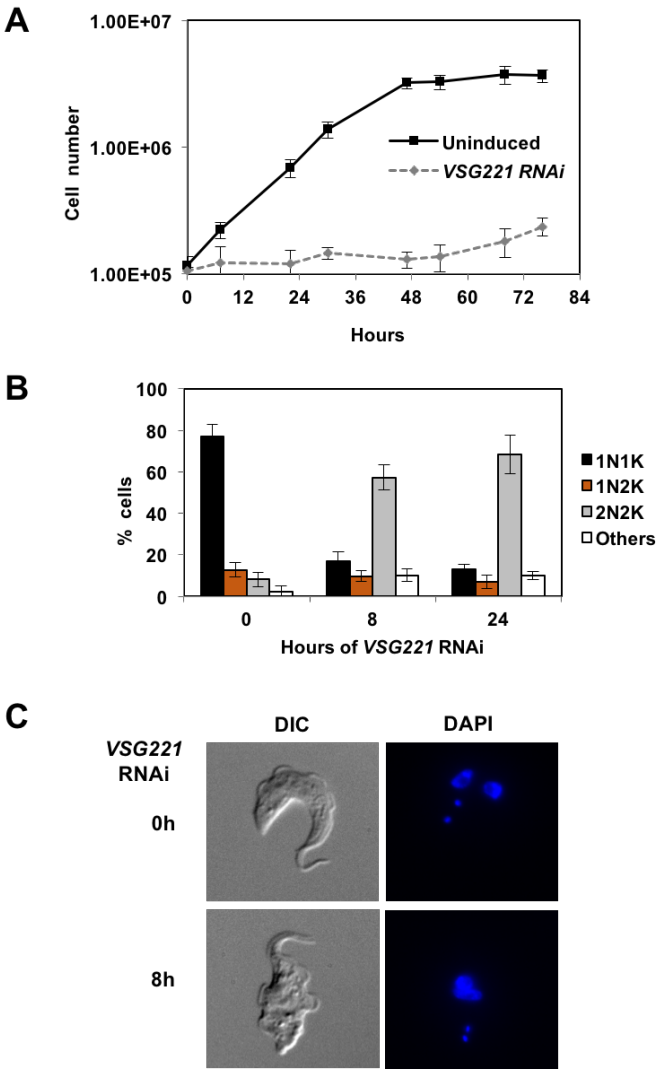



**Figure 3.1. Phenotypes of bloodstream form *T. brucei* after blocking VSG221 synthesis**

**(A)** Growth curves of *T. brucei* 221VG1.1 in the absence and presence of tetracycline induced *VSG221* RNAi. *VSG221* RNAi was induced by the addition of 1 µg/ml tetracycline. Number of viable trypanosomes were counted twice daily using a haemocytometer. Graph shows the result of three independent experiments, with error bars indicating the standard deviations.

**(B)** Cell cycle analysis of *T. brucei* 221VG1.1 after 0, 8 and 24h *VSG221* RNAi induction. Trypanosomes were collected, washed and fixed before analysis using immunofluorescence microscopy. DNA content was stained using DAPI. Trypanosomes were classified based on the arrangement of their nucleus (N) and kinetoplast (K) into: 1N1K, 1N2K, 2N2K and others (multinucleated cells or zoids).

**(C)** Cell morphology changes of *T. brucei* after the induction of *VSG* RNAi. Cells were visualised using differential interference contrast (DIC), whereas their DNA content was visualised using DAPI staining.

### 3.4 Quantification of phagocytosis using the endogenous eGFP signal from *T. brucei* 221VG1.1 after the induction of *VSG221* RNAi

The 221VG1.1 cell line also contains an *eGFP* gene inserted behind the promoter of the active *VSG221* expression site. Therefore, phagocytosis of this cell line by macrophages could be visualised by immunofluorescence microscopy using the endogenous eGFP signal. *VSG221* RNAi was induced in 221VG1.1 cells for 8 hours. 8 hours post-RNAi induction was chosen as the optimal time point because this is the earliest time point with a full cell cycle arrest. At this time point, there is still 60% normal translation, which declines as the global translation arrest takes place (Terry K. Smith *et al*. 2009). Therefore, later time points were not considered to avoid secondary effects due to this reduced translation.

Host molecules including complement C3b or IgG or IgM antibodies adhere to microbial surface and facilitate phagocytosis of the opsonised pathogens (Aderem & Underhill 1999; Bohlson *et al*. 2014). Macrophages attach to these host protein coated pathogens through specific surface receptors recognising these opsonins (Plüddemann *et al*. 2011; Dunkelberger & Song 2010). Trypanosomes were therefore, opsonised with normal mouse serum (NMS), polyclonal anti-VSG221 antibodies or the combination of both NMS and antibodies. This was followed by co-culturing with murine RAW264.7 macrophages. In order to trigger classical activation, macrophages were first stimulated with mouse interferon gamma (IFN-γ) and Lipopolysaccharides from *E. coli* (LPS) for 24 hours prior to co-cultivation with trypanosomes. Phagocytosis was then visualised using immunofluorescence microscopy and characterised according to the distribution of the trypanosome eGFP signal.

The complement used in these experiments was present in normal mouse serum (NMS) from the CD-1 mouse strain. Unlike many laboratory mouse strains, CD-1 mice have functional complement proteins of the terminal complement pathway, and have been shown to

have functional serum complement activity of the classical, lectin and alternative pathways at the level of C9 activation (Kotimaa *et al*. 2016). To verify that the normal mouse serum from the CD-1 mice was complement active, I showed activity of the classical pathway (requiring both antibodies and complement). After opsonisation for 90 minutes with both NMS and anti-VSG antibodies, there was moderate although statistically significant lysis of *T. brucei* after the induction of *VSG221* RNAi for 8 hours (Figure 3.2). The anti-VSG221 antibody used in our experiments was a rabbit polyclonal antibody (1:5000 dilution), which was not in excess in the phagocytosis assays, as shown in Figure 3.3.

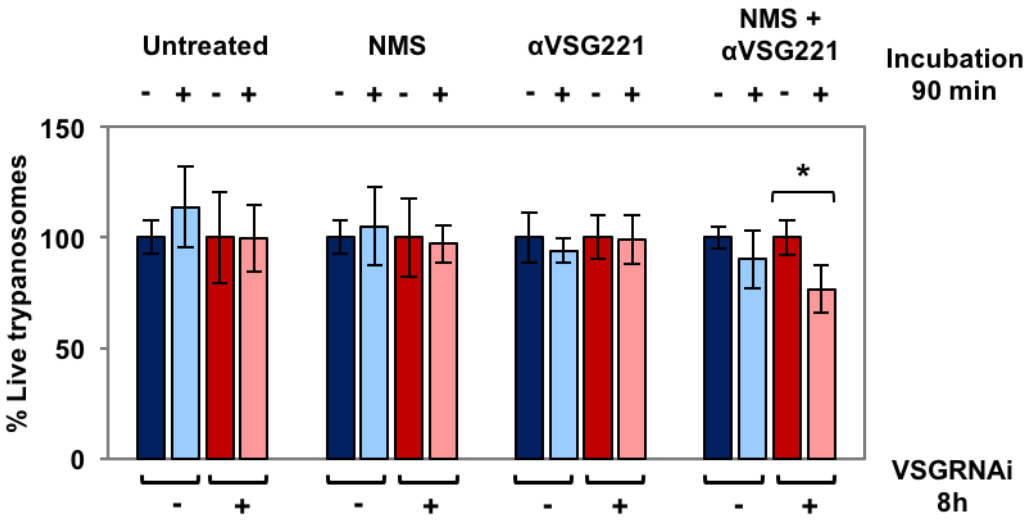



**Figure 3.2. The effect of opsonisation on the viability of *T. brucei* after the induction of *VSG* RNAi.** *VSG221* RNAi was induced in *T. brucei* 221VG1.1 for 8h. Cells were either left untreated, or incubated with 10% normal mouse serum (NMS) from CD-1 mice, rabbit polyclonal anti-VSG221 antibody (1:5000 dilution) or both NMS and anti-VSG221 antibody for 90 minutes. The number of live *T. brucei* was counted using a haemocytometer before and after the 90 minute incubation period. The number of live trypanosomes at 0 minutes is normalised to 100%, and the number after the 90 minute incubation is expressed as a relative percentage. Data show the average percentage (%) of viable trypanosomes from four independent biological replicates. Statistical analysis was performed using the one-way ANOVA with the asterisk (*) indicating *P<0.05.

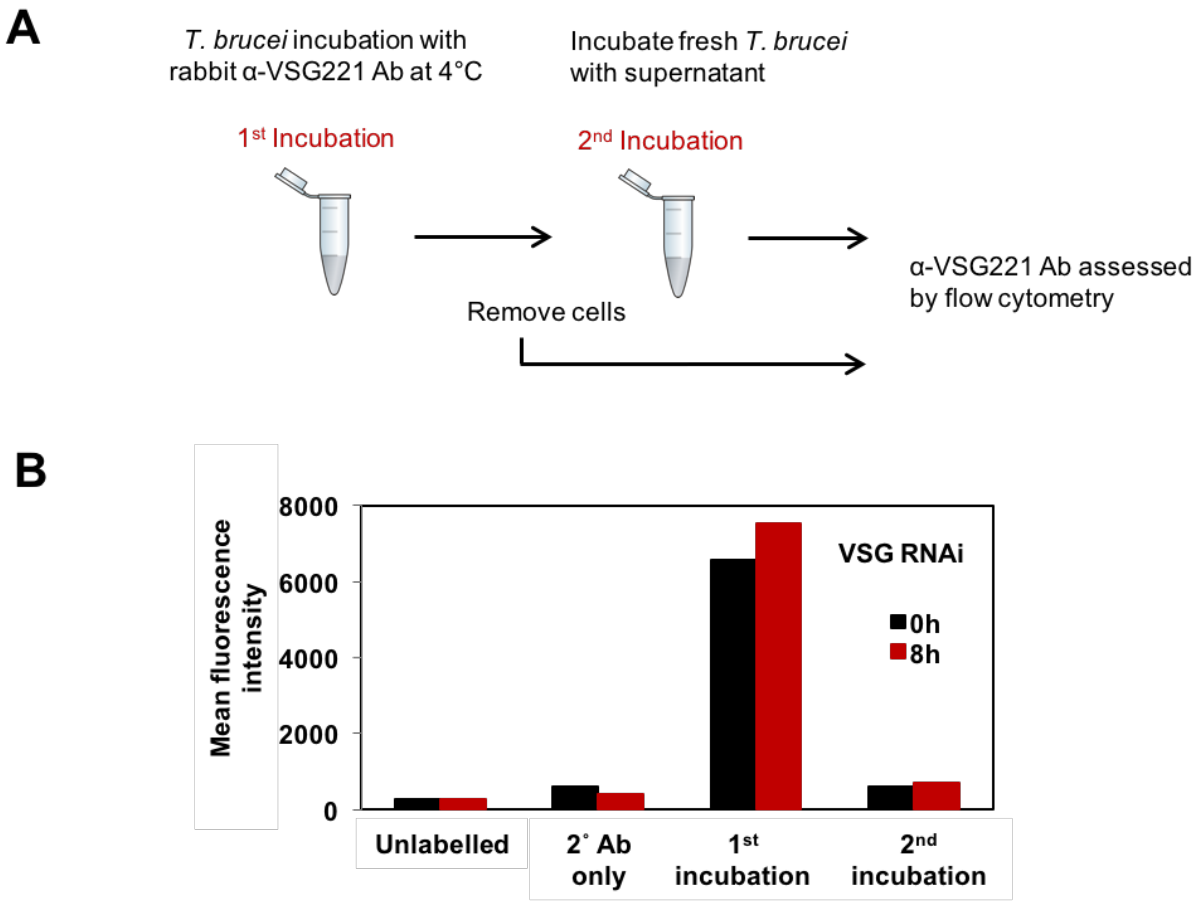



**Figure 3.3. Anti-VSG221 antibody was not in saturation.**
**(A)** *T. brucei* 221VB1.2 was cooled to 4°C to block endocytosis, and incubated with polyclonal rabbit anti-VSG221 antibody (1:5000 dilution) for one hour to coat the cells (1st incubation). The trypanosomes were centrifuged, and the supernatant removed. The supernatant was subsequently incubated with new *T. brucei* (2nd incubation). Cells retrieved after these two incubation steps were fixed in 2% PFA and incubated with the secondary goat anti-rabbit antibody coupled to Alexa Fluor 488. The amount of surface bound anti-VSG221 antibody was assessed using flow cytometry. **(B)** The amount of anti-VSG221 antibody present on the surface of cells which were unlabelled, or incubated with the secondary goat anti-VSG221 antibody (2° Ab only) or using both antibodies after the first incubation. Anti-VSG221 antibody levels were also determined on fresh *T. brucei* after incubation with the supernatant (2nd incubation). These experiments were performed in cells in the presence or absence of *VSG221* RNAi for 8h.

Figure 3.4 shows the various distributions of the eGFP signal before and after the parasites were phagocytosed by macrophages. Whole trypanosomes that adhered to the macrophage surface retained eGFP expressed throughout the cell body (surface macro.), whereas trypanosomes that had been internalised displayed a wider range of fluorescence signal distributions and were categorised accordingly into "vacuole", "punctate" and "dispersed" groups.

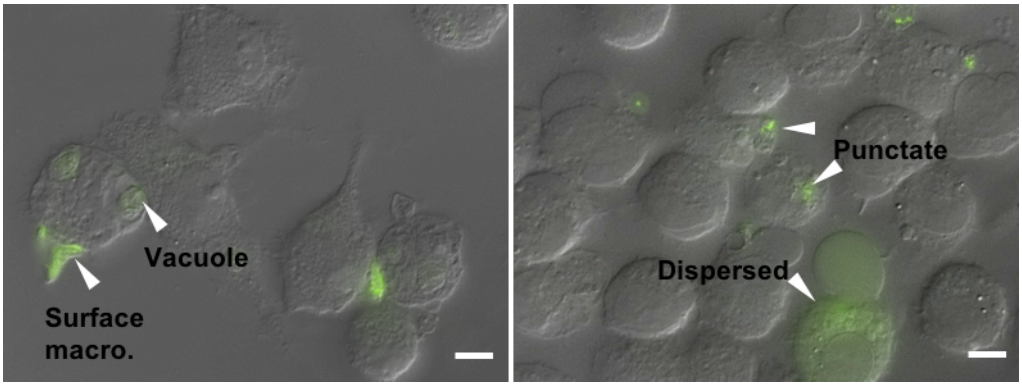



**Figure 3.4. Immunofluorescence microscopy analysis of the phagocytosis of *T. brucei* 221VG1.1 cells.** Phagocytosis was visualised using the 221VG1.1 endogenously expressed eGFP signal. Whole trypanosomes expressing eGFP were identified and counted. Ingested trypanosomes that have lost their normal morphology were described by the distribution of the eGFP signal: 1 or 2 vacuoles, punctate or dispersed distribution. The mean numbers of *T. brucei* adhered to the macrophage surface or internalised into the macrophage were expressed as percentage values of the total number of macrophages counted. Scale bar: 10 μm.

Adherence and internalisation of trypanosomes by macrophages were then quantified according to the aforementioned categories, as seen in Figure 3.5. In the absence of opsonisation, minimal phagocytosis was observed (1.5 %). The addition of normal mouse serum moderately increased the number of trypanosomes attached to the macrophage surface (4.1 % vs 2.4 %) and phagocytosis (4.9 % vs 1.5 %). However, when trypanosomes were opsonised with polyclonal anti-VSG221 antibody, macrophage adherence drastically increased

13.5 times (32.4 % vs 2.4 %). Interestingly, when trypanosomes were opsonised with both NMS and anti-VSG221 antibody, NMS appeared to enhance the effect mediated by anti-VSG221 antibodies and a three-fold increase was observed in phagocytosis.

After the induction of *VSG221* RNAi, there was a moderate but statistically insignificant increase in both adherence to (3.6 % vs 2.4 %) and engulfment by macrophages (5.4 % vs 1.5 %). Opsonisation with NMS alone after blocking VSG synthesis did not improve macrophage adherence but increased phagocytosis by two-fold as 11.1% of macrophages had engulfed trypanosomes compared to 4.9% of uninduced trypanosomes. Incubation of trypanosomes with anti-VSG221 antibodies after the induction of *VSG221* RNAi, not only resulted in high levels of trypanosome attachment to the macrophage surface but also enhanced phagocytosis. However, when both NMS and anti-VSG221 antibodies were added, only phagocytosis was increased. Comparing Figure 3.5C and 3.5D, it appears that while anti-VSG221 antibodies alone increased adherence of parasites to the macrophage surface, the addition of NMS was important in enhancing the process of phagocytosis, as a high percentage of punctate eGFP signal was observed.

Initial observations using the endogenous eGFP signal of the trypanosomes demonstrated the importance of parasite opsonisation in the recognition and engulfment by macrophages. However, using only the eGFP signal to quantify phagocytosis might not have produced the most accurate results. This is because the constitutive expression of eGFP is dependent on the trypanosome cell membrane being intact. Once the cell lyses within the macrophage lysosome, a decrease in pH would cause rapid degradation of eGFP (Campbell & Choy 2001; Roberts *et al*. 2016). As a result, there was a high probability of underestimation of the number of parasites phagocytosed by each macrophage. Moreover, to obtain a large

enough number of cell population for analysis, over 500 macrophages had to be counted for each condition.

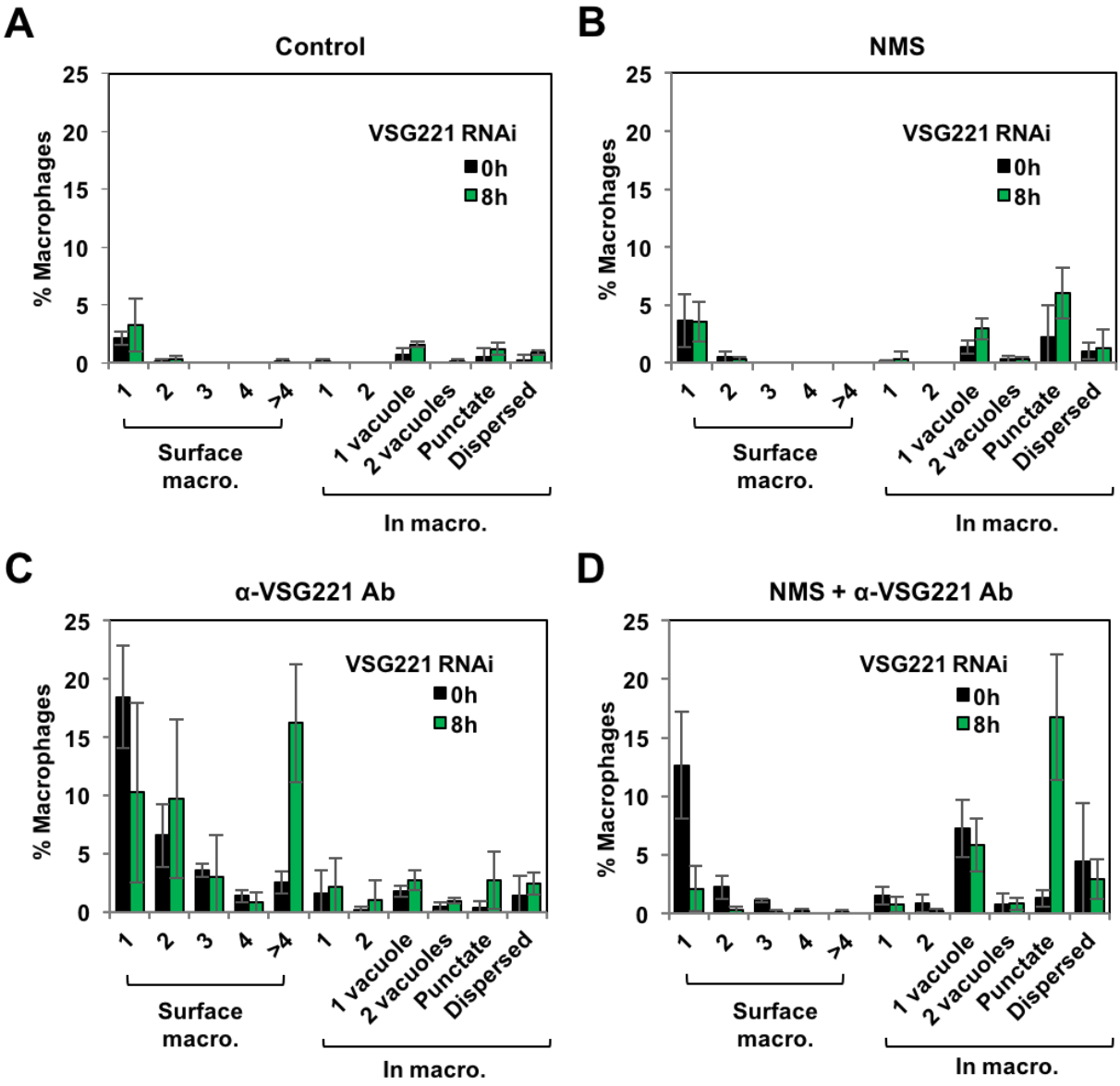



**Figure 3.5.** *T. brucei* 221VG1.1 cells were left **(A)** untreated, or opsonised with **(B)** normal mouse serum (NMS), **(C)** a polyclonal anti-VSG221 antibody or **(D)** both NMS and anti-VSG221 antibody. The number of parasites attached to the macrophage surface (Surface macro.) or ingested by the macrophage (In macro.) was quantified by immunofluorescecne using the endogenously expressed eGFP signal. Ingested trypanosomes that have lost their normal morphology are described by the distribution of the eGFP signal: 1 or 2 vacuoles, punctate or dispersed distribution. The mean numbers of *T. brucei* adhered to the macrophage surface or internalised into the macrophage were expressed as percentage values of the total

number of macrophages counted. The results were obtained from 3 independent biological experiments (n=200) with error bars indicating the standard deviations.

### 3.5 Inhibition of VSG synthesis in *T. brucei* led to an increase in phagocytosis by macrophages in the presence of anti-VSG221 antibodies

In light of this, I decided to quantify trypanosome phagocytosis using a monoclonal antibody (L8C4) against the paraflagellar rod 2 protein (PFR2) of the trypanosome flagellum. Trypanosome flagella remain relatively resistant to degradation in the macrophage phagolysosome, even after the ingested trypanosomes have lysed. After the phagocytosis assay, macrophage and trypanosome were fixed *in situ* on the coverslip and permeabilised using methanol (at -20 ºC). The L8C4 antibody was added, followed by a secondary Alexa Fluor 594 antibody. Using immunofluorescence microscopy, phagocytosis was quantified by counting the number of *T. brucei* flagella inside each macrophage (Figure 3.6A).

Similar to Figure 3.5A, only 2.7 ± 2.3% macrophages showed evidence of trypanosome phagocytosis, indicating that trypanosomes are normally adapted to escape phagocytosis (Figure 3.6B). Opsonisation with NMS from CD-1 mice did not significantly increase phagocytosis (up to 5.2 ± 1.9%). Prior incubation with anti-VSG221 antibodies appeared to have improved phagocytosis (up to 9.8 ± 4.3%) but this increase (up 16.4 ± 6.0%) was only statistically significant when NMS was added in combination with antibodies. These observations not only further support the importance of parasite opsonisation in facilitating macrophage phagocytosis but also highlight the role of the classical activation of the complement pathway.

Next the effect of blocking VSG synthesis on both the recognition and engulfment of trypanosomes by macrophages was investigated. The induction of *VSG221* RNAi appeared to have minimal effect on macrophage phagocytosis, as the percentage of macrophages with

ingested trypanosomes rose only marginally from 2.7 ± 2.3% to 3.9 ± 2.4% (Figure 3.6B). Prior incubation with complement active NMS did not significantly increase phagocytosis (5.2 ± 1.9% to 6.7 ± 3.1%) either. However, the most striking difference was observed when trypanosomes were opsonised with anti-VSG221 antibodies after *VSG221* RNAi had been induced. Phagocytosis of trypanosomes increased 3.4-fold compared to non-induced cells, with 33.5 ± 6.7% of macrophages having ingested one or more trypanosome flagella (*P<0.01). The addition of host complement to anti-VSG antibodies maintained but did not further enhance phagocytosis (34.8 ± 6.6% vs 33.5 ± 6.7%). This demonstrated that anti-VSG antibodies were the major factor which facilitated the recognition and capture of *T. brucei* by macrophages after the induction of a VSG synthesis block.

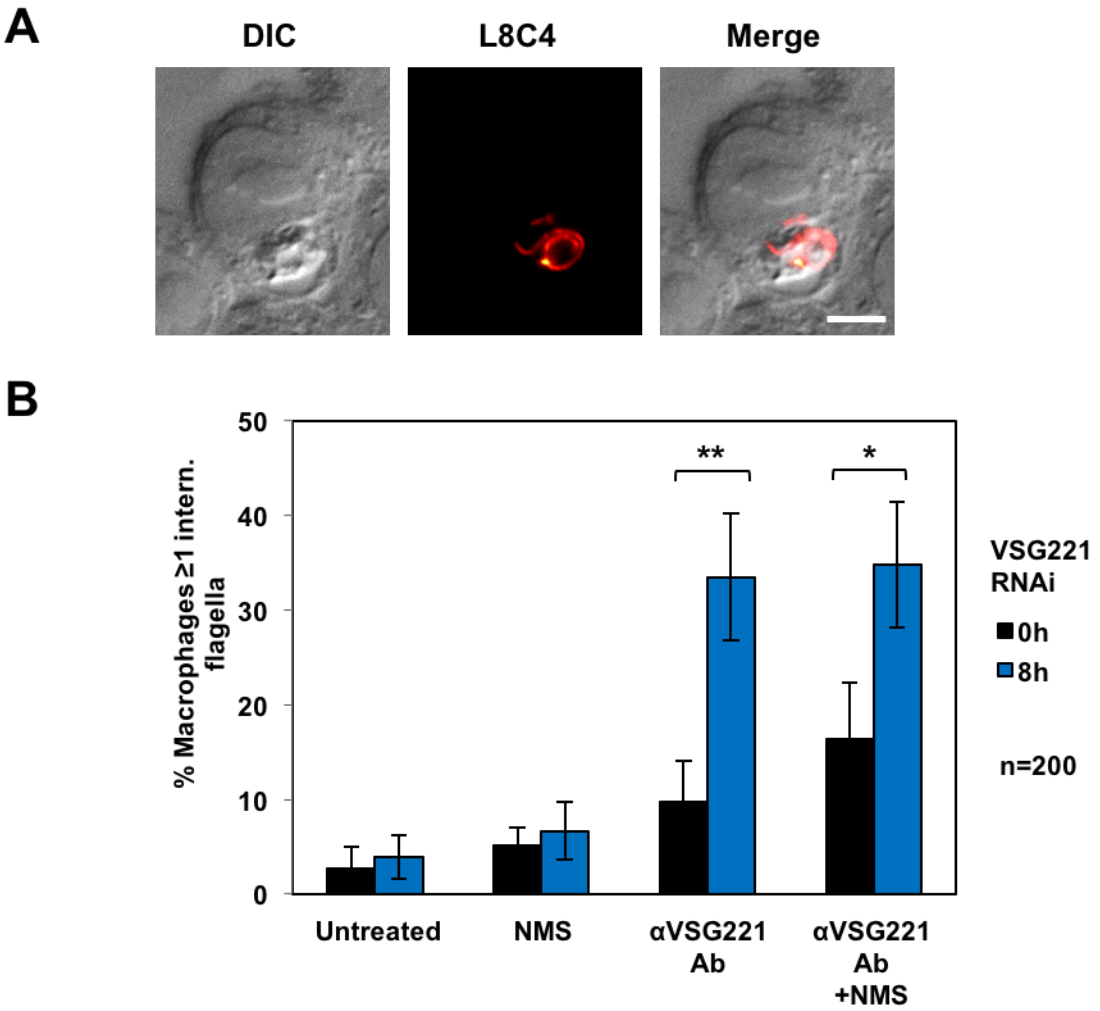



**Figure 3.6. Phagocytosis of *T. brucei* by macrophages increased significantly in the presence of anti-VSG221 antibodies.**

**(A)** Phagocytosis of *T. brucei* 221VG1.1 cells by RAW264.7 mouse macrophages. *T. brucei* cells were visualised using differential interference contrast (DIC). Phagocytosis of *T. brucei* was visualised using a monoclonal antibody against the paraflagellar rod protein PFR2 (L8C4) (red). Scale bar: 5μm.

**(B)** Quantification of the number of macrophages that have ingested one or more *T. brucei* flagella. *VSG221* RNAi was induced for 0 or 8 hours (h) by the addition of tetracycline. Parasites were left untreated, or opsonised with normal mouse serum (NMS), polyclonal anti-VSG221 antibodies (αVSG221 Ab) or the combination of both NMS and αVSG221 Ab. Phagocytosis of *T. brucei* was quantified using immunofluorescence microscopy. The results show the mean values obtained from 3 independent biological experiments (n=200) with error bars indicating the standard deviations. Statistical analysis was performed using the Student's t-test **P<0.01, *P<0.05.

### 3.6 Blocking VSG synthesis in the presence of anti-VSG221 antibodies resulted in an increase in adherence and phagocytosis of trypanosomes by macrophages.

As host opsonins (and especially anti-VSG antibodies) appeared to be crucial in aiding *T. brucei* recognition and phagocytosis, I investigated the extent of trypanosome internalisation by the macrophage as opposed to adherence to the macrophage surface. The limitation of the phagocytosis assay was the 2D nature of using immunofluorescence to differentiate between internalised and attached parasites. Therefore, when determining the difference, I have abided by the rule that the parasite, including the flagellum/flagella must be surrounded entirely by the macrophage cell membrane and also surrounded by a vacuole, either a phagosome or a phagolysosome. Any trypanosome flagellum that does not fit the above description, would be classified as an "attached" parasite.

A detailed analysis in Figure 3.7 showed that trypanosomes that were pre-incubated in host complement did not attach to macrophages significantly better than untreated trypanosomes, regardless of whether *VSG* RNAi was induced (Figure 3.7A and 3.7B). Pre-incubation of uninduced *T. brucei* with anti-VSG221 antibodies lead to a 4.5-fold increase in RAW264.7 macrophages showing adhered trypanosomes, and a 3.4-fold increase in macrophages with internalised flagella. However, the most striking effect was seen when VSG221 synthesis was blocked in trypanosomes which had also been pre-incubated with anti-VSG221 antibodies before co-culturing with macrophages (Figure 3.7C). Here, the majority of the macrophages contained more than one flagellum, and between 5-10% of the macrophages each contained either 1, 2, 3, 4 or more than 4 flagella. Some macrophages efficiently phagocytosed multiple (up to more than four) trypanosomes in the presence of anti-VSG221 antibodies. A VSG synthesis block, with the addition of NMS and anti-VSG antibodies resulted in increased trypanosome adherence and phagocytosis (Figure 3.7D). Anti-

VSG221 antibodies were therefore the most important opsonin facilitating efficient trypanosome uptake in our phagocytosis experiments.

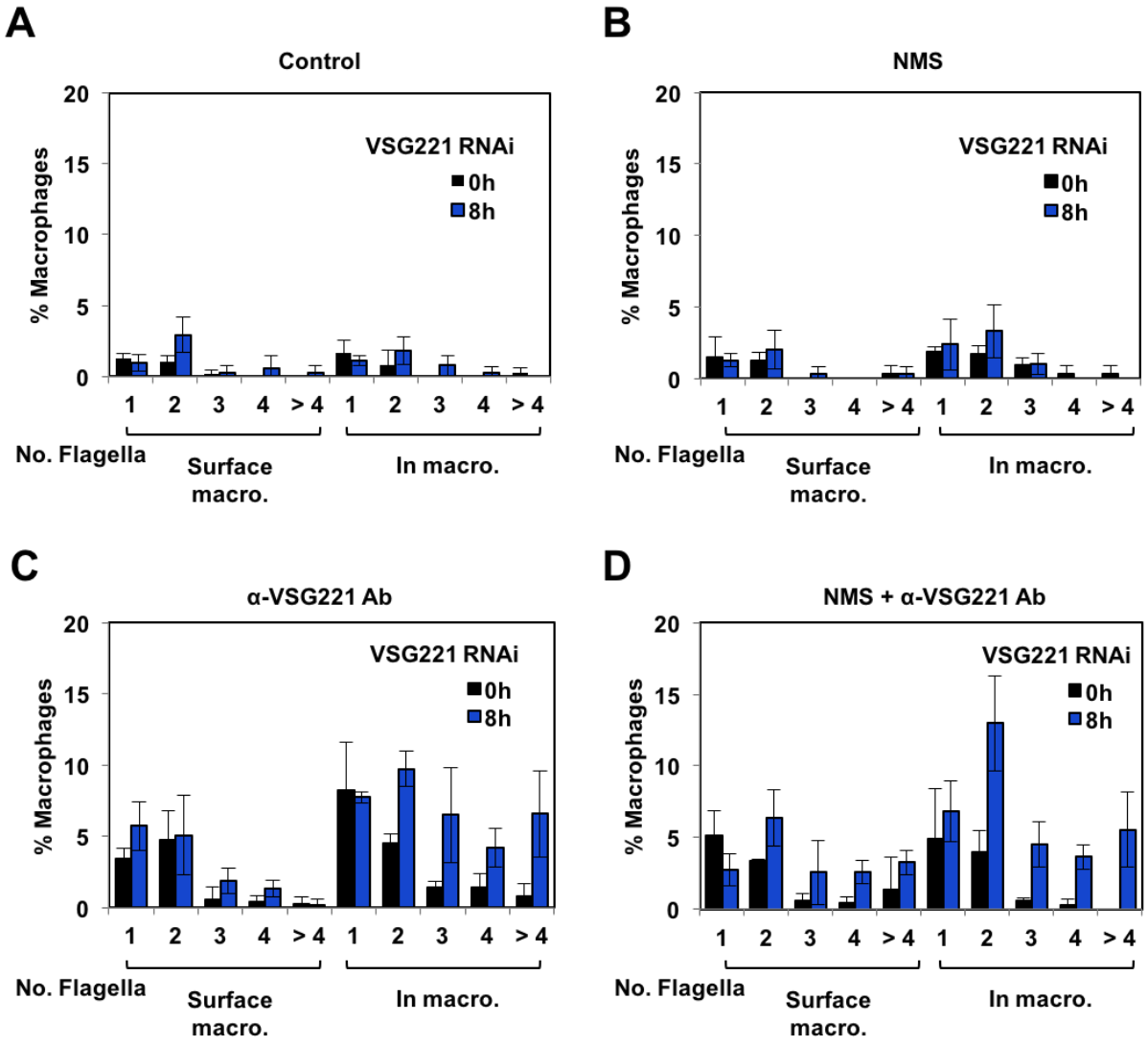



**Figure 3.7. Analysis of *T. brucei* attachment and internalization by RAW264.7 macrophages.**
*T. brucei* 221VG1.1 cells were left **(A)** untreated, or opsonised with **(B)** normal mouse serum (NMS), **(C)** a polyclonal anti-VSG221 antibody or **(D)** both NMS and anti-VSG221 antibody. The number of parasites attached to the macrophage surface (Surface macro.) or ingested by the macrophage (In macro.) was quantified by immunofluorescence using the L8C4 antibody against the parasite flagellar rod protein (PFR2). The mean numbers of *T. brucei* adhered to the macrophage surface or internalised into the macrophage were expressed as percentage values of the total number of macrophages counted. The results were obtained from 3 independent biological experiments (n=200) with error bars indicating the standard deviations.

### 3.7 Discussion

In this chapter, I showed that blocking VSG synthesis significantly increased phagocytosis of bloodstream form *T. brucei* by macrophages but only in the presence of anti-VSG antibodies. These experiments highlighted the effectiveness with which wild-type bloodstream form *T. brucei* normally evades macrophage ingestion. Even after one hour of co-cultivation, only a small percentage of macrophages (2.7 ± 2.3%) had phagocytosed one or more trypanosomes. Phagocytosis levels remained low even with the opsonisation of active mouse complement. Although deposition of the alternative pathway components: C3b and Factor B components have been detected on the trypanosome surface, activation of the C3 convertase did not occur (Devine *et al*. 1986). The C4 binding protein, which features in both the classical and lectin pathway was also observed to bind to *T. brucei* surface, although complement activation never proceeded beyond that point due to unknown mechanisms (Dolinska *et al*. 2013). Recently, a GPI-anchored surface receptor known as the complement factor H (CFH) receptor has been identified in *T. brucei brucei* that binds host CFH (unpublished). Complement factor H is a complement alternative pathway regulator which prevents recognition of self-cells. If *T. brucei* could indeed bind host CFH, it would prevent the alternative complement pathway from progressing, thereby stopping lysis of the parasite. Similarly in my experiments, the effect of host complement could have been sequestered either by the CFH receptor or other unidentified factors, rendering the effect of complement alone ineffective.

Although complement proteins alone had a relatively minor effect, when added in combination with anti-VSG antibodies, the highest levels of phagocytosis were observed, with 16.4 ± 6.0% of the macrophages having internalised more than one flagellum. These results therefore emphasise the importance of host opsonins, specifically the classical pathway of

complement activation in the recognition and subsequent phagocytosis of trypanosomes by professional phagocytes including macrophages.

Macrophages have a range of surface receptors to bind host molecules, such as different types of Fc receptors, which bind the Fc regions of antibodies that have opsonised the surface of pathogens (Nimmerjahn & Ravetch 2007; Guilliams *et al*. 2014). Otherwise, macrophage binding to pathogens can occur through complement proteins deposited through the alternative or the classical pathway of complement activation. Both pathways converge at the point of C3 convertase generation. In the alternative pathway, complement C3 is first cleaved, and the opsonin C3b and its degradation products including iC3b are deposited directly on the microbial surface (Dunkelberger & Song 2010). Monocytes and macrophages have different surface receptors for these host proteins. These include CR1, CR3 and CR4 which bind the C3b and iC3b coated microorganisms, thereby facilitating recognition and phagocytosis (Bohlson *et al*. 2014). In the classical pathway, activation is initiated by binding of the complement protein C1q to the Fc region of antibodies opsonising the microbial surface, which can then be recognised by macrophage receptors including CR1 (Bohlson *et al*. 2014; Sarma & Ward 2011). The synergistic effect of adding both anti-VSG antibodies and normal mouse serum on trypanosome phagocytosis that I observed, was likely a consequence of improved macrophage recognition of parasites opsonised with antibodies as well as different types of complement proteins (including C3b, iC3b and C1q).

Blocking VSG synthesis for 8 hours did not result in a statistically significant increase in macrophage phagocytosis of *T. brucei*, despite this resulting in over 65% of the *T. brucei* population arresting precytokinesis. This was not significantly affected by the addition of normal mouse serum. However, in the presence of anti-VSG antibodies, there was a striking 3.4-fold increase in macrophage phagocytosis of trypanosomes. Classically activated

macrophages were able to internalise multiple trypanosomes, with many phagocytes ingesting more than four parasites. Even under optimal conditions, not all macrophages phagocytosed trypanosomes. This was presumably a consequence of heterogeneity in macrophage activation state after treatment with LPS and interferon γ, as appears to have been observed earlier in the mouse RAW264.7 cell line used in these studies (Noda & Amano 1997).

These experiments emphasised the vital importance for *T. brucei* of rapidly removing host opsonins from its surface, before these can be recognised by macrophage cell surface receptors. *In vivo*, the cell cycle arrest could be a safety mechanism to prevent the parasite to divide in the absence of a full VSG coat. These stalled cells could persist *in vitro* for days but in the presence of an active innate immune system, we showed that opsonins such as complement proteins and anti-VSG antibodies are more likely to adhere to the parasite surface and as a result, attract circulating macrophages to phagocytose the parasite. In the face of a VSG synthesis block, the ability to remove host opsonins may be impaired, resulting in enhanced phagocytosis. The mechanisms behind are still to be elucidated in the upcoming chapters.

# Chapter 4

# Mechanistic effects of a VSG synthesis block on *Trypanosoma brucei* immune evasion

## 4.1 Introduction

Bloodstream form *T. brucei* are known to have one of the highest rates of endocytosis amongst eukaryotes, a process which is crucial to the survival of the parasite in the host bloodstream (Engstler *et al*. 2004). Not only does the rapid endocytic process ensure efficient uptake of nutrients via the flagellar pocket, it also removes any attached host immune components from the parasite cell surface, serving as an important immune evasion mechanism in addition to antigenic variation (Natesan *et al*. 2011).

This high rate of VSG recycling in addition to quality control mechanisms, are key for trypanosome virulence, allowing trypanosomes to multiply without restriction in increasing titres of anti-VSG antibody (Balber *et al*. 1979; Engstler *et al*. 2004). It is only when anti-VSG antibody titres rise above a critical level that targeted trypanosomes are overwhelmed, and parasites expressing the predominant VSG variant are eradicated. High rates of VSG recycling therefore function as a 'coat-cleaning' mechanism to ensure rapid removal of lethal immune complexes from the cell surface (Engstler *et al*. 2007). Motility of the trypanosome appears to facilitate this process. It has been proposed that the hydrodynamic forces generated by a swimming trypanosome would preferentially push VSG-antibody complexes back through the VSG layer towards the flagellar pocket where they are endocytosed (Engstler *et al*. 2007).

As was shown in the previous chapter, the increase of parasite phagocytosis by macrophages after blocking VSG synthesis was largely attributed to the opsonisation with anti-VSG antibodies. However, little is known about the surface of the trypanosome after the

induction of *VSG* RNAi. It has been proposed that the cell cycle arrest acts as a protective mechanism to preserve membrane integrity and prevent severe dilutions to the VSG coat (Sheader *et al*. 2005). Questions such as whether the "coat cleaning" host protein removal mechanism is affected and whether motility of the parasite plays a role in maintaining survival are yet to be explored.

### 4.2 Experimental outline

This chapter aims to delineate the mechanisms behind the enhanced phagocytosis of trypanosomes in the presence of anti-VSG antibodies. I first examined whether antibody clearance by *T. brucei* was affected by the VSG synthesis block both qualitatively by immunofluorescence microscopy and quantitatively by flow cytometry. Since it was shown in (Sheader *et al*. 2005) that both flagellar pockets in the arrested precytokinesis cells remained functional after the induction of *VSG* RNAi, I also investigated whether other forms of endocytosis were affected. Lastly, as motility is essential in bloodstream form *T. brucei* and crucial for the clearance of surface antibodies, different parameters of trypanosome swimming after a VSG synthesis block were measured and analysed.

### 4.3 Blocking VSG synthesis results in reduced clearance of surface-bound anti-VSG221 antibodies

Endocytosis in *T. brucei* can be stopped effectively at low temperatures and at 4°C, molecules can enter the flagellar pocket but further entry into the endocytic system is not possible (Engstler *et al*. 2004). To investigate antibody clearance in our stalled cells, *VSG221* RNAi was first induced for 8 hours. Cells were then cooled to 4°C to allow the binding of anti-VSG221 antibodies. These opsonised cells were subsequently transferred to 37°C to reactivate endocytosis for varying lengths of time before quenching the process by cooling the cells to 4°C again. As a result, a snapshot of the surface antibody clearance was captured and analysed using immunofluorescence microscopy (Figure 4.1). *T. brucei* where no VSG synthesis inhibition was induced, were able to remove almost all anti-VSG221 antibodies within 8 minutes of reactivation of endocytosis (Figure 4.1A). After 8 hours of *VSG221* RNAi induction however, the rate of antibody clearance was greatly impaired. To confirm that the reduction of antibody removal was not the indirect consequence of the growth arrest, I also examined the rate of antibody clearance in the *T. brucei* 90-13TDPC1 cell line. RNAi was induced in this cell line against the chromatin protein gene *TDP1*. *TDP1* is an essential gene encoding an architectural chromatin protein, which has no direct role in VSG trafficking or cellular architecture (Narayanan & Rudenko 2013). The induction of *TDP1* RNAi resulted in a growth arrest 24 hours post-induction but did not appear to alter the rate of anti-VSG221 antibody removal, which occurred within 4 minutes of reinitiation of endocytosis (Figure 4.1B).

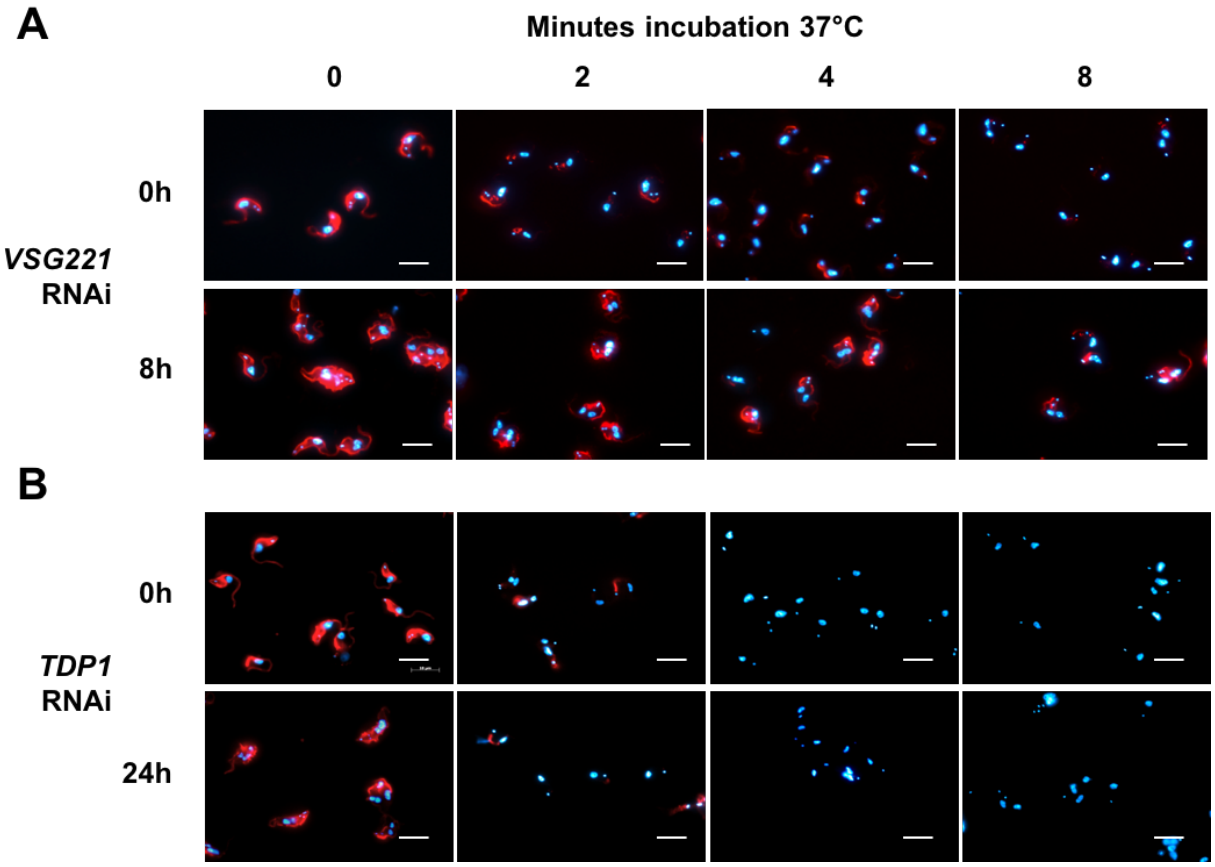



**Figure 4.1. Immunofluorescence microscopy analysis of surface anti-VSG221 antibody clearance by *T. brucei*.**

**(A)** *VSG221* RNAi was induced in *T. brucei* 221VB1.2 for 8h. Cells were harvested and cooled to 4°C to stop endocytosis and to allow the binding of anti-VSG221 antibody. Endocytosis was resumed by transferring cells to 37°C for 0, 2, 4 and 8 min. Cells were immediately fixed afterwards, followed by the binding of the secondary goat anti-rabbit Alexa594 antibody (red) to visualise the remaining anti-VSG221 antibody on the parasite surface using immunofluorescence microscopy. **(B)** The *T. brucei* 90-13TDPC1 cell line was used as control cell line for the non-specific effects of RNAi induced gene knockdown. *TDP1* is an essential gene, which when knocked down, produced a growth arrest within 24h. Scale bar: 10 μm.

As shown in Figure 3.1B, over 65% of cells stalled precisely before cytokinesis at the 2N2K stage, with no further initiation of DNA synthesis. Since the post-VSG RNAi cell population was dominated by these stalled cells, I investigated whether the reduction in antibody clearance was the consequence of the accumulation of 2N2K cells. The rate of antibody clearance in different cell cycle stages was quantitated using flow cytometry. The anti-VSG221 antibodies were visualised using a secondary antibody coupled to Alexa Fluor 488, and trypanosome DNA content was monitored using the propidium iodide stain (Figure 4.2).

From the flow cytometry dot plots, there was no evidence that the rate of antibody clearance differed significantly between cell cycle stages in untreated cells, although it appeared to be slightly slower in 2N2K (G2/M) cells. These cells were able to clear the majority of the surface bound antibodies within 8 minutes (Figure 4.2A), similar to the results obtained from the immunofluorescence microscopy analysis. After the induction of *VSG221* RNAi however, the overall rate of antibody removal decreased significantly. This is particularly striking in the G2/M cells, where even after 16 minutes of reactivation of endocytosis, there was still remaining antibody on the cell surface. Induction of *TDP1* RNAi on the other hand, did not affect the clearance of antibodies from the trypanosome cell surface and showed a comparable degree of antibody removal compared to untreated cells (Figure 4.2B).

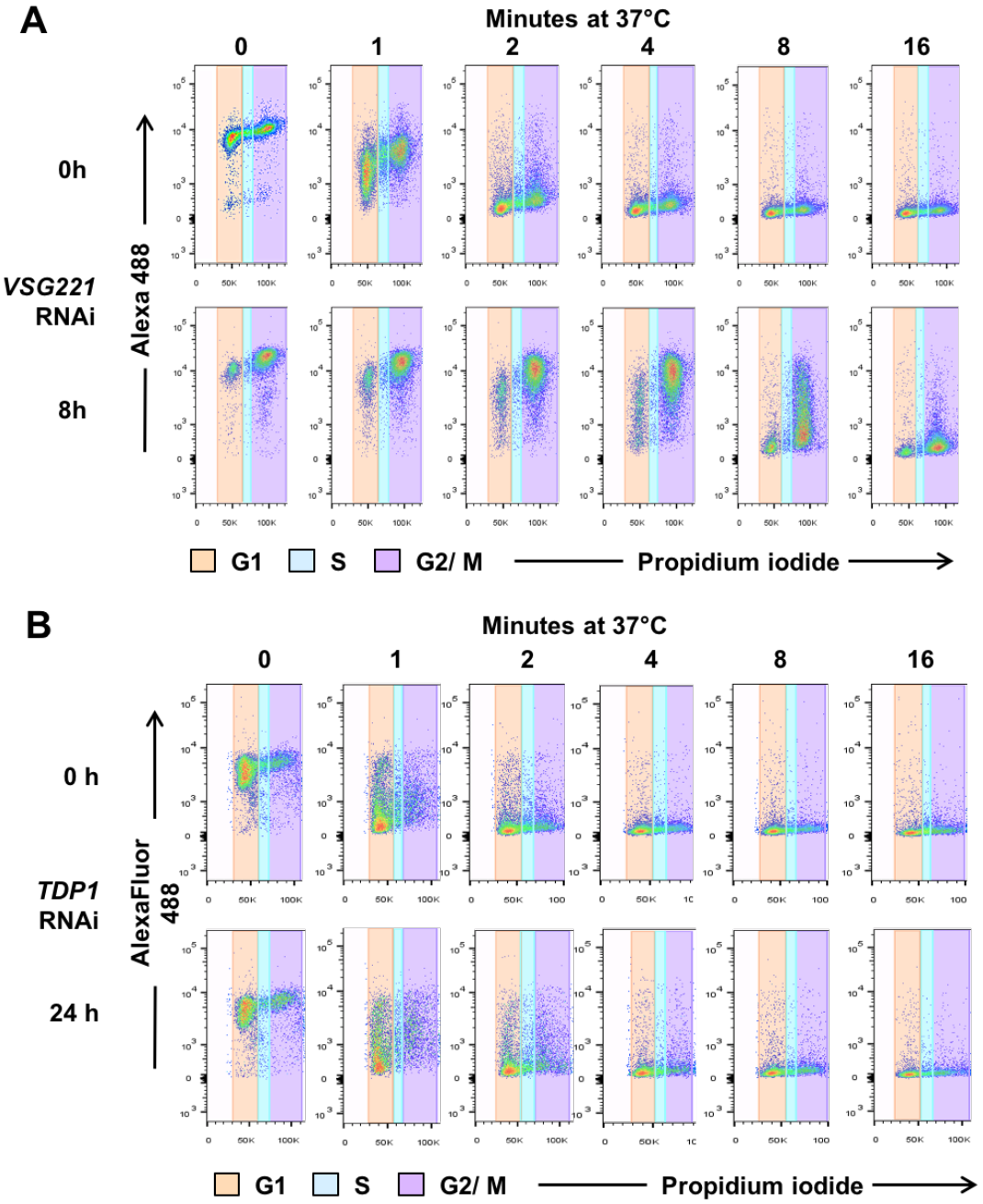



**Figure 4.2. Flow cytometry analysis of the surface clearance of anti-VSG221 antibodies after blocking VSG synthesis.** RNAi was induced against **(A)** *VSG221* in *T. brucei* 221VB1.2 for 0 or 8h or against **(B)** *TDP1* in the *T. brucei* 90-13TDPC1 cell line for 0 or 24h. The cells were cooled to 4ºC to stop endocytosis, and then coated with anti-VSG221 antibodies. Cells were next incubated at 37ºC to reinitiate endocytosis for 0, 1, 2, 4, 8 and 16 minutes. The reaction was subsequently stopped, and the cells were fixed and stained with an AlexaFluor 488 coupled secondary antibody. To visualise DNA content, the cells were simultaneously stained with propidium iodide. The amount of surface anti-VSG221 antibody was determined at the G1 (orange), S (blue) or G2/ M (purple) cell cycle stages.

To obtain a more quantitative measure of the rate of antibody clearance, all mean fluorescence intensity (MFI) values were expressed as a percentage value of that at 0 minute (Figure 4.3). Quantitation of the rate of antibody clearance by trypanosomes at different cell cycle stages showed G2/M cells indeed remove anti-VSG221 antibodies marginally slower than cells at the G1 and S-phase (Figure 4.3A). Basal level of fluorescence from VSG221 antibodies was reached 4 minutes after the reinitiation of endocytosis. After VSG synthesis had been blocked for 8 hours, the rate of antibody removal slowed but only marginally in the G1-phase. This effect was more prominent in S-phase cells but most striking in cells at the G2/M phase. Again, the induction of *TDP1* RNAi had no effect on the rate of antibody removal in all three cell cycle stages (Figure 4.3B).

The half-life of the anti-VSG antibody in the whole population is 36.7 ± 3.7 seconds (Figure 4.3C), which was comparable to the value of 35.3 ± 4.6 seconds found by the Engstler laboratory using polyclonal anti-VSG IgG antibodies (Engstler *et al*. 2007). When the different cell cycle stages were investigated individually, the half-life of the anti-VSG antibody was comparable between the different cell cycle stages, and ranged from 34.3 ± 3.5 seconds for cells in G1, to 39.8 ± 4.7 seconds for cells in S-phase and 39.3 ± 4.2 seconds for cells at G2/M.

However, in cells that were stalled after blocking VSG synthesis, I found significantly reduced clearance of anti-VSG antibodies at all stages of the cell cycle, with an average for the whole population of 79.0 ± 12.8 seconds (Figure 4.3C). If the different cell cycle stages were analysed individually, the half-life increased from 43.6 ± 4.4 seconds for cells in G1 to 75.1 ± 12.5 seconds for cells in S phase, and 99.2 ± 15.9 seconds for cells in G2/M. In the G2/M cell cycle stage anti-VSG antibody clearance was particularly decreased compared with uninduced cells at this cell cycle stage. Again, to ensure that I was monitoring a specific consequence of blocking VSG221 synthesis rather than lethality, the rate of internalisation of anti-VSG221

antibodies after knocking down the highly essential chromatin protein TDP1 was also determined (Narayanan & Rudenko 2013). *TDP1* knock-down also resulted in growth arrest, although not the highly specific precytokinesis cell cycle arrest observed after the induction of *VSG* RNAi, which is to the best of my knowledge unique (Sheader *et al*. 2005; Narayanan & Rudenko 2013). Despite the induction of a rapid growth arrest after *TDP1* knock-down, there was no significant change in the rate of clearance of anti-VSG221 antibodies (41.1 ± 4.0 seconds) (Figure 4.3D).

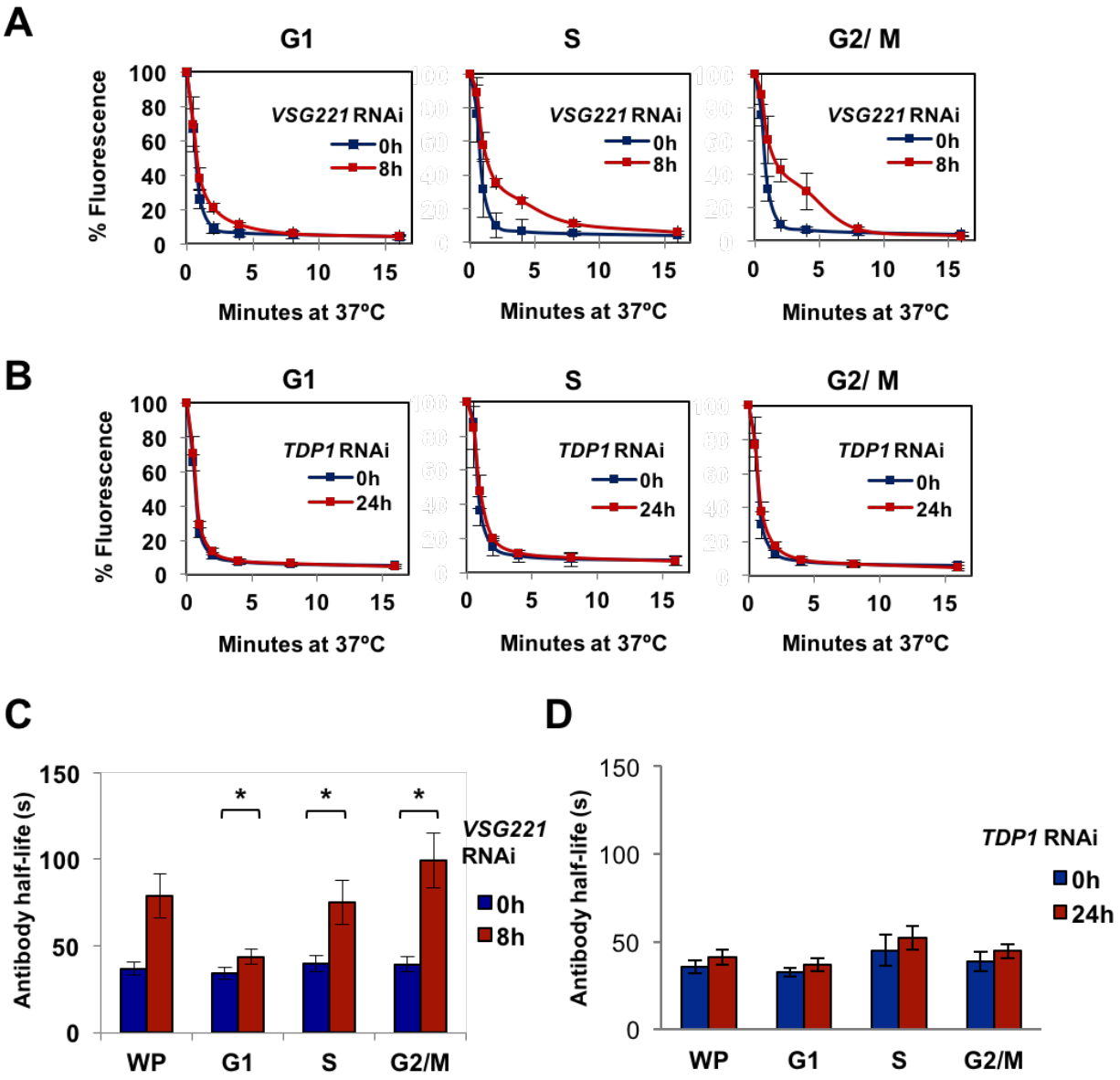



**Figure 4.3. Quantitation of the reduced clearance of anti-VSG221 antibody after blocking (A) VSG221 or (B) TDP1 synthesis.** Surface anti-VSG221 antibody was detected using an Alexa 488-conjugated secondary antibody, and total fluorescence was quantitated by flow cytometry. Mean fluorescence intensity values are expressed as a percentage of the value at 0 minutes. Results shown are the mean of three independent biological replicates with the standard deviation indicated with error bars.

Quantitation of the half-life of anti-VSG221 antibodies after inducing **(C)** *VSG221* RNAi or **(D)** *TDP1* RNAi. Results shown are the mean of three independent biological replicates with the standard deviation indicated with error bars. After fitting each data set to the non-linear regression model, statistical analysis was performed using the Student's t-test *P<0.05.

### 4.4 Decrease in surface VSG corresponded to an increase in anti-VSG antibody binding to the trypanosome surface

A phenomenon that I have observed from the antibody clearance experiments was the apparent increase in antibody binding to the trypanosome cell surface in cells where *VSG221* RNAi had been induced, compared to uninduced cells. To confirm this observation, the total amount of VSG221 in these cells was quantitated using LiCor imaging (Figure 4.4A). The *T. brucei* cell lines SM221pur (expressing VSG221) and HN1(V02+) (expressing VSGVO2) were used as positive and negative controls respectively. Two-fold dilutions of trypanosome cell extract containing 2 x $10^4$ cells were analysed and the amount of VSG221 protein was normalised to that of the *T. brucei* heat shock protein 70 (Hsp70). When VSG synthesis had been blocked for 8 hours, the total amount of VSG decreased to 64 ± 12% of normal levels (Figure 4.4B).

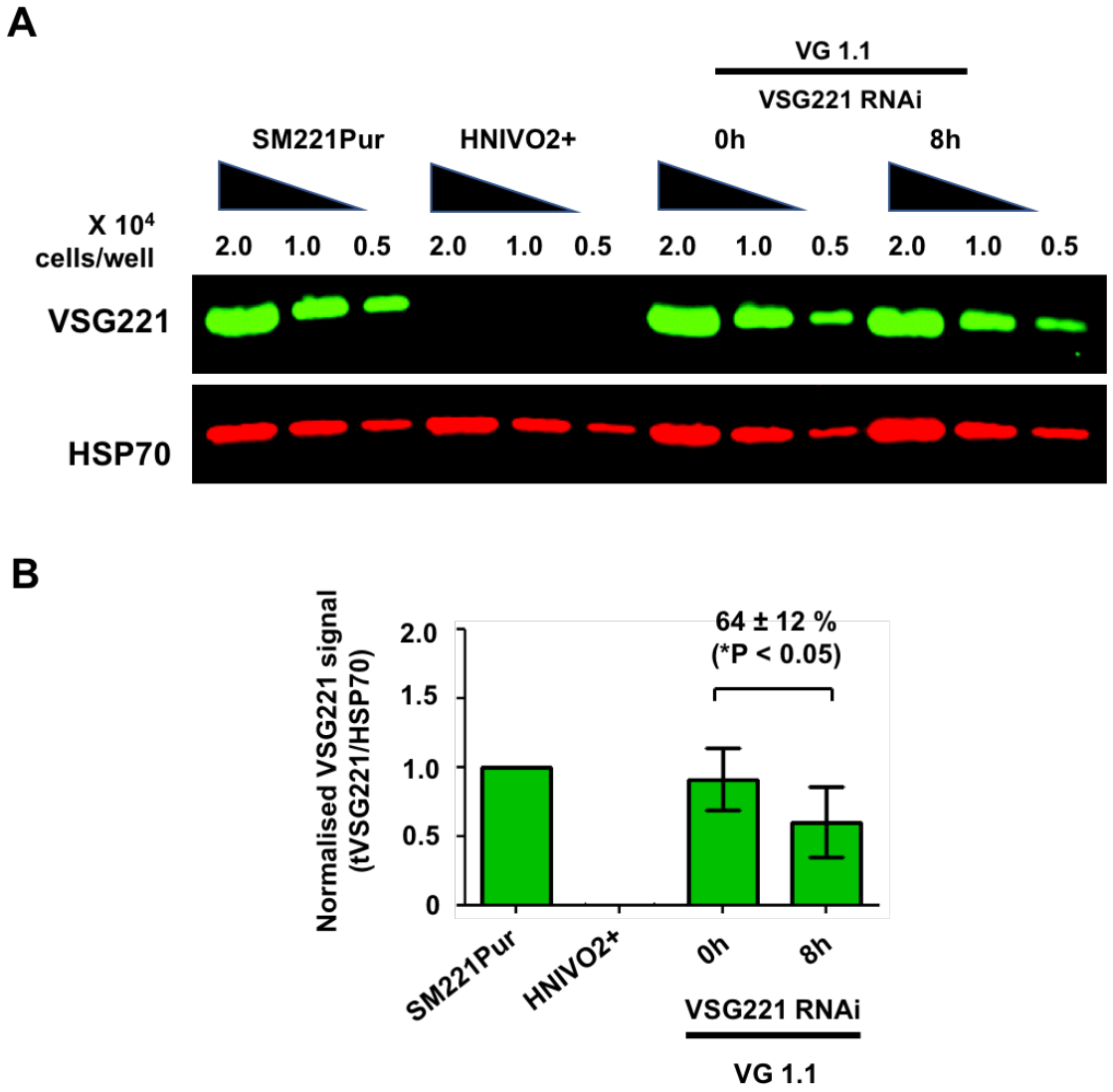



**Figure 4.4. Total amount of VSG221 protein decreased after 8h of *VSG*221 RNAi induction.**

**(A)** Quantitation of total VSG221 in *T. brucei* after the induction of *VSG221* RNAi for eight hours, using LiCor analysis of protein lysates. Two-fold dilutions of *T. brucei* cell extract containing 2 x $10^4$ cells per well are analysed. The *T. brucei* SM221pur cell line expresses VSG221 and *T. brucei* HN1(V02+) expresses VSGV02 (66). The BF *T. brucei* 221VG1.1 is analysed before or after the induction of *VSG221* RNAi for eight hours. The Hsp70 protein was used as a loading control (40).

**(B)** Quantitation of the total amount of VSG221 protein normalised to Hsp70.

**Note**: experiments presented in Figure 4.4 was performed with the help of Dr. CP Ooi and published in (Cheung *et al*. 2016)

Even though the total pool of VSG had reduced after blocking VSG synthesis, it was unclear whether the reduction was on the cell surface or within the endocytic pathway. Therefore, I also measured the amount of surface VSG using biotinylation. *T. brucei* 221VB1.2 cells were cooled to 4 ºC to stop endocytosis and labelled with biotin, followed by flow cytometry analysis to determine the amount of surface VSG. As indicated in Figure 4.5A and Table 4.1, the amount of surface VSG dropped 33% after 8 hours induction of a VSG synthesis block. Equivalent values were obtained if the different cell cycle stages were analysed separately. However, when the amount of anti-VSG221 antibodies was quantitated, approximately twice as much bound to the surface of cells where *VSG* RNAi had been induced (Figure 4.5B). This was particularly apparent in the G2/ M cell cycle stage (213 ± 41%). As I had previously established that blocking VSG synthesis resulted in a moderate reduction in VSG on the cell surface, this observed increase in antibody binding is presumably a consequence of reduced VSG coat density exposing previously inaccessible VSG epitopes to recognition by the polyclonal anti-VSG antibodies.

Gathered from the data so far, the blocking of VSG synthesis caused a moderate reduction of VSG density on the trypanosome cell surface, which resulted in not only the impairment of antibody clearance, but also a drastic increase in anti-VSG antibody binding.

| Cell population | Percentage decrease in surface VSG biotinylation | Percentage increase in αVSG221 antibody binding |
|---|---|---|
| G1 | 34% | 49% |
| S | 31% | 28% |
| G2/M | 36% | 95% |
| Total | 33% | 113% |

**Table 4.1. Changes in the amount of surface VSG versus the amount of anti-VSG221 antibody binding after the induction of *VSG221* RNAi for 8h.** Quantitation of surface VSG was measured by biotinylation, whereas surface antibody binding was assessed using a polyclonal anti-VSG221 antibody. *T. brucei* DNA was simultaneously stained with propidium iodide and cells were analysed according to respective cell cycle stage: G1, S and G2-M. The overall changes in biotinylation and antibody binding are indicated under "Total". Changes in raw mean fluorescence values after the induction of *VSG221* RNAi (8h) are expressed as a percentage of the uninduced control (0h).

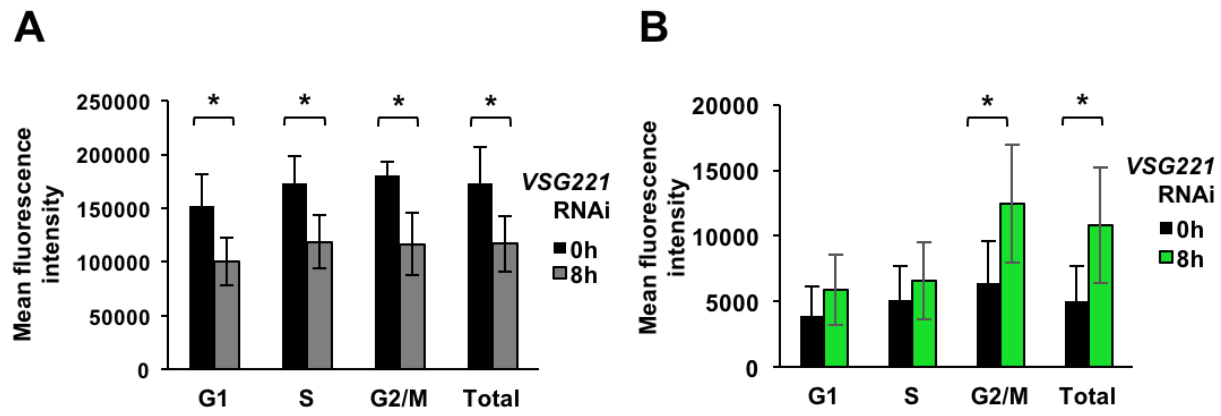



**Figure 4.5. Biotinylation of surface VSG decreased while anti-VSG221 antibody binding increased following the induction of *VSG221* RNAi**

**(A)** The amount of VSG present on the *T. brucei* surface after the induction of VSG RNAi for 8h was assessed using biotinylation. *T. brucei* 221VB1.2 cells were cooled to 4 °C to stop endocytosis, and biotinylated using 1 mM biotin. Cells were fixed, and biotinylation of surface VSG was detected using Alexa488-conjugated streptavidin and quantitated by flow cytometry. *T. brucei* DNA was simultaneously stained with propidium iodide and cells were analysed according to respective cell cycle stage: G1, S and G2-M. The overall change in biotinylation of the whole population is indicated under "Total". Results shown are the mean of three independent biological replicates with the standard deviation indicated with error bars. Statistical analysis was performed using the Student's t-test *P<0.05.

**(B)** Quantification of anti-VSG221 antibody on the trypanosome cell surface in the presence or absence of *VSG221* RNAi for 8 hours. Cells were incubated with anti-VSG221 antibody at 4°C. Surface antibody binding was detected using an Alexa 488-conjugated secondary antibody, and total fluorescence was quantitated by flow cytometry. Results shown are the mean of three independent biological replicates with the standard deviation indicated with error bars. Statistical analysis was performed using the Student's t-test *P<0.05.

As it was now established that there was reduced clearance of anti-VSG antibodies after induction of a VSG synthesis block, I investigated if this effect was due to a reduction in the rate of internalisation of total surface VSG rather than specifically antibody bound VSG. Cells were again cooled to 4ºC to stop endocytosis, before surface VSG was biotinylated (Engstler *et al*. 2004). Cells were subsequently transferred to 37ºC to reinitiate endocytosis for varying lengths of time. Endocytosis was then stopped again and the external biotin was stripped off. This was followed by the fixation and permeabilisation of the cells, which were then incubated

with streptavidin-Alexa Fluor 488 to quantitate the amount of internalised biotinylated VSG by flow cytometry.

However, even after blocking VSG synthesis for 8 hours, the amount of surface VSG that was internalised had not significantly decreased. The half-time of biotinylated VSG internalisation in untreated cells was 23.7 ± 6.1 seconds versus 28.4 ± 7.5 seconds after the induction of *VSG221* RNAi. (Figure 4.6). This demonstrated that in cells arrested by the induction of *VSG221* RNAi, there was a specific reduction in the rate of internalisation of VSG-antibody complexes, rather than a general decrease in the rates of internalisation of all surface VSG.

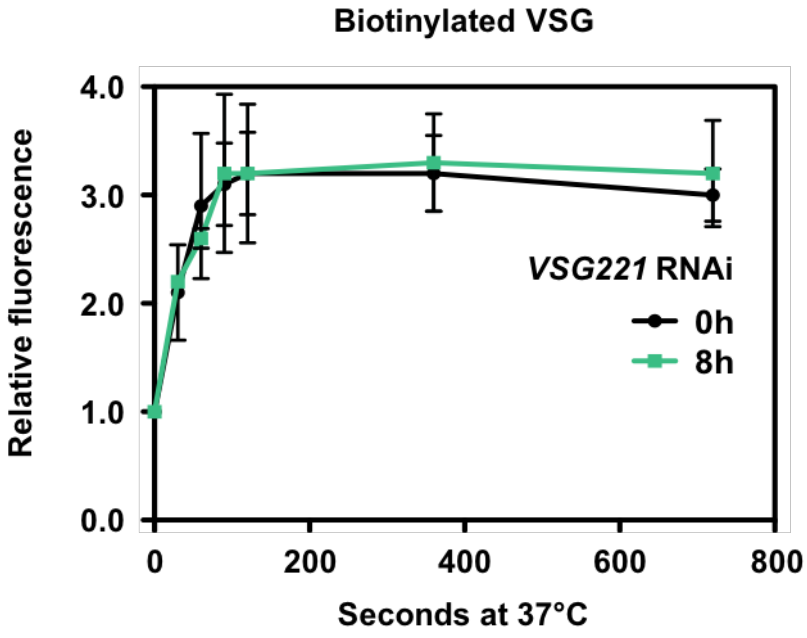



**Figure 4.6. Rate of biotinylated VSG internalisation was unchanged after blocking VSG synthesis.** VSG synthesis was blocked in *T. brucei* 221VB1.2 cells for 8h. Endocytosis was stopped by cooling the cells to 4ºC. Cells were labelled with biotin, and transferred to 37ºC for 0, 30, 60, 90, 180, 360 or 720 seconds to reactivate endocytosis. Remaining surface biotin was removed by the addition of ice cold stripping buffer. Cells were then fixed, permeabilised and incubated with Alexa Fluor 488-conjugated streptavidin. Mean fluorescence intensity (MFI) values were normalised against that of time point 0 seconds. Error bars show the standard deviation of three independent biological replicates.

### 4.5 Blocking VSG synthesis results in impairment of internalisation but not the degradation of anti-VSG antibodies

Although anti-VSG antibody removal from the trypanosome cell surface was shown to be impaired after the induction of *VSG221* RNAi, it was unclear whether this reduction was due to a restriction at the flagellar pocket, preventing the entry of VSG-antibody complexes, or complications further along within the endocytic pathway. I therefore, monitored the internalisation of VSG-antibody complexes using immunofluorescence microscopy. Similar to previous experiments, trypanosomes were first cooled to 4 ºC to stop endocytosis before reactivation by transferring the cells to 37 ºC.

In theory, after resuming endocytosis, the VSG-antibody complexes should enter the cell via the flagellar pocket and progress first through the early, then the late endocytic compartments. The anti-VSG antibodies would then be stripped off the VSG molecules and targeted for degradation within the trypanosome lysosome. However, in order to visualise the accumulation of VSG-antibody complexes in the lysosome, the degradation process was inhibited using the FMK-024 inhibitor. FMK-024 is a lysosomal thiol protease inhibitor that blocks the cathepsin protease TbCat L, allowing the detection of accumulated anti-VSG antibodies in the *T. brucei* lysosome.

As expected, after restarting endocytosis, anti-VSG antibodies (in green) were removed rapidly from the cell surface within 2 minutes (Figure 4.7). The lysosomal compartment was visualised using the lysosomal marker, p67 (in red). In uninduced cells, accumulation of anti-VSG221 antibodies was detected after 8 minutes of reinitiation of endocytosis, where the co-localisation of anti-VSG211 antibodies and p67 was indicated in yellow. After VSG synthesis was blocked, internalisation of VSG221 antibodies still occurred through the flagellar pocket but at a significantly reduced rate. VSG221 antibodies did not reach the lysosomal

compartment until after 16 minutes of reactivation of endocytosis, taking twice as long as untreated cells.

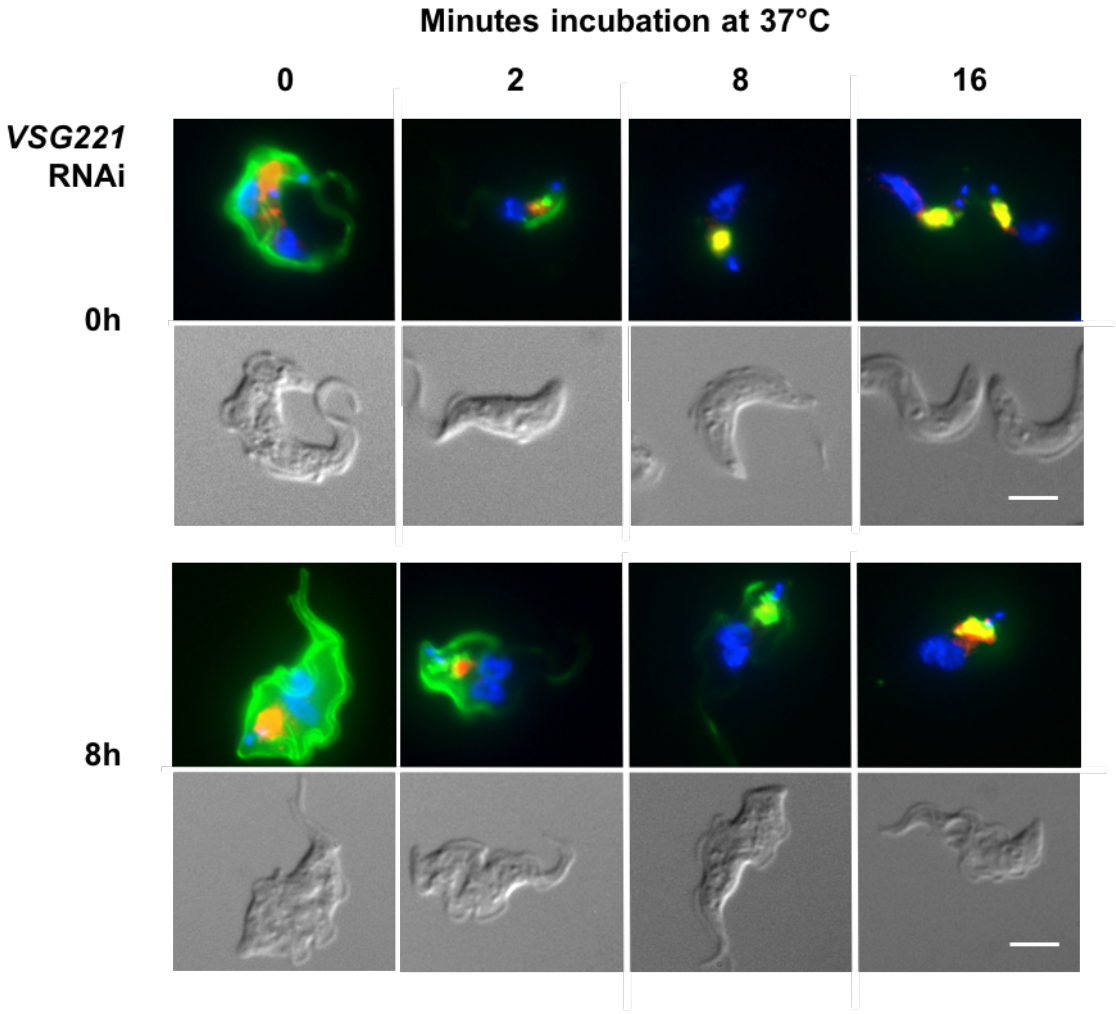



**Figure 4.7. Blocking VSG synthesis impaired the internalisation of VSG221 antibodies**
VSG221 synthesis was blocked in *T. brucei* 221VB1.2 cells by the induction of *VSG221* RNAi for 8h. Cells were coated with an anti-VSG221 antibody at 4ºC, and then transferred to 37ºC to reinitiate endocytosis for 0, 2, 8 and 16 minutes. The lysosomal thiol protease inhibitor FMK-024 was used to inhibit degradation of anti-VSG antibody in the lysosomal compartment, and facilitate its visualisation. Cells were then fixed and stained with an Alexa Fluor 488 coupled secondary antibody (green). The lysosomal compartment was visualised with an antibody against the p67 lysosomal protein stained with an Alexa Fluor 594 coupled secondary antibody (red). The merge of the two signals is shown in yellow. Below are shown panels of the trypanosomes visualised using differential interference contrast. Scale bar: 5 µm.

### 4.6 The early endocytic pathway was not significantly affected by the VSG synthesis block

Endocytosis in bloodstream form *T. brucei* is restricted to the flagellar pocket, and is involved in the removal of surface bound host antibodies, nutrient uptake and the maintenance of homeostasis of the cell surface proteome (Gadelha *et al*. 2015; Shimogawa *et al*. 2015). To determine whether the early endocytic pathway was affected in the stalled cells, the rates of receptor mediated endocytosis were measured by following the uptake of transferrin and tomato lectin, and fluid phase endocytosis was monitored by dextran uptake.

Using flow cytometry to quantify the uptake of human transferrin conjugated to Alexa Fluor 488 fluorescent transferrin, I showed that the half-life of transferrin increased from 1.1 ± 0.3 minutes to 3.3 ± 1.1 minutes, however this result was not statistically significant (Figure 4.8A). Uptake of other endocytic makers was also not significantly affected by the induction of *VSG* RNAi. Receptor-mediated endocytosis was monitored with tomato-lectin coupled to Alexa Fluor 488, which showed an increase in half-life from 3.5 ± 4.2 minutes to 1.5 ± 1.3 minutes (Figure 4.8B). Similarly, fluid phase endocytosis, as monitored by uptake of dextran-Alexa Fluor 488 was also not significantly changed in the stalled cells (7.9 ± 6.3 minutes in cells where *VSG* RNAi had been induced compared with a half-life of 8.3 ± 5.0 minutes in untreated cells) (Figure 4.8C). These results therefore did not provide evidence for a clear impairment in the early endocytic pathway in cells stalled after the induction of a VSG synthesis block.

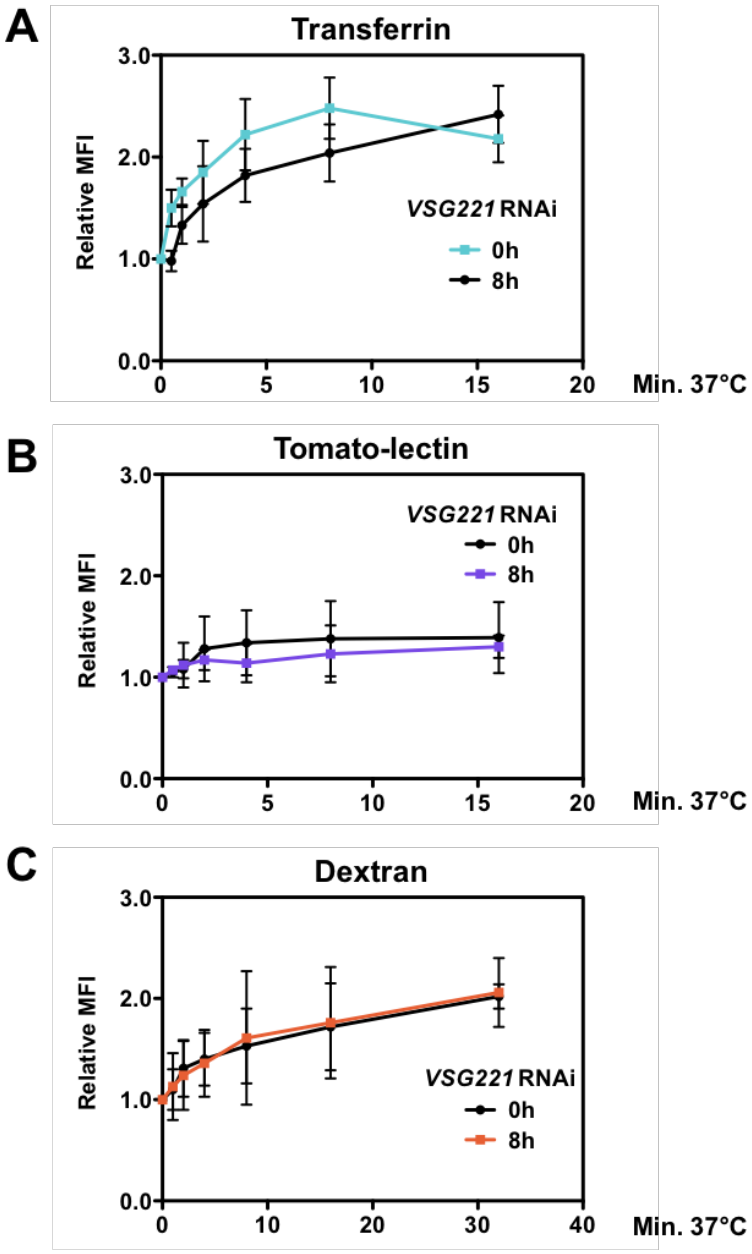



**Figure 4.8. The rate of transferrin, tomato-lectin and dextran internalisation was unaffected by *VSG221* RNAi induction.**

Internalisation of **(A)** transferrin, **(B)** tomato-lectin and **(C)** dextran after the induction of a VSG synthesis block. Cells were incubated with Alexa Fluor 488-conjugated transferrin or Dylight 488-coupled tomato-lectin or Alexa Fluor 488 conjugated dextran at 4ºC. Cells were then transferred to 37ºC to reinitiate endocytosis for the time indicated in minutes. Cells were subsequently fixed and analysed by flow cytometry. Mean fluorescence intensity values were normalised against that of the time point 0 minutes. The standard deviation of three independent biological replicates is indicated with error bars.

### 4.7 Blocking VSG synthesis increased trypanosome swim velocity

Motility is essential for bloodstream form *T. brucei* as it is involved in a wide range of cellular activities, including cell cycle progression, cytokinesis and establishing virulence in the host (Ralston *et al*. 2006; Broadhead *et al*. 2006). Forward motility, as proposed by Engstler *et al* (Engstler *et al*. 2007), is also responsible for the removal of surface bound host opsonins. As the trypanosome swims forward, the hydrodynamic forces created by the forward motion contribute to the preferential backward movement of VSG-antibody complexes into the flagellar pocket. Since motility plays a vital role in the clearance of anti-VSG antibodies, I examined how it was affected after the induction of *VSG* RNAi.

The motility of the trypanosomes was monitored using time-lapse live cell videomicroscopy, where cells were observed under bright-field microscopy in a sealed heated chamber and images were captured every 200 milliseconds for 1.7 minutes (512 frames). Using an intensity maxima algorithm, each cell was identified and their particle tracks were constructed. Through this algorithm, several parameters: cell swim speed, swim velocity and swim directionality were calculated.

Analysis of the whole population did not show a significant change in average swim speed after the induction of *VSG221* RNAi. The distribution of accumulated observation time at each speed interval showed that most uninduced cells spent the most time swimming at 1.4 μm/ s and there was a slight decrease in swim speed to 1.3 μm/ s after blocking VSG synthesis (Figure 4.9A and B). Similarly, the average swim speed of uninduced cells versus that of *VSG221* RNAi induced cells did not change significantly; 1.6 ± 0.014 μm/ s versus 1.7 ± 0.019 μm/ s. Arresting VSG synthesis resulted in a population of stalled trypanosomes that predominantly (>65%) consisted of cells that had arrested before cytokinesis. These stalled cells were characterised by a broader and rounder cell shape, with two external flagella.

Therefore, I investigated the effects on trypanosome swim speed in a cell population dominated by bi-flagellated cells. Only cells with two external flagella were selected from the captured images and their tracks were analysed. Here too, there was no significant change in swim speed after the induction of a VSG synthesis block (1.45 µm/ s vs 1.58 µm/ s).

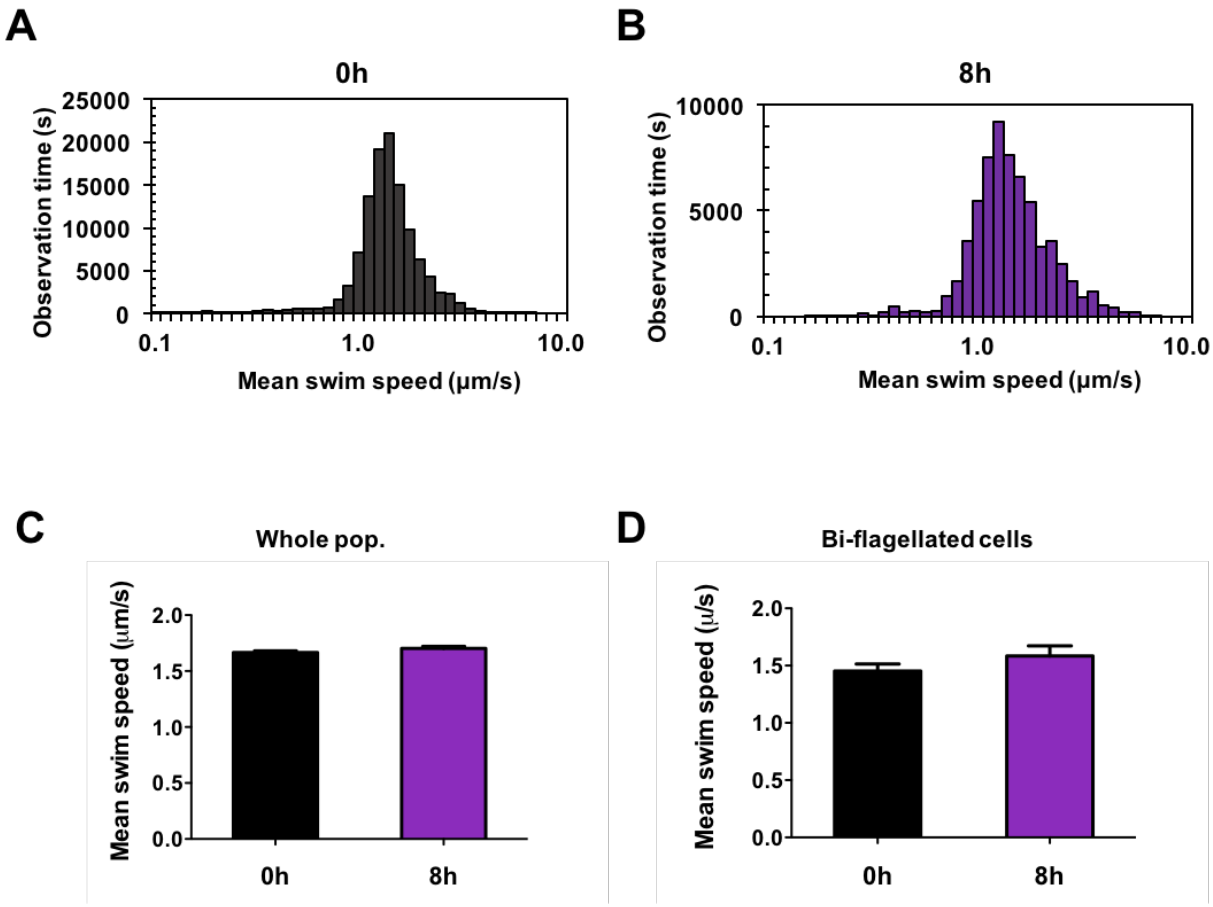



**Figure 4.9. *T. brucei* swim speed was not affected by the VSG synthesis block.**
Histograms showing the distribution of *T. brucei* average swim speed (µm/s) after **(A)** 0h and **(B)** 8h of *VSG221* RNAi induction. The average swim speed within the capture time of 1.7 min for each particle track was calculated and plotted against the accumulated observation time (s) at each swim speed interval. 1500 particle tracks were analysed.
Average swim speed of the **(C)** whole *T. brucei* population and **(D)** bi-flagellated cells after 0h and 8h of *VSG221* RNAi. 1500 particle tracks were analysed and the standard deviation is indicated with error bars.

### 4.8 *VSG221* RNAi induction resulted in reduced tumbling and increased directional swimming

Interestingly, in the population of cells where VSG synthesis had been blocked, there was a clear difference in swimming behaviour as illustrated by the particle motion track plots (Figure 4.10A and B). *T. brucei* motility is known to change depending on the viscosity of the medium; the more viscous the external environment, the more directional the swimming (Engstler *et al*. 2007; Bargul *et al*. 2016). Although tissue culture medium is less viscous compared to blood, it was used in these experiments to replicate the condition of the macrophage phagocytosis assay. In this low viscosity medium, the preferred mode of swimming is tumbling for the majority of uninduced cells, as observed in previous studies of bloodstream form *T. brucei* under standard tissue culture conditions (Engstler *et al*. 2007). However, after blocking VSG synthesis for 8 hours, trypanosomes swam in a much more directional manner, as illustrated by the longer particle tracks (Figure 4.10B).

In light of this, I measured average trypanosome velocity, which is defined as speed in a given direction, or total displacement over track length. In contrast to average speed, which is total distance travelled over track length without considering directionality, the measurement of velocity would include a directional component. After blocking VSG synthesis for 8 hours, the average trypanosome velocity significantly increased from 0.55 ± 0.01 μm/s to 0.90 ± 0.02 μm/s, reflecting the increased directionality of movement (Figure 4.10C). Again, I investigated if this was due to the accumulation of bi-flagellated cells in our arrested population, but found a similar increase in velocity after the induction *VSG* RNAi in these bi-flagellated cells from 0.50 ± 0.06 μm/s to 0.84 ± 0.08 μm/s.

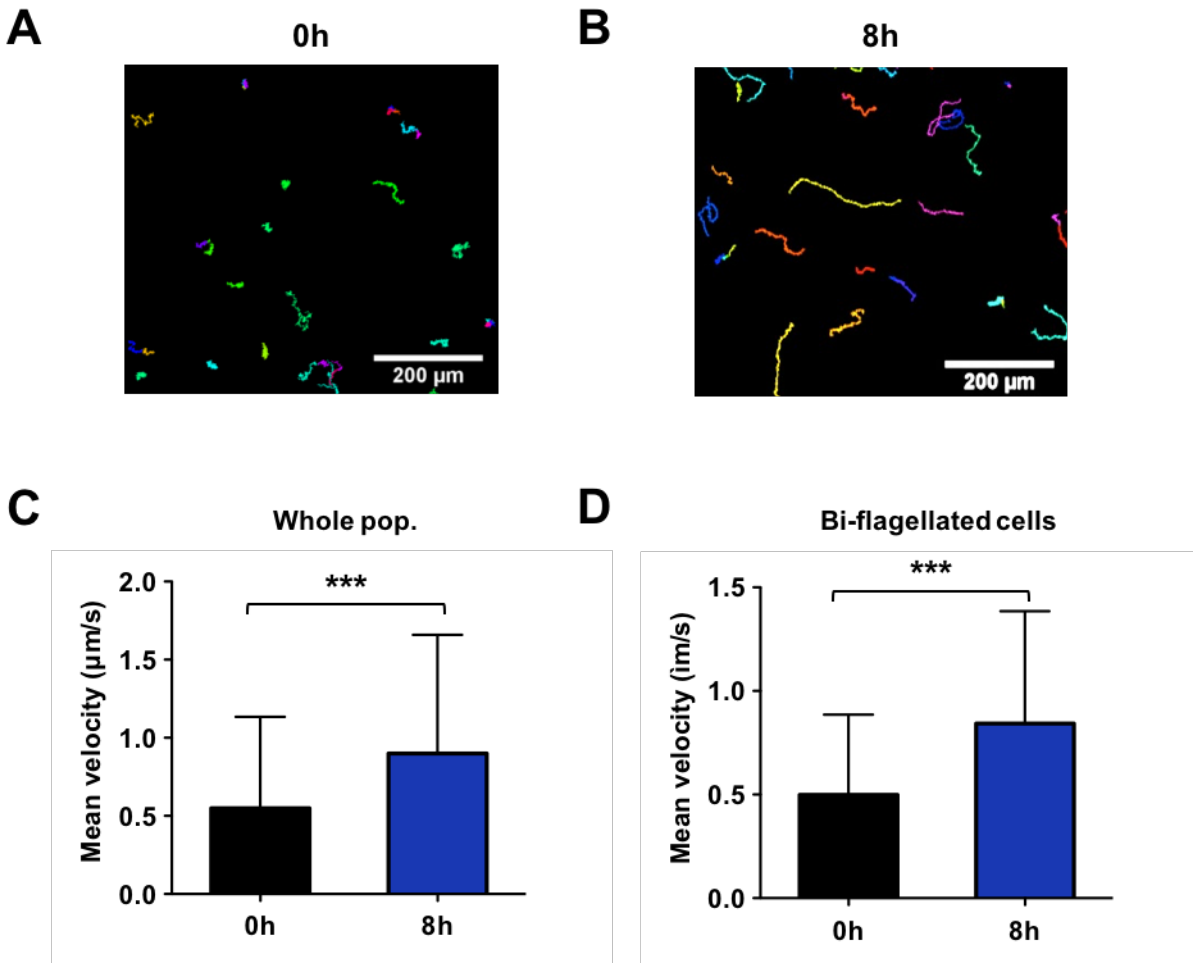



**Figure 4.10. *T. brucei* swim velocity increased after 8h of VSG synthesis block.**
Particle motion tracks of cells where *VSG221* RNAi was induced for **(A)** 0h or **(B)** 8h. Each track represents the distance travelled by an individual cell over the course of measurement. One image was captured every 200 ms (5 Hz) for 1.7 minutes. Scale bar: 200 µm.
Average swim velocity of the **(C)** whole *T. brucei* population and **(D)** bi-flagellated cells after 0h and 8h of *VSG221* RNAi. 1500 particle tracks were analysed and the standard deviation is indicated with error bars. Statistical analysis was performed using the Student's t-test ***P<0.0001.

These results were confirmed by the measurements of average angular persistence. Angular persistence is a mathematical description for how the direction of motion of the cell changes over time (Zaburdaev *et al*. 2011). In this case, directionality was denoted on an arbitrary scale of -1 to 1, where each particle track corresponds to a swimming trypanosome. A value of 1 indicates directional swimming, whereby cells observed after a 2 second period swim in the same direction as in the previous 2 second period. A value of 0 represents random movement (tumbling), whereby the movement of the cell observed after a 2 second period is completely random in direction compared with the previous 2 second period. A value of -1 indicates a reversal in swimming direction, whereby the cell observed after a 2 second period has moved in the reverse direction.

As observed in the particle tracks (Figure 4.10A and B), bloodstream form *T. brucei* primarily tumbled under standard *in vitro* culturing conditions with average angular persistence values of -0.07 ± 0.006 (Figure 4.11A). However, after the induction of *VSG221* RNAi, the average angular persistence increased to 0.20 ± 0.008 units, reflecting the striking shift in the predominant mode of swimming from random to directional. Again, this change in motility after the induction of a VSG synthesis arrest was consistent in both the whole population and in bi-flagellated cells (Figure 4.11B). In bi-flagellated cells the angular persistence increased from -0.18 ± 0.03 units to 0.10 ± 0.04 after VSG synthesis was blocked, which was significantly higher than in bi-flagellated cells in the untreated population.

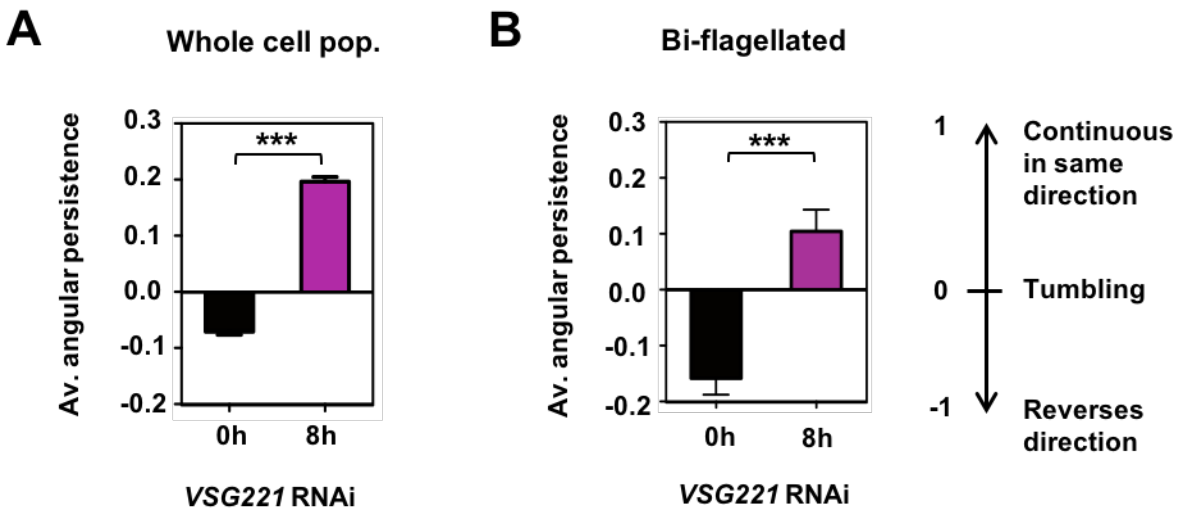



**Figure 4.11. *T. brucei* swam more directionally after the induction of *VSG221* RNAi.** The average (av.) angular persistence is shown in either the **(A)** whole cell population or **(B)** bi-flagellated cells. Angular persistence is denoted on an arbitrary continuous scale of -1 to 1 where a value of 1 indicates continuous swimming in the same direction as observed after a 2 second period, a value of 0 represents cells moving in a random direction after this time period, and a value of -1 represents a trypanosome observed swimming in the reverse direction after 2 seconds. 1500 cells from the whole population (pop.) and 50 bi-flagellated cells were analysed. The Student's t-test was used to analyse the statistical significance of the data set (***P<0.001).

Figure 4.12A and B show a correlation dot-plot between average angular persistence and swim speed. Uninduced cells swam at similar speed to cells where *VSG* RNAi was induced. However, when the component of directionality was considered, there was a clear shift towards the +1 end of the scale after VSG synthesis was blocked, which indicated a preference towards forward directional swimming. At the population level, the heterogeneity of motility phenotypes was greater in cells where VSG synthesis was blocked compared with the non-induced population (Figure 4.12C). In the untreated population, the distribution resembled a normal distribution, with cells spending the most time tumbling, with an angular persistence value of 0.2 units. After the induction of *VSG* RNAi, a wider range of swimming modes was seen. I postulate that this phenomenon may be due to variance in penetrance of the *VSG* RNAi phenotype between cells. However, in general there was a clear increase in directional swimming in cells where VSG synthesis had been blocked. It has been shown earlier that blocking VSG synthesis results in stalled cells which are shorter and broader than normal, although the cell volume remains unchanged (Sheader *et al*. 2005). It was hypothesised that this changed morphology could be a consequence of the cell attempting to minimise its surface area-to-volume ratio and become more spherical in the face of restricted VSG. One would expect that cells with a restricted VSG coat would also be more rigid than normal. This may have reduced their ability to flex, which could explain the reduced tumbling movement that was observed.

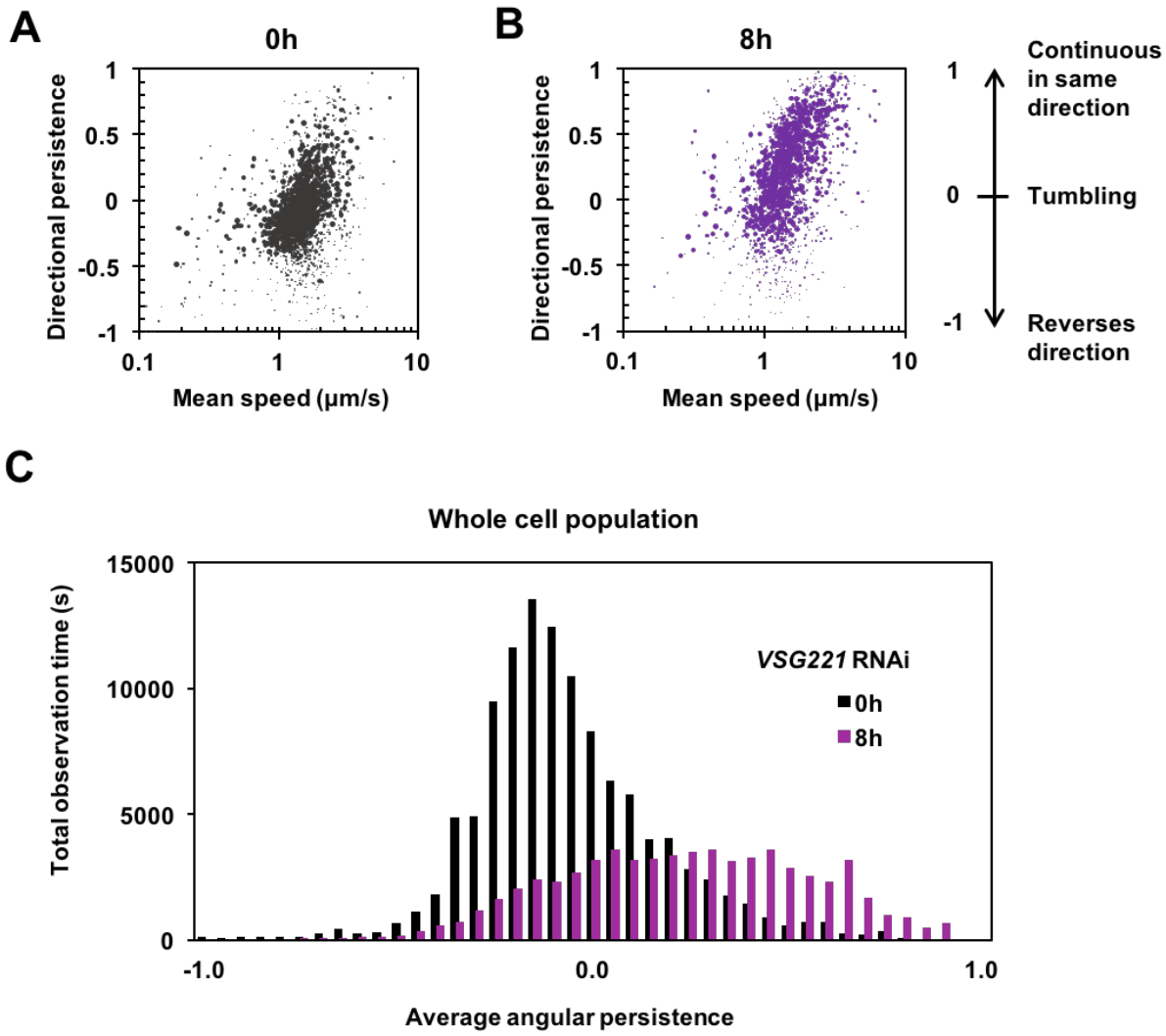



**Figure 4.12. Heterogeneity of angular persistence increased presumably as individual cells were affected differently by *VSG* RNAi.**

**(A)** 0h and **(B)** 8h after the induction of *VSG221* RNAi. The area of each dot is proportional to the length of observation time recorded for that particular trypanosome. Angular persistence is represented on an arbitrary scale of -1 to 1 where a value of 1 indicates continuous swimming of the cell in the same direction as observed after a 2 second period, a value of 0 represents cells moving in a random direction (tumbling) after this time-period, and a value of -1 indicates a trypanosome observed swimming in the reverse direction after 2 seconds.

**(C)** Histogram of average angular persistence of trypanosomes after the synthesis of VSG221 was blocked for 0h and 8h. 1500 cell particle motion tracks were analysed. Histograms show the cumulative observation time in seconds.

## 4.9 Discussion

In this chapter, I investigated the role of the VSG coat and its recycling in the phagocytosis of *T. brucei* by macrophages. As reported in the previous chapter, anti-VSG antibodies were the main host opsonins to enhance macrophage phagocytosis of trypanosomes after VSG synthesis had been blocked.

I showed that blocking VSG synthesis for 8 hours resulted in reduced rates of clearance of anti-VSG antibodies. Arrested cells took twice as long to remove antibodies attached to the trypanosome surface and the half-life of antibodies covering the parasite more than doubled. This was particularly pronounced in G2/ M stage cells, where the half-life of the anti-VSG antibody increased about two and a half fold from 39.3 ± 4.2 seconds to 99 ± 15.9 seconds. At the same time, VSG biotinylation showed that there was a decrease in the amount of surface VSG after the synthesis block, which corresponded to the simultaneous increase in the level of anti-VSG antibody binding. I hypothesise that this could be the result of a dilution in the surface coat after new VSG molecules were no longer being supplied to the cell surface. As a result, the originally dense VSG coat could have exposed some previously inaccessible epitopes to recognition by the polyclonal anti-VSG antibodies.

Conversely, there appeared to be specific perturbation in the removal of VSG-antibody complexes, as rates of internalisation of total biotinylated surface VSG were not significantly changed after blocking VSG synthesis. There was also no evidence of a restriction operating around the flagellar pocket of the stalled cells, as anti-VSG antibodies still reached the lysosomal compartment after a VSG synthesis block, although at slower rates than normal. Interestingly, different components of the trypanosome endocytic pathway also did not seem to be affected by the VSG synthesis block. Endocytosis at the flagellar pocket in bloodstream form *T. brucei* involves clathrin coated pits which bud off the cellular membrane and shed their

clathrin lattice, forming early endosomes (Allen *et al*. 2003; McMahon & Boucrot 2011). The rates of fluid phase and receptor-mediated endocytosis were then monitored using the markers dextran and tomato-lectin respectively. These did not show significant changes after 8 hours induction of *VSG* RNAi. However, a further literature search revealed that tomato-lectin and VSG-antibody complexes do not pass through the same early endosomal compartments. The trypanosome vesicular transport system is defined by the localisation of a family of Rab-GTPases. Bloodstream form *T. brucei* constitutively expresses two Rab5 isoforms: TbRAB5A and TbRAB5B which co-localise with fluid phase and receptor-mediated endocytic cargo (Pal *et al*. 2002; Pal *et al*. 2003). TbRAB5A was found to specifically accompany GPI-anchored cargos i.e. VSG molecules and transferrin receptors. Tomato-lectin along with other non-GPI anchored cargo such as invariant surface glycoproteins (ISGs) is transported via TbRAB5B positive early endosomal compartments (Pal *et al*. 2002). To confirm that TbRAB5A positive compartments which received antibody-VSG complexes were not defective after the VSG synthesis block, I measured the rate of transferrin endocytosis and found no significant impairment in the TbRAB5A positive compartments.

From the experimental data gathered thus far, it appears that the reduction of anti-VSG antibody removal from the trypanosome cell surface was not due to defects in the endocytic pathway. In light of this, I decided to shift my focus to motility, an essential component proposed by Engstler *et al* (Engstler *et al*. 2007) to drive antibody clearance. In this hypothesis, the movement of VSG-antibody complexes towards the flagellar pocket is an active process that requires energy. The addition of 2-deoxyglucose, a metabolic inhibitor reduced the accumulation of anti-VSG antibodies at the posterior end of the cell. Secondly, after knocking down clathrin, antibody-VSG complexes still accumulated at the flagellar pocket but were not internalised. This suggests that antibody sorting on the trypanosome cell surface is independent

of endocytosis. Since energy is needed for the movement of antibody-VSG complexes towards the posterior flagellar pocket, external force must be applied. These authors showed that the hydrodynamic forces generated by the motility of the parasite was the source of energy to push antibodies towards the site of endocytosis.

The swim speed of bloodstream form *T. brucei* 427 grown at 37ºC under standard tissue culture conditions varies between 1.5 to 5.7 μm/ sec (Kisalu *et al*. 2014; Heddergott *et al*. 2012). In more viscous environments, such as blood, directionality of trypanosome swimming has been shown to increase (Bargul *et al*. 2016; Heddergott *et al*. 2012). Although the swim speed measured was low (1.5 μm/ sec), I did not repeat these experiments in high viscosity media, as I was interested in *T. brucei* motility under the conditions used for the macrophage co-cultivation experiments, which was in standard tissue culture medium. In addition to the microenvironment, cellular features have also been shown to affect to trypanosome motility as straighter, more rigid trypanosomes would swim more directionally (Uppaluri *et al*. 2011).

The bloodstream for *T. brucei* used in the motility experiments primarily tumbled *in vitro*, as expected in low viscosity medium. But the induction of a VSG synthesis block caused the cells to swim in a much more directional manner in both the whole population and in the bi-flagellated cells. There was a significant increase in the swim velocity but no change in the swim speed, further confirming the involvement of a directional component.

Cells stalled after the induction of a VSG synthesis block arrest at a precise precytokinesis stage, although these stalled cells differ from wild type precytokinesis cells. The arrested cells are shorter and broader than normal (Sheader *et al*. 2005), although the total cell volume remains unchanged compared with uninduced precytokinesis cells. This change in morphology in the absence of sufficient VSG may be a consequence of a restriction operating

on the VSG surface coat, resulting in increased cellular rigidity. As increased cellular rigidity (as well as an increase in cell width) would be expected to result in increased directional swimming (Uppaluri *et al*. 2011), this could explain why the stalled bi-flagellated cells swim more directionally than wild type bi-flagellated cells.

Selective clearance of VSG-antibody complexes is thought to be facilitated by hydrodynamic forces operating on the trypanosome cell surface generated by directional swimming (Engstler *et al*. 2007). It would appear contradictory to the Engstler theory that after a VSG synthesis block, our cells swam more directionally yet cleared antibodies at a much slower rate. However, even in tumbling cells there is posterior accumulation of anti-VSG immune complexes at the flagellar pocket. Our uninduced cells predominantly tumble, yet are still able to clear anti-VSG antibodies, showing that directional swimming may not be essential for all antibody clearance. It is therefore possible that the flexing activity on the cell surface of a tumbling trypanosome generates enough localised hydrodynamic forces which facilitate the selective movement of VSG-antibody complexes over the cell surface. These forces could be as important in removing surface VSG-antibody complexes as the forces generated through directional swimming through the "wind in the sail" model (Engstler *et al*. 2007). The motility changes I have observed could explain why there was an impairment in the removal of VSG-antibody complexes after the induction of *VSG* RNAi. This adds an interesting argument to the contribution of *T. brucei* motility and its characteristics in facilitating infection in the bloodstream.

The results in this chapter therefore shed light on several issues. Firstly, they highlight the importance of sustained VSG synthesis for bloodstream form *T. brucei* in immune evasion. Blocking VSG synthesis results in viable arrested cells with intact VSG coats that persist for days *in vitro*. This cell cycle arrest could be a parasite safety mechanism preventing a

trypanosome from dividing in the absence of sufficient VSG to cover both daughter cells and may have a protective function *in vivo*. However, the protective nature of this cell-cycle checkpoint would only be effective in the absence of significant anti-VSG antibody titres. The experiments that were shown here, argue that in a host that has been infected long enough to develop a significant antibody response, these stalled cells would be preferentially removed by phagocytes as a consequence of reduced clearance of anti-VSG antibodies.

Secondly, my results directly demonstrate the essentiality of rapid removal of host opsonins from the trypanosome cell surface for effective escape from host macrophages. To the best of my knowledge, these experiments are the first to show that an experimental perturbation leading to impaired anti-VSG antibody clearance directly results in increased trypanosome phagocytosis by macrophages. Lastly, I hypothesise that the motility changes observed after induction of a VSG synthesis block play a direct role in VSG-immune complex removal. These experimental data therefore highlight the importance of high rates of VSG recycling in the removal of host cell opsonins from the trypanosome cell surface, thereby allowing the efficient evasion of professional phagocytes including macrophages during a chronic infection. I therefore showed that the cellular processes of high rates of VSG internalisation coupled with VSG quality control are key virulence factors enabling *T. brucei* to be a highly successful extracellular pathogen.

These experiments also allowed me to gain insight in *T. brucei* evasion of macrophages. I showed here that the increased phagocytosis of trypanosomes in the presence of anti-VSG antibodies after the induction of a *VSG* RNAi, appears to be a direct consequence of a reduction in rates of antibody clearance from the trypanosome cell surface. This chapter highlighted the essentiality of high rates of VSG synthesis and internalisation coupled with VSG quality

control in removing host cell opsonins, thereby enabling trypanosome escape from host phagocytes.

# Chapter 5

# Immunomodulation of human dendritic cells by *T. brucei in vitro*

## 5.1 Introduction

Bloodstream form *T. brucei* is an ancient species of parasite in that its origins can be traced back to over 300 million years ago (Steverding 2008). Over millennia, bloodstream form *T. brucei* has evolved sophisticated immune evasion mechanisms, including antigenic variation and high rates of removal of surface opsonin to evade antibodies, complement and phagocytes (Namangala 2011; Stijlemans *et al*. 2016; Donelson *et al*. 1998). As chronic infection is a feature of Human African Trypanosomiasis, this shows that the innate system alone is insufficient to clear parasitic infection and additional help from the adaptive system is crucial.

Dendritic cells (DCs) are professional antigen presenting cells that form an indispensable link between the innate and adaptive immune systems. Since their discovery by Ralph Steinman and Zanvil Cohn in the 1970s (Steinman & Cohn 1973; Steinman & Cohn 1974), the vital role of DCs has featured heavily in many aspects of immunological disorders. Many parasites and bacteria have evolved to target multiple steps of adaptive responses, ranging from surface receptor downregulation to alterations in cytokine release (Terrazas *et al*. 2010). For example, *Leishmania* inhibits IL-12 production in DCs and macrophages, while upregulating IL-10 release to avoid clearance (Liu *et al*. 2009; Probst *et al*. 1997). As *T. brucei* is a Kinetoplastid parasite like Leishmania, it can be expected that BF *T. brucei* would also target DCs. Modulation of the antigen presentation capacity of macrophages has been reported in mouse models, which show lowered major histocompatibility complex class II (MHCII) expression and defective antigen loading onto the MCHII complexes (B. Namangala *et al*. 2000). Using mice that were either resistant or susceptible to *T. brucei* infection, Dagenais *et*

*al* (Taylor R Dagenais *et al*. 2009) showed that in resistant mice, DC surface co-stimulatory molecules were downregulated. However, the opposite was observed in susceptible mice, altering downstream anti-trypanosomal responses involving T-cells. Since then, there have been few studies detailing trypanosome immunomodulation on DCs. As most studies based their experimental design on mouse models, there is, to the best of my knowledge, no evidence of DC immunomodulation in a human system.

As investigated in the previous chapters, bloodstream form *T. brucei* utilises extremely high rates of endocytosis to remove host opsonins, and thus successfully evade macrophage phagocytosis. In this chapter, immunomodulation mechanisms employed by *T. brucei* against DCs were explored.

**5.2 Experimental outline**

Using an *in vitro* co-culture system, I investigated the effect that bloodstream form *T. brucei* has on the functions of primary human monocyte-derived DCs. These functional tests are designed to test the differentiation and maturation of DCs which include the surface expression of maturation molecules, antigen uptake capacity and cytokine production. To further dissect the direct interaction between the parasite surface and DCs, VSG proteins were isolated and used as a stimulant to moDCs.

### 5.3 *T. brucei* suppresses human dendritic cell maturation markers

After encountering pathogens in the bloodstream, immature DCs acquire several fundamental features in a process known as functional maturation that are essential to their execution of immune surveillance. These include antigen processing and presentation, migration and T-cell stimulation (Dalod *et al*. 2014; Castiello *et al*. 2011). In the resting state, immature DCs express low surface expression of MHC II molecules and co-stimulatory molecules: CD80, CD86 and CD40. Upon interaction with pathogens, these cell surface molecules are upregulated in preparation for inducing clonal expansion of naïve T-cells (Dalod *et al*. 2014). As a result, I decided to first measure the levels of MHCII, CD80, CD86 and CD40 after co-culturing trypanosomes with DCs. As the *T. brucei* cell line used in these experiments are the bloodstream form, I chose to use human monocyte-derived dendritic cells (moDC), isolated from the buffy coat of healthy donors as the model system for the following experiments.

As expected of immature moDCs, they expressed a basal level of all four surface molecules even without trypanosome stimulation (Figure 5.1). Stimulation by LPS showed that these primary moDCs were capable of expressing higher levels of maturation markers after they encountered a pathogen. Bloodstream form 221VB1.2 *T. brucei* was co-cultured with moDCs for 16, 24, 48 and 72 hours to construct a time course of *in vitro* infection. As shown in Figure 5.1, within the first 24 hours of co-culture, the expression all four markers remained at a similar level compared with the untreated control, indicating a degree of maturation suppression exerted on the moDCs by the parasite. This differed significantly from the stimulation by LPS, which showed the expression of MHCII, CD86 and CD80 were more than doubled. However, after 48 hours of co-culture, a slight drop in the expression of MHCII was observed (Figure 5.1A). This was followed by a further significant decrease in the expression

of both MHCII and CD40 after 72 hours of co-culture (Figure 5.1A and D). The expression of CD86 also appeared to be downregulated, although the change was not statistically significant (Figure 5.1B). In addition, the level of the co-stimulatory molecule CD80 was maintained at the level of basal expression level, similar to the untreated control (Figure 5.1C).

This experiment demonstrated that *T. brucei* could suppress the maturation of moDCs within 3 days of co-culture. But whether this was achieved directly by the VSG surface coat or via the secretion of immunomodulatory molecules remained to be investigated.

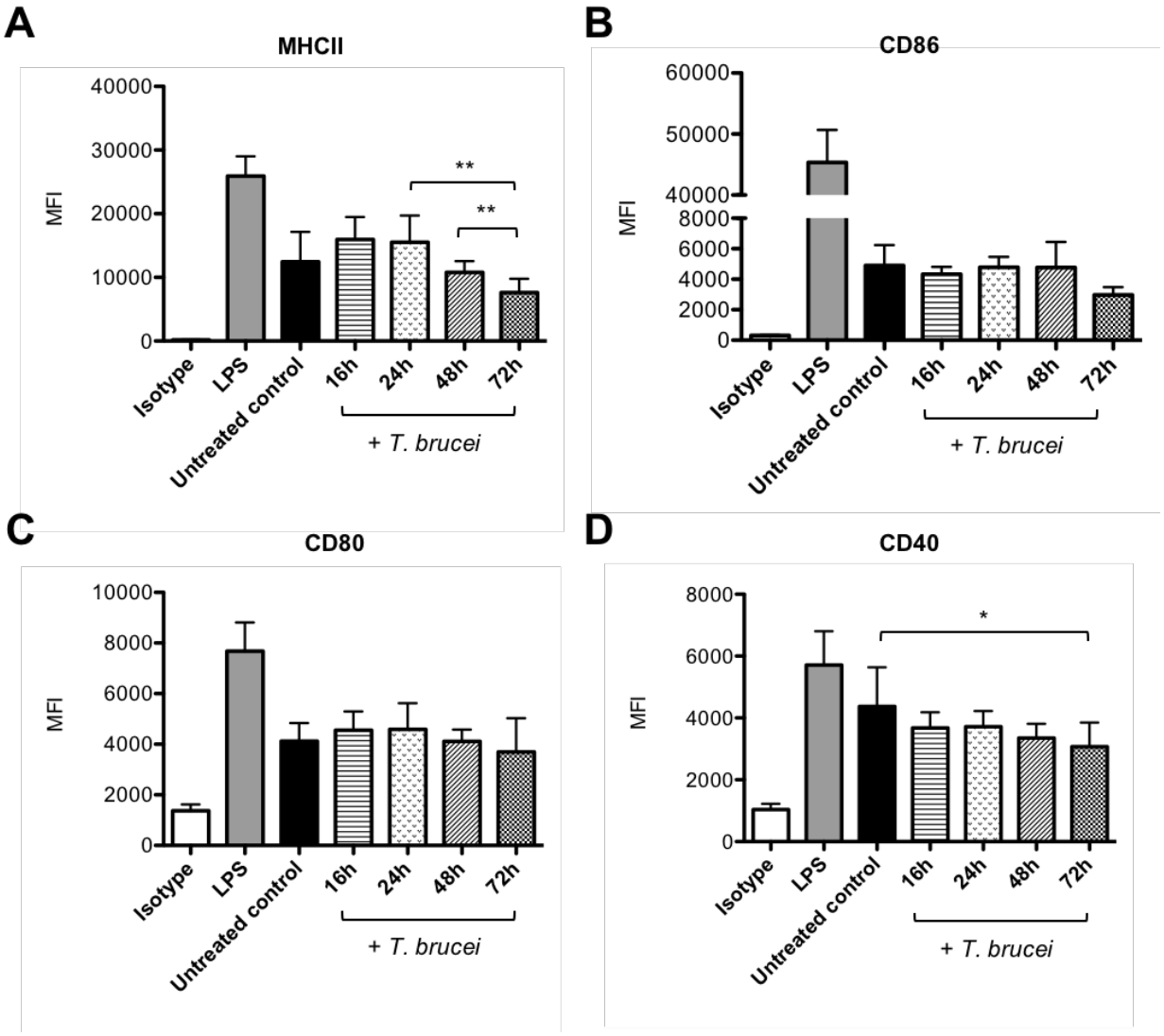



**Figure 5.1 Downregulation of dendritic cell maturation markers by *T. brucei* in a time-dependent manner.** Human monocyte-derived DCs were co-cultured with $1x10^6$ *T. brucei* 221VB1.2 cells for 16, 24, 48 and 72 hours. LPS (100 ng/ml) was used as a DC positive stimulant and was added 24 hours prior to cell staining. MoDCs and *T. brucei* were co-cultured in a 1:1 ratio ($1x10^6$ cells/ condition). Cells were harvested and stained with **(A)** anti-HLADR (MHCII), **(B)** anti-CD86, **(C)** anti-CD80 and **(D)** anti-CD40 antibodies. Expression of each surface marker is expressed as the mean fluorescence intensity (MFI) values. Results shown are the mean of 6 independent biological replicates with SEM indicated with error bars. *P<0.05, **P<0.01.

### 5.4 *T. brucei* reduces the capacity of antigen uptake by moDCs

Dendritic cells are often classified along with macrophages and neutrophils as phagocytes. However, unlike macrophages and neutrophils, DCs are not directly involved in pathogen clearance via phagocytosis. Instead, phagocytosing pathogens through endocytosis serves as the essential first step of antigen presentation. Then the pathogen is disintegrated within the phagolysosome and the resultant peptide or protein antigens are presented to T cells (known as antigen presentation). Then the cascade of adaptive immune response is initiated. This process defines the function of DCs as a bridge between the innate and adaptive immune systems. As seen in the previous experiment, DC maturation appeared to be suppressed to an extent. However, DC maturation is not only defined by the expression of surface co-stimulatory molecules, functional tests are needed to confirm the maturation status. Therefore, I proceeded to investigate whether antigen uptake was affected by *T. brucei* by using the dextran phagocytosis assay. The principle of this test is that matured DCs will no longer phagocytose dextran as the immature DCs does and a measure of dextran uptake would reflect DC maturation status.

*T. brucei* was again co-cultured with moDCs for 16, 24, 48 and 72 hours. Cells were then collected and stained with FITC conjugated dextran, a fluid phase endocytosis marker to monitor active uptake. However, as both *T. brucei* and moDCs are capable of endocytosis, moDCs were stained with an anti-HLADR (MHCII) antibody prior to flow cytometry analysis to distinguish the two cell populations (Figure 5.2A). The level of FITC expression in HLA-DR positive cells was subsequently assessed.

Figure 5.2B and C illustrate the gradual decrease in FITC-dextran signal after moDCs had been treated with *T. brucei*. 24 hours after being co-cultured with *T. brucei*, the phagocytic capacity of DCs reached its peak, a three-fold increase in FITC signal compared with the

untreated control. However, moDCs soon reduced the uptake of dextran as the signal reduced by 2.5-fold by 72 hours (Figure 5.2C). This reduction in dextran uptake demonstrated that the capacity of moDCs to engulf *T. brucei* had decreased over time. There are two potential reasons that could explain this decrease in phagocytic capacity: 1. *T. brucei* can directly downregulate antigen uptake by moDCs. 2. Maturation of DCs after encountering pathogens would also downregulate phagocytosis as changes in the activity of the small GTP-binding proteins, Rac and Cdc42 take place (Nobes & Marsh 2000; Savina & Amigorena 2007). However, as measured in Figure 5.1, DC maturation markers were universally downregulated after *in vitro* co-culture with *T. brucei*, so it would be unlikely that the reduction in phagocytosis was due to DC maturation. Therefore, the suppression of DC functions in terms of reducing uptake of pathogen may have been caused directly by the parasite or indirectly via the secretion of parasite products.

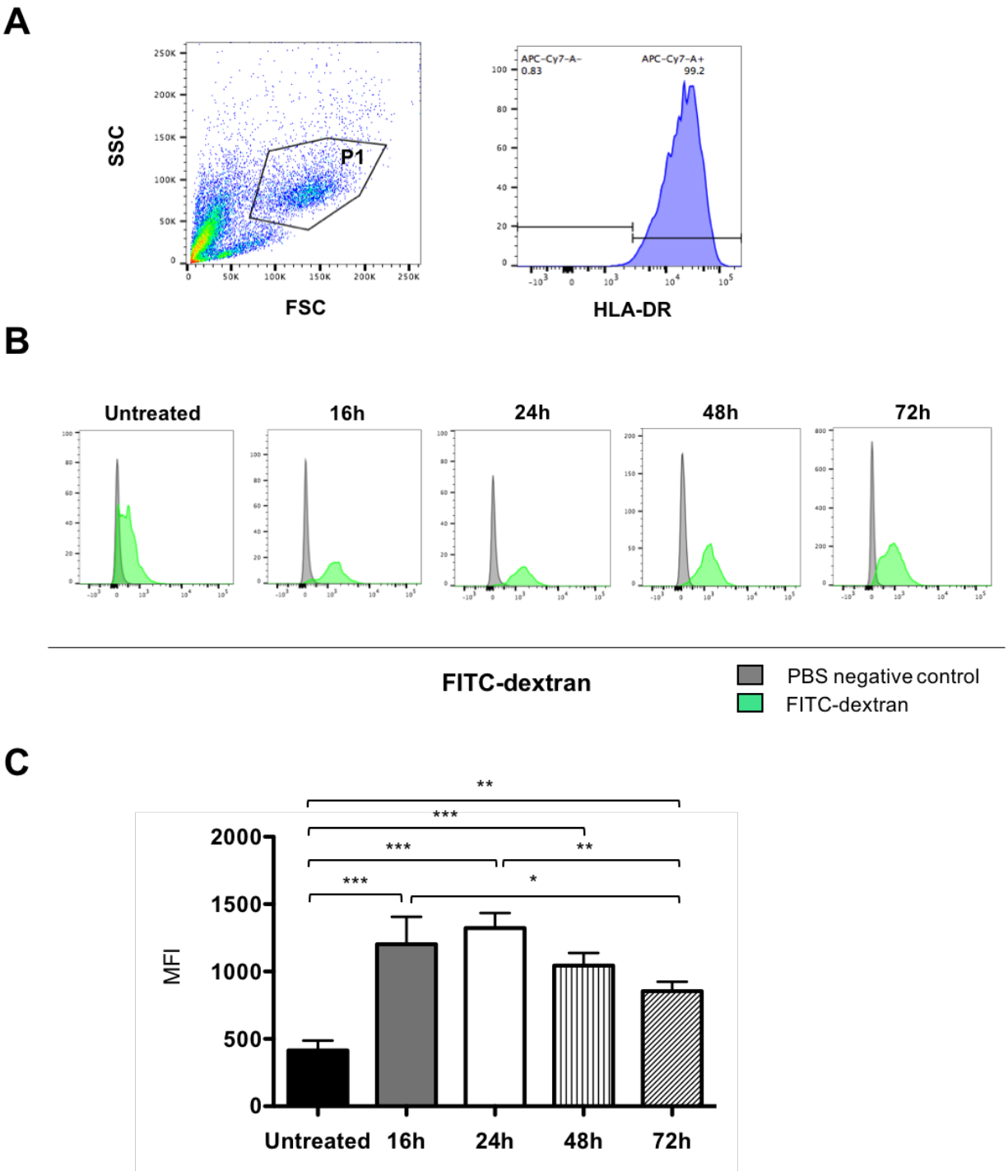



**Figure 5.2 Antigen uptake by dendritic cells decreased over time after co-culture with *T. brucei*.** Human monocyte-derived DCs were co-cultured with 1x10$^6$ *T. brucei* 221VB1.2 cells for 16, 24, 48 and 72 hours. Cells and parasites were collected and stained with **(A)** anti-HLADR (MHCII) antibody to separate DCs from *T. brucei* as both are capable of active endocytosis. P1 shows the gating of viable monocyte-derived DCs. Blue shaded peak shows the P1 expression of HLA-DR positive cells. **(B)** Cells were incubated with FITC conjugated dextran (1 mg/ml) for one hour and excess FITC-dextran was washed away before analysis by

flow cytometry. Representative flow cytometry analysis of FITC-dextran detection (green) compared with the negative control (grey shaded peak; PBS control) in HLA-DR positive cells. **(C)** Quantitation of FITC-dextran uptake using MFI values. Results shown are the mean of 4 independent biological replicates with the SEM indicated with error bars. *P<0.05, **P<0.01, ***P<0.001.

### 5.5 Soluble VSG suppresses maturation of moDCs

During a trypanosome infection, numerous parasite products are released into the bloodstream. One such product is the soluble form of VSG (sVSG), which has been shown to be released in large amounts during infection. Bloodstream form *T. brucei* expresses an endogenous phospholipase-C (PLC), which when activated, cleaves membrane-bound VSG (mfVSG) at the GPI-anchor, and thus liberates the soluble form of VSG. Several theories have been put forward for the reason for the secretion of sVSG. First, the release of sVSG could be a potential immune evasion mechanism, where the selective release of a small amount of VSG of a particular variant could distract the host response, and shield the rest of the trypanosome population from detection by the host (Male *et al*. 2012). Alternatively, the release of sVSG could be a by-product of cell lysis under stress or phagocytosis, which may activate the PLC and the cleavage of mfVSG (Rolin *et al*. 1996).

Although the purpose of VSG release remains debatable, several studies have shown that different components of the VSG molecule can exert virulence on the host during infection (Magez *et al*. 2002; Donna M. Paulnock & Coller 2001). After cleavage by PLC, sVSG retains the glycosylphosphatidyinositol phosphate (GIP) substituent of the original GPI anchor, leaving the dimyristoylglycerol (DMG) lipid component on the trypanosome membrane (Noda & Amano 1997). GIP-sVSG was shown to activate mouse macrophages and potentiate a Th1 response (D M Paulnock & Coller 2001). Further analyses showed that PLC has a role in immunosuppression, alternative macrophage activation and Th2 cytokine production,

revealing a far more complex relationship between soluble VSG, PLC and the host immune system (Boniface Namangala *et al*. 2000; Baetselier *et al*. 2001).

Therefore, I next investigated the role of sVSG in the reduction of moDC maturation and functioning. sVSG were isolated from BF HNI221+ (expressing VSG221) and HNIVO2+ (expressing VSGVO2) by lysing the parasites in ice-cold water to release cell contents. PLC was then activated at 37 ºC to release soluble VSG from the cell membrane. The purity of each fraction was first assessed by Coomassie staining (Figure 5.3A) then confirmed by Western blotting (Figure 5.3B). VSG is the most abundant protein expressed by bloodstream form *T. brucei*, making up 10% of the total protein of the parasite and has a molecular weight between 50-75kDa depending on the VSG variant. As seen in Figure 5.3A, compared to the whole cell extract (WCE), the S1 fraction, contained most of the cellular contents also contained some VSG; VSG221 has a molecular weight of approximately 50kDa, whereas VSGVO2 is more glycosylated and has a molecular weight of 70kDa. The S2 fraction contained soluble VSG of relatively high purity as shown by faint bands that represented other proteins. The rest of the membrane proteins were left in the P3 fraction, which should include proteins such as surface receptors and invariant surface glycoproteins.

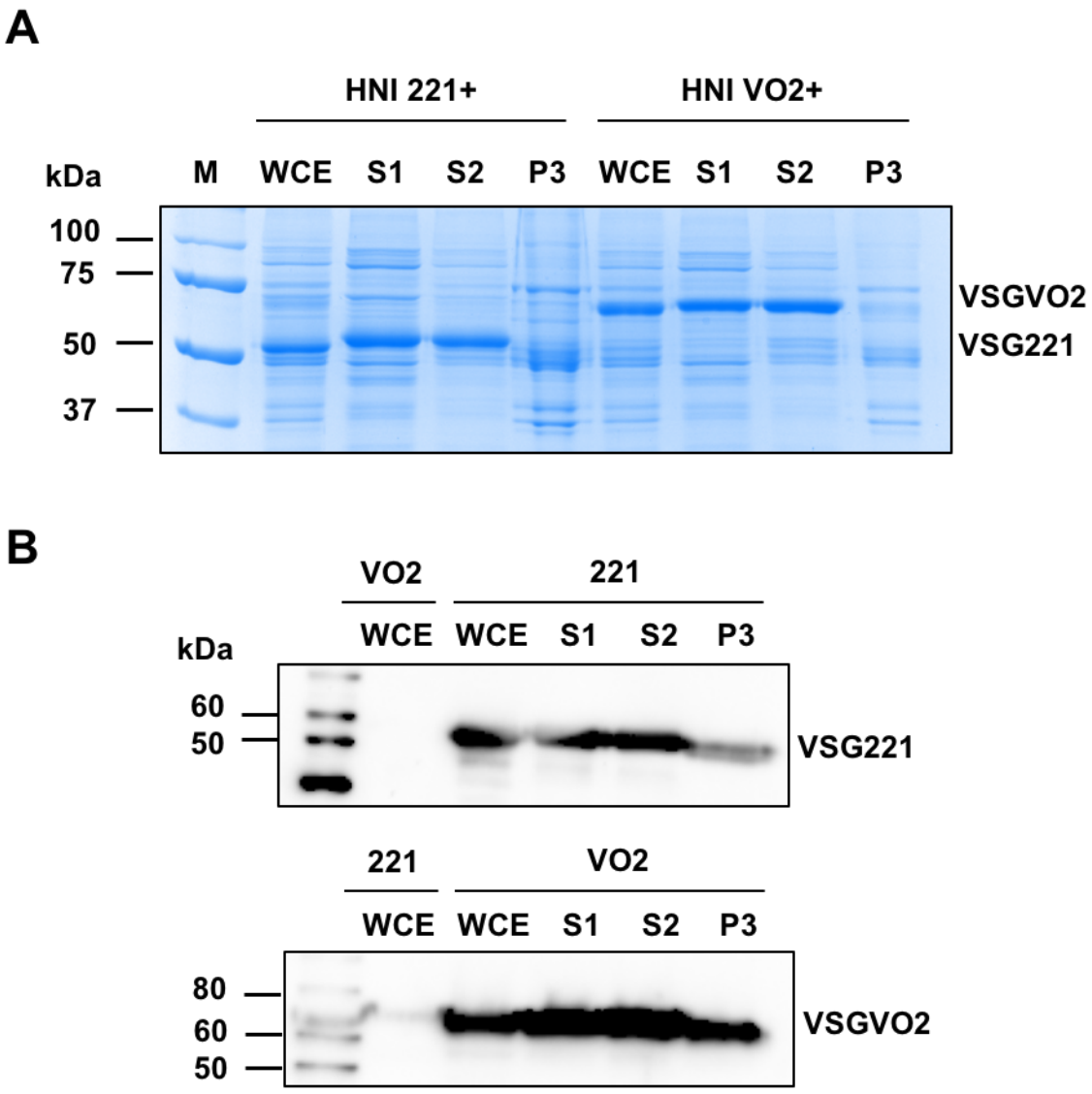



**Figure 5.3 Purification of VSG protein.** BF HNI221+ (expressing VSG221) and HNIVO2+ (expressing VSGVO2) cell lines were lysed at 4ºC using sterile water. Cell contents were centrifuged and the supernatant collected (S1). Cells were then transferred to 37ºC to activate the endogenous trypanosome phospholipase-C (PLC) which cleaves the VSG GPI-anchor, releasing the soluble VSG (S2). The pellet containing the rest of the cellular contents and membrane is indicated as P3. Whole cell extracts (WCE) of both cell lines were used as positive and negative controls. **(A)** Coomassie staining of the total protein content of each isolated cellular fraction of the HNI221+ and HNIVO2+ cell lines. **(B)** Western blot analysis of VSG221 and VSGVO2 protein in each purified fraction. The equivalent of $1x10^6$ cells was loaded in each lane.

Purified soluble VSG from the S2 fraction at three different concentrations, equivalent to $1x10^5$ $5x10^5$ and $1x10^6$ cells, were then used to stimulate moDCs isolated from healthy donors. The level of expression of the same maturation markers: MHCII, CD86, CD80 and CD40 as in Figure 5.1 was measured (Figure 5.4).

After 72 hours of stimulation, there was no significant change in the expression of MHCII and CD86, the levels of which remained similar to that of the untreated control (Figure 5.4A and B). The variant of VSG used did not appear to affect DC maturation significantly, except in the case of CD80 expression. There could be several reasons behind the disparity in the DC stimulation capacity between different VSG variants. As these two variants differ in the amount and arrangement of glycosylation on the N-termini of the VSG molecules, the ability of these external moieties could affect *T. brucei* pathogenicity. Recently, trypanosome growth rate has been linked with the identity of the VSG, indicating that the glycosylation state between VSG variants could affect how fast *T. brucei* proliferates (Schwede *et al*. 2015). It is possible that the expression of VSG221 resulted in a faster growing trypanosome population in comparison with VSGVO2 and would have a more suppressive effect on DC maturation.

Out of the four surface markers, only the expression of the T-cell co-stimulatory molecule CD80 and CD40 appeared to increase when DCs were stimulated with a lower number of VSG221 expressing *T. brucei* ($1x10^5$) (Figure 5.4C and D). However, as the concentration of *T. brucei* increased, the downregulation of their expression also became stronger, although only the suppression of CD80 was statistically significant. The level of CD80 expression decreased by 67% when the number of *T. brucei* was raised from $1x10^5$ to $1x10^6$. This is different to what was observed when moDCs were co-cultivated with live trypanosomes (Figure 5.1), where only MHCII and CD40 were suppressed but not CD80. It is likely that after the cleavage at the VSG GPI anchor by the endogenous PLC, virulent moieties

i.e. glycosylphosphatidyinositol phosphate-sVSG (GIP-sVSG) that were previously hidden became exposed. GIP-sVSG has been shown to activate macrophages and alter their cytokine profile (Donna M. Paulnock & Coller 2001). It is possible that moieties of the soluble VSG molecule were sufficient to block the maturation of moDCs, and therefore no change in costimulatory molecule expression was observed. Further suppression of DC maturation when moDCs were co-cultured with live trypanosomes could be the result of the secretion of other parasite products that were released into the medium.

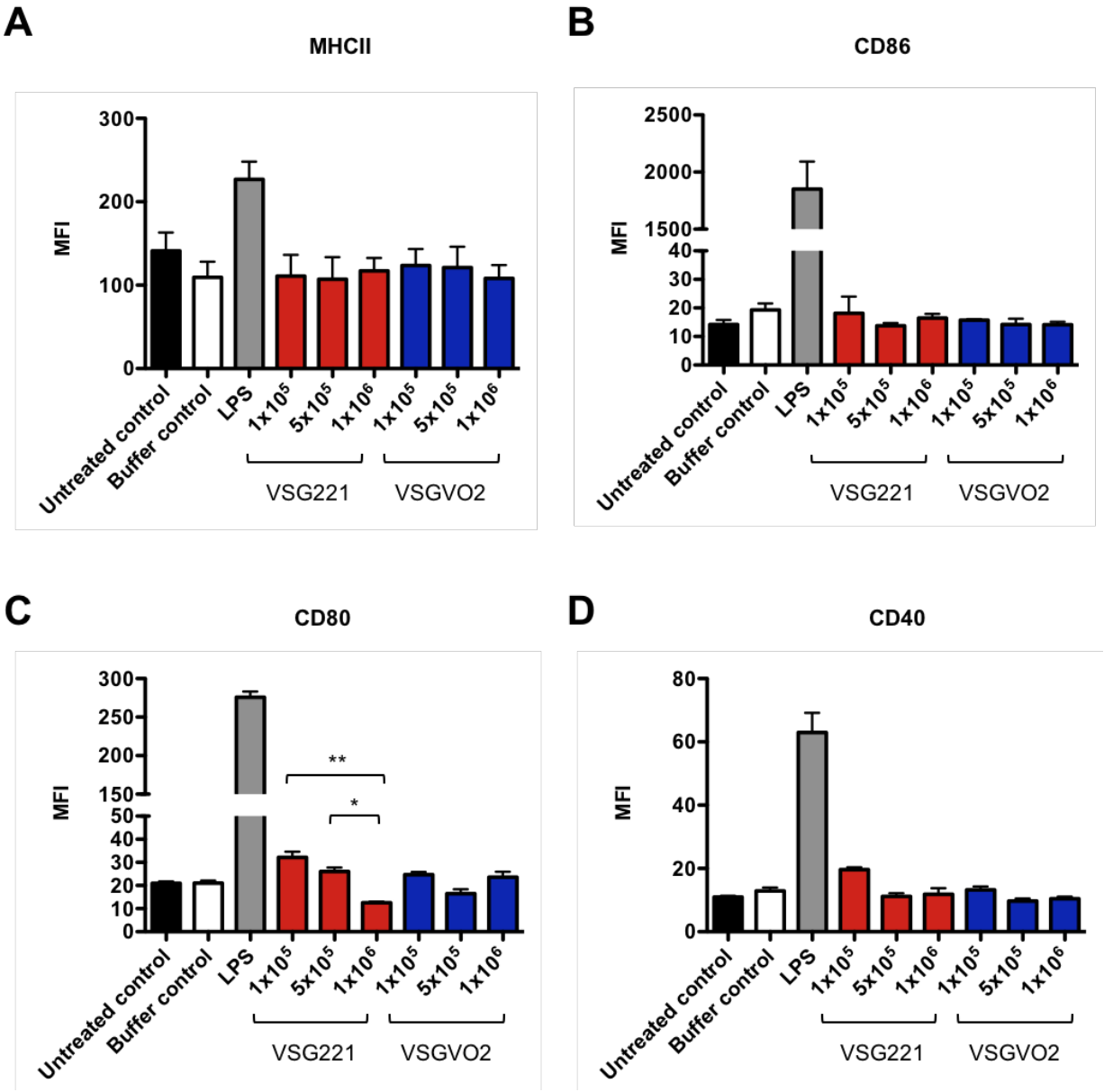



**Figure 5.4 Soluble VSG is insufficient to activate human moDCs.** Soluble VSG isolated from intact BF HNI221+ (expresses VSG221) and HNIVO2+ (expressing VSGVO2) cell lines was incubated with moDCs for 72h. DCs were collected and co-stained with **(A)** anti-HLADR (MHCII), **(B)** anti-CD86, **(C)** anti-CD80 and **(D)** anti-CD40 antibodies. Expression of each surface marker is expressed as the mean fluorescence intensity (MFI) values. Results shown are the mean of 4 independent biological replicates with the SEM indicated with error bars. *P<0.05, **P<0.01.

### 5.6 Inflammatory cytokine regulation

The previous experiments have all consistently shown that DCs were not activated following *in vitro* co-culture with *T. brucei*. However, it was unclear how this would affect the cytokine production of DCs. Cytokines are critical mediators of DC effector functions and directly affect the downstream effector functions including T-cell activation (Blanco *et al*. 2008). At the same time, DCs can also be influenced by cytokines produced by other immune cells in the same microenvironment.

Using a multiplex ELISA screen, the levels of 13 inflammatory cytokines and chemokines were detected and quantified. These included IFN-α, TNF-α, IL-6, IL-8, IL-10, IFN-γ, IL-12p70, IL-23, IL-33, MCP-1, IL-18, IL-1β, IL-17A. Of the 13 cytokines, only 5 were detected above the detection limit. Levels of TNF-α, MCP-1 and IL-6 all increased initially, within the first 24 hours of *T. brucei* stimulation (Figure 5.5). All three cytokines are known to participate in immune cell recruitment and inflammatory response. MCP-1 (CCL2), is a monocyte chemoattractant protein which is a potent chemotactic factor for monocytes (Deshmane *et al*. 2009). MCP-1 regulates the migration and infiltration of monocytes, NK cells and T-cells and has also been shown to enhance T-cell secretion of IL-4. Similarly, TNF-α a key promoter of inflammation and in conjunction with IL-8 and MCP-1, is crucial for leukocyte recruitment (Blanco *et al*. 2008; Kalliolias & Ivashkiv 2015; Bradley 2008). IL-6 on the other hand, has dual properties of pro- and anti-inflammatory functions. In the adaptive immune system, IL-6 not only has a vital role in inducing the maturation of antibody-producing B-cells, it has also been shown to be a key driver in the lineage commitment of Th17 cells (Hunter & Jones 2015).

TNF-α, although expressed at relatively low levels throughout the time course, was initially upregulated 30-fold after 16 hours of co-culture (Figure 5.5B). IL-6 and MCP-1 were

also simultaneously upregulated 9.7 and 1.6-fold respectively after 16 hours (Figure. 5.5A and C). However, this increase in cytokine expression was short-lived and all three cytokines were downregulated 24 hours after the initial spike. TNF-α concentration quickly dropped to 3.8 pg/ml. MCP-1 levels were reduced to only 20% of that in untreated cells, whereas IL-6 expression rapidly declined 6-fold compared to the levels at 16 hours post-stimulation. Levels of TNF-α, IL-6 and MCP-1 were all maintained at similar levels with or lower than that of the untreated controls after 72 hours of co-culture.

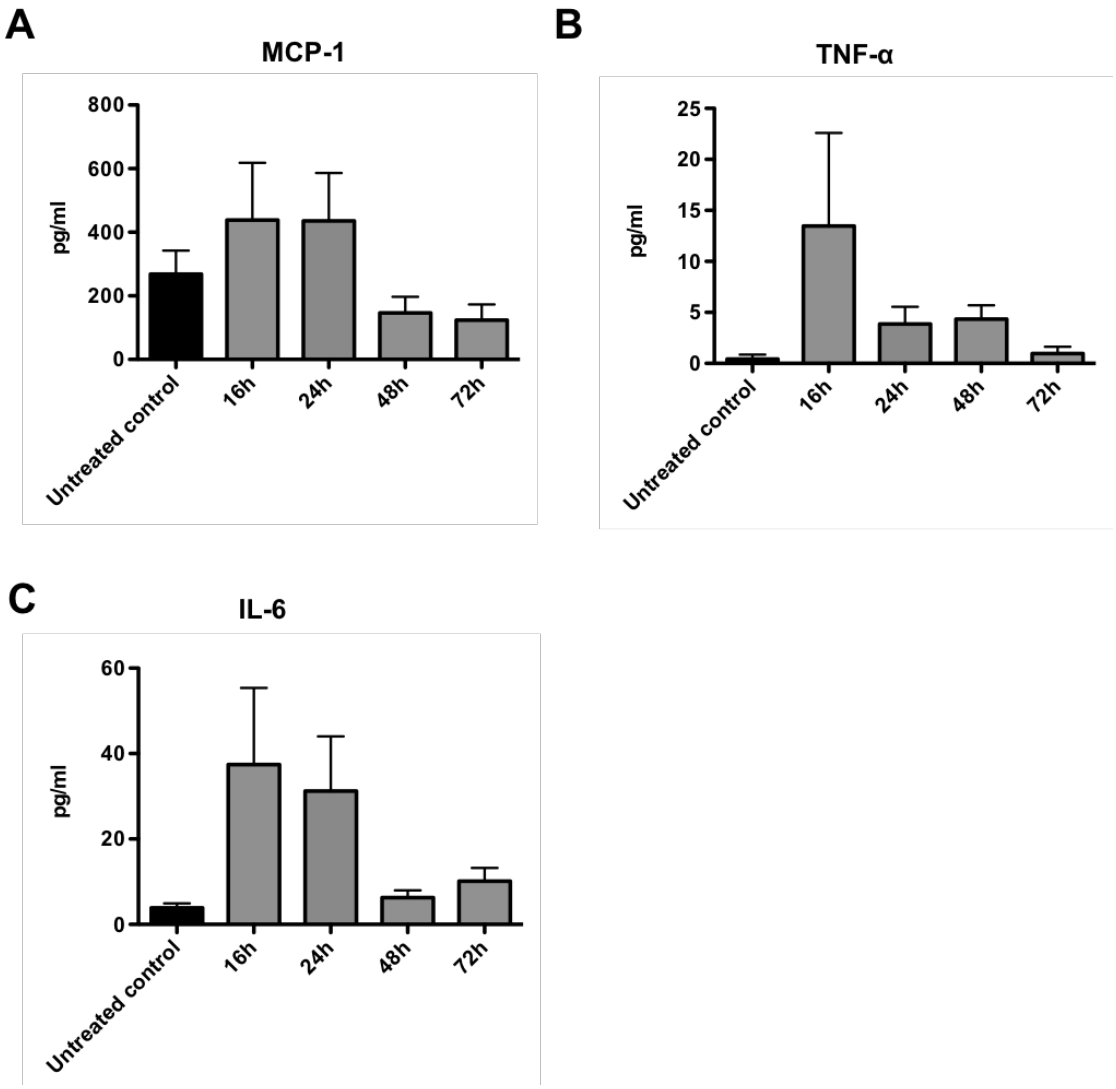



**Figure 5.5 Downregulation of inflammatory cytokines MCP-1, TNF-α and IL-6 by moDCs after stimulation by *T. brucei*.** *T. brucei* was co-cultured with moDCs at a 1:1 ratio for 0, 16, 24, 48 and 72 hours. Culture supernatant was collected and analysed using a bead-based multiplex ELISA kit. The relative concentrations of each cytokine were quantified using the LEGENDplex™ Human Inflammation Panel data analysis software. Results shown are the mean of 5 independent biological replicates with the SEM indicated with error bars.

In contrast, two cytokines were upregulated over time: IL-8 and IL-10 (Figure. 5.6). IL-8 is a chemokine that promotes neutrophil recruitment and induces phagocytosis by neutrophils after they have arrived at the site of inflammation. IL-10 is generally an immunosuppressive cytokine, which represses the host inflammatory response and prevents

the exacerbation of tissue damage by uncontrolled inflammation (Moore *et al*. 2001; Couper *et al*. 2008). In this case, 16 hours of co-culture with *T. brucei* caused a 4.2-fold increase in IL-10 production. Throughout the time course, IL-10 expression continued to surge and reached 18.7 pg/ml after 72 hours. The level of IL-8 meanwhile, was elevated to a staggering 18.5-fold to over 10 ng/ml after 72 hours compared with the untreated control. Fold changes in cytokine expression were calculated by normalising the concentrations against that of the untreated control and are listed in Table 5.1, along with the main functions of each cytokine, including those that were not detected in this assay.

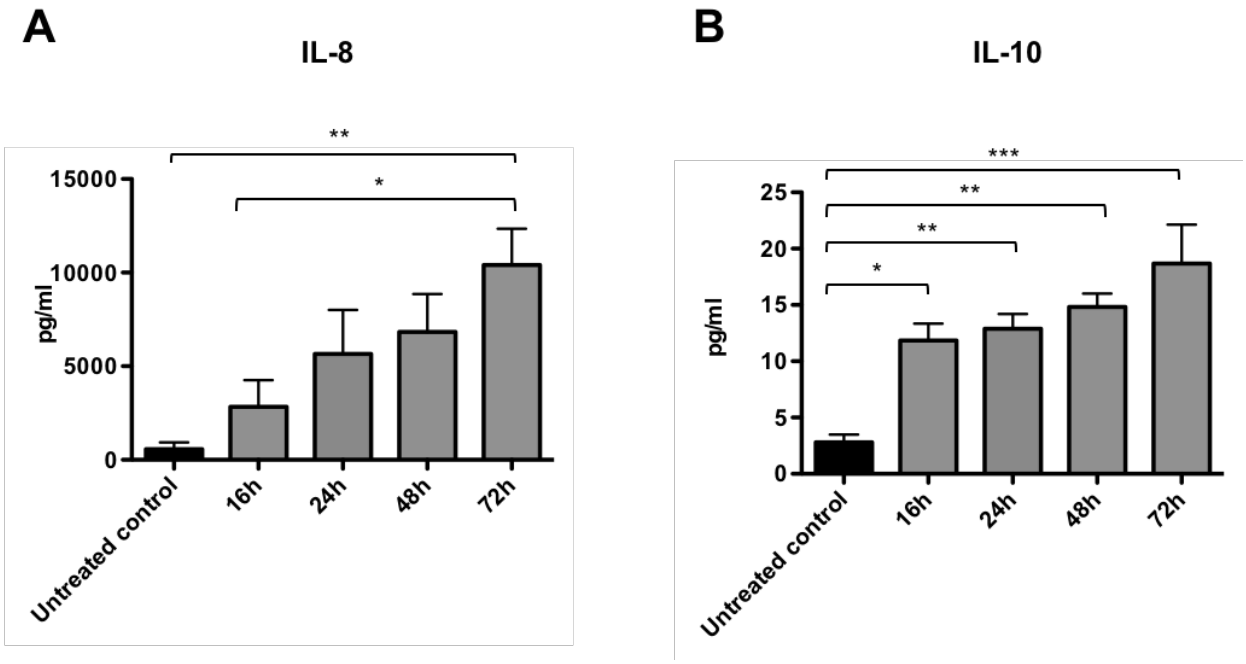



**Figure 5.6 Upregulation of the inflammatory cytokines IL-8 and IL-10 by moDCs after stimulation by *T. brucei*.** *T. brucei* were co-cultured with moDCs at a 1:1 ratio for 0, 16, 24, 48 and 72 hours. Culture supernatant was collected and analysed using a bead-based multiplex ELISA kit. The relative concentrations of each cytokine were quantified using the LEGENDplex™ Human Inflammation Panel data analysis software. Results shown are the mean of 5 independent biological replicates with the SEM indicated with error bars. Statistical analysis was performed using the one-way ANOVA test *P<0.05, **P<0.01, ***P<0.001.

| Cytokine family | Cytokine | Main functions | Detection (in fold change compared to untreated control) | | | |
|---|---|---|---|---|---|---|
| | | | 16h | 24h | 48h | 72h |
| CC chemokines | MCP-1 (CCL2) | Monocyte, memory T-cell, DC recruitment | 1.6 | 1.6 | 0.2 | 0.2 |
| TNF superfamily | TNF-α | Inflammation promotion, neutrophil recruitment | 30.9 | 8.9 | 10.0 | 2.2 |
| IL-6 | IL-6 | Both inflammatory and anti-inflammatory | 9.7 | 8.1 | 1.6 | 2.6 |
| CXC chemokines | IL-8 | Neutrophil recruitment, induce phagocytosis | 5.0 | 10.1 | 12.1 | 18.5 |
| IL-10 | IL-10 | Anti-inflammatory, downregulate Th1 cytokine production | 4.2 | 4.6 | 5.3 | 6.7 |
| IL-1 | IL-1β | Promote inflammation | ND | | | |
| | IL-18 | Promote inflammation, stimulate NK cells to produce IFN-γ | ND | | | |
| | IL-33 | Promote Th2 cytokine release | ND | | | |
| IL-12 | IL-12p70 | Promote Th1 cell differentiation, enhance cytotoxicity of NK and cytotoxic T-cells | ND | | | |
| | IL-23 | Facilitate inflammation with IL-12 | ND | | | |
| Type I interferons | IFN-α | Antiviral | ND | | | |
| Type II interferons | IFN-γ | Induce macrophage activation, induce MHCII expression | ND | | | |
| IL-17 | IL-17A | Pro-inflammatory cytokine produced by T-cells | ND | | | |

**Table 5.1 Summary of the panel of cytokines screened after moDCs were co-cultured with *T. brucei*.** MoDCs from healthy donors were cultured with *T. brucei* for 16, 24, 48 and 72h. Using a bead-based immunoassay, 13 inflammatory cytokines were screened and analysed by flow cytometry. The cytokines are categorised into cytokine families and their main functions are listed.

The concentration of each cytokine was quantified and normalised to that of the untreated control, indicated in fold-change against the control. Cytokines that were screened but not detected are indicated as ND. The fold change represents mean fold change values obtained from 5 independent biological replicates.

## 5.7 Discussion

In the previous chapters, I have shown that bloodstream form *T. brucei* utilises extremely high rates of surface endocytosis to remove host opsonins, and thus successfully evades innate immune attack. Phagocytosis of the parasite by macrophages is therefore hindered unless anti-VSG antibody removal is slowed after blocking VSG synthesis. In this chapter, I explored the mechanisms by which trypanosomes evade the adaptive immune system. DCs represent a central link between the innate and adaptive immunity and are often the target of parasite immunomodulation (von Stebut 2017; Terrazas *et al*. 2010).

Using an *in vitro* co-culture system, it was revealed that bloodstream form *T. brucei* were able to modulate dendritic cell responses. The expression of all four surface maturation markers: MHCII, CD86, CD80 and CD40 were downregulated in a time-dependent manner. In addition, antigen uptake by moDCs also reduced over time. Normally, a decrease in antigen endocytosis is an indicator of DC maturation. However, since maturation markers were universally suppressed, the reduction in endocytosis was likely the result of active immunomodulation by *T. brucei*. Many parasites are known to target DC functions in a bid to alter the host into more a "parasite-tolerant" environment. This can be achieved either through direct interaction between the parasite and DC or through secretion of parasite products to change the host microenvironment.

Kinetoplastid parasites such as the Leishmania family have been found to suppress DC maturation and therefore reduce their capacity to prime T-cells (Gupta *et al*. 2013). *L. donovani* was shown to inhibit DC maturation and subsequently interfere with DC migration (Probst *et al*. 1997). Various strains of *Plasmodium* have also been shown to downregulate the capacity of DCs to prime T-cells (Wykes *et al*. 2007). In the Trypanosoma family, there is evidence that *T. cruzi* trypomastigotes can downregulate the surface expression of CD86, HLA-DR and

CD40 (Poncini *et al*. 2008; Planelles *et al*. 2003). Surface marker expression shown in this chapter showed a degree of maturation hindrance in moDCs after co-cultivation with *T. brucei*. This indicates that members of the *Trypanosoma* genus may share similar strategies in compromising DC function. Antigen uptake was also impaired following co-cultivation with *T. brucei* as the phagocytic capacity of moDCs decreased over time. This reduction in endocytosis was likely the result of a direct downregulation of DC function as opposed to the consequence of maturation.

To determine whether substituents of the *T. brucei* membrane were the cause of DC downregulation, I isolated soluble VSG from two different bloodstream form *T. brucei* cell lines, each expressing a different VSG variant, and used them as stimulants for moDC activation. The effect of soluble VSG on moDC maturation was similar to that induced by whole trypanosomes, where the expression levels of all four markers remained at the same level as untreated DCs. CD80, an important co-stimulatory molecule needed for the priming of naïve T-cells, was further downregulated in a dose dependent manner. Interestingly, the impact of *T. brucei* on DC maturation appeared to be dependent on the VSG variant, with VSG221 being the more potent variant. One of the main functions of VSG N-linked oligosaccharides is to provide structural stability to the parasite surface coat (Schwede *et al*. 2015). As suggested by Schwede *et al*, N-linked glycosylation could also be integral for VSG folding efficiency, which would directly impact on the parasite growth rate. This indicates that the glycosylation state of the VSG could contribute to virulence of trypanosomes on the host immune cells. This may be a potential target for future anti-trypanosome drug design.

Apart from direct interference, parasites can release various products to modulate DC functions. Excreted-secreted products are commonly used by parasites to alter their target cell function, either by suppressing activation or by changing the types of cytokine released by the

cell (Geiger *et al*. 2010; Terrazas *et al*. 2010). The helminth parasite *Trichinella spiralis* is known for secreting products which not only downregulate DC maturation, but also induce expansion of the immunosuppressive regulatory T-cells (Treg) (Langelaar *et al*. 2009; Aranzamendi *et al*. 2012). *P. yoelii* and *P. falciparum* infected red blood cells can change the DC cytokine profile and inhibit IL-12 production (Ocaña-Morgner *et al*. 2008; Ocaña-Morgner *et al*. 2003). Without IL-12, the ability of DCs to elicit a Th1 response is greatly reduced, preventing effective parasite clearance. Recently, the secreted products known as the "secretome" of *T. brucei gambiense* was revealed to impair LPS-induced DC maturation and T-cell stimulation capacity (Garzon *et al*. 2013). Together, these strategies not only affect the targeted immune cell types, but also alter downstream effector cell functions. In most cases, T-cell proliferation, clonal expansion and differentiation are changed to induce a parasite tolerant environment in the host (Rodrigues *et al*. 2014).

Here, I found that incubation of moDCs with *T. brucei* resulted in the secreted cytokines shifting to an increasingly immune-tolerant profile over time. Three cytokines with pro-inflammatory and immune cell recruitment properties (MCP-1, TNF-α and IL-6) were significantly downregulated after 3 days of *T. brucei* exposure. TNF-α has been studied extensively for its role in infection control in Human African Trypanosomiasis and was identified as the key regulator in controlling trypanosome growth (Magez *et al*. 1999; Magez *et al*. 1997). However, excess levels of TNF-α have also been demonstrated to have devastating effects on the host due to uncontrolled inflammation. This ultimately causes anaemia and irreversible tissue damage in Human African Trypanosomiasis patients (Musaya *et al*. 2015; Naessens *et al*. 2005). The reduction of this cytokine by *T. brucei* in combination with MCP-1, the cytokine that is responsible for the migration and infiltration of monocytes, T-cells and NK-cells would impair the ability of host DCs to elicit an effective inflammatory response.

Meanwhile, IL-10 levels continuously increased throughout the co-culture time course, counteracting the effects of TNF-α and creating a more trypanosome-tolerant environment. IL-10 has been shown to have a protective role in *T. brucei* experimental murine models, where mice with increased levels of IL-10 had longer survival and milder inflammatory associated pathology (Namangala *et al*. 2001).

Although the role of IL-6 in experimental Human African Trypanosomiasis models is less well defined, IL-6 has been implicated in the induction of maturation of B cells into antibody-secreting cells as well as the commitment of the Th17 response (Hunter & Jones 2015; Scheller *et al*. 2011). As revealed in previous chapters, anti-VSG antibodies are key to trypanosome phagocytosis by macrophages. If maturation of antibody-producing B-cells can be downregulated by inhibiting the release of IL-6, *T. brucei* could evade both the innate and adaptive arms of the host immune system. Interestingly, one anomaly stood out: the levels of IL-8, a potent chemoattractant for neutrophils, was elevated to over 10 000 pg/ml and over 18.5-fold compared to the untreated control. Judging from the cytokine profile so far, it seemed unusual for an immune cell recruiting cytokine to be upregulated to such extent. One explanation for the phenomenon could be a compensatory mechanism used by the host moDCs in an attempt to counteract the effects of immunosuppression.

Modulation of dendritic cell function is a common survival strategy employed by many intracellular and extracellular parasites. Throughout evolution, parasites have developed various ways to avoid attacks by the immune system and aim to reach a symbiotic co-existent state with their host. One of the most effective ways of survival is to interfere with the functioning of dendritic cells. Bloodstream form *T. brucei* is an extracellular parasite, which means it is in constant contact with dendritic cells during an infection. As a result, *T. brucei* must employ multiple mechanisms to avoid elimination. Antigenic variation and high rates of

host opsonin removal are two of the most efficient evasion mechanisms to avoid antibody-mediated response. However, very little is known about the means by which trypanosomes target DCs.

In this chapter, I aimed to explore the mechanisms of interactions between *T. brucei* and human moDCs using an *in vitro* system. Although the presence of *T. brucei* did not significantly alter the expression of DC co-stimulatory molecules, the phagocytic ability of DCs was visibly reduced. This suggests that there was a degree of hindrance exerted by the parasite to minimise an activating response by the host dendritic cells. There are indications that the types of cytokines released were shifted towards a less inflammatory profile and dampening the ability of the host to mount a parasite clearance response. Nevertheless, future work to investigate the effects of *T. brucei* on LPS or other stimuli-activated dendritic cells could more accurately reflect the immunosuppressive effects of the parasite. As DC activity directly influences T-cell activation, differentiation and ultimately their effector functions, the impact of *T. brucei* treated DCs on the functioning of T-cells will be explored in the next chapter.

# Chapter 6

# Immunomodulation of human T-cells by *T. brucei in vitro*

## 6.1 Introduction

Upon encountering a mature dendritic cell presenting antigen peptide:MHC complexes on its cell surface, along with the aid of co-stimulatory molecules, naïve T-cells become activated and will go through several days of proliferation and mature into effector cells. Several classes of effector T-cells exist, and each subset elicits a range of responses such as cytokine release that define their respective functions.

Bloodstream form *T. brucei* has been shown to modulate the host immune response in multiple ways. Most of these evasion strategies have involved dampening host mechanisms that aid parasite clearance (Stijlemans *et al*. 2016; Donelson *et al*. 1998; Namangala 2011). In the previous chapter, I have shown the immunomodulatory effects that *T. brucei* exerts on dendritic cells, which include downregulating DC maturation, antigen uptake and dampening the pro-inflammatory response. Here I would like to investigate how impaired DC functions could alter the T-cell response elicited by *T. brucei* stimulation.

Through antigen presentation by DCs, T-cells play a crucial role in activating the rest of the adaptive immune system. Studies done using resistant murine models have shown that bloodstream form *T. brucei* elicits a polarised Th1 response in the early stages of infection, with the release of pro-inflammatory cytokines: IFN-γ and TNF-α (Hertz *et al*. 1998; Magez *et al*. 1999). This serves to recruit and activate macrophages to clear the parasite via phagocytosis and the release of nitric oxide (NO) (J M Mansfield & Paulnock 2005). This early pro-inflammatory response, which aims to control the first and most aggressive wave of parasitaemia is then replaced by a switch to a type II response that confers trypanotolerance in

the later stages of infection. This is because excessive inflammation causes tissue damage, anaemia and overwhelms the host, which is not favourable for parasite survival (Naessens *et al*. 2005; Musaya *et al*. 2015).

Like most parasites, bloodstream form *T. brucei* induces an immunosuppressive environment to aid its survival and proliferation. Although there is evidence suggesting that in most trypanosome infection models, a strong Th1 response is protective during the early stage of trypanosomiasis, there is currently no consensus as to the players involved in orchestrating this response (Taylor R Dagenais *et al*. 2009; J. M. Mansfield & Paulnock 2005). In fact, numerous studies have presented contradictory results in terms of cytokine profiles and their function in determining the type of T-cell response (Kato *et al*. 2016). For example, in experimental trypanosomiasis using mouse models, TNF-α was shown to be crucial in control parasite growth and extended the survival of mice (Magez *et al*. 1997). On the contrary, clinical data from trypanosomiasis patients showed TNF-α was associated with the severity of disease progression (MacLean *et al*. 2004).

To this day, most previous studies have focused on the contribution of the Th1 and Th2 polarisation in experimental trypanosomiasis but other subsets of T-cells namely, Th17 and regulatory T-cells (Treg) have not been investigated extensively. In *T. cruzi* and *T. congolense* infections, IL-17 has been shown to mediate control of parasite growth and plays an important role in host defence (Mou *et al*. 2010; Miyazaki *et al*. 2010; da Matta Guedes *et al*. 2010). However, there is currently limited information on T-cell regulation in a trypanosomiasis experimental model, and to the best of my knowledge there is no evidence of Th17 cell involvement in *T. brucei* infections. The network of cytokine production is complex and dynamic, and involves the interaction between multiple subsets of immune cells. Moreover,

cytokine release changes during different stages of infection, making it difficult for a single experimental model to resolve.

In this chapter, I would like to expand on the research question addressed in the previous chapter, which is how an impaired antigen presentation system affects the T-cell response during a *T. brucei* infection. By characterising the cytokine profiles produced by T-cells after activation by *T. brucei* stimulated DCs *in vitro*, I aim to gain better insight into the dynamics and interactions of T-cell responses during a *T. brucei* infection.

## 6.2 Experimental outline

Monocyte derived dendritic cells from healthy human donors were first stimulated by bloodstream form *T. brucei* for 16, 24, 48 or 72 hours. These cells were then irradiated and co-cultured with CD3+ T-cells isolated from the same donor. Three parameters of T-cell function were subsequently studied, which included activation, proliferation and cytokine production by CD4+ T helper cells.

### 6.3 Naïve CD3 positive T-cells were activated by *T. brucei* exposure

Naïve CD3 positive T-cells were isolated from the PBMCs of healthy donors using anti-CD3 microbeads and selected via a magnetic separation column. To ensure the purity of the CD3+ cells after selection remained high (>95%), cells were stained with anti-CD3 antibodies after column selection and analysed by flow cytometry. Figure 6.1 shows the gating strategy of CD3+ T-cells. The average purity of CD3+ T-cells reached 97.5% using the magnetic bead isolation method. These CD3+ T-cells were co-cultured with gamma-irradiated moDCs from the same donor, which had been stimulated by *T. brucei*. On day 5 of the co-culture, cells were harvested and stained for the T-cell activation surface markers: CD25 and CD69.

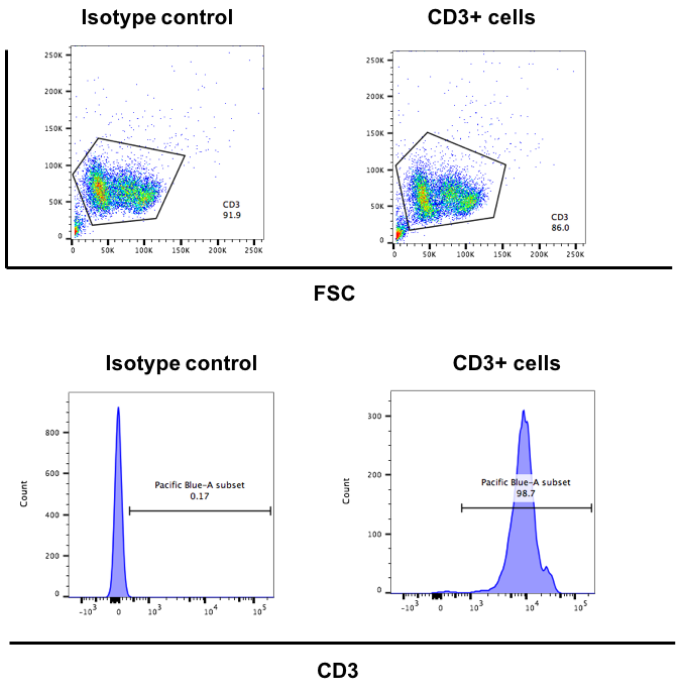
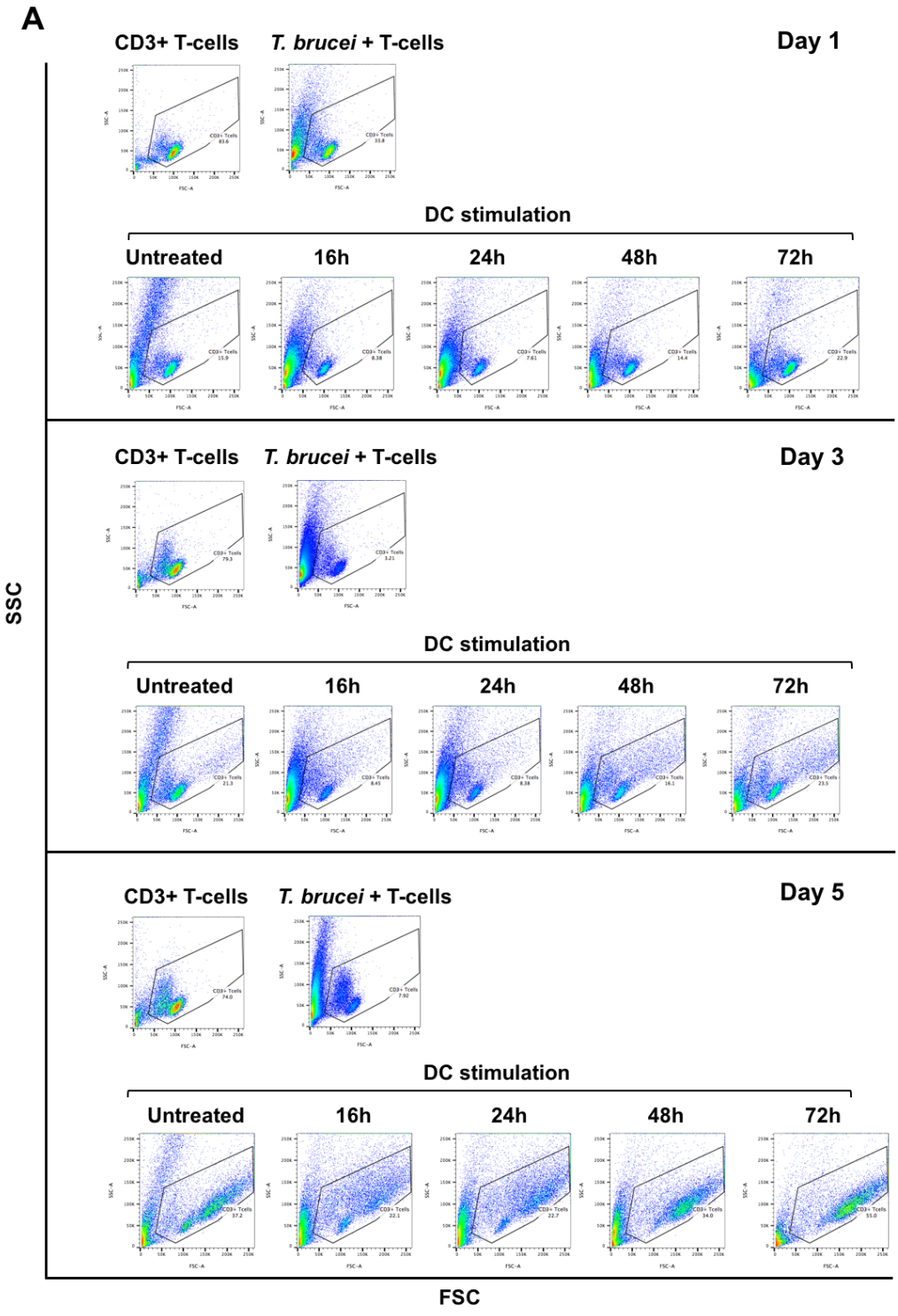



**Figure 6.1 Flow cytometry gating of CD3+ cells after selection. (A)** Viable CD3+ T-cells were incubated with anti-CD3 magnetic microbeads and selected using a magnetic separation system. Cells were then stained with anti-CD3 antibodies to ensure the purity of the population was high (>95%).

Like dendritic cells, T-cells also undergo a range of phenotypical and functional changes upon activation. It has been shown that T-cells increase in size in response to activation, which can be detected by an increase in forward light scatter (FSC) using flow cytometry (MacDonald & Zaech 1982; Böhmer *et al*. 2011). Figure 6.2A illustrates the change in forward light scatter versus side scatter when naïve CD3+ T-cells were exposed to moDCs that were stimulated by *T. brucei* for different lengths of time: 0, 16, 24, 48 and 72 hours. T-cells were co-cultured with gamma-irradiated moDCs for 1, 3 and 5 days before analysis by flow cytometry.

The first day after T-cell and DC co-culture, there was no significant change in FSC values across all conditions (Figure 6.2A and B). To ensure that the T-cell activation effects by *T. brucei* was exerted via dendritic cell antigen presentation and not directly from *T. brucei*, the parasite was added directly to the T-cell culture as a control. LPS was used as a positive stimulant for DC maturation and was included throughout T-cell co-cultivation. However, after 3 days of co-culture, signs of T-cell activation began to show. LPS-treated DCs were able to activate T-cells and shift the population of high FSC ($FSC^{HI}$) cells from 3.9 % to 17.4 % in 3 days (Figure 6.2B). Untreated DCs had also increased T-cell activation marginally from 0.33 % of the gated population to 8.58 %, suggesting that there was a basal level of T-cell activation even when DCs were left untreated. Interestingly, there were indications that DCs that were exposed to *T. brucei* for 16 and 24 hours had immunosuppressive effects on T-cells, where both conditions showed a lower $FSC^{HI}$ population shift, 5.8% and 6.6% respectively, compared with the untreated control. However, the suppressive effect disappeared when moDCs were stimulated with *T. brucei* for over 48 hours, as the percentage of $FSC^{HI}$ T-cells rose to 14.1 % (48 h) and 38.6 % (72 h) (Figure 6.2B). This trend continued through to day 5 of the DC-T-cell co-culture. 16 h and 24 h of *T. brucei* exposure resulted in similar levels of T-cell activation compared with the untreated control (51.4 % and 42.5 % vs 51.2 %). However, 48 h and 72 h

of *T. brucei* treatment generated a significant increase in $FSC^{HI}$ T-cell population of 75.3% and 75.7% by day 5. Consistent with the results from day 3, a basal level of activation could be seen when untreated DCs were co-cultured with T-cells.



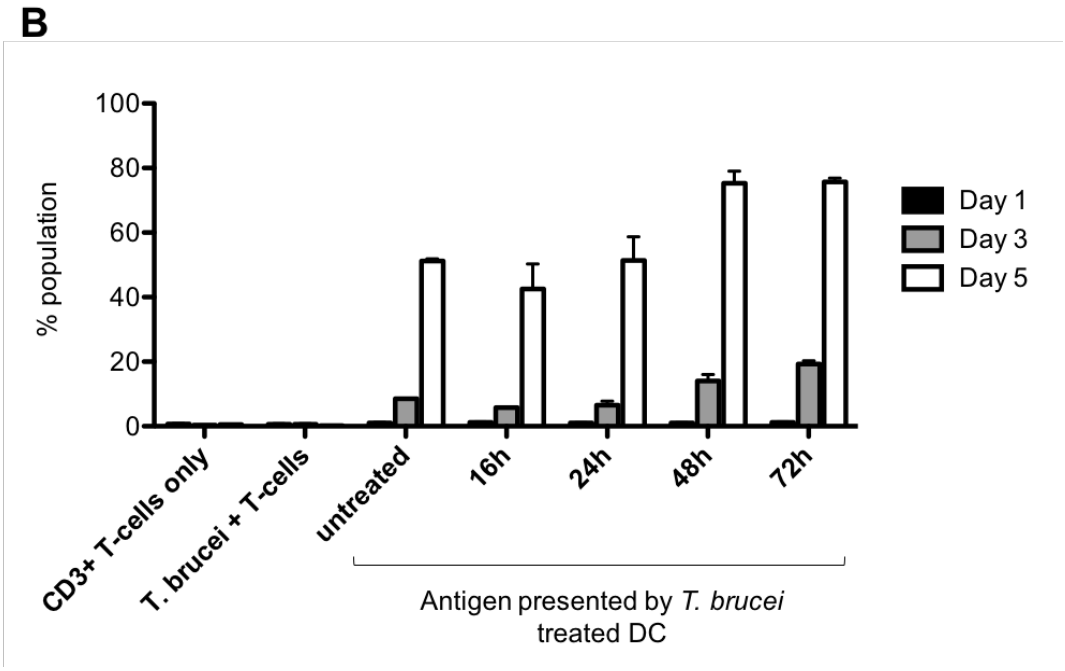



**Figure 6.2 Size of CD3+ T-cells increased after co-culture with moDCs presenting *T. brucei* antigens. (A)** Flow cytometry dot-plot diagrams showing the change in forward scatter (FSC) against side scatter (SSC) after 1, 3 and 5 days of T-cell co-culture with *T. brucei* stimulated moDCs from the same donor. moDCs were stimulated with *T. brucei* for 0, 16, 24, 48 and 72 hours. moDCs and *T. brucei* were then gamma-irradiated before addition to CD3+ T-cells in a 1:5 ratio. **(B)** CD3+ T-cells were gated as shown in (A) and the shift in FSC was gated accordingly. The change in population is expressed as a percentage of the P1 gated parent population and plotted as a bar graph. Results show the mean percentage population change from 2 independent biological replicates with SEM as error bars.

### 6.4 T-cells were activated but activation markers were downregulated upon prolonged co-culture with *T. brucei* stimulated moDCs

The expression of CD69 and CD25 are induced when T-cells become activated and are commonly used as markers for T-cell activation. CD69 is one of the earliest inducible T-cell activation markers and its level was shown to peak around day 4 after stimulation. CD25 forms the alpha chain of the IL-2 receptor and showed a later peak of expression, between days 4 to 8 after activation (Caruso *et al*. 1997; Shipkova & Wieland 2012).

To confirm the increase in T-cell activation as shown in Figure 6.2, CD3+ T-cells were simultaneously stained with anti-CD25 and anti-CD69 antibodies. The expression of both surface activation markers was upregulated; CD25 expression rose 6.7-fold, whereas CD69 levels increased 3.7-fold (Figure 6.3). However, as the exposure time of moDCs to *T. brucei* increased, their ability to activate T-cells dropped. After 72 hours of co-culture of *T. brucei* with stimulated moDCs, CD25 and CD69 expression reduced by 2.2-fold and 4-fold respectively compared with the levels at 16 h. In the case of CD69, its expression level was even lower than that of the untreated control, while CD25 levels remained 3 times above that of the control.

It appears that T-cells were activated by moDCs that were stimulated by *T. brucei,* as shown by the increase in the population of $FSC^{HI}$ cells (Figure 6.2). However, the ability of moDCs to present antigen and elicit a response from T-cells was impaired over time, as indicated by the decrease in activation of marker expression. This was consistent with my previous observation in Chapter 5, where I showed a significant decrease in antigen uptake and maturation by moDCs after prolonged exposure to trypanosomes. However, it was unclear which subsets of T-cells had been activated and what kind of response caused the downregulation of CD25 and CD69.

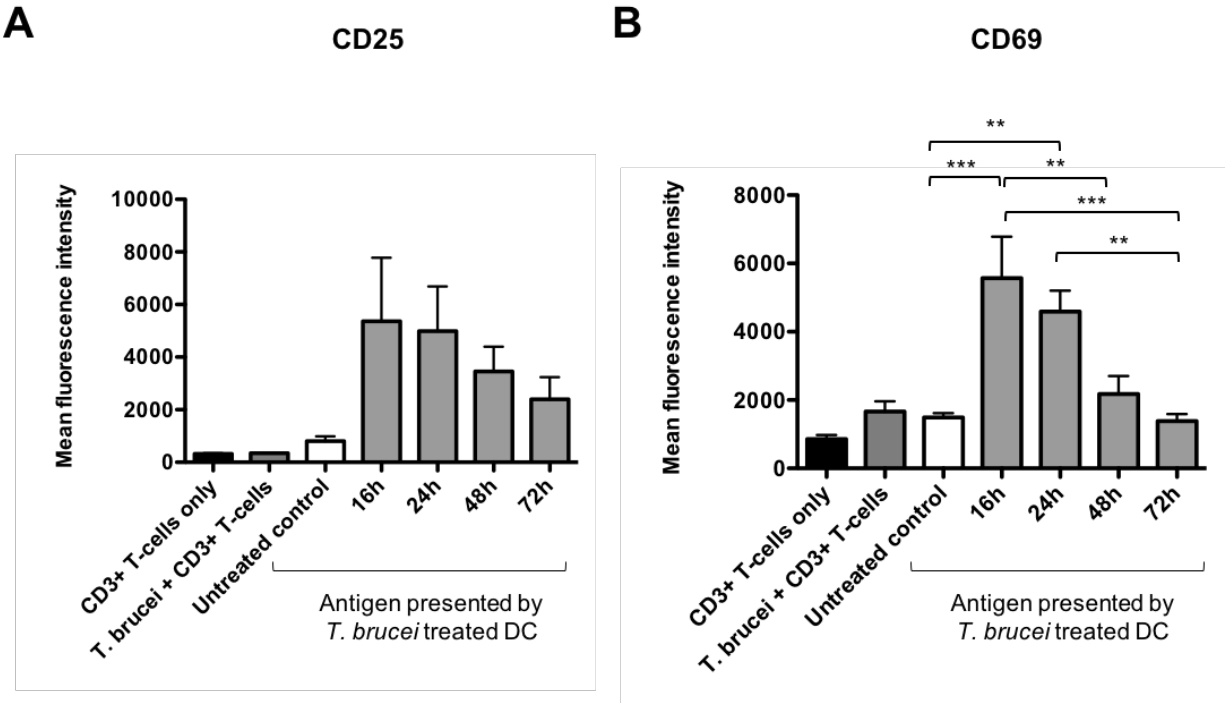



**Figure 6.3 CD3+ T-cells were activated by moDCs presenting *T. brucei* antigens.** Expression levels of the T-cell activation surface markers **(A)** CD25 and **(B)** CD69 five days after co-culture with moDCs. Results show the mean values of 4 independent biological replicates with SEM indicated as error bars. Statistical analysis was performed using the one-way ANOVA test and the Tukey post-test. **P<0.01, ***P<0.001.

### 6.5 *T. brucei* stimulated moDCs triggered CD3+ T-cell proliferation

It was established in the previous section that CD3+ T-cells were activated but gradually downregulated if moDCs were exposed to *T. brucei* over a prolonged period. I next investigated whether changes in T-cell activation state had an impact on T-cell proliferation and the subsets of T-cells that were expressed (Figure 6.4). T-cells were stained with carboxyfluorescein succinimidyl ester (CFSE), a fluorescent dye which stains intracellular molecules. As a CFSE-stained cell divides, its daughter cells will theoretically receive half of the number of CFSE-stained molecules, thus dividing the fluorescence intensity in half. As a

result, the degree of cellular proliferation can be tracked and quantified by the decrease in fluorescence signal using flow cytometry (Quah *et al*. 2007; Parish *et al*. 2009).

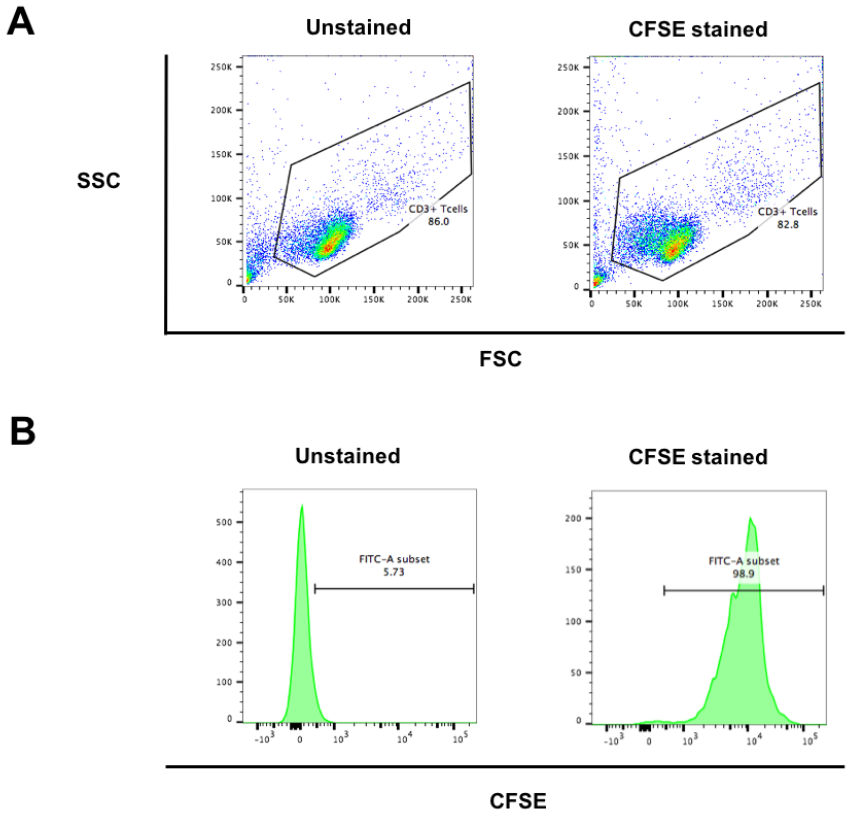



**Figure 6.4 Flow cytometry gating of CFSE-stained CD3+ T-cells.** Following the isolation of CD3+ T-cells, T-cells were stained with 0.05 mM CFSE at 37°C for 20 minutes. Fluorescence expression of CFSE stained T-cells was assessed compared to an unstained control using flow cytometry.

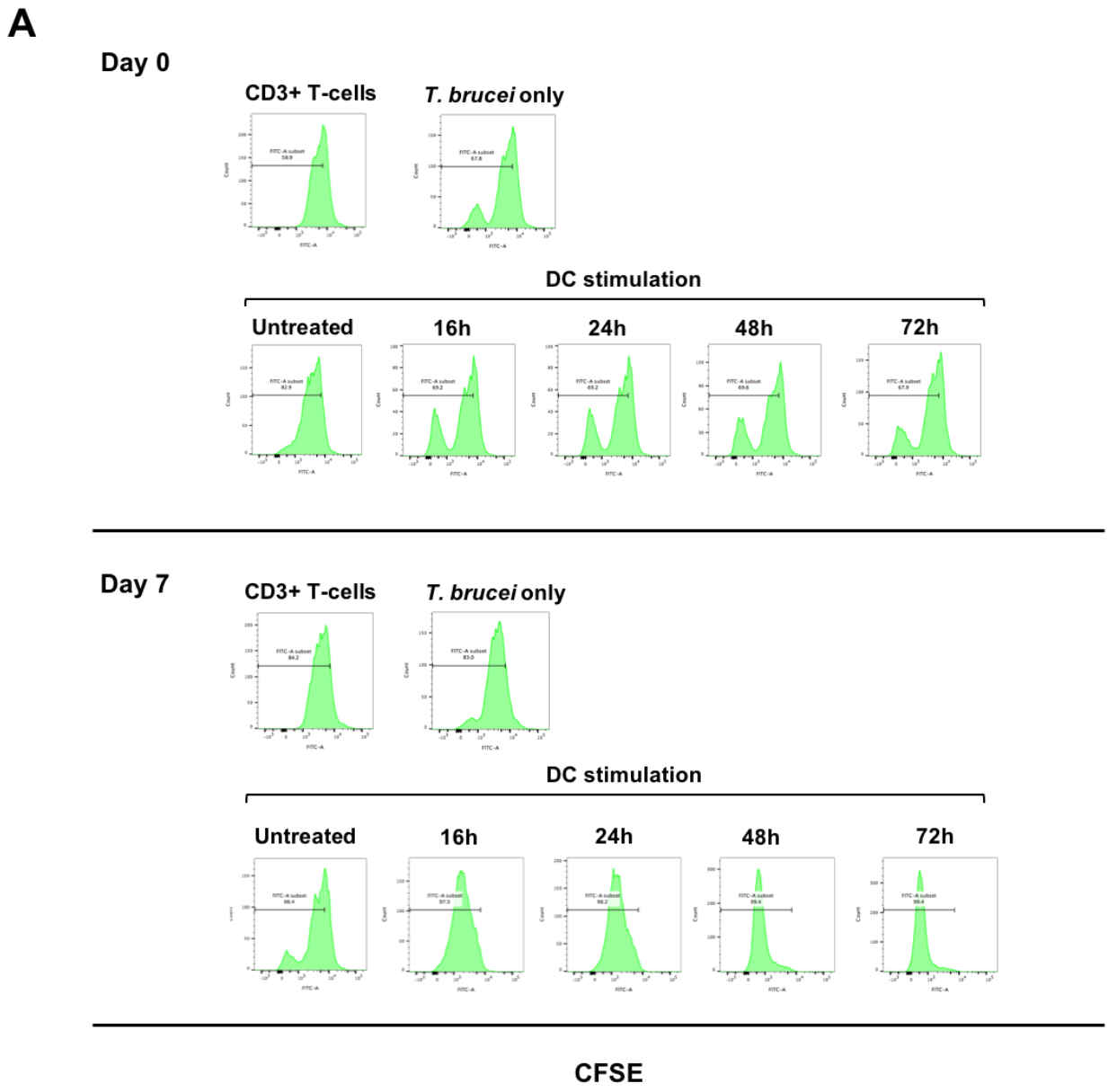
T-cells were stained with CFSE and co-cultivated with irradiated moDCs which had been exposed to *T. brucei* for 0, 16, 24, 48 and 72 hours. CFSE staining was then measured after 0, 2, 3, 5 and 7 days of co-culture by flow cytometry. Figure 6.5A shows the shift in CFSE signal from day 0 to day 7. On day 0, CFSE levels across all conditions were high as expected. However, in the samples where *T. brucei* was present, there was a small peak that showed little to no CFSE staining. This was presumably due to the high endocytosis rate of bloodstream

form *T. brucei*, which caused the rapid degradation of CFSE. After 7 days of co-culture, a significant decrease in CFSE signal was observed compared with the untreated control, indicating that the T-cell population had proliferated in response to *T. brucei* antigen peptides presented by moDCs. The shift of CFSE signal to the left of the histogram increased with the length of time that moDCs were exposed to *T. brucei*.

CFSE staining was subsequently quantified by flow cytometry and a complete representation of T-cell proliferation over 7 days is shown in Figure 6.5B. To ensure that the effects observed in T-cells did not result from non-specific stimulation of DCs, unstimulated DCs were co-cultured with T-cells. The controls with only CD3+ T-cells and *T. brucei* added directly to T-cells showed some degree of CFSE signal loss either through cell proliferation or fluorescence degradation. Consistent with what was shown in Figure 6.2, the untreated control which contained only moDCs and T-cells also displayed a basal level of T-cell proliferation. With the addition of *T. brucei* treated moDCs, significant T-cell proliferation was observed. Theoretically, if the CFSE signal decreased by half, the entire cell population should have completed one cell cycle. Two days after T-cell were stimulated by moDCs that have been treated by trypanosomes for 16 hours, a drop in CFSE signal of 1.72-fold was recorded. On day 3, the signal was further reduced by 2.2-fold, indicating the cell population had gone through 2 rounds of division. This effect was further enhanced when T-cells were treated with moDCs that had been co-cultured with trypanosomes for 72 hours. By day 7, these T-cells cells had undergone an extra cell division compared with 16, 24, and 48 h of *T. brucei* treatment.

This observation seemingly contradicts results in the previous chapter, where I showed that moDC functionality was downregulated by prolonged exposure to *T. brucei*. Therefore, the paradoxical increase in T-cell proliferation must be influenced by additional elements apart from the direct activation by moDC antigen presentation. One possibility is the changes of co-

stimulatory and co-inhibitory molecules expressions profiles caused the functional suppression of moDCs. The pattern resulted may favour the proliferation of some T-cell subsets. However, such postulation needs to be further explored in the future.



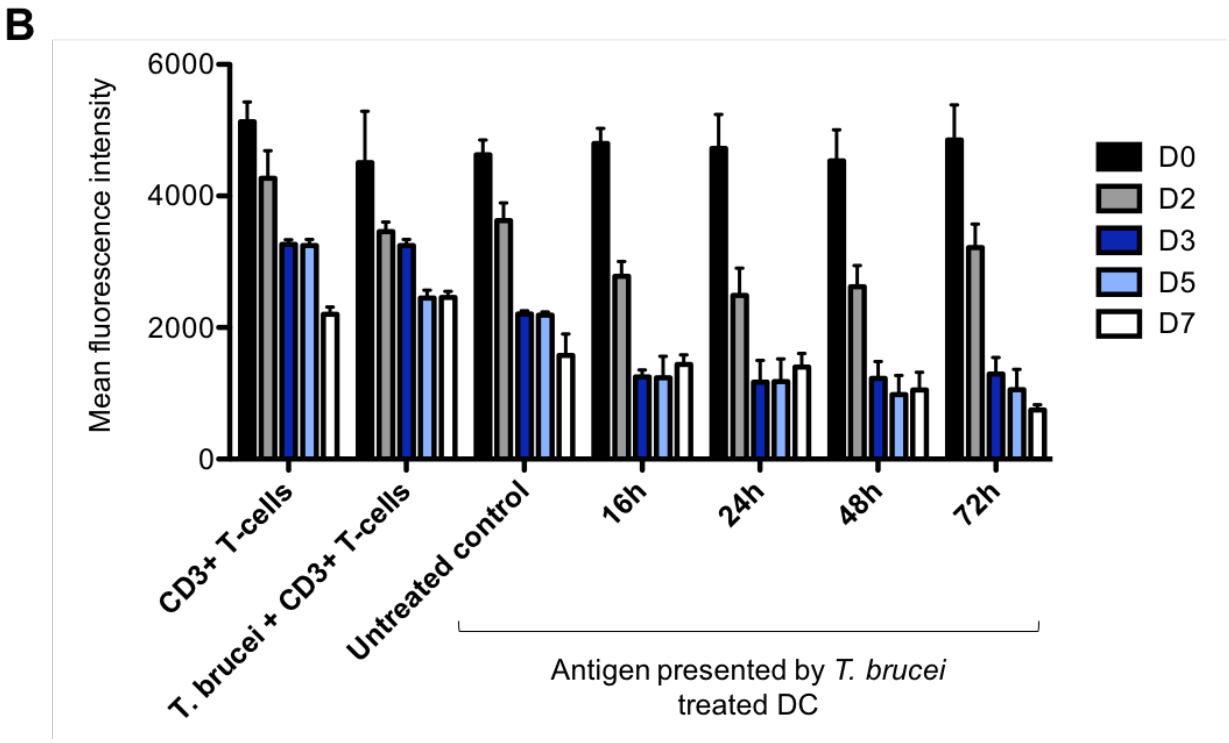



**Figure 6.5 moDCs treated by *T. brucei* for 72h promoted CD3+ T-cell proliferation.** CD3+ T-cells were stained with CFSE to track cell proliferation 0, 2, 3, 5 and 7 days after co-cultivation with moDCs from the same donor. moDCs were stimulated with *T. brucei* for 0, 16, 24, 48 and 72 hours. moDCs and *T. brucei* were then gamma-irradiated before being added to CD3+ T-cells in a 1:5 ratio. CFSE fluorescence was detected using flow cytometry. **(A)** Representative flow cytometry histograms illustrating the change in CFSE signal (green peaks) after 0 and 7 days of co-culture. **(B)** Quantification of the CFSE signal, which was expressed as mean MFI values from 4 independent biological replicates.
Statistical analysis was performed using the two-way ANOVA test. There was a significant interaction in *T. brucei* treatment of DCs and the number of days of co-culture with T-cells, F (7.66), P<0.0001.

### 6.6 Th17 cells were involved in generating a pro-inflammatory microenvironment

To investigate what other factors were involved in triggering the proliferation of T-cells, a cytokine screen was performed. Using a similar bead-based immunoassay that was used to screen cytokine production by dendritic cells, I was able to quantify cytokine release from T-cells by flow cytometry. Interestingly, production of all four of the cytokines (IL-17A, IL-17F, IL-21 and IL-22) associated with the Th17 cell lineage were upregulated (Figure 6.6). Th17 cells are a newly identified T helper cell subtype in addition to Th1 and Th2 cells. Functionally, Th17 cells have been found to play a key role in host defence against extracellular pathogens. Th17 cells are defined by their ability to secrete cytokines in the IL-17 family, primarily IL-17A and F. IL-17A and IL-17F share the greatest homology within the family and are regulated by similar mechanisms due to the proximity of their gene loci on the same chromosome (Crome *et al*. 2010; Kolls & Lindén 2004).

The expression of both IL-17A and IL-17F was upregulated 4-fold and 25-fold respectively after co-cultivation with moDCs that were exposed to *T. brucei* for 16 hours (Figure 6.6A and B). Similar levels of IL-17A were produced by Th17 cells regardless of the amount of time that moDCs were stimulated by trypanosomes. IL-17F levels on the other hand, drastically increased when T-cell came into contact with moDCs that had been co-cultured with *T. brucei* for 72 hours. An increase in IL-17 promotes inflammation and recruitment of immune cells such as macrophages and neutrophils. This coincides with the increase in IL-8 release, which is also a neutrophil attracting chemokine that was produced by moDCs when stimulated by *T. brucei* (Figure 5.6A) in the previous chapter. However IL-17 does not amplify the Th17 population as it does not act as a differentiation factor. Instead, TGF-ß, IL-6 and IL-21 are thought to be responsible as a feedback loop to expand Th17 cells (Korn *et al*. 2007; Zhou *et al*. 2007). IL-6 is a cytokine that closely regulates the activation of Th17 cells and the

production of IL-17A and IL-17F was also shown to be upregulated (Figure 6.6C). In addition, IL-6 has been shown to elicit autocrine IL-21 production (Burkett *et al*. 2015), which surged from 7 pg/ml to 190 pg/ml as the exposure time of moDCs to *T. brucei* increased (Figure 6.6D). IL-21 is also involved in the promotion and maintenance of Th17 lineage commitment and is upregulated by IL-6 during Th17 differentiation (Wei *et al*. 2007). IL-22, although a member of the IL-10 cytokine family, has been identified mostly as a Th17 cytokine and co-expressed with IL-17A and IL-17F *in vivo* (Liang *et al*. 2006; Rutz *et al*. 2013). Its expression rose steadily and increased by 25-fold as the co-culture time between moDCs and trypanosomes increased (Figure 6.6E). In this pro-inflammatory microenvironment, the expression of TNF-α, which is known to contribute to Th17 associated pathology, was also induced (Damsker *et al*. 2010). In the untreated control, TNF-α levels were just above the detection threshold at 52 pg/ml. After 5 days of co-culture with moDCs that were stimulated by *T. brucei* for 72 hours, TNF-α release rose 4.3 times to 224 pg/ml (Figure 6.6F).

The upregulation of all the aforementioned cytokines indicate that *T. brucei* antigen peptides presented by moDCs triggered the proliferation of naïve T-cells, which subsequently differentiated into Th17 cells. Moreover, Th17 cells are known to promote inflammation and play a major role in many chronic inflammation and autoimmune diseases. Therefore, a *T. brucei* infection in this system appeared to shift the T helper cell response towards a pro-inflammatory state.

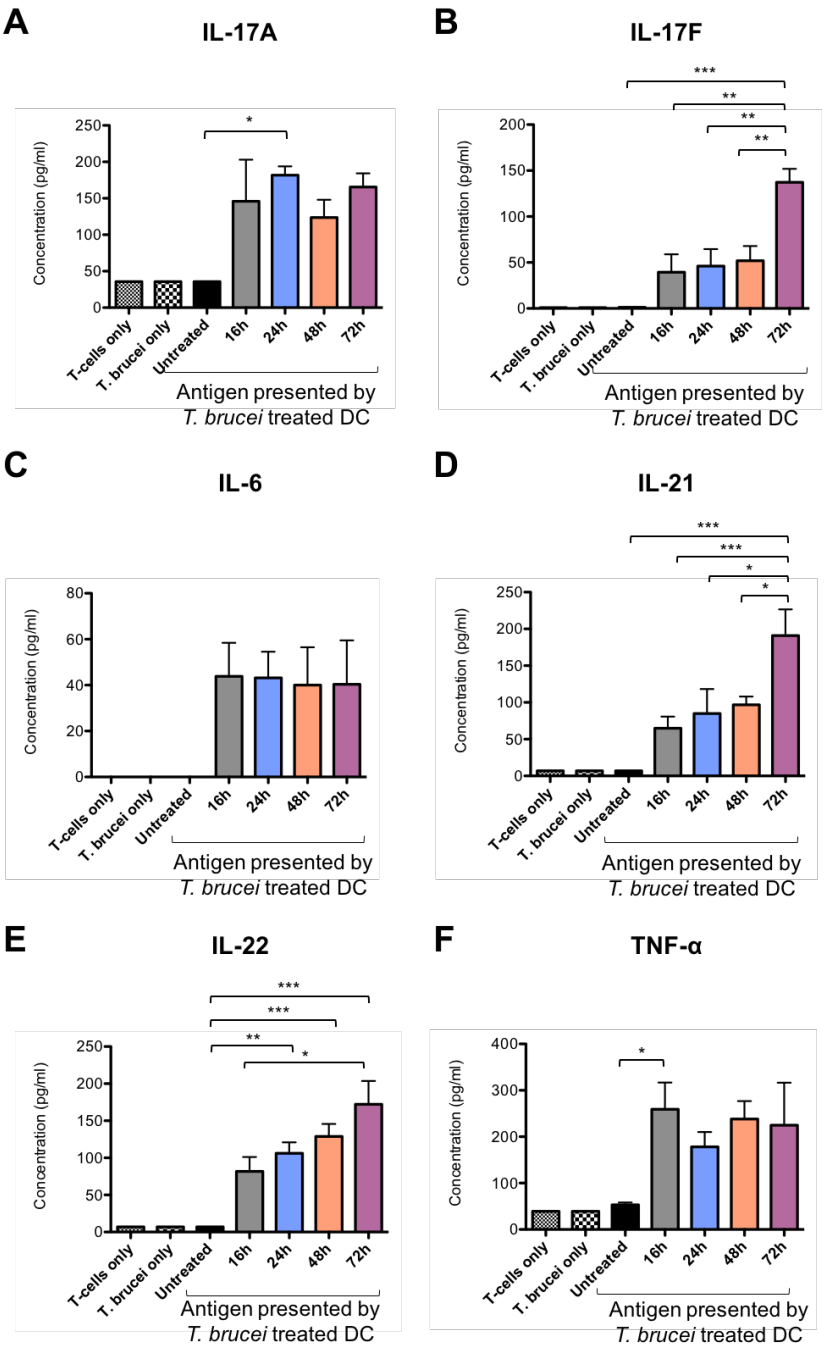



**Figure 6.6 Increase of Th17 cytokine release by CD3+ T-cells after co-culture with *T. brucei*.** moDCs were stimulated by *T. brucei* for 0, 16, 24, 48 and 72 hours before co-cultivation with CD3+ T-cells. 5 days after co-culture, supernatant of the cells was collected and analysed using a bead-based multiplex ELISA kit. The relative concentrations of each cytokine: **(A)** IL-17A, **(B)** IL-17F, **(C)** IL-6 **(D)** IL-21 and **(E)** IL-22 were quantitated using the LEGENDplex™ Human Th Cytokine Panel data analysis software. Results show the mean of 4 independent biological replicates with the SEM indicated with error bars. Statistical analysis was performed using the one-way ANOVA test, followed by the Tukey post-test. *P<0.05, **P<0.01, ***P<0.001.

### 6.7 Th2 cytokines were simultaneously upregulated

In the original Th1 cell and Th2 cell paradigm proposed by Mosmann and Coffman, T-cells were defined by their cytokine secretion profile and categorised into IFN-γ secreting Th1 cells or IL-4 secreting Th2 cells (Coffman 1989). The production of IFN-γ by Th1 cells and the release of IL-4 by Th2 cells antagonises the differentiation of Th2 and Th1 cells respectively. Since the discovery of Th17 cells, the dynamics and relationships between T-cell cytokines have been redefined.

Interestingly, after co-cultivation with moDCs that had been stimulated by bloodstream form *T. brucei*, the expression of these two cytokines was regulated very differently. Whilst IFN-γ levels increased 5.7-fold, to over 1000 pg/ml, expression of IL-4 was reduced 75% (Figure 6.7). Without IL-4, an essential cytokine for the differentiation of naïve T-cells into Th2 cells, the T helper response shifts to a primarily pro-inflammatory state. In addition, IL-4 is known to directly inhibit Th17 cell differentiation and suppress the inflammatory effects brought on by the induction of Th1 and Th17 responses. It would appear that the upregulation of IFN-γ and the reduction in IL-4 would allow the host to more effectively clear the parasite. However, in addition to providing protection to the host, IFN-γ has been shown to promote *T. brucei* growth *in vitro* after exposure to recombinant IFN-γ (Olsson *et al*. 1991). Furthermore, mice with a disrupted IFN-γ gene survived longer and had reduced parasitaemia (Moiz Bakhiet *et al*. 1996). This suggests that IFN-γ could have a dual role in parasitaemia control in a *T. brucei* infection.

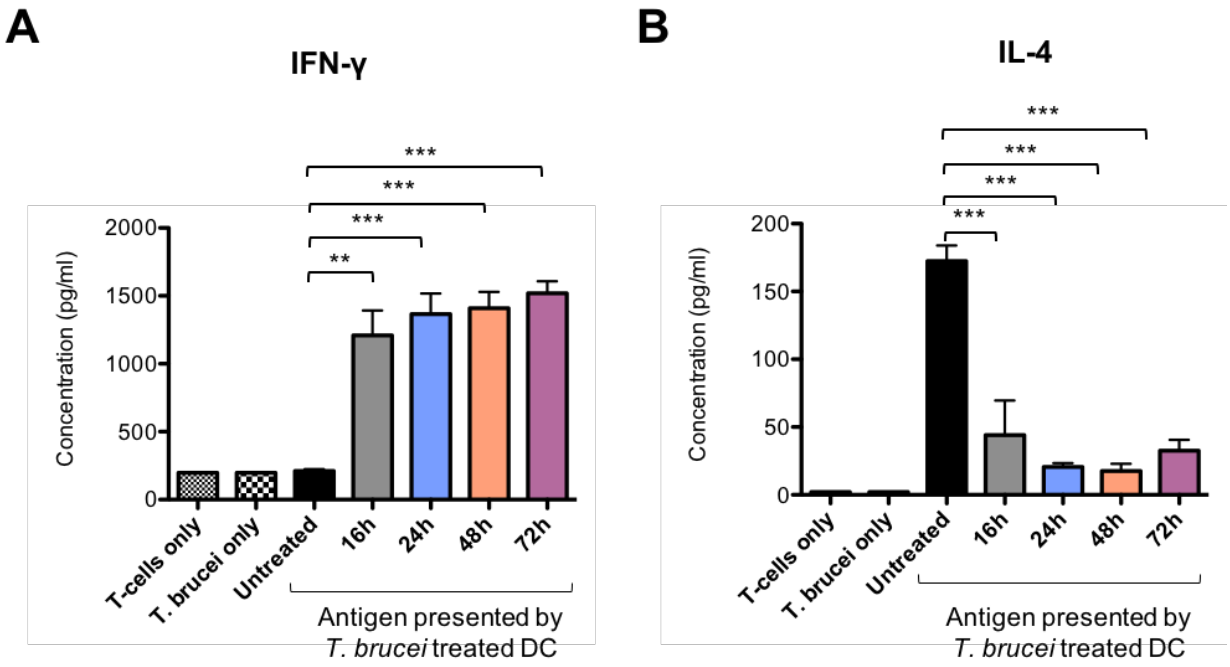



**Figure 6.7 IFN-γ expression increased while IL-4 was downregulated.** moDCs were stimulated by *T. brucei* for 0, 16, 24, 48 and 72 hours before co-cultivated with CD3+ T-cells. 5 days after co-culture, supernatant of the cells was collected and analysed using a bead-based multiplex ELISA kit. The relative concentrations of **(A)** IFN-γ and **(B)** IL-4 were quantitated using the LEGENDplex$^{TM}$ Human T helper cell Cytokine Panel data analysis software. Results shown are the mean of 4 independent biological replicates with the SEM indicated with error bars. Statistical analysis was performed using the one-way ANOVA test, followed by the Tukey post-test. **P<0.01, ***P<0.001.

Further analysis of the cytokine screen revealed the simultaneous upregulation of four anti-inflammatory, Th2 cytokines: IL-5, IL-9, IL-10 and IL-13 (Figure 6.8). Again, the increase in these cytokine levels was directly proportional to the exposure time of moDCs to *T. brucei*. IL-10, a key anti-inflammatory cytokine was upregulated over 50-fold when moDCs were co-cultured with DCs that had been stimulated by *T. brucei* for 72 hours (Figure 6.8A). IL-13, a cytokine that has diverse functions in IgE antibody production, parasite expulsion and inflammation suppression, increased 3-fold (Figure 6.8B). When IL-13 was first characterised, it was thought to be functionally redundant to IL-4 based on its sequence and structure similarity. However, the development of knockout models has shown a much more diverse and complex role of IL-13 (Wynn 2003). Other Th2 cytokines, IL-5 and IL-9 were similarly upregulated by trypanosome treated moDCs (Figure 6.8C and D). Interestingly, in addition to being a conventional Th2 cytokine, IL-9 has also been shown to be a product of Th17 cells. IL-9 secreted by Th17 was shown by Elyaman *et al* to enhance the suppressive effect of regulatory T-cells (Treg) (Elyaman *et al*. 2009).

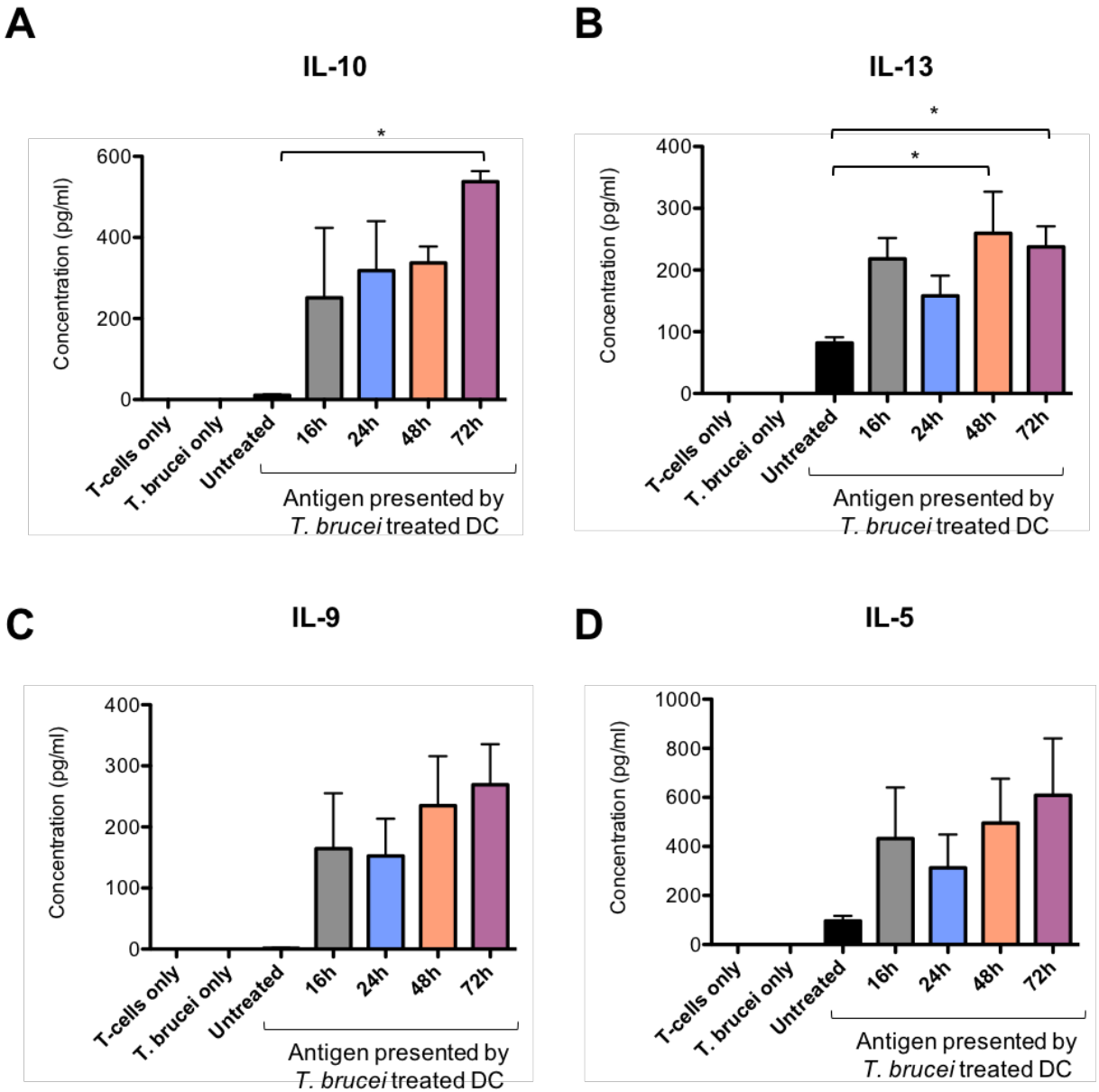



**Figure 6.8 Expression of Th2 cytokines were simultaneously upregulated.** moDCs were stimulated by *T. brucei* for 0, 16, 24, 48 and 72 hours before co-cultivation with CD3+ T-cells. 5 days after co-culture, supernatant of the cells was collected and analysed using a bead-based multiplex ELISA kit. The relative concentrations of **(A)** IL-10, **(B)** IL-13, **(C)** IL-9 and **(D)** IL-5 were quantitated using the LEGENDplex™ Human T helper Cytokine Panel data analysis software. Results shown are the mean of 4 independent biological replicates with the SEM indicated with error bars. Statistical analysis was performed using the one-way ANOVA test, followed by the Tukey post-test. *P<0.05.

## 6.8 Discussion

This chapter explored the effect that *T. brucei* stimulated DCs have on the T-cell response in the context of activation, proliferation and cytokine release. T-cells are critical for the control of trypanosome infections, as the coordination of the adaptive immune response lies in the effector functions of T-cells. These responses were quantified using moDCs from healthy donors which had been stimulated by bloodstream form *T. brucei* for different lengths of time. After 5 days of co-culture, moDCs were able to activate CD3+ T-cells, and stimulate their subsequent proliferation into the different subsets of T effector cells. This effect proportionately increased with the amount of time for which moDCs were exposed to *T. brucei*. Prolonged exposure of moDCs to *T. brucei* also downregulated T-cell activation markers CD25 and CD69, further confirming that the antigen presentation ability was impaired in DCs.

Currently, a large body of evidence suggests that in the acute phase of *T. brucei* infection, the host mounts a polarised Th1 pro-inflammatory response to control the infection. Activation of macrophages causes the release of IFN-γ and IL-12, which in turn primes macrophages to become fully polarised to the M1 phenotype (Paulnock *et al*. 2010; Mansfield 1994). M1 macrophages then release pro-inflammatory cytokines such as TNF-α and NO needed for parasite control. However, Th1 cells are not the only source of IFN-γ. Th17 cells, a T-cell subset that is functionally distinct from Th1 and Th2 cells also elicit a pro-inflammatory response. Th17 cells are characterised by their ability to secrete IL-17, and contribute to the clearance of pathogens that are not effectively cleared by either the Th1/Th2 responses. Apart from IL-17 (IL-17A), Th17 cells also secrete IL-17F, IL-21, IL-6 and IL-22 (Kolls & Lindén 2004; Korn *et al*. 2009). All these cytokines were found to be upregulated significantly after naïve T-cells were co-cultured with *T. brucei* stimulated moDCs, demonstrating that Th17 cells play a major role in the host response against bloodstream form *T. brucei* infection *in vitro*

(Figure 6.6). This has, to the best of my knowledge, never been reported in experimental trypanosomiasis, although the consensus is a dominant pro-inflammatory response at the initial stages of infection.

Th17 cytokines act on a range of cells such as epithelial cells, fibroblasts and macrophages and protects the mucosal layer. The downstream effects of a Th17 response include inducing pro-inflammatory cytokine TNF-α and chemokines such as G-CSF and IL-8, recruiting eosinophils, basophils and neutrophils (Ouyang *et al*. 2008; Kolls & Lindén 2004). Coincidentally, the generation of IL-8 was reported to be enhanced in dendritic cells that were stimulated by *T. brucei* in Chapter 5 (Figure 5.6A). It is likely that neutrophils could play a role in the infection control and clearance of *T. brucei* but little evidence has been reported so far.

Although a pro-inflammatory response is advantageous to infection control and the clearance of the parasite, excessive inflammation has been reported to cause tissue damage and contribute to the pathology of Human African Trypanosomiasis. Trypanosoma-associated anaemia is a hallmark of the overwhelming type I response and is the major cause of death in the cattle form of trypanosomiasis, nagana. This is because the lipid composition of erythrocytes are altered during a trypanosome infection, which results in the preferential phagocytosis of red blood cells by the host phagocytes (Stijlemans *et al*. 2015). Like most parasites, it is vital for *T. brucei* to exist in a symbiotic state with its host to maintain survival and a strong pro-inflammatory response is detrimental to parasite and host survival. As a result, after the initial acute inflammation state, a type II response is activated and anti-inflammatory cytokines such as IL-10, IL-6 and TGF-β have been shown to be upregulated in both mouse models and in Human African Trypanosomiasis patients, resulting in a switch to the chronic stage of the disease (Kato *et al*. 2015; Ngotho *et al*. 2006). This correlates with my data

showing the upregulation of IL-10, IL-5, IL-9 and IL-13 (Figure 6.8) after DCs have been co-cultured with T-cells for 5 days. This dampens the inflammatory response and produces a more favourable immune-tolerant environment for a sustained *T. brucei* infection.

However, the level of IL-4 produced by T-cells was suppressed by the addition of *T. brucei* treated DCs. IL-4 is the key cytokine that triggers the differentiation of naïve CD4+ T-cells into Th2 cells and is important for the activation of B-cells to produce IgG1 and IgE antibodies. The role of IL-4 however has yet to be characterised fully during a trypanosome infection. Experimental trypanosomiasis mouse models have shown that the severity of trypanosomiasis is linked to the ability of the host to control the secretion of IL-4 in mice (M Bakhiet *et al*. 1996). In contrast, clinical data of Human African Trypanosomiasis displayed low levels of IL-4 in all stages of *T. brucei rhodesiense* (MacLean *et al*. 2001). The low levels of IL-4 observed in this study appears to resemble clinical data, and is presumably an immunomodulatory mechanism exerted by the parasite to reduce B-cell and antibody involvement.

Here, I showed that in addition to impairing DC functions, bloodstream form *T. brucei* also targets T-cell functions probably via modulating the antigen presentation response. Apart from altering the balance between Th1 and Th2 cytokines as reported by numerous studies of both experimental trypanosomiasis and clinical data of Human African Trypanosomiasis patients, *T. brucei* was revealed for the first time to upregulate Th17 cytokines. Interestingly, Th17 cells have been demonstrated to be more protective than Th1 cells in a *Trypanosoma cruzi* infection, a parasite that causes Chagas disease (Cai *et al*. 2016). Despite this promising observation, more analysis must be done to confirm the involvement of Th17 cells in *T. brucei* clearance. Markers for Th17 cell differentiation including IL-23 and TGF-β that are involved in lineage commitment need to be measured. Moreover, it will be important to distinguish the

immune response and cytokines profile during the acute phase and chronic phase of infected patients. There may be more profound immune interactions in patients under chronic infection.

Nevertheless, cytokine regulation is extremely complex and dynamic and may be influenced by other confounding factors such baseline immune status of the subjects. The complexity is reflected by the large amounts of contradictory data presented in current literature regarding cytokine profiles throughout the course of a *T. brucei* infection. There have been numerous attempts to use cytokines as disease stage biomarkers but due to insufficient sensitivity in their detection, clinical use of such markers have been limited (Kato *et al*. 2016). My model utilized a reductionist approach and can help to clarify some basic immune response that may take place in the host.

Overall, trypanosomes have evolved extremely effective immune evasion mechanisms to modulate the host's adaptive immune response to create an environment suitable for parasite survival and proliferation. During the course of infection, the host's capacity to respond becomes impaired, and a chronic infection accompanied with persistent inflammation is established. Therefore, understanding the interplay between different T-cell subsets and the influence of cytokines on parasite control and clearance is a crucial step for the development of appropriate alternative treatments.

# Chapter 7

# Potential therapeutic use of pegylated-arginase (BCT-100) in the treatment of Human African Trypanosomiasis

## 7.1 Introduction

Human African Trypanosomiasis is caused by two human infectious *Trypanosoma brucei* sub-species, *T. b. rhodesiense* and *T. b. gambiense*. Both subspecies are extracellular parasites which cycle between the Tsetse fly vector and the human host. *Trypanosoma b. rhodesiense* is found in East and southern Africa and causes an acute form of the disease, whereas *T. b. gambiense* occurs in West and Central Africa and is associated with chronic infection of HAT (Simarro *et al*. 2012). Currently, only four drugs are available to treat HAT: suramin, pentamidine, eflornithine and melarsoprol. With the exception of eflornithine, all were chemotherapy drugs that were discovered in the late 19$^{th}$ and early 20$^{th}$ century (Babokhov *et al*. 2013). However, all these agents have their limitations. Unfortunately, vaccination against HAT is not a viable option due to the ability of bloodstream form *T. brucei* to change its VSG coat periodically and evade from antibody recognition. Therefore, the need to find a cure with minimal side-effects remains a global health priority.

In the 20$^{th}$ century, three epidemics were recorded in sub-Saharan Africa. The first one lasted a decade from 1896 to 1906, killing over 300, 000 people and devastating the economy in the Congo Basin (Steverding 2008). Due to the scale and impact of this epidemic, efforts were put into developing a cure. In 1916, a team of scientists in collaboration with the German pharmaceutical company Bayer, successfully developed the first effective treatment for HAT, which is now known as suramin. Suramin is effective in treating early *T. b. rhodesiense* infections and is used until this day. This was followed by the discovery of a second drug,

pentamidine, which was used to target early stage *T. b. gambiense* infections in the 1930s. Later in 1949, the arsenical compound, melarsoprol was introduced for the treatment of late stage HAT. However, all these drug treatments are chemotherapy drugs with high toxicity and severe side-effects, including nausea, seizures and sometimes death (Steverding 2008; Steverding 2010b).

It was not until the discovery of eflornithine (alpha-Difluoromethylornithine; DFMO), that a drug that is effective against both early and late stages of *T. b. gambiense* was discovered to have trypanostatic effects and was used for Trypanosomiasis treatment. DFMO was developed in the 70s as an anti-cancer chemotherapeutic agent. DFMO is an irreversible inhibitor of ornithine decarboxylase (ODC), the first enzyme involved in polyamine biosynthesis, an essential process for cell proliferation and cytokinesis. This results in the depletion of essential polyamines such as the putrescine and spermidine, and reduces proliferation by blocking the ability of the bloodstream form trypanosomes to divide. DFMO inhibition of ODC is extremely effective against *T. b. gambiense* because the turnover rate of ODC is much slower (18-19 hours) compared to the human ODC (10-30 minutes). The half-life of *T. b. rhodesiense* is shorter than *T. b. gambiense*, at approximately 4 hours. Therefore, DFMO is more effective against *T. b. gambiense*. Eflornithine has also been reported to be a safer option compared with melarsoprol, with fewer neurological and cutaneous adverse effects (Chappuis *et al*. 2005).

Recent treatments of HAT also include a combination therapy involving both eflornithine and nifurtimox, a trypanocide that has shown promise against melarsoprol-refractory *T. b. gambiense* patients. However, there is currently no drug treatment that is effective against both early and late stage infections of *T. b. rhodesiense* as well as *T. b. gambiense* (Babokhov *et al*. 2013; Bacchi 2009). Despite a drop in number of cases due to

better education and preventative measures, the problem of drug toxicity and resistance still remain and alternative treatments are needed.

In the mean time, as cancer becomes the leading cause of death worldwide, research into finding a cure has become a global effort and the priority of many research organisations. As a result, cancer drug development has sky rocketed over the years. However, little attention has been paid to HAT due to a decrease in case numbers in recent years. Consequently, drug development for the treatment of HAT has been lagging behind other tropical neglected diseases.

BCT-100, a pegylated human recombinant arginase is a patented compound developed by Dr. Paul Cheng's group (Bio-Cancer Treatment International Ltd., HK), which has been to shown to be effective against both human hepatocellular carcinoma (HCC) and acute myeloid leukaemia (AML) in early phases of clinical trials. Our team also showed that it can induce apoptosis on acute lymphoblastic leukaemia and neuroblastoma cells *in vitro* (Kwong-Lam & Chi-Fung 2013).

BCT-100 works by competing with the endogenous human arginase enzyme to deplete the target cells of its source of arginine. Normal human arginase has a short half-life of 10-20 minutes, which greatly limits the therapeutic use of recombinant arginase. However, the addition of polyethylene glycol (PEG) polymer chains to recombinant arginase can extend the arginase half-life to 3.5 days, without significant loss of enzyme activity. This modification significantly improves both the stability and circulation time of the drug.

Since many of the anti-trypanosomal drugs in use today are anti-cancer drugs originally developed in the early years of last century, current chemotherapeutic drugs may offer an alternative cure for HAT. Coincidentally, L-arginine is an essential substrate for polyamine synthesis in bloodstream form *T. brucei*. Figure 7.1 illustrates the initial steps of *T. brucei*

polyamine synthesis and where DFMO and BCT-100 target *al*ong this pathway. Seeing this potential opportunity, I decided to investigate the effects of BCT-100 on bloodstream form *T. brucei*.

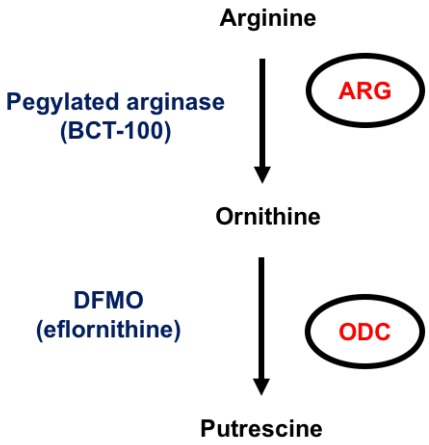



**Figure 7.1 Schematic illustration of the first steps of trypanosome polyamine synthesis.** Arginine is converted into ornithine by the enzyme arginase (ARG). The enzyme ornithine decarboxylase (ODC) then converts ornithine into putrescine. BCT-100 is a recombinant human arginase which competes with the endogenous arginase to deplete arginine. DFMO is a suicide inhibitor of ODC and binds irreversibly to the enzyme to block the generation of putrescine.

## 7.2 Experimental outline

Different concentrations of BCT-100 were tested on the bloodstream form 221VG1.1 cell line *in vitro*. DFMO (eflornithine), an existing drug for HAT treatment was used as a positive control. Toxicity and efficacy of BCT-100 were tested by monitoring trypanosome growth and characterising cell morphological changes.

### 7.3 BCT-100 inhibited *T. brucei* growth and caused parasite lysis *in vitro*

Toxicity of BCT-100 was tested on the bloodstream form 221VG1.1 *T. brucei* cell line. Three concentrations of BCT-100: 0.1, 1 and 10 U/ml were used to test the effect on *T. brucei* growth (Figure 7.2). DFMO, also known as eflornithine is an existing drug used to treat Human African Trypanosomiasis (HAT), and targets the same polyamine synthesis pathway as BCT-100. A titration of effective DFMO concentrations was performed by a fellow PhD student, Louise Kerry, who showed that 200 μM was the lowest effective concentration to inhibit trypanosome growth (unpublished). Therefore, this concentration was chosen as the positive control in the subsequent experiments. As expected, DFMO had an inhibitory effect on trypanosome growth. After 24 hours of growth, DFMO-treated *T. brucei* stopped dividing and their numbers remained at $2x10^5$/ml until the end of the experiment. 0.1 U/ml BCT-100 proved to be ineffective against trypanosome growth control, as the population expanded uninterrupted. Increasing the dose to 1 U/ml improved the effect of trypanosome growth inhibition similar to that of DFMO. Adding DFMO to 1 U/ml BCT-100 had an additive effect and eliminated trypanosomes within 60 hours. The most toxic dose of BCT-100 was 10 U/ml, as BCT-100 at this concentration was sufficient to kill all trypanosomes by 53 hours. For the purpose of studying the effect that BCT-100 on the morphology and cellular functions of *T. brucei*, 1 U/ml was chosen for the subsequent experiments as it was the lowest effective dose and allowed a longer trypanosome viability window to be studied.

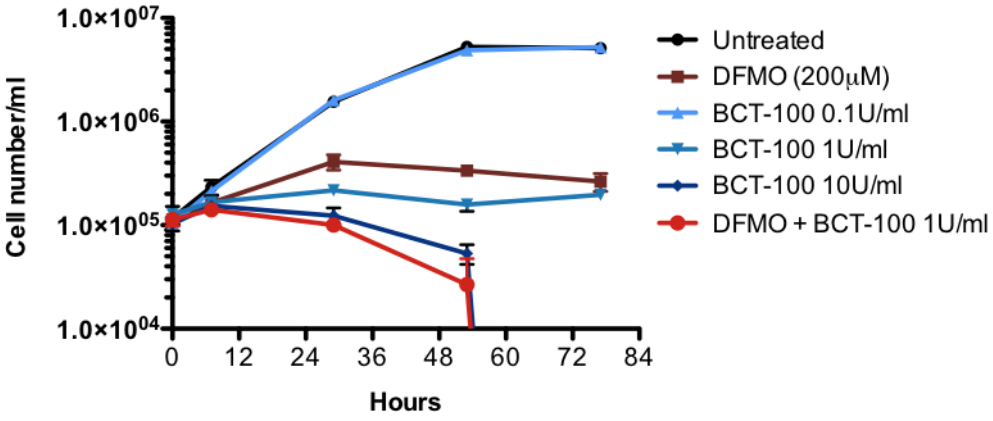



**Figure 7.2 Growth of bloodstream form 221VG1.1 *T. brucei* after BCT-100 treatment.** *T. brucei* were treated with 0.1, 1 or 10 U/ml BCT-100 or a combination of 1 U/ml BCT-100 and 200 μM DFMO. 200 μM DFMO (eflornithine) was used as a positive control. Growth of *T. brucei* was monitored by counting the number of viable trypanosomes twice a day using a haemocytometer.

Further analysis using fluorescence microscopy revealed that both DFMO and BCT-100 had similar effects on the morphology of *T. brucei* (Figure 7.3). After 24 hours of treatment, both DFMO and BCT-100 (1 U/ml) treated parasites were showing abnormal cellular morphology. Vacuoles began to form within the cytoplasm (indicated with white arrows). A large proportion of the cell population appeared to arrest at the 2N2K (G2/M) stage, characterised by two nuclei and two kinetoplasts. These cells also displayed two external flagella, which emerged on either side of the parasite from the flagellar pockets. After 48 hours of treatment, BCT-100 appeared to have a more severe effect on the parasite compared with DFMO, as approximately 40 % of cells showed signs of flagellar detachment and cell lysis. Although the phenotype was less severe in the DFMO-treated cells, similar morphological changes were observed.

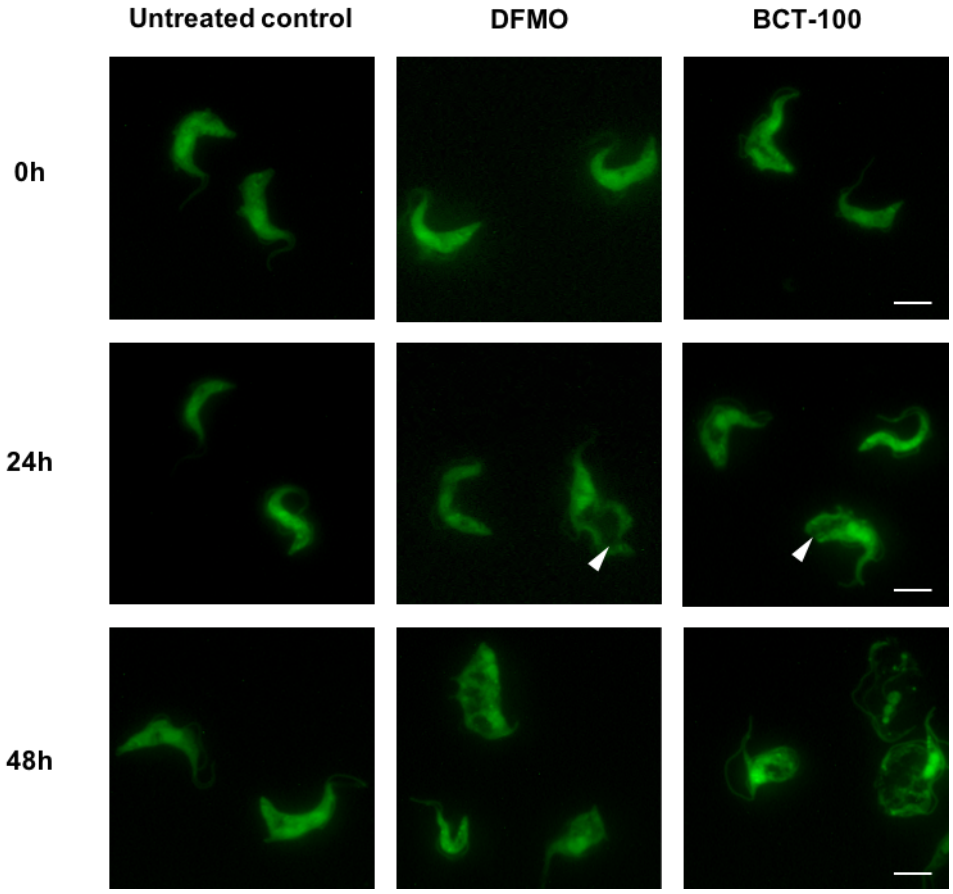



**Figure 7.3 *T. brucei* were lysed by BCT-100 after 24 hours of treatment.** 221VG1.1 *T. brucei* were treated with 1 U/ml BCT-100, 200 μM DFMO or left untreated for 0, 24 and 48 hours. Cells were collected, fixed with 2% PFA and mounted onto microscopy slides. The 22VG1.1 cell line endogenously express eGFP and was visualised using fluorescence microscopy. Scale bar =10 μm.

### 7.4 Number of abnormal parasites in the G2/M cell cycle stage increased after BCT-100 treatment

To confirm my observations of an increased proportion of 2N2K cells, the DNA content was stained with propidium iodide (PI), which was then analysed using flow cytometry Figure 7.4. Untreated cells showed a normal DNA profile, where the percentage of cells in G1: S: G2/M phase was approximately 62 %: 12.7 %: 25.9 % respectively. As expected, treatment with 0.1 U/ml BCT-100 had no effect on the cell cycle, as the ratio of cells in G1: S: G2/M remained similar to that of the untreated control even after 48 hours (59.3%: 11.2%: 27.1%). The effect of DFMO was apparent after 24 hours of stimulation. Similar to what was observed in the fluorescence microscopy analysis, there was a significant decrease in the proportion of cells in S-phase (1N2K), dropping from 13.1 % to only 4.7 %. Meanwhile, after 48 hours there was a corresponding increase in the number of 2N2K (G2/M) cells by 10 %, compared with the 0 h control. Similar effects were seen when trypanosomes were treated with 1 U/ml BCT-100, as a 12 % increase in 2N2K cells and a 14 % decrease in 1N2K cells were recorded after 48 hours. This effect occurred earlier at 24 hours when 10 U/ml BCT-100 was added. The addition of both BCT-100 and DFMO did not result in significant exacerbation of depletion of 1N2K cells, suggesting that a saturation effect could have been reached.

The abnormal DNA profile displayed by BCT-100 treated trypanosomes indicated a cell cycle arrest was triggered by drug treatment. The accumulation of 2N2K cells suggested that cells arrested after DNA replication and before cytokinesis. At the same time, new rounds of DNA synthesis were not initiated, which led to a depletion of 1N2K cells. This phenotype was surprisingly similar to that exhibited by trypanosomes after VSG synthesis had been blocked. In both cases, a cell cycle arrest with a significant accumulation of 2N2K cells was observed. The cellular morphology of the arrested cells also resembled *VSG* RNAi cells, with

two external flagella and a broader cell shape. The only difference between *VSG* RNAi induced cells and BCT-100-treated cells was the nature of cell cycle arrest. Whilst the phenotype of *VSG* RNAi could be reversed and cells remained viable in culture for days, cells treated by BCT-100 were lysed after 48 hours.

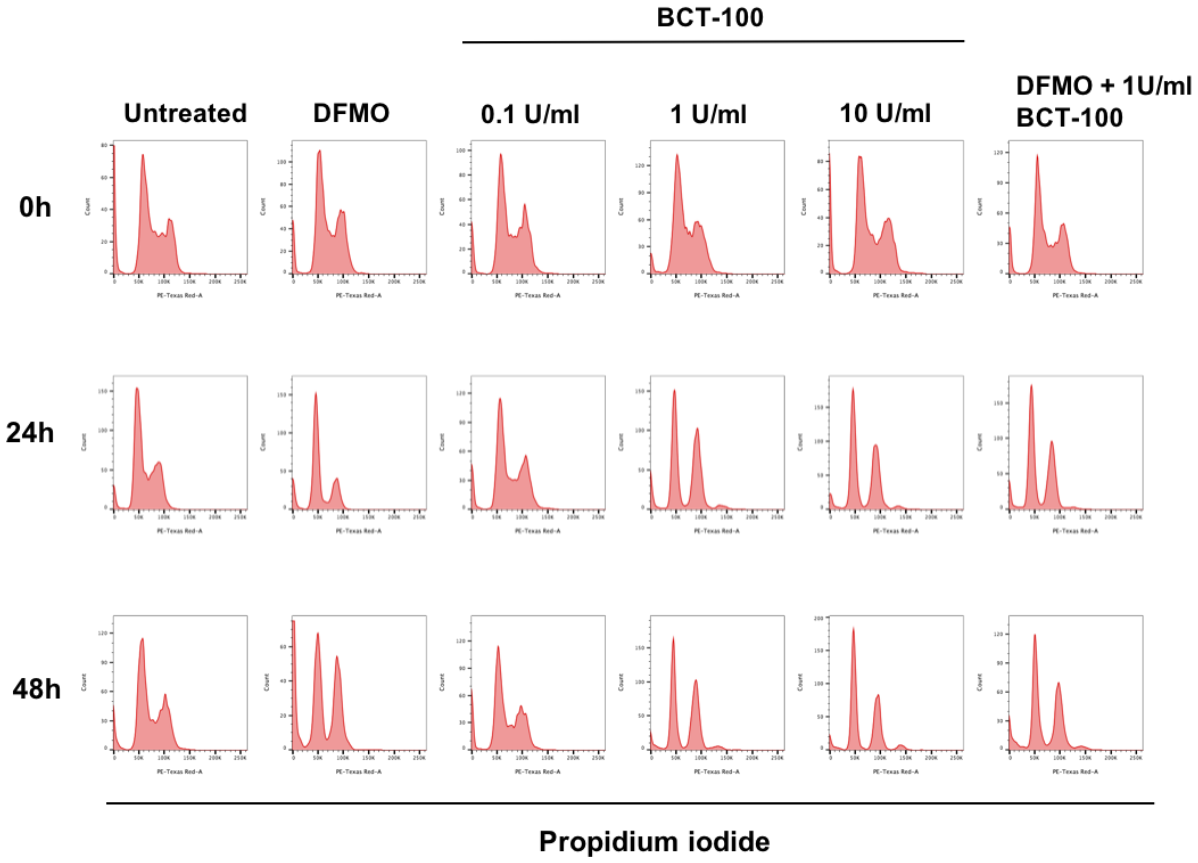



**Figure 7.4 Proportion of *T. brucei* in the G2/M cell cycle stage increased after BCT-100 treatment.** 221VG1.1 *T. brucei* were treated with 0.1, 1 or 10 U/ml BCT-100, 200 µM DFMO or a combination of 200 µM DFMO and 1 U/ml BCT-100 for 0, 24 and 48 hours. Cells were collected, fixed with 2% PFA and permeabilised using 0.1% Triton X-100. DNA content was then stained with propidium iodide and analysed by flow cytometry.

### 7.5 *T. brucei* cell cycle arrest was coupled with DNA arrangement abnormalities

To further characterise the cell cycle arrest phenotype of BCT-100 treated trypanosomes, I decided to stain the DNA content of the trypanosomes and categorise the arrangement of the nucleus and kinetoplast. The relative positioning and morphology of the nucleus and kinetoplast gives an indication of the specific cell cycle stage (Chapter 1.4, Figure 1.3). The untreated control population displayed a normal DNA profile, where most cells (67 %) were in the 1N1K stage, 18 % was in 1N2K and 8 % 2N2K cells. Finally, approximately 6 % of cells had abnormal phenotypes, these included cells with no nucleus, known as zoids or multi-nucleated cells. Schematic illustrations of the phenotypes are shown in Figure 7.6.

Trypanosomes that were treated with BCT-100 experienced a steep decline of 17.7 % (from 20.3 % to 2.6 % in 1N2K cells 24 hours post-treatment. This was further reduced to 0 % after 48 hours. As shown in Figure 7.4, the depletion of 1N2K cells corresponded to an increase in cells in the 2N2K stage. However, further analysis by microscopy revealed that these 2N2K cells did not have normal arrangements of nuclei and kinetoplasts. Untreated bloodstream form trypanosomes in the 2N2K stage, contain two nuclei spaced apart on the anterior end of the cell and two kinetoplasts on the posterior end. However, after BCT-100 treatment, the arrangement of both nuclei and kinetoplasts appeared closer together and positioned in a parallel manner. Both nuclei and kinetoplasts have divided successfully and the presence of two full-length external flagella indicated that replication of other internal organelles had completed before the cell cycle arrest (Figure 7.6). Approximately 38 % of the whole population was made up of these abnormal 2N2K cells after 24 hours of treatment. Nevertheless, these cells were unable to proceed through cytokinesis and accumulated as arrested 2N2K cells until their eventual lysis. In addition, there was also an accumulation of multi-nucleated cells and cells without a nucleus. This suggested that a proportion of cells had

undergone uneven cell division or multiple rounds of replication under the effects of BCT-100 treatment.

Like BCT-100, DFMO also acts to inhibit polyamine synthesis in BF *T. brucei* and induced similar phenotypes in the treated trypanosomes. The accumulation of 2N2K P cells was substantial at 24 hours (22 %) but only reached similar levels to the BCT-100 treated cells after 48 hours of incubation (Figure 7.6). Again, the addition of BCT-100 and DFMO did not produce a more severe phenotype, presumably because of a saturation effect mentioned earlier and both drugs targeted the same trypanosome metabolic pathway.

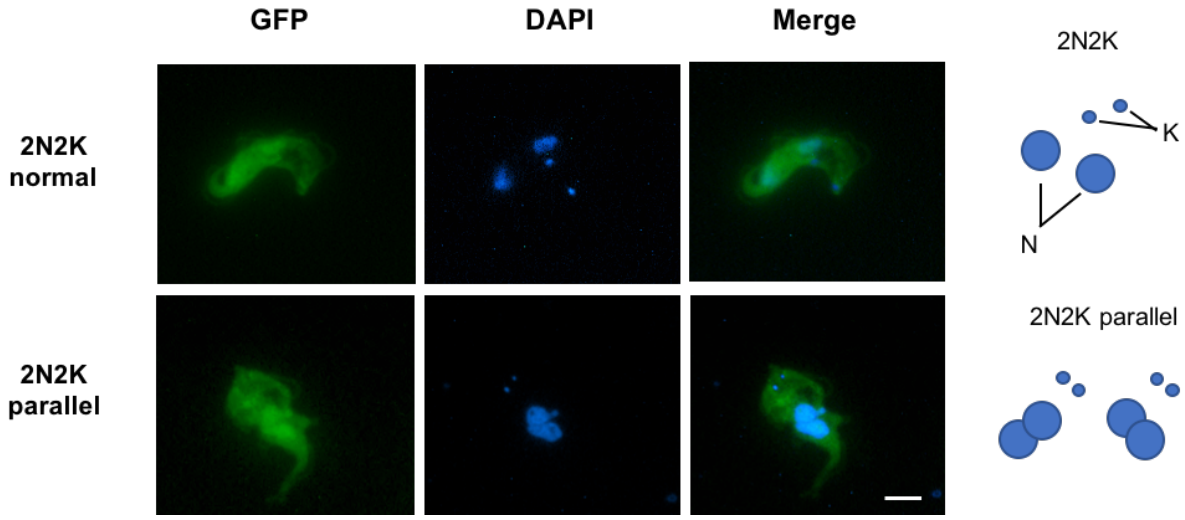



**Figure 7.5 Changes in DNA arrangement in 2N2K cells after BCT-100 treatment.** *T. brucei* were treated with 1 U/ml BCT-100 for 24 hours. Cells were fixed and the DNA content stained with DAPI. Schematic illustrations showed DNA positioning in normal and abnormal 2N2K cells. Cells with abnormal DNA arrangements were classified as 2N2K parallel.

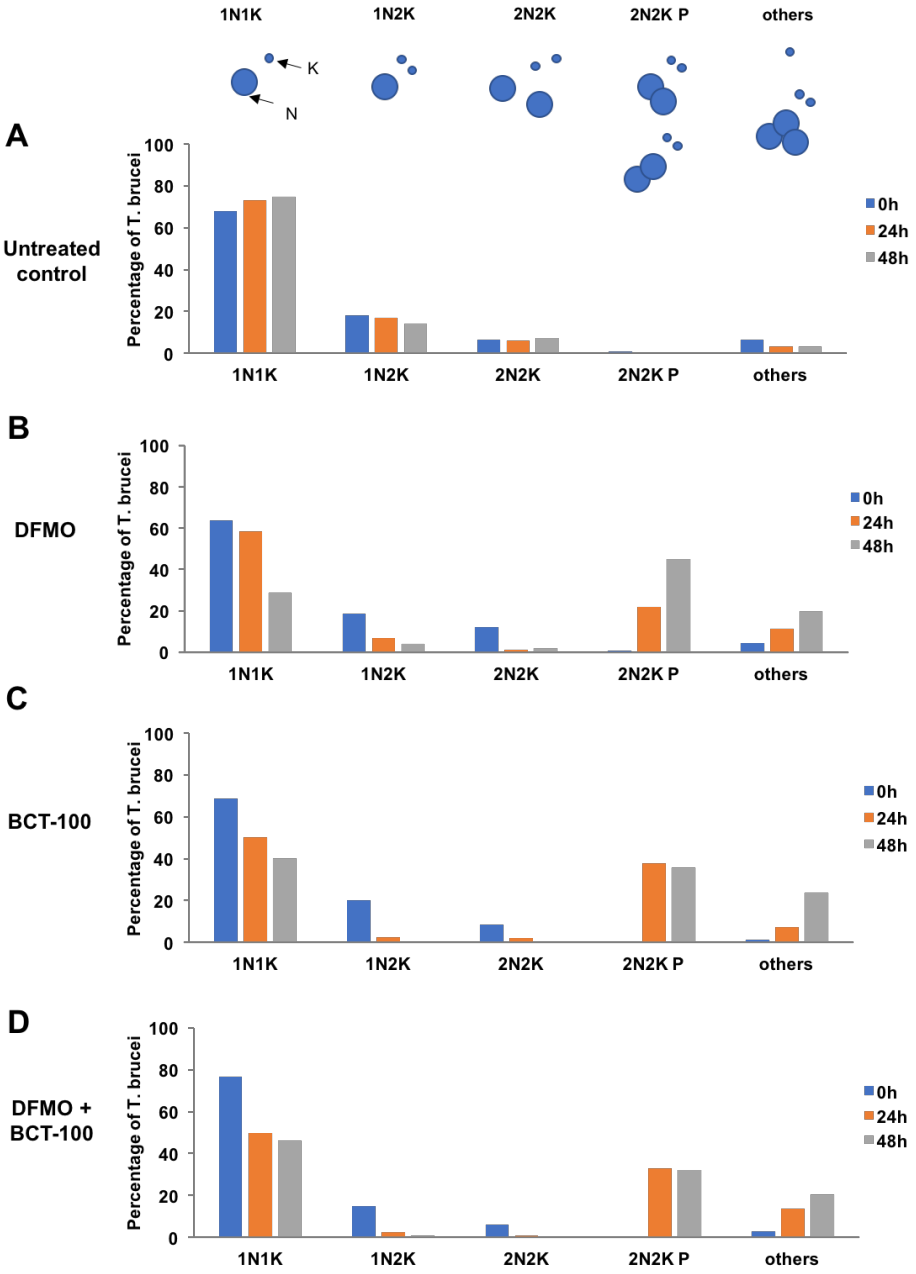



**Figure 7.6 Characterisation of DNA content arrangement in BF 221VG1.1 after BCT-100 treatment.** Trypanosomes were treated with either 1 U/ml BCT-100, 200 µM DFMO or the combination of both for 0, 24 and 48 h. Cells were then fixed and the DNA content stained with DAPI before analysis by fluorescence microscopy. Trypanosomes were categorised based on the arrangement of their nucleus (N) and kinetoplast (K) into: 1N1K, 1N2K, 2N2K and others (multinucleated cells or zoids). Cells with an abnormal arrangement of nuclei and kinetoplasts in the 2N2K stage were classified into the 2N2K P group. The results were obtained from 2 independent biological experiments (n=200). The mean number of cells in each category were expressed as percentage values of the total number of trypanosomes counted.

## 7.6 Discussion

This chapter documents the initial characterisation of the effect of the anti-cancer drug, BCT-100 against bloodstream form *T. brucei*. Similar to DFMO, which inhibits the first step of trypanosome polyamine synthesis, BCT-100 also possesses trypanostatic effects and inhibited the growth of the parasite within 24 hours *in vitro*. Furthermore, parasite growth inhibition was the consequence of an arrest triggered in the G2/M phase of the cell cycle, which eventually led to parasite death. Similar cell cycle arrest observations were found when the human hepatocellular carcinoma (HCC) cell line, Hep3B was treated with BCT-100 (Lam *et al*. 2009).

BCT-100 has shown promise against HCC and acute myeloid leukaemia (AML) and melanoma. The $IC_{50}$ concentration of BCT-100 ranged between 0.058 – 0.616 U/ml depending on the cell line tested against melanoma (Lam *et al*. 2011), while the BCT-100 $IC_{50}$ concentration against the HCC cell line, Hep3B was 0.1 U/ml. Although it is worth noting that the mechanisms of anti-tumour effects from arginine depletion may vary between cell lines (Lam *et al*. 2009). Here, I showed that the lowest effective concentration of BCT-100 against BF *T. brucei in vitro* was 1 U/ml. Two BCT-100 phase II clinical trials for the treatment of HCC and AML showed significant improvements in overall survival and tolerable safety profiles, with no life-threatening Grade 3 and above adverse events recorded (Yau et al. 2014; F.J. et al. 2014).

L-arginine is an essential amino acid for bloodstream form *T. brucei* and the parasite has been shown to have high affinity transporters to obtain L-arginine from the mammalian host (Mathieu *et al*. 2017). *T. brucei* is highly dependent on the host as a source of L-arginine as RNAi against the genes of two of these transporters, *TbAAT5* and *TbAAT16* led to a reduction in trypanosome growth within a day. This resembles the growth inhibition that was shown

when BCT-100 was added, demonstrating the importance of L-arginine availability to trypanosome survival. Apart from cell proliferation and cellular component synthesis, L-arginine is needed in *T. brucei* for the synthesis of a kinetoplastid-specific compound called trypanothione. Trypanothione is a form of glutathione containing two molecules of glutathione joined by a spermidine molecule. It is the kinetoplastid counterpart of the mammalian glutathione and helps to defend against oxidative stress by creating a reducing environment (Fairlamb & Cerami 1992; Manta *et al*. 2013).

Mechanistically, BCT-100 functions differently compared with DFMO, an existing drug for the treatment of HAT. DFMO is an irreversible enzyme inhibitor, whereas BCT-100 is a recombinant enzyme that depletes arginine supplies. Nevertheless, both of these drugs produced similar effects on the parasites by halting the progression of polyamine synthesis. Despite DFMO being the safest current option for HAT treatment, there are still multiple disadvantages to this drug. Firstly, the half-life of DFMO is short lasting and is only 2-4 hours in adults. This means DFMO treatment requires constant dosing, adding to the complication of drug administration, especially in developing countries. Secondly, DFMO is effectively mostly against *T. b. gambiense* but not *T. b. rhodesiense*, as the ODC enzyme in *T. b. rhodesiense* has a shorter half-life and is less sensitive to DFMO inhibition. To reduce the required duration and dose of eflornithine administration, nifurtimox was introduced to be used in combination with eflornithine. This combination therapy has now become an essential medicine on the WHO list. However, after enjoying 30 years of success, drug resistance against eflornithine has begun to emerge. This is perhaps not entirely unexpected, as it is relatively easy to select for eflornithine-resistance trypanosomes in vitro. DFMO is actively taken up by the parasite using a transporter (TbAAT6). Selection of DFMO resistant parasites led to the deletion of the *TbAAT6* gene and the elimination of this transporter (Vincent *et al*. 2010). In contrast, BCT-

100 appears able to bypass the aforementioned problems presented by treatment with DFMO. The pegylation of the human recombinant arginase increases the half-life of arginase by almost 300 times, thus reducing the need for constant drug administration (Cheng *et al*. 2007). Furthermore, the use of arginase as a competitive enzyme would not in theory, be subspecies specific like DFMO, as both *T. b. rhodesiense* and *T. b. gambiense* require arginase to proliferate. This would also eliminate the problem of drug resistance as BCT-100 only interferes with the conversion of L-arginine in the bloodstream and does not require uptake by *T. brucei*. One could question the impact that the citrulline-NO cycle has on the effectiveness of arginine depletion, as this pathway can recycle citrulline into arginine. However, the enzyme, argininosuccinate synthase (ASS), which is responsible for the conversion of citrulline and aspartate into argininosuccinate is not found in the *Trypanosoma* genus (Lakhal-Naouar *et al*. 2012), meaning *T. brucei* would have no alternative means to obtain arginine. This hypothesis is further supported by previous studies showing a decrease in levels of serum putrescine and spermidine in arginine depleted HCC cells, indicating that downstream compounds of the arginine pathway cannot be sourced elsewhere to compensate for the loss of L-arginine. In addition, BCT-100 against HCC and AML did not cause significant toxicity both *in vitro* and *in vivo* (Tsui *et al*. 2009; F.J. *et al*. 2014). In the phase I clinical trial of BCT-100 treatment against HCC, no treatment related death was observed and only one out of 15 patients recruited experienced dose limiting toxicity, who was receiving the highest dose of BCT-100 (2500 U/kg) (Yau *et al*. 2014). The use of BCT-100 is now undergoing phase II clinical trials for the treatment of both HCC and AML.

Nevertheless, modifying the availability of L-arginine during a trypanosome infection has its consequences, as the balance of host arginine and nitric oxide production is intimately linked to the effectiveness of parasite clearance. Mammalian arginine metabolism is complex

and varies between cell types. The biology of macrophages and arginine metabolism are fundamentally regulated by the M1/M2 functional phenotypes. Essentially, the M1/M2 classification can be divided into two competing pathways, both using arginine as their main substrate (Rath *et al*. 2014). M1 macrophages preferentially metabolise arginine into nitric oxide (NO) and citrulline via nitric oxide synthase (NOS), which promotes pathogen killing. M2 macrophages on the other hand, promote cell healing and repair by converting arginine into ornithine and urea via arginase. This dichotomous regulation of arginine metabolism is central to the functioning of macrophages. Therefore, the availability of arginine would have a direct effect on macrophage function and subsequent T-cell polarisation.

In *T. brucei* infected mice, Gobert *et al* observed a drastic decrease in plasma arginine and a corresponding increase in macrophage arginase activity, suggesting the shift towards an M2 phenotype. This resulted in a reduction in NO activity and impaired parasite killing (Gobert *et al*. 2000). One must therefore, take into account the balance of the two competing pathways that utilise L-arginine as their substrate when using BCT-100 to treat HAT.

The data presented in this chapter are only the initial steps to explore the potential use of BCT-100 as a therapeutic treatment for HAT. Although preliminary data showed promise in trypanosome killing, more detail analysis regarding cellular toxicity must be performed.

# Chapter 8

# Final conclusions and future perspectives

## 8.1 High rate of host antibody clearance is key to macrophage evasion

The African trypanosomes are an ancient species, its origins could be traced back 350 million years (Steverding 2008). Through millennia, trypanosomes have evolved extremely sophisticated mechanisms to co-exist with their host. The mammalian infectious *T. brucei* utilises a dense coat of surface glycoproteins (VSG) to shield itself from the continuous attack by the host immune system. The importance of the VSG was demonstrated by blocking VSG synthesis via an inducible RNAi system (Sheader *et al*. 2005). Two mechanisms were found to be crucial for immune evasion: antigenic variation and high rates of endocytosis. Antigenic variation primarily aids the parasite evasion from host antibody response by continuously switching VSG variants throughout the infection. However, since an effective antibody response takes approximately a week to develop, high rates of surface opsonin removal is critical for trypanosome survival and proliferation in the early stages of infection.

In this study, I showed for the first time that efficient anti-VSG antibody clearance is key to trypanosome evasion from macrophage phagocytosis. By blocking the synthesis of VSG, a increased in trypanosome phagocytosis was observed. This was due to selective perturbation of the internalisation of antibody-VSG complexes. The cell cycle arrest triggered by the VSG synthesis block is presumably a protective mechanism to prevent the lethal dilution of the VSG coat (Sheader *et al*. 2005). However, this protection is only effective in the absence of significant antibody titres. If the host is left to build an antibody response, these arrested cells would be preferentially phagocytosed by macrophages as a consequence of reduced anti-VSG antibody clearance (Chapter 3.5, Figure 3.6).

While complement proteins could enhance antibody-mediated phagocytosis of trypanosomes, they did not appear to be effective alone. This observation supports previous study reports where the deposition of complement proteins C3b, the C4 binding protein and Factor B have been detected but for unknown reasons, complement activation never occurred (Devine *et al*. 1986; Dolinska *et al*. 2013). Recently, the Carrington group has identified a receptor on the trypanosome surface, known as the complement factor H (CFH) receptor, which may hinder complement activation (unpublished), suggesting a novel immune evasion mechanism may exist.

Investigations into the molecular mechanisms behind the impaired antibody clearance revealed no defects in endocytosis, as internalisation rates of tomato-lectin, transferrin and dextran did not change (Chapter 4.6, Figure 4.8). Anti-VSG antibodies that were in complex with VSG molecules could enter the trypanosome via the flagellar pocket and reach the lysosome but the kinetics at which antibodies were internalised was reduced. In the "wind in sail model" proposed by the Engstler group, antibody removal from the trypanosome surface is dependent on the hydrodynamic forces generated by forward directional swimming (Engstler *et al*. 2007). This is thought to be an important process in the bloodstream, where the viscosity is much higher than the culture medium that was used in my experiments. Trypanosome motility changes depending on the microenvironment As the viscosity of the medium increases, tumbling will be replaced by directional swimming (Heddergott *et al*. 2012). In trypanosome culture medium, the swim speed of the uninduced cells was low (1.5 μm/s) and predominantly tumbled (Chapter 4.7 Figure 4.9). Surprisingly, antibodies still accumulated at the posterior end of the cell and could effectively remove surface bound antibodies, arguing that directional swimming is not essential for all antibody clearance. After blocking VSG synthesis for 8 hours, the arrested cells showed a change in swimming behaviour and a significant increase in

directional swimming was recorded. It appeared to contradict the Engstler theory that after a VSG synthesis block, the stalled cells swam more directionally yet cleared antibodies at a much slower rate. One possible explanation for this observation is that directional swimming is not the only mechanism that generates hydrodynamic forces. It is possible that the flexing activity on the cell surface of a tumbling trypanosome generates enough localised hydrodynamic forces which facilitate the selective movement of VSG-antibody complexes over the cell surface. Therefore, the type of cellular motility may influence the rate at which host opsonins are removed from the parasite surface. To test this hypothesis further, additional motility measurements could be performed in medium that resemble the viscosity of blood.

### 8.2 *T. brucei* dampens dendritic cell response to avoid activating T-cells

Apart from antigenic variation and rapid antibody internalisation, bloodstream form *T. brucei* has been shown to utilise other mechanisms to evade active immune response from other branches of immunity. Early in a trypanosome infection, large amounts of parasite products such as soluble VSGs are released into the host bloodstream as the parasite multiplies. The causes the host to launch a strong proinflammatory response to control the infection. This includes polarising macrophages to the M1 phenotype, which elevates the production of cytokines such as TNF-α and IFN-γ (Hertz *et al*. 1998; Namangala *et al*. 2009). Several studies have demonstrated the importance of an early inflammatory response, which is linked to host resistance to *T. brucei* infections. However, it is neither beneficial to the host nor the parasite when the state of excess inflammation is sustained. HAT pathology including anaemia and liver damage have been recorded in both experimental mouse models and in HAT patients (Naessens *et al*. 2005; Musaya *et al*. 2015). Therefore, after the initial, most aggressive waves of parasitaemia, anti-inflammatory cytokines and chemokines are often seen upregulated and

the infection switches to the chronic stage. However, what factors mediate the global switch from a pro-inflammatory to a parasite-tolerant state remain to be studied.

Dendritic cells form the essential link between the innate and adaptive immune system and are often the target of immunomodulation parasitic infections. Here, I have shown that human dendritic cells were functionally suppressed by *T. brucei* in a time-dependent manner. The expression of all four maturation markers: HLA-DR, CD86, CD80 and CD40 were diminished upon co-cultivation with trypanosomes, which also coincided with a decrease in antigen capture ability over time. As a result, the cytokine production shifted towards a trypanotolerant environment, where proinflammatory cytokines such as MCP-1, TNF-α and IL-6 were downregulated and the levels of the anti-inflammatory cytokine, IL-10 increased (Chapter 5.6 Figure 5.5 and 5.6). This observation is in line with the existing literature where the proinflammatory response would be gradually dampened. However, there was one anomaly that stood out; IL-8, a neutrophil recruiting chemokine was upregulated over 18-fold after 72 hours of trypanosome exposure (Chapter 5.6 Figure 5.6A). A possible explanation is that this is a host response to compensate for the dissipating proinflammatory response. In the absence of crucial immune cell recruiting cytokines like TNF-α, MCP-1 and IL-6, clearance of the parasites may rely on neutrophils. Early studies by Clayton *et al* had demonstrated in mice that a marked increase in neutrophils was seen after a week of infection (Clayton et al. 1980), further supporting my observation in the upregulation of IL-8. Nevertheless, current information on the role of neutrophils in a *T. brucei* infection is limited and their contributions remain largely undefined.

NETosis is a novel cell killing mechanism where the decondensed neutrophil DNA along with granule proteins and histones are ejected into the extracellular environment in a mesh (neutrophil extracellular trap; NET) that traps and kills the pathogen (Brinkmann *et al*.

2004). Several studies have in fact shown that members of the *Leishmania* family can elicit NET formation (Guimarães-Costa *et al*. 2009; Gabriel *et al*. 2010). The involvement of NETs in *Trypanosoma* infection was confirmed in a recent study on *Trypanosoma cruzi*, the causative agent of Chagas disease. This study showed that *T. cruzi* could induce the formation and release of NETs in a time and dose-dependent manner (Sousa-Rocha *et al*. 2015). Release of NETs is now regarded as an important host defense mechanisms, which surprisingly only surfaced recently. In my opinion, it is highly likely that NETs are involved in the process of *T. brucei* clearance, as evident in the surge in IL-8 in this study.

### 8.3 Th17 cells are involved in to the perpetuation of the pro-inflammatory response against *T. brucei* infection

Despite a diminished capacity to present antigen, dendritic cells were able to activate naïve CD3+ T-cells and initiate proliferation (Chapter 6.3 and 6.5, Figure 6.2 and 6.5). But activation was soon downregulated in a time-dependent manner by *T. brucei* stimulated DCs. In addition, *T. brucei* alone were unable to stimulate naïve T-cells, suggesting that the immunosuppressive effect is perpetuated through antigen presentation by DCs. Screening of T helper cytokines revealed a complex network of cytokines and chemokines at play. Upregulation of IFN-γ release was coupled with a corresponding inhibition of IL-4, indicating the polarisation of a Th1 response was elicited to control the infection. In the absence of IL-4, Th2 cytokines still showed some residual effects and were upregulated in an attempt to ameliorate inflammation.

Until recently, T helper response has always been viewed as the Th1/Th2 paradigm but identification of new T-cell subsets such as Th17 and regulatory T-cells (Treg), has shed light on the complexity of T-cell regulation. For the first time, Th17 cells were shown to play a role

in controlling a *T. brucei* infection as six Th17 related cytokines: IL-17A, IL-17F, IL-21, IL-22, IL-6 and TNF-α were markedly upregulated (Chapter 6.6, Figure 6.6). Th17 are a subset of CD4+ T-cells are known to play a role in the defence against some extracellular bacteria and fungi. IL-17 and IL-21 secreted by Th17 cells were also shown to enhance the functions of cytotoxic T-cells and exert protective effects against *T. cruzi* infection (Cai *et al*. 2016). However, the involvement of Th17 cells have never been demonstrated in a *T. brucei* infection until now. To further dissect the role of Th17 cells, beyond cytokine secretion, functional tests must be performed.

### 8.4 BCT-100 as a potential drug treatment for Human African Trypanosomiasis

Because of the effectiveness of antigenic variation, vaccines against *T. brucei* have enjoyed little success. As a result, current HAT treatments still rely heavily on chemotherapeutic drugs that were discovered decades ago, which are often accompanied by toxicity and severe side effects (WHO 2017; Steverding 2010b). Choices of drugs are also limited; melarsoprol and eflornithine (DFMO)-nifurtimox are the only drugs available to treat *T. b. rhodesiense* and *T. b. gambiense* respectively. No new drugs have been introduced since the 1980s.

Several parameters should be considered in the drug development. Firstly, the drug should be relatively easy to administer because most affected areas are remote and lack professional medical staff. These areas are often affected by social and political instability, with minimal medical services (WHO 2017). For the same reasons as above, the half-life of the drug should be long enough that it does not require constant dosing. Thirdly, the treatment should be *T. brucei*-specific with minimal side-effects to prevent treatment associated deaths.

BCT-100, a patented pegylated human recombinant arginase has shown promise against both human hepatocellular carcinoma (HCC) and acute myeloid leukaemia (AML) (Cheng *et al*. 2007; Yau *et al*. 2014). Arginine is essential for *T. brucei* polyamine synthesis and BCT-100 actively competes for arginine with the parasite. Depletion of arginine using BCT-100 led to parasite growth inhibition, coupled with a cell cycle arrest (Chapter 7.3 and 7.4, Figure 7.2 and 7.4). This is comparable to the effects seen in BCT-100 treated melanoma cell lines (Lam *et al*. 2011). Whilst DFMO, which also targets the same polyamine synthesis pathway and showed similar effects in *T. brucei*, BCT-100 has several advantages over DFMO. DFMO is an irreversible inhibitor of ornithine decarboxylase (ODC), the enzyme responsible for the conversion of ornithine into putrescine. However, it is only effective against *T. b. gambiense* but not *T. b. rhodesiense* due to the short half-life of its ODC. Since BCT-100 does not require uptake of the drug, its use in theory, should not be limited to specific trypanosome species. Furthermore, pegylation of BCT-100 greatly increases its stability, which would eliminate the need for constant administration. Although preliminary results showed promise, further investigations into toxicity and efficacy of administering this drug must be performed.

African trypanosomes are one of the most evolutionarily successful parasites, having evolved highly sophisticated mechanisms to manipulate their host and remain as one of the most difficult parasitic disease to eradicate. In this study, I have highlighted the importance of several key issues regarding *T. brucei* immune evasion. Firstly, I demonstrated the importance of the efficient antibody removal by *T. brucei* in the evasion from macrophages. Secondly, I showed that trypanosomes are able to dampen the response of human dendritic cells by downregulating their functions and altering the cytokine profiles. Thirdly, I showed for the first time the involvement of Th17 cells in controlling *T. brucei* infection, although further investigation is required to confirm the mechanisms of action. Lastly, a preliminary drug study

revealed the potential of a pegylated human recombinant arginase (BCT-100) as an alternative HAT treatment. Further investigation will hopefully allow us to gain insight into the mechanisms involved in mounting an effective response against *T. brucei* infections and develop novel therapies for the treatment of Human African Trypanosomiasis.

# References


Acosta-Serrano, a et al., 2001. The surface coat of procyclic Trypanosoma brucei: programmed expression and proteolytic cleavage of procyclin in the tsetse fly. *Proceedings of the National Academy of Sciences of the United States of America*, 98(4), pp.1513–8. Available at: http://www.pubmedcentral.nih.gov/articlerender.fcgi?artid=29288&tool=pmcentrez&rendertype=abstract.

Aderem, A. & Underhill, D.M., 1999. Mechanisms of phagocytosis in macrophages. *Annual review of immunology*, 17, pp.593–623. Available at: http://www.ncbi.nlm.nih.gov/pubmed/10358769.

Akira, S. & Takeda, K., 2004. Toll-like receptor signalling. *Nature reviews. Immunology*, 4(7), pp.499–511. Available at: http://www.ncbi.nlm.nih.gov/pubmed/15229469 [Accessed July 15, 2012].

Allen, C.L., Goulding, D. & Field, M.C., 2003. Clathrin-mediated endocytosis is essential in Trypanosoma brucei. *EMBO Journal*, 22(19), pp.4991–5002.

Alsford, S. et al., 2001. Diversity and dynamics of the minichromosomal karyotype in Trypanosoma brucei. *Molecular and Biochemical Parasitology*, 113(1), pp.79–88.

Alsford, S. et al., 2012. High-throughput decoding of antitrypanosomal drug efficacy and resistance. *Nature*, 482(7384), pp.232–236. Available at: http://dx.doi.org/10.1038/nature10771.

Aranzamendi, C. et al., 2012. Trichinella spiralis-secreted products modulate DC functionality and expand regulatory T cells in vitro. *Parasite Immunology*, 34(4), pp.210–223.

Babokhov, P. et al., 2013. A current analysis of chemotherapy strategies for the treatment of human African trypanosomiasis. *Pathogens and global health*, 107(5), pp.242–52. Available at: http://www.pubmedcentral.nih.gov/articlerender.fcgi?artid=4001453&tool=pmcentrez&rendertype=abstract.

Bacchi, C.J., 2009. Chemotherapy of human african trypanosomiasis. *Interdisciplinary perspectives on infectious diseases*, 2009, p.195040.

Baetselier, P.D. et al., 2001. Alternative versus classical macrophage activation during

experimental African trypanosomosis. *Int J Parasitol*, 31(5–6), pp.575–587. Available at: http://www.sciencedirect.com/science?_ob=MImg&_imagekey=B6T7F-42WX3BM-R-16&_cdi=5057&_user=687336&_pii=S0020751901001709&_origin=search&_coverDate=05%2F01%2F2001&_sk=999689994&view=c&wchp=dGLbVlz-zSkWb&md5=50a12722f13ce6432c92bd7fc71ec31d&ie=/sdarticle.pd.

Baker, N. et al., 2013. Drug resistance in African trypanosomiasis: The melarsoprol and pentamidine story. *Trends in Parasitology*, 29(3), pp.110–118.

Bakhiet, M. et al., 1996. Control of parasitemia and survival during Trypanosoma brucei brucei infection is related to strain-dependent ability to produce IL-4. *J. Immunol.*, 157(8), pp.3518–3526.

Bakhiet, M. et al., 1996. Human and rodent interferon-y as a growth factor for Trypanosoma brucei. *European Journal of immunology*, 26(6), pp.1359–1364.

Balber, A.E. et al., 1979. Inactivation or elimination of potentially trypanolytic, complement-activating immune complexes by pathogenic trypanosomes. *Infection and Immunity*, 24(3), pp.617–627.

Bargul, J.L. et al., 2016. Species-Specific Adaptations of Trypanosome Morphology and Motility to the Mammalian Host. *PLoS pathogens*, 12(2), p.e1005448. Available at: http://dx.doi.org/10.1371/journal.ppat.1005448 [Accessed January 12, 2017].

Barrett, M.P. et al., 2003. The trypanosomiases. *Lancet*, 362(9394), pp.1469–1480.

Barry, J.D., 1979. Capping of variable antigen on Trypanosoma brucei, and its immunological and biological significance. *Journal of cell science*, 37, pp.287–302.

Berriman, M. et al., 2005. The genome of the African trypanosome Trypanosoma brucei. *Science (New York, N.Y.)*, 309(5733), pp.416–422.

Beschin, A. et al., 2014. African trypanosome control in the insect vector and mammalian host. *Trends in Parasitology*, 30(11), pp.538–547.

Blanco, P. et al., 2008. Dendritic cells and cytokines in human inflammatory and autoimmune diseases. *Cytokine & growth factor reviews*, 19(1), pp.41–52. Available at: http://www.ncbi.nlm.nih.gov/pubmed/18258476%5Cnhttp://www.pubmedcentral.nih.gov/articlerender.fcgi?artid=PMC2413068.

Van Bogaert, I. & Haemers, A., 1989. Eflornithine. A new drug in the treatment of sleeping sickness. *Pharmaceutisch weekblad. Scientific edition*, 11(3), pp.69–75.

Bohlson, S.S. et al., 2014. Complement, c1q, and c1q-related molecules regulate macrophage polarization. *Frontiers in immunology*, 5(August), p.402. Available at: http://www.pubmedcentral.nih.gov/articlerender.fcgi?artid=4139736&tool=pmcentrez&rendertype=abstract.

Böhmer, R.M., Bandala-Sanchez, E. & Harrison, L.C., 2011. Forward light scatter is a simple measure of T-cell activation and proliferation but is not universally suited for doublet discrimination. *Cytometry Part A*, 79 A(8), pp.646–652.

Bradley, J.R., 2008. TNF-mediated inflammatory disease. *Journal of Pathology*, 214(2), pp.149–160.

Brinkmann, V. et al., 2004. Neutrophil extracellular traps kill bacteria. *Science*, 303(5663), pp.1532–1535.

Broadhead, R. et al., 2006. Flagellar motility is required for the viability of the bloodstream trypanosome. *Nature*, 440(7081), pp.224–227.

Brun, R. et al., 2010. Human African trypanosomiasis. *The Lancet*, 375(9709), pp.148–159. Available at: http://dx.doi.org/10.1016/S0140-6736(09)60829-1.

Bülow, R., Overath, P. & Davoust, J., 1988. Rapid lateral diffusion of the variant surface glycoprotein in the coat of Trypanosoma brucei. *Biochemistry*, 27(7), pp.2384–2388.

Burkett, P.R., Zu Horste, G.M. & Kuchroo, V.K., 2015. Pouring fuel on the fire: Th17 cells, the environment, and autoimmunity. *Journal of Clinical Investigation*, 125(6), pp.2211–2219.

Cai, C.W. et al., 2016. Th17 Cells Are More Protective Than Th1 Cells Against the Intracellular Parasite Trypanosoma cruzi. *PLoS Pathogens*, 12(10).

Campbell, T.N. & Choy, F.Y.M., 2001. The effect of pH on Green Fluorescent Protein: a brief review. *Molecular Biology Today*, 2, pp.1–4.

Carrington, M. et al., 1991. Variant specific glycoprotein of Trypanosoma brucei consists of two domains each having an independently conserved pattern of cysteine residues. *Journal of Molecular Biology*, 221(3), pp.823–835. Available at: http://www.sciencedirect.com/science/article/pii/002228369180178W.

Caruso, A. et al., 1997. Flow cytometric analysis of activation markers on stimulated T cells and their correlation with cell proliferation. *Cytometry*, 27(1), pp.71–6. Available at: http://www.researchgate.net/profile/Maria_Francesco/publication/14207004_Flow_cytometric_analysis_of_activation_markers_on_stimulated_T_cells_and_their_correlation_

with_cell_proliferation/links/54bcda880cf253b50e2d6b1a.pdf%5Cnhttp://www.ncbi.nlm.nih.gov/p.

Castiello, L. et al., 2011. Monocyte-derived DC maturation strategies and related pathways: A transcriptional view. *Cancer Immunology, Immunotherapy*, 60(4), pp.457–466.

Chappuis, F. et al., 2005. Eflornithine is safer than melarsoprol for the treatment of second-stage Trypanosoma brucei gambiense human African trypanosomiasis. *Clinical infectious diseases : an official publication of the Infectious Diseases Society of America*, 41(table 2), pp.748–751.

Checchi, F. et al., 2007. Nifurtimox plus eflornithine for late-stage sleeping sickness in Uganda: A case series. *PLoS Neglected Tropical Diseases*, 1(2).

Checchi, F. et al., 2008. The natural progression of Gambiense sleeping sickness: what is the evidence? *PLoS neglected tropical diseases*, 2(12), p.e303.

Cheng, P.N.M. et al., 2007. Pegylated recombinant human arginase (rhArg-peg5,000mw) inhibits the in vitro and in vivo proliferation of human hepatocellular carcinoma through arginine depletion. *Cancer Research*, 67(1), pp.309–317.

Cheung, J.L.Y. et al., 2016. Blocking Synthesis of the Variant Surface Glycoprotein Coat in Trypanosoma brucei Leads to an Increase in Macrophage Phagocytosis Due to Reduced Clearance of Surface Coat Antibodies K. L. Hill, ed. *PLoS Pathogens*, 12(11), p.e1006023. Available at: http://www.ncbi.nlm.nih.gov/pmc/articles/PMC5125712/.

Chung, W.L., Carrington, M. & Field, M.C., 2004. Cytoplasmic targeting signals in transmembrane invariant surface glycoproteins of trypanosomes. *Journal of Biological Chemistry*, 279(52), pp.54887–54895.

Clayton, C.E. et al., 1980. Murine trypanosomiasis: Cellular proliferation and functional depletion in the blood, peritoneum, and spleen related to changes in bone marrow stem cells. *Infection and Immunity*, 28(3), pp.824–831.

Coffman, T.R.M. and R.L., 1989. TH1 AND TH2 CELLS : Different Patterns of Lymphokine Functional Properties. *Ann. Rev. Immunol*, 7, pp.145–173.

Couper, K., Blount, D. & Riley, E., 2008. IL-10: the master regulator of immunity to infection. *Journal of immunology*, 180(9), pp.5771–5777.

Crome, S.Q., Wang, A.Y. & Levings, M.K., 2010. Translational Mini-Review Series on Th17 Cells: Function and regulation of human T helper 17 cells in health and disease. *Clinical and Experimental Immunology*, 159(2), pp.109–119. Available at:

http://www.ncbi.nlm.nih.gov/pmc/articles/PMC2810379/.

Cross, G.A.M., 1975. Identification, purification and properties of clone-specific glycoprotein antigens constituting the surface coat of Trypanosoma brucei. *Parasitology*, 71(3), pp.393–417. Available at: https://www.cambridge.org/core/article/div-class-title-identification-purification-and-properties-of-clone-specific-glycoprotein-antigens-constituting-the-surface-coat-of-span-class-italic-trypanosoma-brucei-span-div/C54E539958EE5AE7CA66088222426B5D.

Dagenais, T.R. et al., 2009. Processing and presentation of variant surface glycoprotein molecules to T cells in African trypanosomiasis. *Journal of immunology (Baltimore, Md. : 1950)*, 183(5), pp.3344–55. Available at: http://www.pubmedcentral.nih.gov/articlerender.fcgi?artid=2730433&tool=pmcentrez&rendertype=abstract [Accessed May 21, 2013].

Dagenais, T.R. et al., 2009. T-cell responses to the trypanosome variant surface glycoprotein are not limited to hypervariable subregions. *Infection and Immunity*, 77(1), pp.141–151.

Dalod, M. et al., 2014. Dendritic cell maturation: Functional specialization through signaling specificity and transcriptional programming. *EMBO Journal*, 33(10), pp.1104–1116.

Damsker, J.M., Hansen, A.M. & Caspi, R.R., 2010. Th1 and Th17 cells: Adversaries and collaborators. *Annals of the New York Academy of Sciences*, 1183, pp.211–221. Available at: http://www.ncbi.nlm.nih.gov/pmc/articles/PMC2914500/.

Delespaux, V. & de Koning, H.P., 2007. Drugs and drug resistance in African trypanosomiasis. *Drug Resistance Updates*, 10(1–2), pp.30–50.

Deshmane, S.L. et al., 2009. Monocyte Chemoattractant Protein-1 (MCP-1): An Overview. *Journal of Interferon & Cytokine Research*, 29(6), pp.313–326. Available at: http://www.liebertonline.com/doi/abs/10.1089/jir.2008.0027.

Devine, D. V., Falk, R.J. & Balber, A.E., 1986. Restriction of the alternative pathway of human complement by intact Trypanosoma brucei subsp. gambiense. *Infection and Immunity*, 52(1), pp.223–229.

Dolinska, S. et al., 2013. Trypanosoma brucei brucei binds human complement regulatory protein C4BP. In A. de Almeida et al., eds. *Farm animal proteomics 2013: Proceedings of the 4th Management Committee Meeting and 3rd Meeting of Working Groups 1, 2 {&} 3 of COST Action FA1002 Ko{š}ice, Slovakia 25-26 April 2013*. Wageningen:

Wageningen Academic Publishers, pp. 132–134. Available at: http://dx.doi.org/10.3920/978-90-8686-776-9_35.

Donelson, J.E., Hill, K.L. & El-sayed, N.M.A., 1998. Multiple mechanisms of immune evasion by African trypanosomes. *Molecular and Biochemical Parasitology*, 91, pp.51–66.

Drennan, M.B. et al., 2005. The induction of a type 1 immune response following a Trypanosoma brucei infection is MyD88 dependent. *Journal of immunology (Baltimore, Md. : 1950)*, 175(4), pp.2501–2509.

Drennan, M.B. et al., 2012. Trypanosoma brucei Infection Is MyD88 Dependent 1.

Dunkelberger, J.R. & Song, W.C., 2010. Complement and its role in innate and adaptive immune responses. *Cell research*, 20(1), pp.34–50.

Elyaman, W. et al., 2009. IL-9 induces differentiation of T(H)17 cells and enhances function of FoxP3(+) natural regulatory T cells. *Proceedings of the National Academy of Sciences of the United States of America*, 106(31), pp.12885–12890. Available at: http://www.ncbi.nlm.nih.gov/pmc/articles/PMC2722314/.

Engstler, M. et al., 2007. Hydrodynamic Flow-Mediated Protein Sorting on the Cell Surface of Trypanosomes. *Cell*, 131(3), pp.505–515.

Engstler, M. et al., 2004. Kinetics of endocytosis and recycling of the GPI-anchored variant surface glycoprotein in Trypanosoma brucei. *Journal of cell science*, 117(Pt 7), pp.1105–1115.

F.J., M. et al., 2014. Cytotoxicity of the recombinant human arginase (BCT-100) against acute myeloid leukaemia (AML). *Blood*, 124(21), p.no pagination. Available at: http://www.bloodjournal.org/content/124/21/2317%5Cnhttp://ovidsp.ovid.com/ovidweb.cgi?T=JS&PAGE=reference&D=emed16&NEWS=N&AN=71759980.

Fairlamb, a H. & Cerami, a, 1992. Metabolism and functions of trypanothione in the Kinetoplastida. *Annual review of microbiology*, 46, pp.695–729.

Ferguson, M.A., 1999. The structure, biosynthesis and functions of glycosylphosphatidylinositol anchors, and the contributions of trypanosome research. *Journal of Cell Science*, 112(17), p.2799 LP-2809. Available at: http://jcs.biologists.org/content/112/17/2799.abstract.

Ferguson, M. a et al., 1988. Glycosyl-phosphatidylinositol moiety that anchors Trypanosoma brucei variant surface glycoprotein to the membrane. *Science (New York, N.Y.)*,

239(4841 Pt 1), pp.753–759.

Ferrante, A. & Allison, A.C., 1983. Alternative pathway activation of complement by African trypanosomes lacking a glycoprotein coat. *Parasite Immunology*, 5(5), pp.491–498.

Field, M.C. & Carrington, M., 2009. The trypanosome flagellar pocket. *Nat Rev Micro*, 7(11), pp.775–786. Available at: http://dx.doi.org/10.1038/nrmicro2221.

Franco, J.R. et al., 2014. Epidemiology of human African trypanosomiasis. *Clinical Epidemiology*, 6(1), pp.257–275.

Gabriel, C. et al., 2010. Leishmania donovani promastigotes evade the antimicrobial activity of neutrophil extracellular traps. *Journal of immunology (Baltimore, Md. : 1950)*, 185(7), pp.4319–4327.

Gadelha, C. et al., 2015. Architecture of a host-parasite interface: complex targeting mechanisms revealed through proteomics. *Molecular & cellular proteomics : MCP*, pp.1911–1926. Available at: http://www.ncbi.nlm.nih.gov/pubmed/25931509.

Garzon, E. et al., 2013. The Trypanosoma brucei gambiense secretome impairs lipopolysaccharide-induced maturation, cytokine production, and allostimulatory capacity of dendritic cells. *Infection and Immunity*, 81(9), pp.3300–3308.

Geiger, A. et al., 2010. Exocytosis and protein secretion in Trypanosoma. *BMC microbiology*, 10, p.20.

Glover, L. et al., 2013. Antigenic variation in African trypanosomes: The importance of chromosomal and nuclear context in VSG expression control. *Cellular Microbiology*, 15(12), pp.1984–1993.

Gobert, A.P. et al., 2000. L-arginine availability modulates local nitric oxide production and parasite killing in experimental trypanosomiasis. *Infection and Immunity*, 68(8), pp.4653–4657.

Grünfelder, C.G. et al., 2003. Endocytosis of a Glycosylphosphatidylinositol-anchored Protein via Clathrin-coated Vesicles, Sorting by Default in Endosomes, and Exocytosis via RAB11-positive Carriers □ V. *Molecular Biology of the Cell*, 14, pp.2029–2040.

Guermonprez, P. et al., 2002. Antigen Presentation and T Cell Stimulation by Dendritic Cells. *Annual Review of Immunology*, 20(1), pp.621–667. Available at: http://www.annualreviews.org/doi/abs/10.1146/annurev.cellbio.19.111301.153011%5Cnhttp://www.ncbi.nlm.nih.gov/pubmed/15189156%5Cnhttp://www.annualreviews.org/doi/10.1146/annurev.biochem.73.030403.080419%5Cnhttp://www.annualreviews.org/doi/

abs/10.1146/annur.

Guilliams, M. et al., 2009. IL-10 dampens TNF/inducible nitric oxide synthase-producing dendritic cell-mediated pathogenicity during parasitic infection. *Journal of immunology (Baltimore, Md. : 1950)*, 182(2), pp.1107–1118.

Guilliams, M. et al., 2014. The function of Fcγ receptors in dendritic cells and macrophages. *Nature reviews. Immunology*, 14(2), pp.94–108. Available at: http://www.ncbi.nlm.nih.gov/pubmed/24445665.

Guimarães-Costa, A.B. et al., 2009. Leishmania amazonensis promastigotes induce and are killed by neutrophil extracellular traps. *Proceedings of the National Academy of Sciences of the United States of America*, 106(16), pp.6748–6753.

Gupta, G., Oghumu, S. & Satoskar, A.R., 2013. Mechanisms of Immune Evasion in Leishmaniasis. *Advances in Applied Microbiology*, 82, pp.155–184.

Hammarton, T.C., 2007. Cell cycle regulation in Trypanosoma brucei. *Molecular and Biochemical Parasitology*, 153(1), pp.1–8.

Heddergott, N. et al., 2012. Trypanosome Motion Represents an Adaptation to the Crowded Environment of the Vertebrate Bloodstream. *PLoS Pathogens*, 8(11).

Hertz-Fowler, C. et al., 2008. Telomeric expression sites are highly conserved in Trypanosoma brucei. *PLoS ONE*, 3(10).

Hertz, C.J., Filutowicz, H. & Mansfield, J.M., 1998. Resistance to the African trypanosomes is IFN-gamma dependent. *J.Immunol.*, 161(0022–1767 (Print)), pp.6775–6783.

Hirumi, H. & Hirumi, K., 1989. Continuous cultivation of Trypanosoma brucei blood stream forms in a medium containing a low concentration of serum protein without feeder cell layers. *The Journal of parasitology*, 75(6), pp.985–989. Available at: http://eutils.ncbi.nlm.nih.gov/entrez/eutils/elink.fcgi?dbfrom=pubmed&id=2614608&retmode=ref&cmd=prlinks%5Cnpapers2://publication/uuid/90E651E7-D9B2-4497-8B15-6C38A7DCF953.

Horn, D. & McCulloch, R., 2010. Molecular mechanisms underlying the control of antigenic variation in African trypanosomes. *Current Opinion in Microbiology*, 13(6), pp.700–705.

Hugues, S., 2010. Dynamics of dendritic cell-T cell interactions: A role in T cell outcome. *Seminars in Immunopathology*, 32(3), pp.227–238.

Hunter, C. a & Jones, S. a, 2015. IL-6 as a keystone cytokine in health and disease. *Nature*

*immunology*, 16(5), pp.448–457. Available at: http://www.ncbi.nlm.nih.gov/pubmed/25898198.

Jones, N.G. et al., 2008. Structure of a glycosylphosphatidylinositol-anchored domain from a trypanosome variant surface glycoprotein. *Journal of Biological Chemistry*, 283(6), pp.3584–3593.

Kalliolias, G.D. & Ivashkiv, L.B., 2015. TNF biology, pathogenic mechanisms and emerging therapeutic strategies. *Nature Reviews Rheumatology*, 12(1), pp.49–62. Available at: http://www.nature.com/doifinder/10.1038/nrrheum.2015.169.

Kato, C.D. et al., 2015. Interleukin (IL)-6 and IL-10 Are Up Regulated in Late Stage Trypanosoma brucei rhodesiense Sleeping Sickness. *PLOS Neglected Tropical Diseases*, 9(6), p.e0003835. Available at: http://dx.doi.org/10.1371%2Fjournal.pntd.0003835.

Kato, C.D. et al., 2016. The role of cytokines in the pathogenesis and staging of Trypanosoma brucei rhodesiense sleeping sickness. *Allergy, asthma, and clinical immunology : official journal of the Canadian Society of Allergy and Clinical Immunology*, 12, p.1. V. A, C. RD, E. JD, in Essentials of Glycobiolo. Available at: http://www.pubmedcentral.nih.gov/articlerender.fcgi?artid=4722787&tool=pmcentrez&rendertype=abstract.

Kennedy, P.G., 2013. Clinical features, diagnosis, and treatment of human African trypanosomiasis (sleeping sickness). *Lancet neurology*, 12(2), pp.186–94. Available at: http://www.ncbi.nlm.nih.gov/pubmed/23260189.

Kisalu, N.K. et al., 2014. Mouse infection and pathogenesis by Trypanosoma brucei motility mutants. *Cellular Microbiology*, 16(6), pp.912–924.

Kohl, L., Sherwin, T. & Gull, K., 1999. Assembly of the paraflagellar rod and the flagellum attachment zone complex during the Trypanosoma brucei cell cycle. *The Journal of eukaryotic microbiology*, 46(2), pp.105–109.

Kolls, J.K. & Lindén, A., 2004. Interleukin-17 family members and inflammation. *Immunity*, 21(4), pp.467–476.

Korn, T. et al., 2009. IL-17 and Th17 Cells. *Annual review of immunology*, 27(1), pp.485–517. Available at: http://dx.doi.org/10.1146/annurev.immunol.021908.132710%5Cnhttp://www.annualreviews.org/doi/pdf/10.1146/annurev.immunol.021908.132710.

Korn, T. et al., 2007. IL-21 initiates an alternative pathway to induce proinflammatory T(H)17 cells. *Nature*, 448(7152), pp.484–487.

Kotimaa, J. et al., 2016. Sex matters: Systemic complement activity of female C57BL/6J and BALB/cJ mice is limited by serum terminal pathway components. *Molecular Immunology*, 76, pp.13–21. Available at: http://www.sciencedirect.com/science/article/pii/S0161589016301067.

Kwong-Lam, F. & Chi-Fung, C.G., 2013. Vincristine could partly suppress stromal support to T-ALL blasts during pegylated arginase I treatment. *Experimental hematology & oncology*, 2(1), p.11. Available at: http://www.pubmedcentral.nih.gov/articlerender.fcgi?artid=3655039&tool=pmcentrez&rendertype=abstract.

Lakhal-Naouar, I. et al., 2012. Leishmania donovani Argininosuccinate Synthase Is an Active Enzyme Associated with Parasite Pathogenesis. *PLOS Neglected Tropical Diseases*, 6(10), p.e1849. Available at: http://dx.doi.org/10.1371%2Fjournal.pntd.0001849.

Lam, T.L. et al., 2009. Recombinant human arginase inhibits proliferation of human hepatocellular carcinoma by inducing cell cycle arrest. *Cancer Letters*, 277(1), pp.91–100.

Lam, T.L. et al., 2011. Recombinant human arginase inhibits the in vitro and in vivo proliferation of human melanoma by inducing cell cycle arrest and apoptosis. *Pigment Cell Melanoma Res*, 24(2), pp.366–376.

Langelaar, M. et al., 2009. Suppression of dendritic cell maturation by Trichinella spiralis excretory/secretory products. *Parasite Immunology*, 31(10), pp.641–645.

Lee, S.H., Stephens, J.L. & Englund, P.T., 2007. A fatty-acid synthesis mechanism specialized for parasitism. *Nature reviews. Microbiology*, 5(4), pp.287–297.

Li, Z., 2012. Regulation of the cell division cycle in Trypanosoma brucei. *Eukaryotic Cell*, 11(10), pp.1180–1190.

Liang, S.C. et al., 2006. Interleukin (IL)-22 and IL-17 are coexpressed by Th17 cells and cooperatively enhance expression of antimicrobial peptides. *The Journal of Experimental Medicine*, 203(10), pp.2271–2279. Available at: http://www.ncbi.nlm.nih.gov/pmc/articles/PMC2118116/.

Lila Koumandou, V. et al., 2013. Evidence for recycling of invariant surface transmembrane domain proteins in African trypanosomes. *Eukaryotic Cell*, 12(2), pp.330–342.

Liu, D. et al., 2009. Leishmania major phosphoglycans influence the host early immune response by modulating dendritic cell functions. *Infection and Immunity*, 77(8), pp.3272–3283.

MacDonald, H.R. & Zaech, P., 1982. Light scatter analysis and sorting of cells activated in mixed leukocyte culture. *Cytometry*, 3(1), pp.55–58.

MacLean, L. et al., 2004. Severity of human African trypanosomiasis in East Africa is associated with geographic location, parasite genotype, and host inflammatory cytokine response profile. *Infection and Immunity*, 72(12), pp.7040–7044.

MacLean, L. et al., 2012. Stage Progression and Neurological Symptoms in Trypanosoma brucei rhodesiense Sleeping Sickness: Role of the CNS Inflammatory Response. *PLoS Neglected Tropical Diseases*, 6(10).

MacLean, L., Odiit, M. & Sternberg, J.M., 2001. Nitric oxide and cytokine synthesis in human African trypanosomiasis. *The Journal of infectious diseases*, 184(8), pp.1086–90. Available at: http://www.ncbi.nlm.nih.gov/pubmed/11574928.

Magez, S. et al., 1997. Specific uptake of tumor necrosis factor-alpha is involved in growth control of Trypanosoma brucei. *The Journal of cell biology*, 137(3), pp.715–727.

Magez, S. et al., 2008. The Role of B-cells and IgM Antibodies in Parasitemia, Anemia, and VSG Switching in Trypanosoma brucei–Infected Mice S. Black, ed. *PLoS Pathogens*, 4(8), p.e1000122. Available at: http://dx.plos.org/10.1371/journal.ppat.1000122 [Accessed May 3, 2012].

Magez, S. et al., 1999. Tumor necrosis factor alpha is a key mediator in the regulation of experimental Trypanosoma brucei infections. *Infection and Immunity*, 67(6), pp.3128–3132.

Magez, S. et al., 2002. VSG-GPI anchors of African trypanosomes: their role in macrophage activation and induction of infection-associated immunopathology. *Microbes and infection / Institut Pasteur*, 4(9), pp.999–1006. Available at: http://www.ncbi.nlm.nih.gov/pubmed/12106794.

Magnus, E., Vervoort, T. & Van Meirvenne, N., 1978. A card-agglutination test with stained trypanosomes (CATT) for the serological diagnosis of T. b. gambiense trypanosomiasis. *Annales De La Societe Belge De Medecine Tropicale*, 58(3), p.169.

Male, D. et al., 2012. *Immunology* 8th ed., Saunders.

Mansfield, J.M., 1994. T-cell responses to the trypanosome variant surface glycoprotein: A

new paradigm? *Parasitology Today*, 10(7), pp.267–270.

Mansfield, J.M. & Paulnock, D.M., 2005. Regulation of innate and acquired immunity in African trypanosomiasis. *Parasite Immunology*, 27(10–11), pp.361–371.

Mansfield, J.M. & Paulnock, D.M., 2005. Regulation of innate and acquired immunity in African trypanosomiasis. *Parasite immunology*, 27(10–11), pp.361–71. Available at: http://www.ncbi.nlm.nih.gov/pubmed/16179030.

Manta, B. et al., 2013. Trypanothione: A unique bis-glutathionyl derivative in trypanosomatids. *Biochimica et Biophysica Acta - General Subjects*, 1830(5), pp.3199–3216.

Marcello, L. & Barry, J.D., 2007. Analysis of the VSG gene silent archive in Trypanosoma brucei reveals that mosaic gene expression is prominent in antigenic variation and is favored by archive substructure. *Genome Research*, 17(9), pp.1344–1352.

Mathieu, C. et al., 2017. Arginine and Lysine Transporters Are Essential for Trypanosoma brucei. *PLOS ONE*, 12(1), p.e0168775. Available at: http://dx.doi.org/10.1371%2Fjournal.pone.0168775.

da Matta Guedes, P.M. et al., 2010. IL-17 produced during Trypanosoma cruzi infection plays a central role in regulating parasite-induced myocarditis. *PLoS neglected tropical diseases*, 4(2).

Matthews, K.R., 2005. The developmental cell biology of Trypanosoma brucei. *Journal of cell science*, 118(Pt 2), pp.283–90. Available at: http://www.pubmedcentral.nih.gov/articlerender.fcgi?artid=2686837&tool=pmcentrez&rendertype=abstract [Accessed March 6, 2012].

McKean, P.G., 2003. Coordination of cell cycle and cytokinesis in Trypanosoma brucei. *Current Opinion in Microbiology*, 6(6), pp.600–607. Available at: http://linkinghub.elsevier.com/retrieve/pii/S1369527403001462 [Accessed March 30, 2012].

McMahon, H.T. & Boucrot, E., 2011. Molecular mechanism and physiological functions of clathrin-mediated endocytosis. *Nature reviews. Molecular cell biology*, 12(8), pp.517–533. Available at: http://dx.doi.org/10.1038/nrm3151.

Mitashi, P. et al., 2012. Human African Trypanosomiasis Diagnosis in First-Line Health Services of Endemic Countries, a Systematic Review. *PLOS Neglected Tropical Diseases*, 6(11), p.e1919. Available at:

http://dx.doi.org/10.1371%2Fjournal.pntd.0001919.

Miyazaki, Y. et al., 2010. IL-17 is necessary for host protection against acute-phase Trypanosoma cruzi infection. *Journal of immunology (Baltimore, Md. : 1950)*, 185(2), pp.1150–1157.

Moore, K.W. et al., 2001. INTERLEUKIN-10 AND THE INTERLEUKIN-10 RECEPTOR. *Annual Review of Immunology*, 19, pp.683–765.

Mou, Z. et al., 2010. Interleukin-17-Mediated Control of Parasitemia in Experimental Trypanosoma congolense Infection in Mice . *Infection and Immunity*, 78(12), pp.5271–5279. Available at: http://www.ncbi.nlm.nih.gov/pmc/articles/PMC2981335/.

Musaya, J. et al., 2015. Role of cytokines in Trypanosoma brucei-induced anaemia: A review of the literature. *Malawi Medical Journal*, 27(2), pp.45–50. Available at: http://www.ncbi.nlm.nih.gov/pmc/articles/PMC4562079/.

Naessens, J. et al., 2005. TNF-α mediates the development of anaemia in a murine Trypanosoma brucei rhodesiense infection, but not the anaemia associated with a murine Trypanosoma congolense infection. *Clinical and Experimental Immunology*, 139(3), pp.405–410.

Namangala, B. et al., 2000. Attenuation of Trypanosoma brucei is associated with reduced immunosuppression and concomitant production of Th2 lymphokines. *The Journal of Infectious Diseases*, 181, pp.1110–1120.

Namangala, B., 2011. How the African trypanosomes evade host immune killing. *Parasite Immunology*, 33(8), pp.430–437.

Namangala, B. et al., 2001. Relative contribution of interferon-gamma and interleukin-10 to resistance to murine African trypanosomosis. *The Journal of infectious diseases*, 183(12), pp.1794–800. Available at: http://www.ncbi.nlm.nih.gov/pubmed/11372033.

Namangala, B. et al., 2000. Trypanosoma brucei brucei infection impairs MHC class II antigen presentation capacity of macrophages. *Parasite Immunology*, 22(7), pp.361–370.

Namangala, B., De Baetselier, P. & Beschin, A., 2009. Both type-I and type-II responses contribute to murine trypanotolerance. *Journal of Veterinary Medicine*, 71, pp.313–318.

Narayanan, M.S. & Rudenko, G., 2013. TDP1 is an HMG chromatin protein facilitating RNA polymerase i transcription in African trypanosomes. *Nucleic Acids Research*, 41(5), pp.2981–2992.

Natesan, S.K.A. et al., 2011. Trypanosoma brucei brucei: Endocytic recycling is important

for mouse infectivity. *Experimental Parasitology*, 127(4), pp.777–783.

Ngotho, M. et al., 2006. IL-10 is up regulated in early and transitional stages in vervet monkeys experimentally infected with Trypanosoma brucei rhodesiense. *Parasitology International*, 55(4), pp.243–248.

Nimmerjahn, F. & Ravetch, J. V., 2007. Fc-Receptors as Regulators of Immunity. *Advances in Immunology*, 96, pp.179–204.

Nimmerjahn, F. & Ravetch, J. V., 2006. Fc gamma receptors: Old friends and new family members. *Immunity*, 24(1), pp.19–28.

Nobes, C. & Marsh, M., 2000. Dendritic cells: New roles for Cdc42 and Rac in antigen uptake? *Current Biology*, 10(20).

Noda, T. & Amano, F., 1997. Differences in nitric oxide synthase activity in a macrophage-like cell line, RAW264.7 cells, treated with lipopolysaccharide (LPS) in the presence or absence of interferon-gamma (IFN-gamma): possible heterogeneity of iNOS activity. *Journal of biochemistry*, 121(1), pp.38–46.

Ocaña-Morgner, C., Mota, M.M. & Rodriguez, A., 2003. Malaria blood stage suppression of liver stage immunity by dendritic cells. *The Journal of experimental medicine*, 197(2), pp.143–51. Available at: http://www.pubmedcentral.nih.gov/articlerender.fcgi?artid=2193811&tool=pmcentrez&rendertype=abstract.

Ocaña-Morgner, C., Wong, K. a & Rodriguez, A., 2008. Interactions between dendritic cells and CD4+ T cells during Plasmodium infection. *Malaria journal*, 7, p.88. Available at: http://www.pubmedcentral.nih.gov/articlerender.fcgi?artid=2423365&tool=pmcentrez&rendertype=abstract.

Olsson, T. et al., 1991. Bidirectional activating signals between Trypanosoma brucei and CD8+ T cells: A trypanosome-released factor triggers interferon-γ production that stimulates parasite growth. *European Journal of Immunology*, 21(10), pp.2447–2454. Available at: http://dx.doi.org/10.1002/eji.1830211022.

Ooi, Y.M. & Colten, H.R., 1979. Genetic defect in secretion of complement C5 in mice. *Nature*, 282, p.207–8.

Ouyang, W., Kolls, J.K. & Zheng, Y., 2008. The Biological Functions of T Helper 17 Cell Effector Cytokines in Inflammation. *Immunity*, 28(4), pp.454–467.

Overath, P. & Engstler, M., 2004. Endocytosis, membrane recycling and sorting of GPI-

anchored proteins: Trypanosoma brucei as a model system. *Molecular Microbiology*, 53(3), pp.735–744.

Pal, A. et al., 2002. Differential endocytic functions of Trypanosoma brucei Rab5 isoforms reveal a glycosylphosphatidylinositol-specific endosomal pathway. *Journal of Biological Chemistry*, 277(11), pp.9529–9539.

Pal, A. et al., 2003. Rab5 and Rab11 mediate transferrin and anti-variant surface glycoprotein antibody recycling in Trypanosoma brucei. *The Biochemical journal*, 374(Pt 2), pp.443–451.

Parish, C.R. et al., 2009. Use of the intracellular fluorescent dye CFSE to monitor lymphocyte migration and proliferation. *Current Protocols in Immunology*, (SUPPL. 84).

Paulnock, D.M. & Coller, S.P., 2001. Analysis of macrophage activation in African trypanosomiasis. *J. Leukoc. Biol.*, 69(May), pp.685–690. Available at: http://www.jleukbio.org/content/69/5/685.abstract.

Paulnock, D.M. & Coller, S.P., 2001. Analysis of macrophage activation in African trypanosomiasis. *Journal of leukocyte biology*, 69(5), pp.685–690.

Paulnock, D.M., Freeman, B.E. & Mansfield, J.M., 2010. Modulation of innate immunity by African trypanosomes. *Parasitology*, 137(14), pp.2051–63. Available at: http://www.ncbi.nlm.nih.gov/pubmed/21087532 [Accessed May 22, 2013].

Pays, E. et al., 1985. Telomeric reciprocal recombination as a possible mechanism for antigenic variation. *Nature*, 316(6028), pp.562–4.

Planelles, L. et al., 2003. Differential CD86 and CD40 co-stimulatory molecules and cytokine expression pattern induced by Trypanosoma cruzi in APCs from resistant or susceptible mice. *Clinical and Experimental Immunology*, 131(1), pp.41–47. Available at: http://www.ncbi.nlm.nih.gov/pmc/articles/PMC1808596/.

Plüddemann, A., Mukhopadhyay, S. & Gordon, S., 2011. Innate immunity to intracellular pathogens: macrophage receptors and responses to microbial entry. *Immunological reviews*, 240(1), pp.11–24. Available at: http://www.ncbi.nlm.nih.gov/pubmed/21349083 [Accessed January 12, 2017].

Poncini, C.V. et al., 2008. Trypanosoma cruzi induces regulatory dendritic cells in vitro. *Infection and Immunity*, 76(6), pp.2633–2641.

Priotto, G. et al., 2007. Nifurtimox-eflornithine combination therapy for second-stage

Trypanosoma brucei gambiense sleeping sickness: a randomized clinical trial in Congo. *Clin Infect Dis*, 45(11), pp.1435–1442. Available at: http://www.ncbi.nlm.nih.gov/entrez/query.fcgi?cmd=Retrieve&db=PubMed&dopt=Citation&list_uids=17990225.

Priotto, G. et al., 2008. Safety and effectiveness of first line eflornithine for Trypanosoma brucei gambiense sleeping sickness in Sudan: cohort study. *BMJ (Clinical research ed.)*, 336(7646), pp.705–708. Available at: http://www.bmj.com/content/336/7646/705.long%5Cnhttp://ovidsp.ovid.com/ovidweb.cgi?T=JS&PAGE=reference&D=med5&NEWS=N&AN=18321960.

Probst, P. et al., 1997. A Leishmania protein that modulates interleukin (IL)-12, IL-10 and tumor necrosis factor-α production and expression of B7-1 in human monocyte-derived antigen-presenting cells. *European Journal of Immunology*, 27(10), pp.2634–2642. Available at: http://dx.doi.org/10.1002/eji.1830271024.

Quah, B.J.C., Warren, H.S. & Parish, C.R., 2007. Monitoring lymphocyte proliferation in vitro and in vivo with the intracellular fluorescent dye carboxyfluorescein diacetate succinimidyl ester. *Nature protocols*, 2(9), pp.2049–2056.

Ralston, K.S. et al., 2006. Flagellar motility contributes to cytokinesis in Trypanosoma brucei and is modulated by an evolutionarily conserved dynein regulatory system. *Eukaryotic Cell*, 5(4), pp.696–711.

Ralston, K.S. et al., 2009. The Trypanosoma brucei flagellum: moving parasites in new directions. *Annual Review of Microbiology*, 63, pp.335–62. Available at: http://www.ncbi.nlm.nih.gov/pubmed/19575562%5Cnhttp://www.pubmedcentral.nih.gov/articlerender.fcgi?artid=PMC3821760.

Raschke, W.C. et al., 1978. Functional macrophage cell lines transformed by abelson leukemia virus. *Cell*, 15(1), pp.261–267.

Rath, M. et al., 2014. Metabolism via arginase or nitric oxide synthase: Two competing arginine pathways in macrophages. *Frontiers in Immunology*, 5(OCT).

Reinitz, D.M., Aizenstein, B.D. & Mansfield, J.M., 1992. Variable and conserved structural elements of trypanosome variant surface glycoproteins. *Molecular and Biochemical Parasitology*, 51(1), pp.119–132. Available at: http://www.sciencedirect.com/science/article/pii/016668519290207Z.

Roberts, T.M. et al., 2016. Identification and Characterisation of a pH-stable GFP. *Scientific*

*Reports*, 6, p.srep28166. Available at: http://www.nature.com/articles/srep28166.

Robinson, N.P. et al., 1999. Predominance of duplicative VSG gene conversion in antigenic variation in African trypanosomes. *Molecular and cellular biology*, 19(9), pp.5839–5846.

Rodrigues, V. et al., 2014. Impairment of T Cell Function in Parasitic Infections. *PLoS Neglected Tropical Diseases*, 8(2).

Rodríguez, J. a et al., 2009. Propulsion of African trypanosomes is driven by bihelical waves with alternating chirality separated by kinks. *Proceedings of the National Academy of Sciences of the United States of America*, 106(46), pp.19322–19327.

Rolin, S. et al., 1996. Simultaneous but independent activation of adenylate cyclase and glycosylphosphatidylinositol-phospholipase C under stress conditions in Trypanosoma brucei. *Journal of Biological Chemistry*, 271(18), pp.10844–10852.

Rotureau, B. et al., 2014. Flagellar adhesion in Trypanosoma brucei relies on interactions between different skeletal structures in the flagellum and cell body. *Journal of Cell Science*, 127(1), pp.204–215. Available at: http://jcs.biologists.org/cgi/doi/10.1242/jcs.136424.

Rudenko, G. et al., 1998a. Selection for activation of a new variant surface glycoprotein gene expression site in Trypanosoma brucei can result in deletion of the old one. *Molecular and Biochemical Parasitology*, 95(1), pp.97–109.

Rudenko, G. et al., 1998b. Selection for activation of a new variant surface glycoprotein gene expression site in Trypanosoma brucei can result in deletion of the old one. *Molecular and Biochemical Parasitology*, 95(1), pp.97–109.

Rutz, S., Eidenschenk, C. & Ouyang, W., 2013. IL-22, not simply a Th17 cytokine. *Immunological Reviews*, 252(1), pp.116–132.

Salmon, D. et al., 2012. Adenylate Cyclases of Trypanosoma brucei Inhibit the Innate Immune Response of the Host. *Science*, 337(6093), pp.463–466.

Sarma, J.V. & Ward, P.A., 2011. The complement system. *Cell and Tissue Research*, 343(1), pp.227–235.

Savina, A. & Amigorena, S., 2007. Phagocytosis and antigen presentation in dendritic cells. *Immunological Reviews*, 219(1), pp.143–156.

Scheller, J. et al., 2011. The pro- and anti-inflammatory properties of the cytokine interleukin-6. *Biochimica et Biophysica Acta (BBA) - Molecular Cell Research*, 1813(5),

pp.878–888. Available at: http://www.sciencedirect.com/science/article/pii/S0167488911000425.

Schleifer, K.W. et al., 1993. Characterization of T helper cell responses to the trypanosome variant surface glycoprotein. *Journal of Immunology*, 150(7), pp.2910–2919. Available at: http://www.ncbi.nlm.nih.gov/pubmed/8454863.

Schopf, L.R. et al., 1998. Interleukin-4-dependent immunoglobulin G1 isotype switch in the presence of a polarized antigen-specific Th1-cell response to the trypanosome variant surface glycoprotein. *Infection and Immunity*, 66(2), pp.451–461.

Schwede, A. et al., 2015. How Does the VSG Coat of Bloodstream Form African Trypanosomes Interact with External Proteins? *PLoS Pathogens*, 11(12).

Schwede, A. et al., 2011. The VSG C-terminal domain is inaccessible to antibodies on live trypanosomes. *Molecular and Biochemical Parasitology*, 175(2), pp.201–204.

Schwede, A. & Carrington, M., 2010. Bloodstream form trypanosome plasma membrane proteins: antigenic variation and invariant antigens. *Parasitology*, 137(14), pp.2029–2039. Available at: http://www.journals.cambridge.org/abstract_S0031182009992034%5Cnpapers2://publication/doi/10.1017/S0031182009992034.

Sheader, K. et al., 2005. Variant surface glycoprotein RNA interference triggers a precytokinesis cell cycle arrest in African trypanosomes. *Proceedings of the National Academy of Sciences of the United States of America*, 102(24), pp.8716–8721.

Sheader, K., Te Vruchte, D. & Rudenko, G., 2004. Bloodstream Form-specific Up-regulation of Silent VSG Expression Sites and Procyclin in Trypanosoma brucei after Inhibition of DNA Synthesis or DNA Damage. *Journal of Biological Chemistry*, 279(14), pp.13363–13374.

Shi, M., Pan, W. & Tabel, H., 2003. Experimental African trypanosomiasis: IFN-gamma mediates early mortality. *European journal of immunology*, 33(1), pp.108–18. Available at: http://www.ncbi.nlm.nih.gov/pubmed/12594839.

Shimogawa, M.M. et al., 2015. Cell surface proteomics provides insight into stage-specific remodeling of the host-parasite interface in Trypanosoma brucei. *Molecular & cellular proteomics : MCP*, 14(7), pp.1977–1988. Available at: http://www.mcponline.org/content/14/7/1977.abstract?etoc.

Shipkova, M. & Wieland, E., 2012. Surface markers of lymphocyte activation and markers of

cell proliferation. *Clinica Chimica Acta*, 413(17–18), pp.1338–1349.

Silverman, J.S. et al., 2011. Late endosomal Rab7 regulates lysosomal trafficking of endocytic but not biosynthetic cargo in Trypanosoma brucei. *Molecular Microbiology*, 82(3), pp.664–678.

Simarro, P.P. et al., 2012. Estimating and Mapping the Population at Risk of Sleeping Sickness. *PLoS Neglected Tropical Diseases*, 6(10).

Smith-Garvin, J. & Koretzky, G., 2009. T cell activation. *Annual Review of Immunology*, 27, pp.591–619. Available at: http://www.ncbi.nlm.nih.gov/pmc/articles/PMC2740335/.

Smith, T.K. et al., 2009. Blocking variant surface glycoprotein synthesis in Trypanosoma brucei triggers a general arrest in translation initiation. *PLoS ONE*, 4.

Smith, T.K. et al., 2009. Blocking variant surface glycoprotein synthesis in Trypanosoma brucei triggers a general arrest in translation initiation. *PloS one*, 4(10), p.e7532. Available at: http://www.pubmedcentral.nih.gov/articlerender.fcgi?artid=2762041&tool=pmcentrez&rendertype=abstract [Accessed March 9, 2012].

Sousa-Rocha, D. et al., 2015. Trypanosoma cruzi and its soluble antigens induce NET release by stimulating toll-like receptors. *PLoS ONE*, 10(10).

von Stebut, E., 2017. Parasites Dampen Dendritic Cell Activation to Ensure Their Survival. *Trends in Parasitology*, 33(2), pp.78–80. Available at: http://dx.doi.org/10.1016/j.pt.2016.12.001.

Steinman, R. & Cohn, Z., 1974. Identification of a novel cell type in peripheral lymphoid organs of mice. II. Functional properties in vitro. *The Journal of Experimental Medicine*, 139(2), pp.380–97. Available at: http://www.pubmedcentral.nih.gov/articlerender.fcgi?artid=2139525&tool=pmcentrez&rendertype=abstract.

Steinman, R.M. & Cohn, Z.A., 1973. Identification of a novel cell type in peripheral lymphoid organs of mice. *Journal of Experimental Medicine*, 137(1), pp.1142–1162. Available at: http://eutils.ncbi.nlm.nih.gov/entrez/eutils/elink.fcgi?dbfrom=pubmed&id=17182535&retmode=ref&cmd=prlinks.

Sternberg, J.M., 2004. Human African trypanosomiasis: clinical presentation and immune response. *Parasite Immunology*, 26(11–12), pp.469–476. Available at:

http://www.ncbi.nlm.nih.gov/pubmed/15771682%5Cnhttp://doi.wiley.com/10.1111/j.0141-9838.2004.00731.x.

Steverding, D., 2010a. The development of drugs for treatment of sleeping sickness: a historical review. *Parasites & vectors*, 3(1), p.15. Available at: http://www.pubmedcentral.nih.gov/articlerender.fcgi?artid=2848007&tool=pmcentrez&rendertype=abstract.

Steverding, D., 2010b. The development of drugs for treatment of sleeping sickness: a historical review. *Parasites & vectors*, 3(1), p.15.

Steverding, D., 2008. The history of African trypanosomiasis. *Parasites & vectors*, 1(1), p.3. Available at: http://www.pubmedcentral.nih.gov/articlerender.fcgi?artid=2270819&tool=pmcentrez&rendertype=abstract%5Cnhttp://www.ncbi.nlm.nih.gov/pubmed/18275594%5Cnhttp://www.pubmedcentral.nih.gov/articlerender.fcgi?artid=PMC2270819.

Steverding, D., 2000. The transferrin receptor of Trypanosoma brucei. *Parasitology International*, 48(3), pp.191–198.

Stijlemans, B. et al., 2015. Development of a pHrodo-Based Assay for the Assessment of In Vitro and In Vivo Erythrophagocytosis during Experimental Trypanosomosis. *PLoS Neglected Tropical Diseases*, 9(3).

Stijlemans, B. et al., 2016. Immune evasion strategies of Trypanosoma brucei within the mammalian host: Progression to pathogenicity. *Frontiers in Immunology*, 7(JUN).

Stijlemans, B. et al., 2010. Scrutinizing the mechanisms underlying the induction of anemia of inflammation through GPI-mediated modulation of macrophage activation in a model of African trypanosomiasis. *Microbes and Infection*, 12(5), pp.389–399.

Taylor, J.E. & Rudenko, G., 2006. Switching trypanosome coats: what's in the wardrobe? *Trends in genetics : TIG*, 22(11), pp.614–20. Available at: http://www.ncbi.nlm.nih.gov/pubmed/16908087 [Accessed March 7, 2012].

Taylor, P.R. et al., 2005. Macrophage receptors and immune recognition. *Annu Rev Immunol*, 23, pp.901–944. Available at: http://www.ncbi.nlm.nih.gov/pubmed/15771589%5Cnhttp://www.annualreviews.org/doi/abs/10.1146/annurev.immunol.23.021704.115816.

Terrazas, C.A., Terrazas, L.I. & Gómez-García, L., 2010. Modulation of dendritic cell responses by parasites: A common strategy to survive. *Journal of Biomedicine and*

*Biotechnology*, 2010.

Triggs, V.P. & Bangs, J.D., 2003. Glycosylphosphatidylinositol-dependent protein trafficking in bloodstream stage Trypanosoma brucei. *Eukaryotic cell*, 2(1), pp.76–83. Available at: http://www.pubmedcentral.nih.gov/articlerender.fcgi?artid=141176&tool=pmcentrez&rendertype=abstract.

Tsui, S.-M. et al., 2009. Pegylated derivatives of recombinant human arginase (rhArg1) for sustained in vivo activity in cancer therapy: preparation, characterization and analysis of their pharmacodynamics in vivo and in vitro and action upon hepatocellular carcinoma cell (HCC). *Cancer Cell International*, 9(1), p.9. Available at: http://dx.doi.org/10.1186/1475-2867-9-9.

Uppaluri, S. et al., 2011. Impact of microscopic motility on the swimming behavior of parasites: Straighter Trypanosomes are more directional. *PLoS Computational Biology*, 7(6).

Vincent, I.M. et al., 2010. A molecular mechanism for eflornithine resistance in African trypanosomes. *PLoS Pathogens*, 6(11).

Wang, J., Böhme, U. & Cross, G.A.M., 2003. Structural features affecting variant surface glycoprotein expression in Trypanosoma brucei. *Molecular and Biochemical Parasitology*, 128(2), pp.135–145.

Wei, L. et al., 2007. IL-21 is produced by Th17 cells and drives IL-17 production in a STAT3-dependent manner. *Journal of Biological Chemistry*, 282(48), pp.34605–34610.

WHO, 2017. Trypanosomiasis, human African (sleeping sickness). Available at: http://www.who.int/mediacentre/factsheets/fs259/en/#.WKQRI2MZYes.mendeley [Accessed February 15, 2017].

Wickstead, B., Ersfeld, K. & Gull, K., 2002. Targeting of a tetracycline-inducible expression system to the transcriptionally silent minichromosomes of Trypanosoma brucei. *Molecular and biochemical parasitology*, 125(1–2), pp.211–216.

Williams, R.O., Young, J.R. & Majiwa, P.A.O., 1982. Genomic environment of T. brucei VSG genes: presence of a minichromosome. *Nature*, 299(5882), pp.417–421. Available at: http://dx.doi.org/10.1038/299417a0.

Wilson, L.G., Carter, L.M. & Reece, S.E., 2013. High-speed holographic microscopy of malaria parasites reveals ambidextrous flagellar waveforms. *Proc Natl Acad Sci U S A*, 110(47), pp.18769–18774. Available at:

http://www.ncbi.nlm.nih.gov/pubmed/24194551.

Wirtz, E. et al., 1999. A tightly regulated inducible expression system for conditional gene knock-outs and dominant-negative genetics in Trypanosoma brucei. *Molecular and Biochemical Parasitology*, 99(1), pp.89–101.

Wykes, M.N. et al., 2007. Plasmodium strain determines dendritic cell function essential for survival from malaria. *PLoS Pathogens*, 3(7), pp.0904–0912.

Wynn, T.A., 2003. IL-13 E FFECTOR F UNCTIONS *. *Annual Review of Immunology*, 21(1), pp.425–456. Available at: http://www.annualreviews.org/doi/10.1146/annurev.immunol.21.120601.141142.

Yau, T.C. et al., 2014. Preliminary efficacy, safety, pharmacokinetics, and quality of life study of pegylated recombinant human arginase 1 in patients with advanced hepatocellular carcinoma. *J Clin Oncol*, Abstract e.

Zaburdaev, V. et al., 2011. Langevin dynamics deciphers the motility pattern of swimming parasites. *Physical Review Letters*, 106(20).

Zhou, L. et al., 2007. IL-6 programs T(H)-17 cell differentiation by promoting sequential engagement of the IL-21 and IL-23 pathways. *Nature immunology*, 8(9), pp.967–974.

Ziegelbauer, K. & Overath, P., 1993. Organization of two invariant surface glycoproteins in the surface coat of Trypanosoma brucei. *Infection and Immunity*, 61(11), pp.4540–4545.

# Publication

Cheung, J.L.Y. *et al*., 2016. Blocking Synthesis of the Variant Surface Glycoprotein Coat in Trypanosoma brucei Leads to an Increase in Macrophage Phagocytosis Due to Reduced Clearance of Surface Coat Antibodies K. L. Hill, ed. *PLoS Pathogens*, 12(11), p.e1006023.

# Award

Imperial College London, Department of Life Sciences Travel Award (April 2015)

# Conference Presentations

**Jackie L.Y Cheung** N.V Wand, S. Ridewood, R. Wheeler, G. Rudenko and GCF Chan
Mechanistic evidence for the clearance of *Trypanosoma brucei* by macrophages and the potential therapeutic use of the pegylated arginase, BCT-100
Asian Society for Paediatric Research Meeting – Bangkok, Thailand, 10-11 November 2016
(Poster Presentation)

**Jackie L.Y Cheung**, N.V Wand, R. Wheeler, E. Gluenz, K. Gull and G. Rudenko
The role of Variant Surface Glycoprotein in evasion of *T. brucei* from macrophage phagocytosis
Kinetoplastid Molecular Cell Biology Meeting – Woods Hole, MA, USA, 25-29 April 2015
(Oral presentation)

**Jackie L.Y Cheung**, N.V Wand, R. Wheeler, E. Gluenz, K. Gull and G. Rudenko
The role of Variant Surface Glycoprotein in *Trypanosoma brucei* evasion of phagocytosis by macrophages
Trypanosomatid GPLF Annual Meeting – Paris, France, 14-16 October 2014
(Oral presentation)

**Jackie L.Y Cheung**, N.V Wand, R. Wheeler, E. Gluenz, K. Gull and G. Rudenko
The role of Variant Surface Glycoprotein in *Trypanosoma brucei* evasion of phagocytosis by macrophages
British Society For Parasitology 52nd Annual Spring Meeting – Cambridge, UK, 6-9 April 2014
(Poster presentation)